

AD695925

FTD-MT-24-135-69-Vol II of II

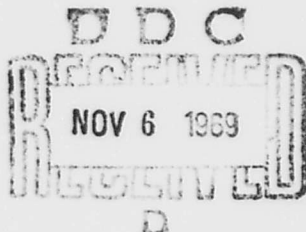
FOREIGN TECHNOLOGY DIVISION



LIQUID FUEL ROCKET ENGINES -
DESIGN FUNDAMENTALS

by

M. V. Dobrovolskiy



Distribution of this document is
unlimited. It may be released to
the Clearinghouse, Department of
Commerce, for sale to the general
public.

Reproduced by the
CLEARINGHOUSE
for Federal Scientific & Technical
Information Springfield Va. 22151

317

FTD-MT- 24-135-69-Vol II of II

EDITED MACHINE TRANSLATION

LIQUID FUEL ROCKET ENGINES — DESIGN FUNDAMENTALS

By: M. V. Dobrovolskiy

English pages: 302-615

THIS TRANSLATION IS A RENDITION OF THE ORIGINAL FOREIGN TEXT WITHOUT ANY ANALYTICAL OR EDITORIAL COMMENT. STATEMENTS OR THEORIES ADVOCATED OR IMPLIED ARE THOSE OF THE SOURCE AND DO NOT NECESSARILY REFLECT THE POSITION OR OPINION OF THE FOREIGN TECHNOLOGY DIVISION.

PREPARED BY:

TRANSLATION DIVISION
FOREIGN TECHNOLOGY DIVISION
WPAFB, OHIO.

FTD-MT- 24-135-69-Vol II of II

Date 27 June 1969

U. S. BOARD ON GEOGRAPHIC NAMES TRANSLITERATION SYSTEM

Block	Italic	Transliteration	Block	Italic	Transliteration
А а	А а	A, a	Р р	Р р	R, r
Б б	Б б	B, b	С с	С с	S, s
В в	В в	V, v	Т т	Т т	T, t
Г г	Г г	G, g	У у	У у	U, u
Д д	Д д	D, d	Ф ф	Ф ф	F, f
Е е	Е е	Ye, ye; E, e*	Х х	Х х	Kh, kh
Ж ж	Ж ж	Zh, zh	Ц ц	Ц ц	Ts, ts
З з	З з	Z, z	Ч ч	Ч ч	Ch, ch
И и	И и	I, i	Ш ш	Ш ш	Sh, sh
Й я	Й я	Y, y	Щ щ	Щ щ	Shch, shch
К к	К к	K, k	ѣ ѿ	ѣ ѿ	"
Л л	Л л	L, l	ы ы	ы ы	Y, y
М м	М м	M, m	ѣ ѿ	ѣ ѿ	'
Н н	Н н	N, n	Э э	Э э	E, e
О о	О о	O, o	Ю ю	Ю ю	Yu, yu
П п	П п	P, p	Я я	Я я	Ya, ya

* ye initially, after vowels, and after ѿ, ѿ; e elsewhere.
When written as є in Russian, transliterate as ye or є.
The use of diacritical marks is preferred, but such marks
may be omitted when expediency dictates.

C H A P T E R V

CHAMBERS OF LIQUID PROPELLANT ROCKET ENGINES

5. 1. Shapes and Examples of Existing Chambers of Liquid Propellant Rocket Engines

The chamber of the engine is the main unit of a rocket engine installation.

The following basic shapes of combustion chambers of liquid propellant rocket engines [LPRE] (Fig. 5.1).

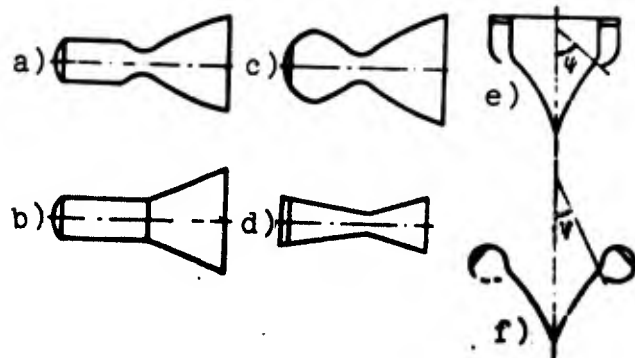


Fig. 5. 1. Shapes of combustion chambers: a) cylindrical; b) semithermal nozzle; c) spherical; d) conical; e, f) annular.

1. Cylindrical.
2. Spherical (or pear-shaped).
3. Conical.

BLANK PAGE

4. Annular.

Let us consider the special features of each of these forms.

Cylindrical Combustion Chambers, Average and Relative Specific Weight Flow

Cylindrical combustion chambers are the most widely used at present. They are used for chambers of engines of all thrusts. Their basic advantage is simplicity of manufacture. The simple shape facilitates the application of light stiffened walls with many connections and tubes. The LPRE with detachable nozzle units and injection assemblies usually have cylindrical combustion chamber. The application of cylindrical chambers in multichamber propulsion systems facilitates arrangement of cluster engines. A deficiency of cylindrical chambers as compared to spherical chambers is the poor strength properties; another is the large cooling surface.

As a characteristic of cylindrical combustion chambers it is convenient to use the concept of specific weight flow.

The average specific weight flow of the combustion chamber over the section is

$$r = \frac{G}{f_r} \text{ kg/s} \cdot \text{cm}^2, \quad (5.1)$$

where f_r - area of combustion chamber cross section.

Let us express the flow rate G thorough the complex β (1.9):

$$G = \frac{f_{sp} p_2}{\beta};$$

then

$$r = \frac{f_{sp}}{\beta} 10^6 p_2 \text{ g/s} \cdot \text{cm}^2 \quad (5.2)$$

where p_2 - pressure in combustion chamber in kgf/cm^2 .

Since the quantity β has an approximately constant value for a given fuel; the magnitude of specific weight flow is directly proportional to the pressure in the chamber, i. e.,

$$r_p = r_0 \cdot p_0 \quad (5.3)$$

where $r_p = \frac{r}{p_0}$ is specific weight flow referred to the pressure in the chamber and is called the relative specific weight flow. Frequently the quantity r_p is used in place of r for appraisal of specific weight flow.

In accordance with equation (5.2),

$$r_p = \frac{f_{sp}}{f_m} \cdot 10^3 \text{ g/kgf}\cdot\text{s.} \quad (5.4)$$

Thus r_p depends only on the type of propellant and the ratio f_w/f_m and for given signal it is constant, independently of chamber pressure.

Since for the propellants in use $\beta=170-240 \text{ kgf}/\text{s/kg}$, in accordance with equality (5.4) at $f_w/f_m=2-6$ the values of relative specific weight flow are within the limits 1-2 g/kg·s. At smaller values of f_w/f_m the values of r_p are correspondingly greater.

A distinction is made between isobaric and high-speed combustion chamber. Combustion chambers in which the pressure is approximately constant along the length are sometimes called isobaric chambers. These include chambers in which $f_w/f_m > 3$.

The ratio f_w/f_m is usually called the dimensionless area of the combustion chamber. If the value of $f_w/f_m < 3$, then during combustion the flow rate considerably increases in the chamber along its length, while the pressure drops in accordance with the equation of the law of conservation of energy. Such combustion chambers (with $f_w/f_m < 3$) cannot be called isobaric; they are called high-speed chambers. In the limit $f_w/f_m=1$ engine chambers carry the name semithermal nozzle. [Translator's note: This term may be equivalent to the U.S. expression "thermally choked."] (Fig. 5. 1b).

High-speed combustion chambers with small ratios ρ_2/ρ_3 have somewhat greater losses in connection with losses on thermal drag [1]. However, since at large ρ_2 these losses are small, it is frequently expedient to use more compact, high-speed chambers [110].

The diameter of the cylindrical part of the combustion chamber is determined by finding either the ratio L_k/D_k , which is taken as equal to 1-1.5, or the value of specific weight flow or r_p (or, which is the same thing, the quantity ' dL/dr_p ')

The accepted values of relative specific weight flow are $r_p=1-2$, which corresponds to values of $L_k/D_k = 6$. In conclusion let us note that sometimes the diameter of the combustion chamber is determined by the diameter of the injection assembly necessary for distribution of the injectors.

Upon the appearance of high-frequency oscillations in the combustion chamber it is sometimes possible to stabilize engine operation by changing the accepted ratio L_k/D_k , making it larger or smaller.

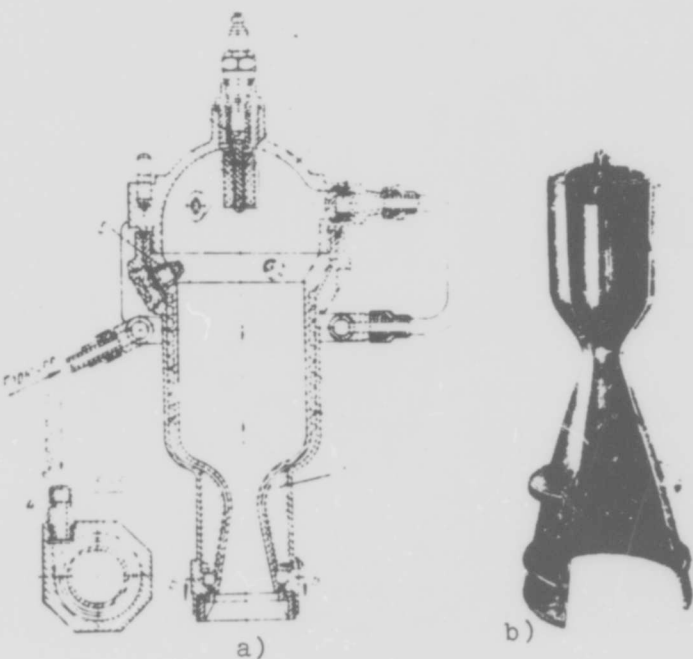


Fig. 5.2. Engines with cylindrical combustion chambers: a) ORM-65 (1936); b) RD-107 (1954-1957);
1 - inner shell of chamber; 2 - casing; 3 - insert; 4 - oxidizer supply connection; 5 - oxidizer injector; 6 - injector assembly; 7 - fuel injector; 8 - glow filament; 9 - igniter composition; 10 - igniter grain.

Examples of LPRE with cylindrical combustion chambers include the chambers ORM-65 of the engine, described in detail in [25], the RD-107 and RD-119 (see section 6.8), and also the can-type chamber of the RZ-2 engine (Figs. 5.2 and 5.3).

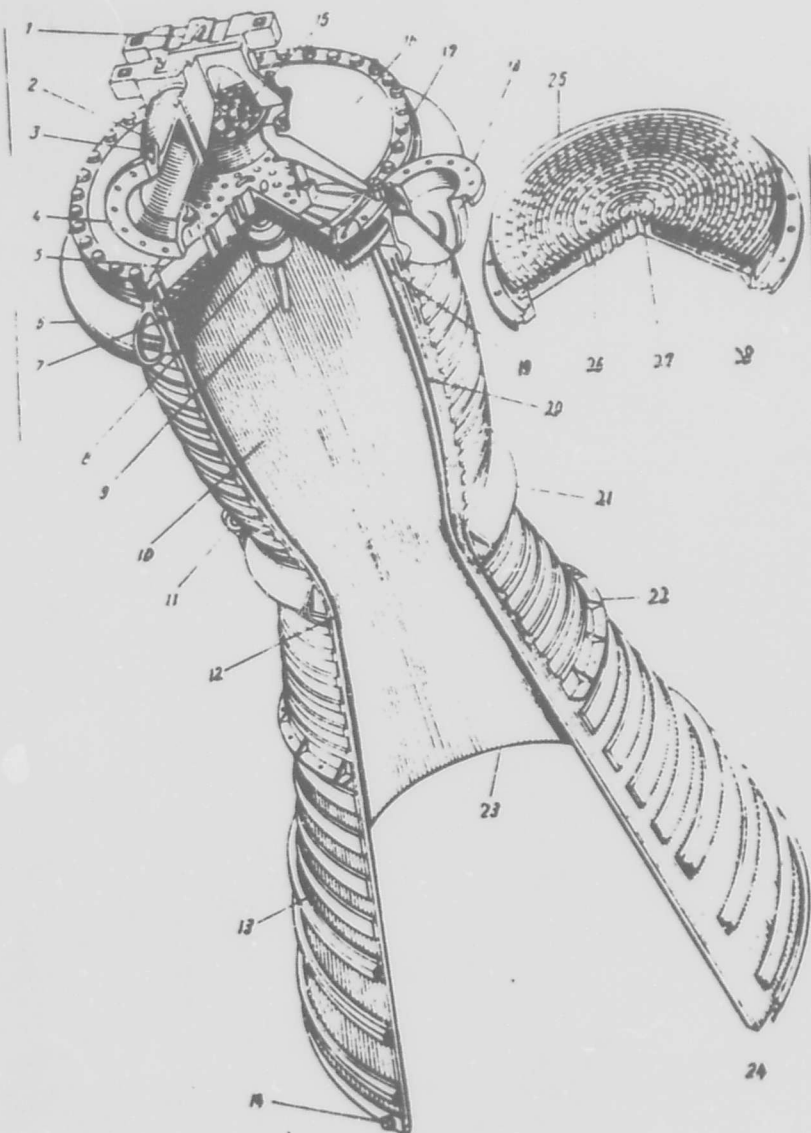


Fig. 5.3. Can-type engine chamber: 1 - cardan suspension; 2 - liquid O_2 supply; 3 - pressure measurement connection; 4 - flange; 5 - injector assembly; 6 - kerosene inlet manifold; 7 - sealing ring; 8 - squib; 9 - [ignition] cable; 10 - combustion chamber; 11 - ring for attachment of lever for thrust vector control; 12 - critical section; 13 - [reinforcing] bands; 14 - drain connection; 15 - honeycomb; 16 - injector assembly cover; 17 - starting fuel supply; 18 - flange; 19 - fuel inlet; 20 - tubes; 21 - power ring in critical section; 22 - flange for attachment of screen; 23 - nozzle exit section; 24 - fuel manifold; 25 - injector assembly housing; 26 - oxygen feed; 27 - starting fuel feed; 28 - fuel feed.

Can-Type Engine Chamber

Figure 5.3 shows the can-type chamber of the RZ-2 engine, operating on a liquid oxygen + kerosene propellant. The thrust of the engine on the ground is 62 T ($\sim 620\text{ kN}$); the specific thrust is $245\text{ kgf}\cdot\text{s/kg}$ ($24\cdot 10^2\text{ N}\cdot\text{s/kg}$); ratio $f_w/f_{w_0}=1.8$, i. e., the combustion chamber is high-speed; nozzle expansion ratio equals 8; pressure in combustion chamber is 38 [atm(abs.)] [3.73 N/m^2].

The chamber shell is made of 312 soldered nickel tubes. To increase the strength set of tubes is wrapped with reinforcing rings 13, which will form a solid conical casing on the combustion chamber section. Kerosene, cooling the wall of the chamber, is fed into inlet manifold 6 and enters the tubes through holes 19. Cooling is produced in "two passes" [regenerative]. The coolant passes along one tube into nozzle collector 24 and returns through the neighboring tube, after which it enters the injector face of injector assembly 5.

Liquid oxygen enters the injector assembly through angled pipe 2. From the injection assembly the oxygen and kerosene enter the combustion chamber, where the mixture is ignited by pyrotechnic igniter 8, which in turn is ignited by an electrical spark.

Spherical Combustion Chambers

An advantage of spherical and close-to-spherical pear-shaped combustion chambers is the smaller chamber surface for a given volume, which lowers its weight and facilitates cooling. Furthermore, the strength properties of a spherical chamber are higher than those of a cylindrical chamber.

The major deficiency of spherical chambers is their complexity of nozzles, which means it is sometimes necessary to make precombustion chambers in the chamber head; this further complicates the manufacturing process. Furthermore, relatively little room is left in spherical chambers for arrangement.

The indicated merits and deficiencies of spherical chambers lead to their preferential application in LPRE with high thrusts, where the dimensions of the combustion chambers are quite great, so that the gain in chamber weight becomes perceptible.

An example of a spherical chamber is the engine chamber of the A-4 rocket, operating on oxygen and 75% ethyl alcohol (Fig. 5.4). Engine thrust is 25 T (245 kN).

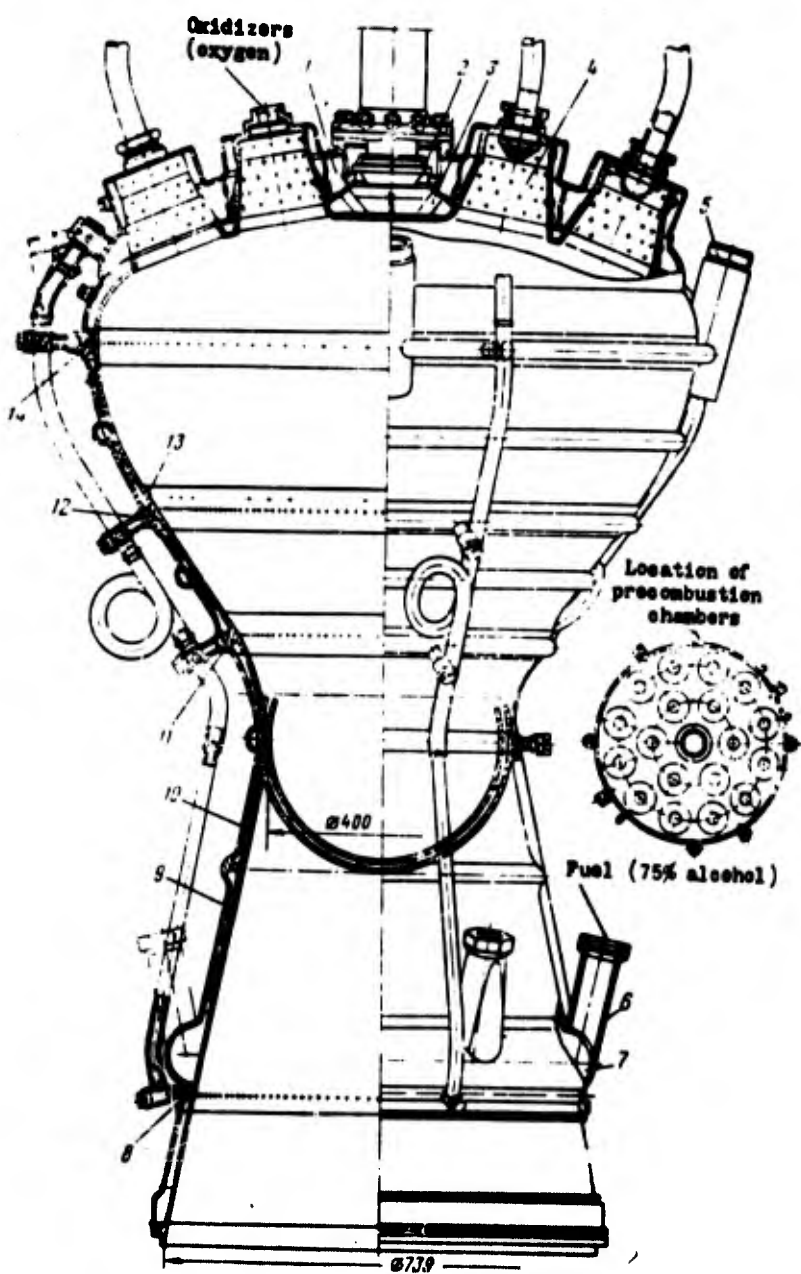


Fig. 5.4. Chamber of engine of A-4 rocket: 1 - upper annulus; 2 - main fuel valve; 3 - lower fuel annulus; 4 - precombustion chamber; 5 - stop for transmission of thrust to frame; 6 - fuel feed nozzle; 7 - manifold; 8 - lower internal cooling band; 9 - inner shell of chamber; 10 - outer shell of chamber; 11, 12 - internal cooling bands; 13 - additional internal cooling band; 14 - upper internal cooling band.

Conical Combustion Chambers

In conical combustion chambers (see Fig. 5.1d) in essence the entire chamber is the inlet part of the nozzle. Their P_{m} is reduced as compared to other types of chambers and due to this they are not used, presenting only historical interest.

The basic cause of the reduction in P_{m} is the high speeds of the combustion products in the chamber. Due to this the transformation of thermal energy into work of expansion is less than complete, i. e., large thermal drag losses occur. Furthermore, in conical chambers the zone of atomization and evaporation occupies a considerable part of the total volume; the zone of combustion is decreased, which leads to poor combustion or requires an increase in the total volume of the chamber.

Annular Combustion Chambers

The application of annular combustion chambers in LPRE stems from the use of nozzles with a center body and plates. Diagrams of annular combustion chambers with rectangular and round sections are shown in Figs. 5.1e and f and in 5.5.

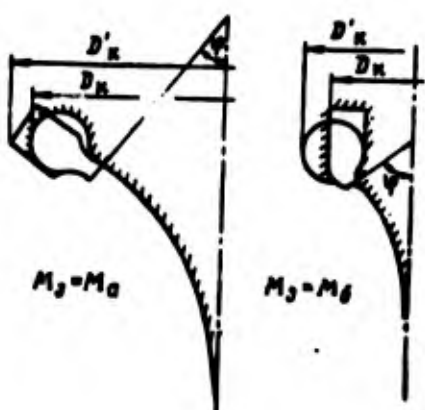


Fig. 5.5. Selection
of form of annular
combustion chamber,
 $M_a > M_b$.

It is advisable to use annular chambers with round sections during the acceleration of gas in a nozzle with a center body to high Mach. In connection with the necessity for a large turn of the flow, the angled of the slope of the surface of critical speed is reduced, so that application of a chamber with a rectangular section would lead to an increase in the dimension D_n of the chamber.

As compared to other types, annular combustion chambers have a number of deficiencies. Their surface is considerably greater, which leads to an increase in weight and hampers chamber cooling. The annular combustion chamber is complicated to manufacture, and to ensure its rigidity either special external stiffeners or cooled struts, connecting the external contour of chamber with the internal, are required. As merits of the annular combustion chamber we can point out the possibility of thrust vector adjustment and a decreased probability of appearance of vibration burning with division of chamber into a series of separate sections along the circumference.

Figures 2.26 and 2.32 show diagrams of engines with annular combustion chambers and center bodies.

5.2. Determining the Volume of the Combustion Chamber

It is accepted to consider the volume of the combustion chamber, V_n to be the volume of the chamber up to the critical section.

One of the following parameters is used for determination of the necessary volume V_n .

1. Conditional time of stay of fuel and combustion products in chamber $\tau_{y,n}$.
2. Reduced (or characteristic) length of combustion chamber l_n .
3. Volumetric thrust P_n .

We will examine the determination of combustion chamber volume by each of these parameters.

Determining Combustion Chamber Volume by Conditional Time of Stay

The conditional time of stay of fuel and combustion products in the chamber is determined by the expression (3.3)

$$\tau_{yes} = \frac{V_2}{Gp_2}$$

Substituting the value of v_2 from the equation of state, we obtain

$$\tau_{yes} = \frac{V_2 p_2}{GR_2 T_2}, \quad (5.5)$$

from which we obtain the calculation expression

$$V_2 = \frac{\tau_{yes} GR_2 T_2}{p_2}. \quad (5.6)$$

For chambers with constant area A , the ratio G/p_2 is practically constant. Examining equation (5.5) and disregarding influence of pressure on $R_2 T_2$, we see that for a given fuel in the first approximation (neglecting the influence of p_2 on processes of transformation) the quantity τ_{yes} does not depend on pressure p_2 (or on fuel consumption). The value of τ_{yes} depends on the type of propellant used and the quality of carburetion. For different fuels necessary value of τ_{yes} is determined experimentally and is within the limits

$$\tau_{yes} = 0.0015 \pm 0.005 \text{ s.}$$

At large pressures the values of τ_{yes} are closer to the lower limit. During selection of τ_{yes} it is necessary also to consider the circuit of the propulsion system. In propulsion systems with a closed circuit part of the fuel (or all of it with the circuit "Gas + Gas") is atomized and partially burns in gas generator prior to entry into the combustion chamber, while afterburning of fuel occurs in the chamber. Therefore for the engines of systems with closed circuits it is necessary to take τ_{yes} as 1.3-1.8 times less than in an engine with an open circuit.

Determining Combustion Chamber Volume by Reduced Length

The reduced (or characteristic) length of the combustion chamber is the name given the quantity

$$l_{sp} = \frac{V_1}{f_{sp}}, \quad (5.7)$$

from which the calculation formula has the form

$$V_1 = l_{sp} f_{sp} A^2, \quad (5.8)$$

or

$$V_1 = 10^4 l_{sp} f_{sp} A.$$

Values of l_{sp} depend on the type of propellant used and are determined experimentally. For different fuels propellants the quantity l_{sp} is within limits of 1000 to 5000 mm. Table 5.1 gives values of l_{sp} for certain propellants [4], [32].

Table 5.1. Values of l_{sp} for certain propellants for LPRE.

Fuel	$\frac{l_{sp}}{mm}$	Fuel	$\frac{l_{sp}}{mm}$
Nitric acid + aniline	1000—1300	Oxygen + kerosene	1000—1500
Nitric acid + kerosene	1250—1600	Oxygen + ethyl alcohol	1300—2700
Nitric acid + UDMH	1300	Nitromethane (single-component)	5000
Oxygen + hydrogen	500—1000	Fluorine + ammonia	1000—1500

It is not difficult to show that the reduced length l_{sp} and the conditional time of stay τ_{yes} are proportional parameters.

Actually, according to equation (1.9)

$$f_{sp} = \frac{M}{P_2} = \frac{\sqrt{R_2 T_1}}{A_e} \frac{a}{P_2}$$

Putting this value of t_{sp} in formula (5.7), we obtain

$$t_{sp} = \frac{V_p A_s}{\sqrt{R_2 T_2}} \quad (5.9)$$

Comparing equations (5.9) and (5.5), we obtain

$$t_{sp} = t_{yca} A_s \sqrt{R_2 T_2} \quad (5.10)$$

For a given propellant the product $A_s V_p T_2$ can be considered constant; consequently

$$t_{sp} = \text{const } t_{yca} \quad (5.11)$$

It is obvious that t_{sp} , like t_{yca} , depends little on the pressure in the combustion chamber. Knowing t_{sp} , we always can determine t_{yca} .

Thus, for example, if for oxygen + kerosene we take $t_{sp}=1250$ mm, then considering approximately $\alpha_n=1.13$, (i. e., $\alpha_n=1.98$), $FR_2 = 35 \text{ kgf}\cdot\text{m/kg} \times \text{deg}(343 \text{ J/kg}\cdot\text{deg})$ and $T_2=3550^\circ\text{K}$, we obtain the value of t_{yca} corresponding to the given t_{sp} .

$$t_{yca} = \frac{t_{sp}}{A_s \sqrt{R_2 T_2}} = \frac{1.25}{1.98 \sqrt{3.3550}} = 0.0018 \text{ s.}$$

Determining Combustion Chamber Volume by Volumetric Thrust

Sometimes chamber volume is determined by proceeding from the value of volumetric thrust P_v , i. e., the thrust of the LPRE referred to one liter of vclume of the combustion chamber:

$$P_v = \frac{P}{V_e} \text{ kgf/l (or N/l)} \quad (5.12)$$

whence

$$V_e = \frac{P}{P_v}$$

The volumetric thrust P_v does not reflect a basic factor determining combustion efficiency — the time available for flow of the combustion

process. Values of P_s depend on the pressure in the chamber and for current LPRE engines they vary in wide limits, from 100 to 10,000 kgf/l ($\approx 1-100$ kN/l).

In analyzing the above-considered parameters for determining combustion chamber volume — V_m , t_m and P_m — the following conclusions can be drawn. None of the parameters reflects the influence of chamber shape and the structure of the injection assembly on V_m , although such influence undoubtedly exists. The use of volumetric thrust as a parameter for determining V_m is possible only in the case when recommended values of P_s at a given pressure in the chamber are known. It is most expedient to use conditional time of stay or reduced length for determination of V_m .

It is necessary to note also that an increase in pressure and improvement of the organization of the processes of carburetion and combustion lead to a decrease in the necessary time of stay in combustion chamber, i. e., to decrease in the necessary t_m or l_m . Thus, with development of LPRE and an increase in the chamber pressure there is a tendency to decrease the volume of the combustion chamber.

5.3. Unstable Burning

In certain cases unstable (vibration) burning appears in LPRE chambers. There are oscillations of pressure, accompanied by oscillations of the temperature, composition, and velocity of the gas in the chamber. Oscillations of pressure can occur in wide range of amplitudes, from fractions of an atmosphere up to the magnitude of the average pressure in the chamber, with oscillation frequencies from tens to several thousand cycles per second.

Under unstable burning we understand not random and immediately damped oscillation (bursts) of pressure, but periodic oscillations with definite frequencies and amplitudes which, starting from one or another cause, are supported due to appearance of a regular self-oscillation process.

Usually two basic types of oscillations are distinguished:

Low-frequency oscillations, having frequencies from tens to several hundred cycles per second.

High-frequency oscillations with frequencies up to 10-12 thousand cycles per second. Figure 5.6 shows typical graphs of the change in pressure during low-frequency and high-frequency oscillations. The boundary between low-frequency and high-frequency oscillations can be established by comparing the period of oscillations T and time of stay in the combustion chamber τ . If $T \gg \tau$, the gases in the chamber oscillate as a single whole. Such oscillations relate to low-frequency. Thus, for example, at $\tau = 0.002$ s, oscillations with a frequency of $f < 500$ cps ($T > 0.002$ s) fall in the low-frequency group. If $T < \tau$, it is possible to trace the propagation of the wave over the chamber. Such oscillations are high-frequency. Sometimes oscillations with intermediate frequency are distinguished [107]; they appear due to oscillations of mixture ratio fed into the chamber.

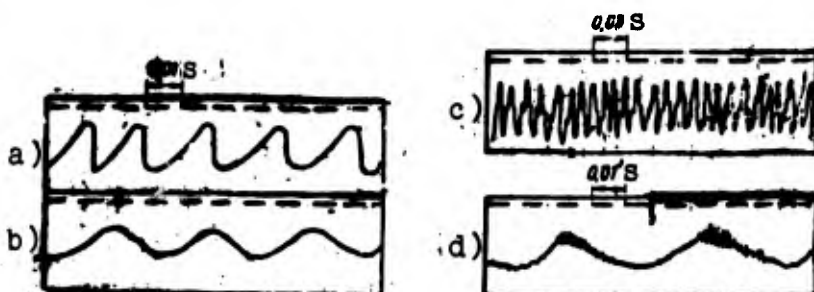


Fig. 5.6. Oscillations of pressure in chamber: a) b) low-frequency instability; c) high-frequency instability; d) superposition of low-frequency and high-frequency oscillations.

The appearance of combustion instability in LPRE is extremely undesirable. During low-frequency instability there can occur oscillations of pressure with amplitudes leading to destruction of the chamber, strong vibrations of the entire propulsion system, and a decrease in specific thrust. A basic consequence of high-frequency oscillations is intensification of heat exchange due to destruction (washout) of the boundary layer, leading to burnout of the chamber.

The processes occurring during unstable burning have as yet been insufficiently studied and are a subject for thorough theoretical and experimental investigation. Although a number of works exist in which a broad analysis is conducted of phenomena during unstable burning [105], [109], [4], [66], no general theory of unstable burning in LPRE has as yet been published.

Let us consider the basic phenomena during unstable burning.

Low-Frequency Instability

A characteristic criterion of low-frequency oscillations is an oscillation period which exceeds the time of stay, i. e., oscillations of pressure proceed immediately in the entire chamber volume. The causes of the appearance and maintaining of low-frequency oscillations are connected in the first place with presence of an ignition delay time and also with the dynamic characteristics of the elements of supply system. Thus, it is possible to present the mechanism of the appearance of instability as follows (Fig. 5.7).

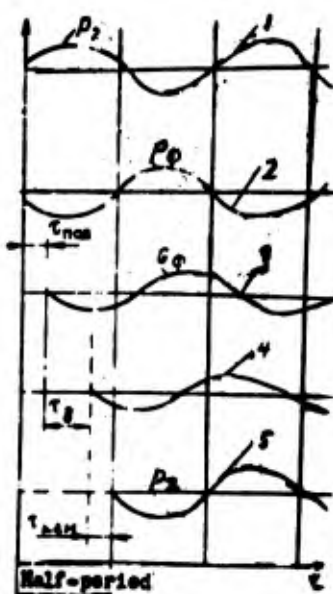


Fig. 5.7. Mechanism of appearance of low-frequency instability.

Let us assume that for some reason a random oscillation of pressure (curve 1) occurs in the combustion chamber. In the initial

moment with the increase in chamber pressure the drop Δp_4 on the injectors is correspondingly decreased (curve 2). However, the flow rate of the supplied components does not change immediately, since the supply system cannot react instantly to the change in Δp_4 . This requires a certain time τ_{REA} , during which fuel consumption will decrease in accordance with the decrease in Δp_4 . In other words, the change in supply with a change in pressure p_2 will occur with a delay for the time τ_{REA} (curve 3). Ignition of the propellant will lag additionally with respect to supply for the ignition delay time τ_i (curve 4). But since the combustion chamber has a definite capacity, the change in the quantity of burning fuel will be reflected as a change of pressure in chamber not at once, but with a delay by a certain time τ_{KAV} (curve 5).

Thus, change in pressure p_2 in the chamber at some moment after time $\tau_{\text{REA}} + \tau_i + \tau_{\text{KAV}}$ will appear in the form of an influence on pressure due to the change in the quantity of burning fuel. If the sum $\tau_{\text{REA}} + \tau_i + \tau_{\text{KAV}}$ is equal to the half-period of the pressure oscillation, the influence of the decrease in the quantity of burning fuel on p_2 will appear at exactly the moment when this pressure is least. This will lead to a new decrease in pressure, in consequence of which oscillations of pressure, once they appear, will be supported without damping.

Analogously, with a decrease in pressure the influence of an increase in the flow rate of components will be manifested at the greatest pressure in the chamber. Thus, due to the phase shift the pressure change and the influence of this change on pressure self-excitation of oscillations occurs in the chamber.

Oscillations of pressure in the chamber lead to oscillations of the feed and, consequently, also of propellant pressure in the supply system. That is, during low-frequency oscillations there will be oscillations in the entire propellant supply system.

In certain cases it is possible to have excitation of low-frequency oscillations only inside the chamber, with preservation of constant fuel feed. This is the so-called intrachamber low-frequency instability, appearing independently of the characteristics of the supply system. The cause of its appearance is oscillation of ignition delay time τ , due to oscillation of the values of the parameters (pressure, temperature, etc.) of gas in the chamber.

A theoretical analysis of low-frequency instability for different cases of its appearance is given in [105] and [4]. The experimental data given in these works agree quite well with theory and make it possible to establish the influence of certain parameters of LPRE operation on low-frequency instability.

The frequency and amplitude of oscillations depend first of all on the pressure in the chamber and on the type of propellant. An increase in pressure leads to an increase in oscillation frequency and to a decrease in amplitude. A considerable reduction of pressure can lead to a dangerous increase in amplitude. Hypercyclic fuels are characterized by an increase of frequencies and a decrease in the amplitude of oscillations; increasing the chamber volume leads to decreases in both frequency and amplitude of oscillations; an increase in the pressure drop on the injectors leads to a rise in frequency.

The component ratio ω has little effect on the frequency of oscillations. However, burning stability strongly depends on the value of ω . Figure 5.8 gives the results of experimental investigation of stability of operation of LPRE on $\text{HNO}_3 + \text{furfuryl alcohol}$ with a change of the excess oxidant ratio α and chamber pressure p_2 .

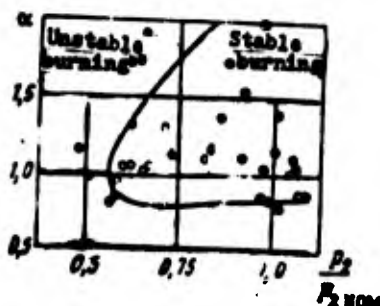


Fig. 5.8. Influence of α and pressure on stability of burning.
HOM = nominal

High-Frequency Instability

Besides low-frequency oscillations, it is also possible to see in the chamber of an LPRE the appearance of high-frequency oscillations with frequencies of order of several thousand Hz (in certain cases to 10-12 thousand Hz). Here the period of the oscillations is less than time of stay of combustion products in the chamber, so that it is possible to trace the propagation of the pressure wave over the chamber. Thus in contrast to low-frequency instability, during high-frequency instability oscillations of pressure appear locally and but not at once in the entire volume; this leads to heterogeneity of pressure (and other parameters) over the chamber volume at a given moment. High-frequency oscillations in the chamber have practically no effect on feed pressure and the flow rate of the components.

Depending upon conditions in the combustion chamber of an LPRE and on its geometry, excitation of two basic types of oscillations is possible: longitudinal and transverse. In turn, lateral oscillations are divided into tangential and radial.

During longitudinal oscillations the parameters of the gases in the chamber (pressure, temperature, etc.), vary along the axis of the chamber. Moreover, in section of the chamber perpendicular to the axis the parameters of the gas have identical values.

During lateral oscillations (tangential or radial) the change of the parameters occurs in a plane perpendicular the chamber axis; the parameters of the gas along every line parallel to the chamber axis remain constant.

Tangential oscillations can exist in two forms: in form of a standing wave, with which node surfaces are stationary, and in form of a rotating wave, in which the nodal surfaces rotate. Figure 5.9 gives diagrams of the different forms (modes) of oscillations [109]. The dotted lines show the line of equal values of pressures; the arrows indicate the direction of the pulsational motion of gas masses. On the left is shown the moment when the masses move to the right,

and on the right, after a half period. During longitudinal oscillations (see Fig. 5.9a) the gases move along the chamber axis, so that pulsational components are added with average speed. During tangential oscillations (see Fig. 5.9b), because the cross section of the chamber is a circle, the lines of equal pressures cease to be straight lines. During radial oscillations (see Fig. 5.9c) the axis of symmetry is the axis of the combustion chamber.

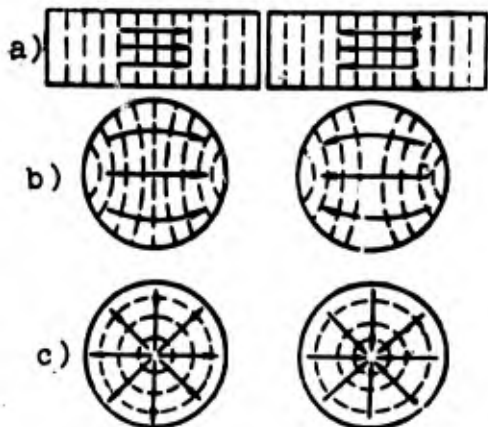


Fig. 5.9. Forms (modes) of high-frequency oscillations in LPRE chamber: a) longitudinal; b) tangential; c) radial; ---- line of equal pressures.

In the chamber of an LPRE oscillations are not always excited in the form of "pure" longitudinal or lateral oscillations. Frequently mixed (combined) oscillations occur; they constitute a combination of longitudinal and lateral oscillations or a combination of different forms (modes) of lateral oscillations. Furthermore, for every form (mode) of oscillations the appearance of first, second, etc., modes of oscillations is possible. Figure 5.10 shows different forms of lateral oscillations.

The theoretical analysis of high-frequency instability is very complicated. Although there are tens of works dedicated to analysis of the individual forms of high-frequency oscillations, in particular works [105], [109], [106], [107], and [108], the study of the mechanism of the appearance and maintaining of high-frequency oscillations is, at present, far from complete.

Experimental data show that high-frequency instability in LPRE chambers is affected by system of fuel injection systems, chamber

geometry, and the process of expansion in the nozzle. Different propellants possess different inclinations to the appearance of high-frequency oscillations. There are a number of empirically obtained recommendations on the struggle with high-frequency instability arrangement of various kinds of partitions in combustion chamber [112], etc.).

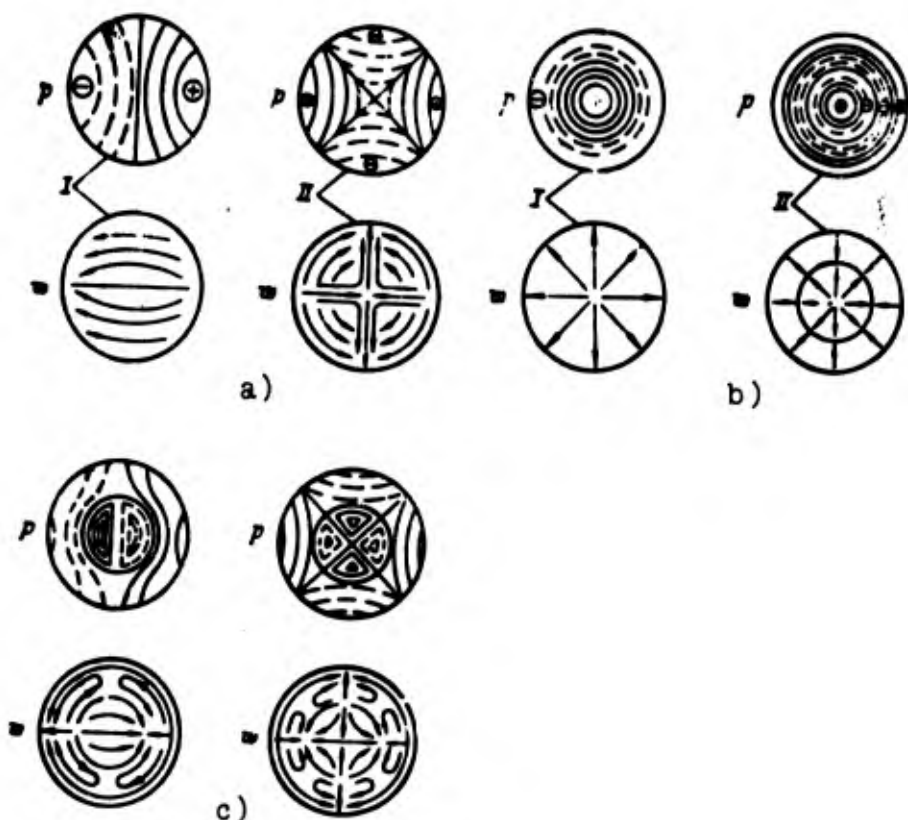


Fig. 5.10. Forms of lateral oscillations: a) purely tangential modes; b) purely radial modes; c) mixed modes.

5.4. Start and Shutdown of Engine

Start and shutdown of an engine are the most critical stages of its operation. The main requirement faced by systems for start and shutdown is reliability. To this, depending upon the intended function of the engine, there are added other requirements connected with the character and duration of start and shutdown processes.

Engine Start

Reliability of LPRE start requires, in the first place, guaranteed ignition of propellant with the minimum possible time of approach to regime. [Translator's note: Time required to achieve the nominal operating regime]. Reduction of the time of approach to regime permits decreasing the necessary reserve of fuel and consequently, decreasing the initial weight; this is especially important for space and ballistic rockets.

In certain cases, furthermore, there must be assurance of the possibility of multiple starting and starting of the engine in high-altitude conditions or under conditions of space flight. Specific requirements for start organization arise during starting of chambers of high-thrust engines.

Depending upon the character of the approach to regime it is possible to distinguish smooth, step, and "bang" [extremely rapid] starts.

In a smooth start ignition occurs with small fuel consumption and with subsequent comparatively smooth accretion of fuel consumption. Smooth starting is characteristic for small and average-thrust LPRE with turbopump supply systems. The smoothness of accretion of propellant consumption is ensured due to the inertia of the turbopump assembly [TNA]. The duration of start is determined basically by the time required for the turbopump assembly to reach the nominal regime ("spin-up of turbopump assembly").

Step start is characterized by the introduction of an intermediate (or preliminary) stage of LPRE operation and is sometimes advisable for starting high-thrust engines. The need to introduce an intermediate stage is caused by the fact that with growth of thrust and, consequently, also of the power of the turbopump assembly, the time expended on spin-up of the turbopump assembly (inertness of turbopump assembly) decreases. As a result the influence of turbopump assembly inertia on the pressure rise rate becomes insignificant, so that

starting must be cushioned by the introduction of an intermediate regime.

During starting of LPRE operating on nonhypergolic components, the introduction of a preliminary stage ensures heating of chamber and formation of a reliable flame.

"Bang" starting is a mode in which a full flow of propellant is supplied immediately. Bang starting is not applied in pure form, since it would cause very great overpressure in the chamber; therefore the supply system or the engine injection assembly are always equipped with devices which cushion the start. Starts close to the bang type are possible with the use of displacement supply systems.

Methods of ignition

Depending upon the propellant, the type of engine, and the operating conditions, methods of ignition can be divided into categories:
— chemical; — pyrotechnic; -- electrical.

Chemical ignition is self-ignition of appropriately selected propellant components. Such ignition always occurs in engine operation on hypergolic components. Multiple starting of the engine is possible.

Chemical ignition is also applied in engines operating on nonhypergolic components. In this case hypergolic components are first fed into the combustion chamber for starting; the basic components are introduced only after formation in the chamber of a powerful flame.

To ensure starting are when using nonhypergolic components, various additives to one of the components are also used; they lead to the formation of a hypergolic mixture (for example, addition to the fuel of triethyl aluminum, which ignites with oxygen).

Pyrotechnic ignition is ignition with the help of a special cartridge, which burns for several seconds and gives a high-temperature flame. The cartridge is either mounted in the head (as, for example, in the LPRE ORM-65 and in the engine RZ-3) or is introduced from the side of nozzle on a special holder. After ignition of the cartridge the liquid propellant is fed in, first at a small flow rate; then the propellant feed is increased to the nominal flow rate. The cartridges are usually ignited with help of an electrical glow filament.

Pyrotechnic ignition can be used in chambers of all thrusts for single-use and reusable single-start engines. In reusable LPRE (for example, aircraft LPRE) pyrotechnic ignition is unacceptable.

Electrical ignition is produced with help of electrical spark or flame plug and finds application in oxygen-hydrogen engines (for example, the RL-10), in aviation LPRE, in low-thrust engines and in experimental engines intended for bench tests.

A deficiency of this method is the comparatively small thermal power of the electrical spark plug. Therefore with application of electrical ignition the propellant is frequently ignited with a spark plug at a low flow rate in a precombustion chamber, creating a duty flame which ignites propellants at the basic flow rate. Furthermore, electrical ignition requires a source of electrical energy, which is not always available on the vehicle. Electrical ignition is convenient for use in reusable and multiple-start chambers.

For ignition of certain propellants (for example, hydrogen peroxide) it is possible to use catalytic surfaces, which promote the appearance of a reaction.

Pressure change in combustion chamber during starting

Important characteristics of starting are the rate of pressure buildup in the chamber during starting ($\frac{\Delta p}{\Delta t}$) and the magnitude of pressure excess (or peak), i. e., the value of the ratio of the greatest pressure in the chamber during starting to the nominal pressure.

The rate of pressure buildup and the pressure excess characterize the severity of starting. The greater are these values, the more severe is the start. On Fig. 5.11 gives typical graphs of the pressure change in the combustion chamber during starting. The starting proceeding in accordance with curve 3 is obviously the most severe.

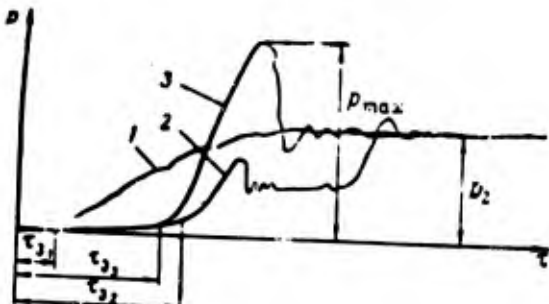


Fig. 5.11. Change of pressure in chamber during starting: 1 - smooth start; 2 - step start; 3 - severe start; τ_i - ignition delay time.

At high values of dp/dt and large overpressures there is danger of disruption and even explosion of the chamber, both due to its loss of strength and as a result of the appearance of detonation burning of the propellant.

The basic influence on severity of starting is rendered by the propellant ignition delay time, τ_i . Obviously, the greater the value of τ_i , the more propellant will be accumulated prior to the beginning of ignition and the greater will be the overpressure.

We will evaluate approximately the value of maximum overpressure P_{max} during starting.

The quantity of propellant entering the combustion chamber from the beginning of supply to the beginning of ignition equals

$$\int G(\tau) d\tau = G_{avg} \tau_i, \quad (5.13)$$

where G_{avg} - certain average starting flow rate;
 τ_i - ignition delay time.

If we assume that combustion occurs instantaneously at the moment of ignition, then in accordance with equation of state the maximum overpressure will be

$$P_{\max} = G_{\text{sys}} \tau_s \frac{RT}{V_s}, \quad (5.14)$$

where T and R - temperature of combustion and gas constant of combustion products during starting.

According to equation (5.5) during steady-state operation the pressure in the combustion chamber is

$$P_2 = G\tau_{\text{yes}} \frac{R_2 T_2}{V_s}. \quad (5.15)$$

Comparing equation (5.14) and (5.15) and considering the values of R and T during starting to be equal to the values R_2 and T_2 in the steady-state regime, we obtain

$$\frac{P_{\max}}{P_2} = \frac{G_{\text{sys}} \tau_s}{G\tau_{\text{yes}}}.$$
 (5.16)

This expression permits rough estimation of the highest possible excess pressure during starting.

In reality, since combustion is not instantaneous and, furthermore, the value of RT during starting is less than that of $R_2 T_2$

$$\frac{P_{\max}}{P_2} < \frac{G_{\text{sys}} \tau_s}{G\tau_{\text{yes}}}.$$
 (5.17)

During starts which are close to "bang" $G_{\text{sys}} = (1.5-2)G$, during a smooth start $G_{\text{sys}} \sim G$. Ignition delay time τ_s is usually a few times larger than τ_{yes} . Therefore it is τ_s which renders a decisive influence on the value of the maximum overpressure during starting.

For hypergolic propellants applied in LPRE τ_s is equal to the delay time of self-igniting and lies within the limits 0.01-0.03 s. For nonhypergolic propellants τ_s basically depends on the kind of propellant and the power of the igniting device and is approximately

on order smaller than for hypergolic fuels. In the general case the value of τ , and, consequently, the severity of starting are essentially affected also by a number of factors determined by the conditions of carrying out starting and by the construction of the LPRE.

Influence of conditions of engine starting

- a) Initial temperature of propellant. A change in the initial temperature leads to a change in the chemical activity and also of the physical properties of the propellant (viscosity, surface tension), affecting its mixing during injection with a decrease in initial temperature, τ is increased. Thus, for example, for a propellant consisting of nitric acid and a mixture of furfuryl alcohol with aniline, with a decrease in temperature from -10 to -30°C ignition delay time is increased from 0.015 to 0.040 s, i. e., more than doubled.
- b) Initial pressure in combustion chamber. The question of the influence of initial pressure in the chamber on ignition is very important during organization of engine starting in high-altitude conditions. Lowering of the pressure leads to an increase in τ , and, as a result to an increase in overpressure during starting. With a large decrease in pressure can, in general, certain hypergolic fuels lose the ability of self-ignition. Such conditions can, in particular, appear during starting of an engine in space, where the ambient pressure is equal to zero. Fortunately in such cases the propellant, upon entering a chamber with a pressure close to zero, turns out to be in overheated state. Very rapid sublimation of the propellant occurs and the pressure in the combustion chamber is increased by the vapors.
- c) Composition of Propellant. The value of τ is influenced both by a change in the propellant component ratio and by presence of various diluents or additives — sometimes unavoidable (for example, water) and sometimes specially introduced.

The least value of τ_s of a number of propellants does not correspond to the stoichiometric ratio.

Thus, for example, for nitric acid + 50% xylyidine and 50% furfuryl alcohol a change in τ_s occurs with a change in α as is shown on Fig. 5.12a, and the minimum value of τ_s corresponds to $\alpha = 1.1$ [9].

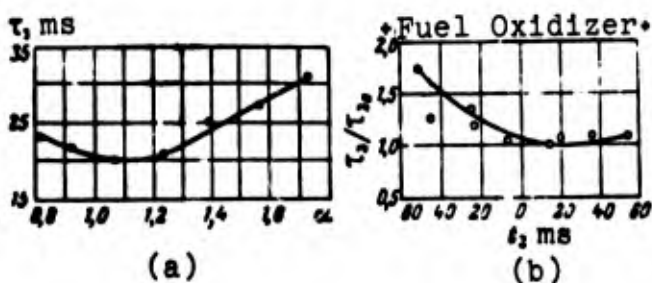


Fig. 5.12. Influence of propellant composition (a) and early injection on τ_s (b).

Analogous graphs can be obtained for other propellants. In every case a particular α will correspond to the least value of τ_s .

Varicous additives in the propellant can increase or decrease τ_s . Thus, for example, an increase in the content of water in nitric acid leads to a growth in τ_s .

d) Premature supply of one component. In LPRE it is difficult to ensure simultaneous supply of oxidizer and fuel; a delay of one of them can lead to an increase (and sometimes to a decrease) in τ_s . Thus, from the graph of the change in τ_s as a function of early supply t for nitric acid + furfuryl alcohol (Fig. 5.12b) it is clear that for this propellant early feeding of the oxidizer reduces τ_s , i. e., improves starting. The magnitude of rational advance in supplying one or the other component depends on the composition of the propellant and also on the structure of the injection assembly, so that for every propellant and injection assembly construction there is one most expedient order of supplying the components.

Sometimes during selection of the advance of supplying fuel or oxidizer the fact that a powerful flame is formed behind the engine nozzle during afterburning of fuel which was not burned in the chamber.

e) Other influences. Besides the indicated basic factors τ_0 and engine starting are affected also by the physical properties of the propellant, the pressure drop on injectors Δp_0 (increase in Δp_0 usually decreases τ_0), the form and volume of the chamber, the quantity of component supplied (an increase in the quantity of propellant supplied frequently leads to a decrease in τ_0), the number of restarts, etc.

Engine Shutdown

The requirements for LPRE shutdown sequence are determined by the engine's function. Shutdown is provided either by complete exhaustion components from the tanks or by shutting the propellant cutoff valves at a given moment (forced shutdown).

Engine operation to exhaustion of components is used on guided AA missiles, torpedoes, and (in certain cases) on the first stages of multistage rockets.

Forced shutdown of the engine is necessary on ballistic or space rockets, when the engine must cease operation at an assigned moment - for example, when the rocket achieves a certain speed. Frequently the engine is first shifted to a smaller thrust regime and then is completely shutoff. Cessation of propellant feed is accomplished with pneumatic hydraulic or pyrotechnic cutoff valves. An important criterion of the quality of forced engine shutdown is the value of the so-called aftereffect impulse.

5.5. Aftereffect Impulse

The aftereffect impulse J_a is the value of engine impulse from the moment of arrival of the valve shutoff command to full cessation of engine operation, i. e.

$$J_n = \int_0^{\tau} P d\tau, \quad (5.18)$$

where P — engine thrust;

τ — time from moment of arrival of cutoff valve cut command to full cessation of engine operation.

The presence of the aftereffect impulse strongly affects the accuracy of insertion of a spaceship into orbit or that of the flight of a rocket to the assigned target.

Total absence of the aftereffect impulse ($J_n=0$) would be ideal. In real conditions, however, a definite aftereffect impulse is inevitable; its value depends on a whole series of structural and operational parameters and yields reluctantly to exact calculation.

We will examine the basic factors on which the value of the aftereffect impulse depends.

Expressing thrust as thrust in vacuum, from expression (5.18) we obtain

$$J_n = \int_0^{\tau} P_{y_{n,n}} G d\tau - \int_0^{\tau} f_3 p_n d\tau. \quad (5.19)$$

Since engine shutdown is normally produced at high altitude, where pressure p_n is close to zero, the second components can be disregarded and we can consider that

$$J_n = \int_0^{\tau} P_{y_{n,n}} G d\tau. \quad (5.20)$$

Change in propellant consumption Δ during the time τ is determined, first, by law of covering of the cutoff valves and after they are shut, by the conditions of outflow of liquid and evaporated components from the cavities of the engine chamber and adjacent pipeline sections to the cutoff valve.

In the same time τ the specific thrust in vacuum is changed by impairment of β , both due to the drop in the quality of the combustion process with a decrease in the pressure in the combustion chamber and the change in the ratio of components v . It is necessary to emphasize that at constant β the pressure $P_{n,0}$ is also unchanged with a decrease in the flow rate G , since in vacuum specific thrust does not depend on propellant consumption.

Schematically the change of thrust in vacuum, $P_n = P_{n,0} \cdot G$ during time τ can be represented in the form of the graph shown in Fig. 5.13.

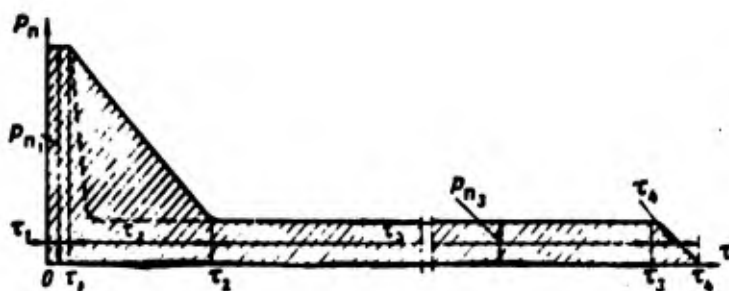


Fig. 5.13. Evaluating the aftereffect impulse.

Here the period of time τ , in accordance with essence of the processes determining thrust, can be simply presented in the form of the sum

$$\tau = \tau_1 + \tau_2 + \tau_3 + \tau_4 \quad (5.21)$$

Accordingly, the aftereffect impulse is also presented in the form of a sum

$$J_n = J_{n1} + J_{n2} + J_{n3} + J_{n4} \quad (5.22)$$

We will examine the components of time τ and estimate the corresponding components of the aftereffect impulse.

The τ [τ_1 ?] - chamber inertia time. During this time combustion chamber is still operating, due to the transformation of the liquid fuel available in the chamber at the moment of sending the command to close the valves. This fact is that at any moment engine operation

there is in the combustion a reserve of propellant equal to the product of the flow rate per second and the time of transformation (see section 3.1). Independently of whether or not shutting of the cutoff valves is started at this instant, the thrust of the engine during the further transformation of this reserve of propellant remains constant. Due to this, for a certain time τ_1 after the command to close the valves engine thrust P_m remains constant and equal to the engine thrust prior to the moment when engine shutdown began. Time τ_1 can be considered equal to the time of transformation, i. e., $\tau_1 = 0.003-0.008$ s.

The value of the aftereffect impulse during time τ_1 is equal to

$$J_{m1} = P_m \tau_1. \quad (5.23)$$

The quantity J_{m1} will be the smaller, the less the thrust of the propulsion system before engine shutdown. Therefore to decrease component J_{m1} and, as we will see below, all remaining components of total aftereffect impulse the engine must be shutdown in conditions the smallest possible thrust. For this step engine shutdown is used. Sometimes, to decrease the aftereffect impulse the main engine is cutoff first and the rocket is "brought up" to the assigned speed with help of the control engines which, having smaller thrust, have accordingly smaller values of aftereffect impulse.

The τ_2 - cutoff valve closing time. During this time the propellant flow rate drops from nominal to zero. Time τ_2 is determined by the type of cutoff valve and its construction. For pneumatic valves $\tau_2 = 0.1-0.3$ s; for pyrotechnic valves it is considerably less, comprising 0.001-0.005 s.

Although closing of the valve starts from moment of arrival of the cutoff signal, time τ_2 should be counted directly after time τ_1 , since the change in flow rate during covering of the valves will begin to affect engine thrust with displacement by the apparent time τ_1 of transformation, i. e., with displacement by the time τ_2 is equal to

$$J_m = \int P_{m,n} G_n d\tau \quad (5.24)$$

For determination of J_m by formula (5.24) it is necessary to know law of change in flow rate G over the time of shutting for the given construction of the valve.

The value of $P_{m,n}$ can be considered constant and equal to value of $P_{m,n}$ on the nominal operating regime (a certain change in $P_{m,n}$ due to of impairment of the combustion process in the chamber is ignored).

During cutoff of propellant feed by a pyrotechnic valve the thrust drops considerably faster (dotted line on Fig. 5.13). Accordingly, the aftereffect impulse J_m will clearly be less with application of pyrotechnic valves.

The τ_3 - time of chamber operation due to entry of components remaining in cavities after shutting of valves. After the valves are closed propellant components remain in cavities of pipelines and in the engine chamber in the sections from the cutoff valves to the injectors (chamber manifolds, coolant tract, cavities of injection assembly, etc.). Since the external pressure is close to zero, the pressure in the cavities also drops to values at which boiling of the components begins. As a result in the cavities a pressure is established which is equal to the pressure of saturated vapors of the component at its temperature. Under the action of the pressure of the saturated vapors, and also due to the pressure of the liquid column and the action of forces of acceleration, liquid or evaporated components (depending upon location of the component with respect to the nozzles) begin to flow into the combustion chamber. Arriving in the chamber, the components burn and the outflow of the combustion products gives thrust P_m .

The value of τ_3 depending upon the physical properties of the propellant components, their temperature, and the volume of the cavities, varies in wide limits - from several to tens of seconds.

The component of the aftereffect impulse (Fig. 5.14) after that time is

$$J_{\text{ss}} = \int_{t_0}^{\infty} P_{y_{A,\text{ss}}} G_s dt. \quad (5.25)$$

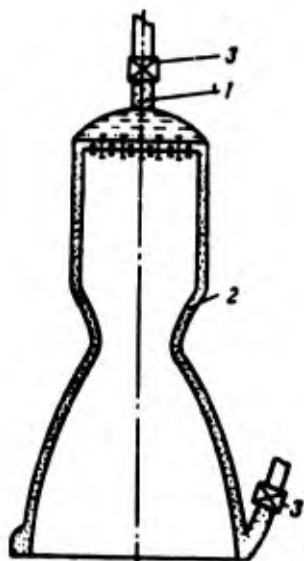


Fig. 5.14. At the appearance of components of aftereffect impulse
 J_{ss} : 1 - oxidizer vapor; 2 - fuel vapor; 3 - cutoff valve.

In the first approximation of the insignificant pressure of the column of the liquid component and the action of forces of inertia on the flow rate can be disregarded and we can consider that during time t_s , the flow rate through the injectors is determined only by the value of the pressure of the saturated vapors. The pressure of the saturated vapors depends on the temperature of the components and during time t_s it can be considered to be constant. Thus and the flow rate of components through the injectors will be constant.

Specific thrust in vacuum $P_{y_{A,\text{ss}}}$ depends on the component ratio and the quality of the process in the combustion chamber; with a constant ratio of flow rates of the components it also can be considered a constant quantity. Then

$$J_{\text{ss}} = P_{y_{A,\text{ss}}} G_s t_s = P_{\text{ss}} t_s. \quad (5.26)$$

The value of J_{ss} can be reduced, first, by decreasing the total quantity of fuel remaining in the cavities, i. e., by decreasing the volume of the cavities. For this it is necessary to locate the cutoff valves as close as possible to the engine chamber. If for some reason (strength, technological, etc.) open volumes are left in the injector assembly or coolant passage and their reduction will not influence on the quality of flow of the process, it is desirable to reduce these volumes by filling them with some light material.

To decrease J_{ss} by approximately two times it is possible also to use drainage of cavities; the drainage holes in the cavities are opened simultaneously with shutting of the cutoff valves. It is also possible to blow out the cavities with a gas which is inert with respect to the components.

The τ_4 - time of outflow of the last portion of propellant from the combustion chamber. During this time engine thrust drops from P_{ss} to zero. Since due to boiling of propellant in the cavities the last portion will enter in the gaseous state, time τ_4 can be taken as equal to the conditional time of stay τ_{gca} , or 0.0015-0.005.s.

The component of aftereffect impulse during time τ_4 is

$$J_{\text{ss}} = \int_{\tau_0}^{\tau_4} P_{\text{gca}} G_4 d\tau. \quad (5.27)$$

Assuming that during the time τ_4 thrust drops on a straight line, we obtain approximately

$$J_{\text{ss}} = \frac{1}{2} P_{\text{ss}} \tau_4. \quad (5.28)$$

Since P_{ss} and τ_4 are comparatively small, the value of J_{ss} is considerably less than the remaining components of the aftereffect impulse and its calculation during practical calculation of the total aftereffect impulse quickly becomes academic.

We will present a comparative appraisal of the components of the aftereffect impulse. J_m and J_{m2} are small due to small time of action of τ_1 and τ_2 . With use of pyrotechnic valves, due to their very brief operating time τ_2 the quality J_{m2} is also insignificant; now the main component of the total aftereffect impulse is J_m — the aftereffect impulse appearing due to operation of the engine chamber on the components remaining in the cavities after shutting of the cutoff valves.

With pneumatic cutoff valves, due to the comparatively great time τ_2 required for them to close the value of J_{m2} becomes comparable with that of J_m ; this leads to an increase in the total aftereffect impulse.

The magnitude of the total aftereffect impulse can be reduced by using all the factors which promote a decrease of its components, namely:

1. Turning off the propulsion system in the smallest possible thrust regime. This leads to a decrease of all components of the aftereffect impulse.
2. Application of pyrotechnic cutoff valves, which have a small closing time τ_2 .
3. Decreasing the volume of cavities on the section from the cutoff valve to the injectors.
4. Opening drains of cavities after cutoff of the supply of components.
5. Venting out the chamber and the cavities.

5.6. Engine Chamber Strength Calculation

An engine chamber can be destroyed by two causes: insufficient strength and loss of form. In the first case destruction will occur due to appearance in elements of the shell of stresses which exceed

the tensile strength of the material; this can occur as the result of insufficient total carrying capacity or insufficient strength of individual elements of the chamber (fastenings, shells, etc.). In second case sagging of shells leads to an increase of the section of the coolant passage and disturbance of the cooling regime. As a result the conditions of cooling are impaired, [4.1], the temperature of the inner shell rises, and this in turn leads to a further increase in sag and to impairment of cooling. Finally, the temperature of the gas wall is increased to the melting point and the chamber is destroyed by burnout of the shell. Practice shows that with few connections the chamber usually becomes disabled prior to the appearance of destructive forces in elements of shell and burnout due to great sag of the shells. Thus the second cause of chamber destruction is characteristic for LPRE whose chambers have widely separated fastenings. With frequently [spaced] connections the cause of destruction is loss of overall carrying capacity by the chamber or insufficient strength of its individual elements.

Special Features of Operating Conditions and Strength Calculation of LPRE Chambers

The specific character of strength calculations LPRE chambers emanates from peculiarities of the structural forms of the engine chamber and its operating conditions.

The first feature consists in the fact that usually the engine chamber is a double-walled shell, fastened by connections, and is subject to force and temperature influences.

Schematically the methods of fastening double-walled shells can be divided into three basic types (Fig. 5.15): longitudinal, helical, and point. The type of fastening is of essential significance during calculations of the shell for local sags. During calculations of the total carrying capacity it does not play an essential role.

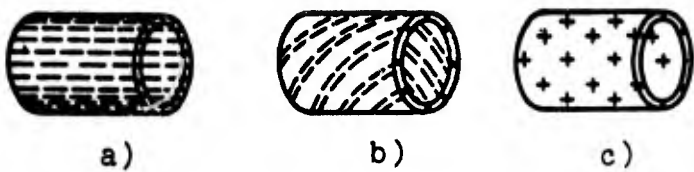


Fig. 5.15. Types of fastenings of double-walled shells: a) longitudinal; b) helical; c) point.

During operation of the LPRE the temperatures of the external and inner shells are different and vary both along the shell and through its thickness. Figure 4.1 shows a typical graph of the change in temperature through the thickness of the external and inner shells of a chamber, from which it is clear that the inner shell works in the most severe temperature conditions. Its average temperature is much higher than that of the external shell and, furthermore, the temperature varies considerably through its thickness (it varies the more, the greater the heat flow q through the wall and the smaller the thermal conductivity of the wall).

With such operational temperature conditions large temperature stresses appear in the walls and the mechanical properties of the material are worsened. In view of this during strength calculations of an LPRE chamber it is necessary to consider temperature and its nonuniformity through the thickness of the inner shell, as well as the change in the mechanical properties of the material with an increase in temperature.

The second feature consists in the fact that the difference Δp between the pressure in the coolant passage p_{cool} and the static pressure in the chamber p_s , and also the temperature of the internal wall t_{cp} vary along the length of the engine chamber (Fig. 5.16).

From consideration of the change in Δp and t_{cp} it is clear that from the point of view of the strength of the inner shell, the following of its sections are subject to the most difficult working conditions: in the combustion chamber, where pressure p_s is greatest; at the nozzle exit section, where the pressure difference Δp is greatest; and the sections near the critical section, where due to the high temperature of the wall the strength properties of the metal are poorest.

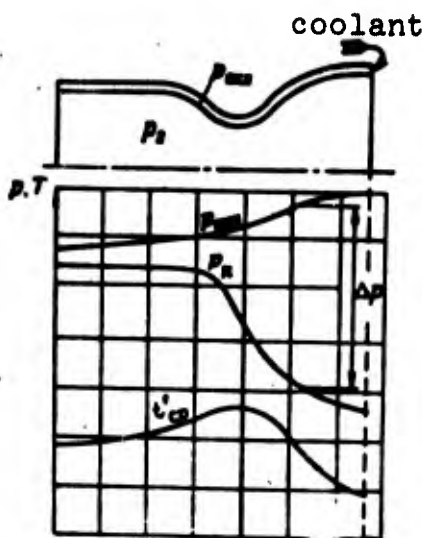


Fig. 5. 16. Distribution of pressures and means temperature of the inner shell over the length of the chamber.

Due to this the strength calculations of the inner shell must be conducted, at a minimum, for two sections: the section of the greatest difference of pressures Δp and the section with the highest temperature of the inner shell.

The third feature of conditions of operation and strength calculation of the engine chamber lies in the fact that calculation in terms of permissible stresses is not always acceptable. The fact is that temperature stresses alone in the walls of the chamber can significantly exceed the limit of elasticity, so that the material of the engine chamber operates in the region of plastic deformations under the simultaneous effect of force and temperature influences.

In carrying out strength calculations in the plastic region of operation for highly plastic materials (such as the materials utilized for LPRE chambers), judging the degree of reliability of operation of the structure by the value of the stresses which appear is very difficult, since in this region small changes of stresses correspond to large deformations, while the actual stresses still do not attain ultimate strength. However, as mentioned above, these deformations can be sufficient to lead to disturbance of the engine operating conditions and, as a result, to its burnout. Therefore as the basic criterion of suitability of an LPRE chamber it is advisable to take

not the magnitude of appearing stresses, but the magnitude of the deformations of both the shell as a whole and of its individual elements.

Finally, the fourth feature is the fact that strength calculations of an LPRE chamber have the character of control calculations.

All the basic dimensions of the shells, the methods of fastening, and also load on shell and its temperature of are determined in the first place by the conditions of reliability of the cooling system and ensuring the assigned thrust of the engine; only after this are conditions of strength determining.

If some elements of chamber do not satisfy the conditions for strength, we cannot change their dimensions without the introduction of essential corrections in the cooling or thermal calculation of the chamber. Thus, for example, we cannot increase the thickness of the wall of the inner shell, since this will cause a sharp change in the cooling conditions.

Sequence of Strength Calculation of LPRE Chamber

Proceeding from the above-stated peculiarities of the conditions of operation and strength calculations of an LPRE chamber, the following procedure for carrying out strength calculations of an LPRE chamber is presented as the most expedient.

First to be calculated is the total carrying capacity of the fastened shell of the engine chamber. The shell of the chamber is examined as a compound thin-walled vessel subjected to the influence of the pressure in the chamber.

After this local sags of the inner shell in the combustion chamber, in the critical section and at the nozzle exit section are determined by calculation. Local sags must not ready a value at which the regime of cooling the chamber is disturbed and burnout of the wall becomes possible. If the shell fastenings are widely spaced,

instead of calculation for local sags it is necessary to conduct calculation of the inner shell for stability.

Calculation for local sags, like calculation of fastenings, should be conducted under two conditions of load: operating conditions, where the high temperature of the walls causes impairment of the strength properties of their material, and in conditions of hydraulic pressurization used during technological tests. Regimes close to that of hydraulic pressurization, when the pressure drop Δp is greatest, can appear also during engine operation at the time of starting, when pressure in combustion chamber has not yet been raised, the wall is still cold, and high pressure has already been created in the coolant passage.

With very closely spaced fastenings calculation for local sags loses its meaning, since in this case a sag of the inner shell so great that it leads to disturbance of the cooling regime is impossible.

The thickness of the inner shell in this case is small and therefore its influence on the general strength properties of the chamber is insignificant. The main load is carried by the external shell and therefore in the first approximation the strength properties of the engine chamber shell can be estimated by proceeding from the calculation of its external shell alone. It is calculated by the usual methods as a thin-walled shell, taking into account the change in the strength properties of the material at raised temperatures, which can reach $300\text{--}400^{\circ}\text{C}$.

Then strength calculations are carried out for the injector assembly, its attachment and bracing to the combustion chamber, fastenings, etc. If the injectors are attached by brazing, the face is calculated as a double-walled system with fastenings (injectors). If, however, the injectors are rolled in, the goal of the calculation is to determine the conditions leading to disturbance of the impermeability of the injector attachment.

The procedure for strength calculations of LPRE is examined in detail in works [111], [104], and [103].

5.7. Additional Remarks

Inasmuch as the LPRE is the engine of a flight vehicle, it must ensure the greatest possible specific thrust for a given propellant with the smallest possible mass of the engine itself.

For a satisfactorily designed engine the losses of specific thrust in the design operating conditions comprise 3-5%, which corresponds to a specific thrust coefficient $\varphi=0.95-0.97$.

The specific weight (ratio of mass of installation to thrust) of a single-action propulsion system without tanks is a quantity on the order of 7-10 kg/T. For low-thrust propulsion systems and also for units designed to meet special requirements (repeated start and stop, profound control, etc.), the specific weight exceeds these limits and can reach 30-50 kg/T. For high-thrust propulsion systems value of specific weight approaches the lower limits (7-10 kg/T) [24].

The specific weight of the engine chamber makes up approximately one third of the specific weight of the installation without tanks.

High values of the specific thrust coefficient with small specific weight are attained by rational design of all elements of the engine chamber. Here it is frequently necessary to solve the problem of simultaneous satisfaction of incompatible requirements. Thus, for example, a shaped nozzle with smallest losses is unable to meet requirements with respect to mass and cannot be fitted into the allowed dimensions of the installation; application of a spherical chamber having the least cooling surface and mass may cause unjustified technological difficulties; and so on.

It is impossible to give universal recommendations for solution of such problems. In every particular case it is necessary to find the optimum solution, depending upon the set of concrete conditions with respect to specific thrust, dimensions, mass, unit reliability, etc.

We will give certain additional considerations concerning the selection of materials and also the designing of separate elements of the engine.

Selection of material. The material of the engine chamber should as durable as possible, light, and should possess good plastic properties. For material of the inner shell a combination of high thermal conductivity and satisfactory strength properties at high temperatures is desirable; however, as a rule, heat-resistant alloys have poor thermal conductivity. For the outer shell thermal conductivity is not of great significance and therefore the main requirement here for the material is high strength and the lowest possible density. In certain cases, with highly heat-conducting fastenings, the temperature of the external shell can attain $300-400^{\circ}\text{C}$ and then the material should possess sufficiently good heat resistance.

Furthermore, depending upon type of construction and the applied components, the material should satisfy the conditions of weldability and acid-resistance and should be noncatalytic.

Application of adapter to nozzle. In contemporary engines with great maximum-power altitudes of nozzle unit adapters are sometimes applied. Such adapters increase the expansion ratio of the nozzle, which increases specific thrust correspondingly. Thus, for example, in the AJ10-104 engine the application of the adapter increases the ratio from 20 to 40. The convenience of the adapter consists in the fact that ground tests and finishing of the engine are produced without it. Adapters are usually prepared from heat-resistant alloys based on titanium or niobium and do not have special systems of regenerative cooling. Ablative or radiation cooling is often used for cooling of adapters.

The basic difficulties in application of adapters consist, first, in their low rigidity. To ensure sufficient rigidity special stiffeners are made on the external surface. There are proposals to use as adapters very thin-walled shells, a section of which is shown on Fig. 4.26d. The equivalent thickness of these materials (sometimes called "space" materials) comprises 0.4-0.5 mm. [33].

Definite difficulties in the use of adapters are connected with attachment of the adapter to the main chamber, and also with necessity of thorough organization of the near-wall layer to avoid the formation at the walls of the adapter of high-temperature "tongues" of combustion products, which sharply disturb the conditions of cooling it.

Single-chamber and multichamber [cluster] propulsion systems.

For the same thrust a single-chamber high-thrust engine requires more finishing time than a multichamber cluster engine. There is also an increased probability of appearance of high-frequency oscillations. Furthermore, the cluster engine has smaller dimensions in terms of height and fills the motor section volume better. The mass of the cluster is comparable with the mass of the single-chamber engine.

However, an increase in the number of chambers leads to an increase in the quantity of different units supporting the operation of the engine, this lowers the reliability of the system. With application of propulsion systems with closed loops (see Chap. VIII), an increase in the number of chambers can strongly hamper the supply of high-temperature combustion products from the turbine of the turbopump assembly to the combustion chamber.

C H A P T E R VI

PROPULSION SYSTEMS

The propulsion system consists of the engine chamber and the feeding system. In turn, the feeding system can be divided into three main parts.

1. Unit for creating component feed pressure.
2. System of units and pipelines to ensure starting, stopping, and operation of the engine. In general, such a system will be a hydro-, pyro-, pneumatic electrosystem. In each particular case in a system the pneumatic, electrical, or pyrotechnic part can be absent.
3. Tanks. (With a turbopump feed system, the tanks frequently are not shown on the diagram of a propulsion system although they are a component part of the propulsion system).

6.1. Feed Systems

Depending upon its purpose a liquid fuel rocket engine [ZhRD] is presented with different requirements in respect to value of thrust, duration and conditions of operation. This leads to a great variety of applied methods of feed of components and propulsion system plans on the whole. At present it is possible to cite several tens of types of propulsion systems, distinguished in plant circuit, fuel, method of its supply, construction of basic units (chamber, nozzle, turbopump assembly[TNA]), etc.

One of the important elements characterizing the propulsion system on the whole is the feed system.

According to the type of unit creating feed pressure, they are classed as turbopump and pressure feed systems.

The most widely used in a ZhRD are turbopump systems ensuring supply of components in a wide range of pressures and flow rates. An elementary diagram of a turbopump feed system is presented in Fig. 6.1.

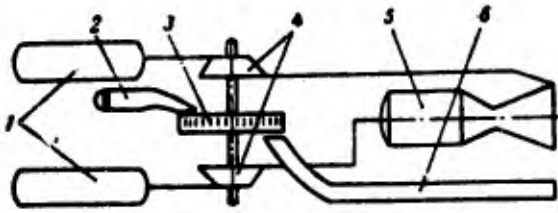


Fig. 6.1. Elementary dia-gram of a system with a turbopump assembly. 1 - tanks; 2 - gas generator; 3 - turbine; 4 - pumps; 5 - engine chamber; 6 - exhaust duct.

Components from tanks 1 proceed to pumps 4 and move into combustion chamber 5. The main element of the feed system is the TNA, by means of which there is created the necessary feed pressure of components and the prescribed flow rate is ensured.

Depending on the further use of the working substance coming from the turbine of the TNA, propulsion systems with a TNA are classed as working on open and on closed circuit. In systems working on open circuit, the working substance from the TNA through exhaust ducts 6 is ejected into the atmosphere. With an enclosed circuit (sometimes such circuits are also called closed or circuits with afterburning) working in a turbine, the working substance enters the combustion chamber (afterburning), where it is burned and used to create thrust (see. Chap. VIII).

Recently the possibility has been investigated of using gas jet pumps for feed of components in a ZhRD [13].

Less widely used are pressurized feeding systems, in which the components are displaced from the tanks by means of a high-pressure gas container.

Pressurized feeding systems are divided according to type of high-pressure gas container into gas-pressure feed systems and systems with solid propellant (PAD) pressure accumulator or liquid propellant (ZhAD) pressure accumulator (see section 9.6). Elementary diagrams of pressurized feeding systems are shown in Figs. 9.2, 9.23 and 9.29.

The basic advantage of turbopump systems consists in the fact that the fuel tanks are not under feed pressure of components. This permits making large volume fuel tanks with comparatively small mass. A disadvantage of turbopump systems consists in the relative complexity of the TNA.

Pressurized feeding systems on the whole are simpler, however their main disadvantage consists in the fact that the fuel tanks are under feed pressure of components. Due to this the required thickness of walls of the tank and their mass grows, which is expressed in decisive form on the mass of the whole propulsion system both with increase in time of operation of ZhRD (i. e., volume of tanks) and also with increase in required feed pressure. Therefore a propulsion system with a pressurized feeding system can successfully compete with a system having a turbopump system of supply only with small general pulse of the system P_T (i. e., with small volume fuel tanks) and with low pressures in the chamber (i. e., with low feed pressures).

In Fig. 6.2 there are shown regions of rational use of turbopump and gas-pressurized systems of feeding by cold gas depending upon thrust and duration of operation of the engine (analysis of operation of propulsion systems with a pressurized feeding system is provided in Chap. IX).

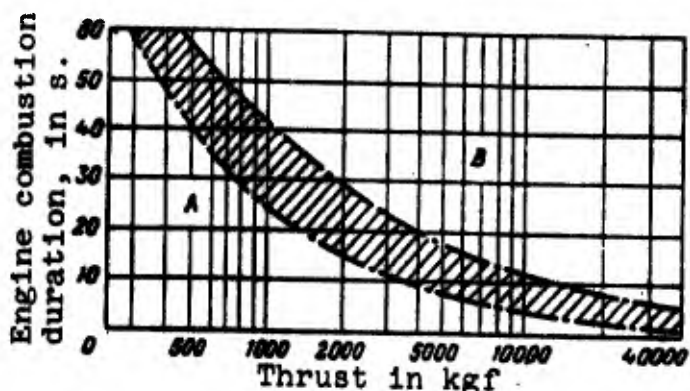


Fig. 6.2. Regions of use of pump and pressurized feeding systems. A - Pressurized feeding. B - TNA feeding.

6.2. Propulsion Systems with a Turbopump Feeding System

Basic Methods of Producing the Working Substance for a Turbopump Assembly

One of the basic criteria determining the distinction in turbopump feed systems is the method of producing the working substance for the drive of the TNA. According to this criterion turbopump feed systems can be divided into:

- a) systems with liquid gas generator (ZhGG), in which the working substance will be formed as a result of combustion of a fuel and an oxidizer;
- b) systems with steam and gas generator (PGG), in which the working substance will be formed as a result of decomposition of components (hydrogen peroxide, isopropyl nitrate, assymetric dimethylhydrazine [NDMG], etc.);
- c) systems with drive of turbine by vapor forming in the coolant passage;
- d) systems with drive of turbine by hot gases removed from the combustion chamber;
- e) systems with drive of turbine by products of powder combustion.

The most widely used are systems with ZhGG and PGG.

Liquid gas generators usually work on the basic components of a ZhRD and therefore their chief merit is the absence of necessity of placing a third component on board the rocket.

The components in a ZhGG are usually fed by the same basic pumps which feed the components into the chamber of a ZhRD (Fig. 6.3). However in so doing the necessity arises for a special device for spin-up of the TNA during starting.

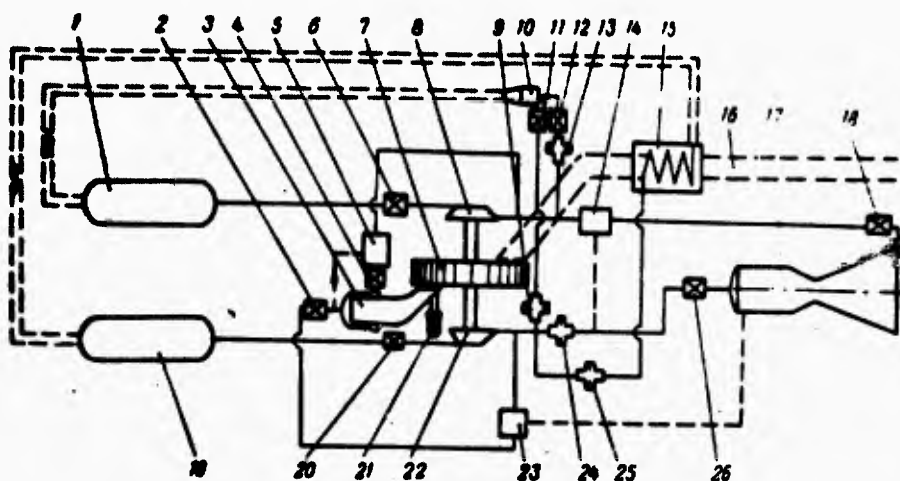


Fig. 6.3. Generalized diagram of a feed system with ZhGG. 1 - fuel tank; 2, 4 - ZhGG cutoff valves; 3 - ZhGG; 5 - regulator of equivalence ratio in ZhGG; 6, 18, 20, 26 - cutoff valves; 7 - turbine; 8 - fuel pump; 9, 13, 24, 25 - throttles; 10 - ZhGG fuel pressurization tank; 11, 12 - cutoff valves of ZhGG pressurization; 14 - regulator of equivalence; 15 - evaporator; 16 - exhaust duct; 17 - combustion chamber; 19 - oxidizer tank; 21 - starting PAD; 22 - oxidizer pump; 23 - regulator of pressure in the chamber
 — liquid, - - - pressure, = == gas.

Systems with PGG (Fig. 6.4) are very reliable in operation. Furthermore, in using PGG, working, for example on products of decomposition of hydrogen peroxide, the problem of starting the whole system is simplified. However, a great disadvantage of such a system is the necessity to have on board the rocket a third component for feeding the PGG, since, as a rule, the basic components of a ZhRD are impracticable to decompose in the PGG. This leads to requirement for additional capacity and a separate system of units and main lines

for servicing the capacities and supply of working substance in the PGG, which complicates the propulsion system and hampers its utilization. Due to this deficiency, steam gas generators are being displaced by ZhGG working on the same components as the TNA.

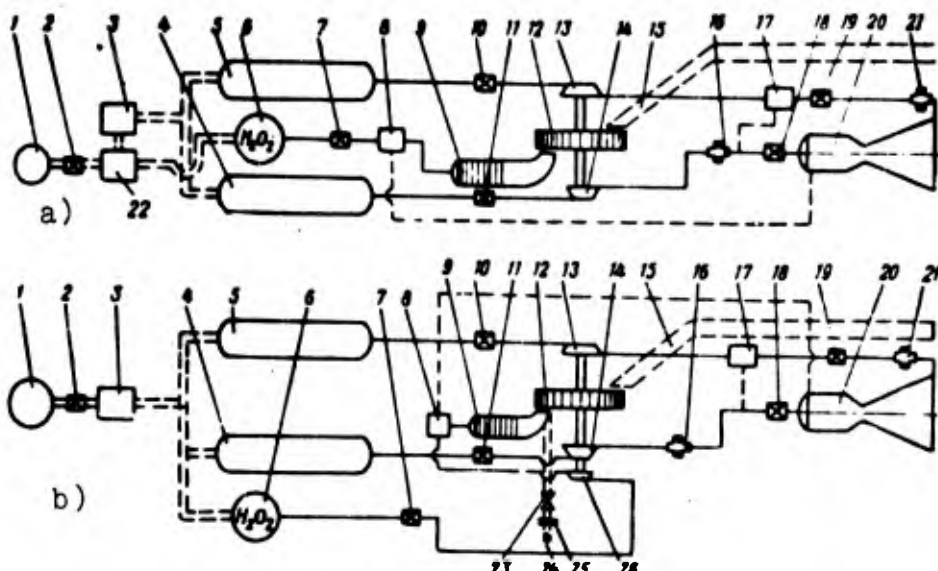


Fig. 6.4. Generalized diagrams of feed systems with PGG. a) pressurized feed of peroxide. b) pump feed of peroxide. 1 - air (or gas) pressure accumulator; 2 - cutoff valve; 3 - pressurization reduction valve; 4 - tank of oxidizer; 5 - tank of fuel; 6 - tank of peroxide; 7 - peroxide cutoff valve; 8 - regulator of pressure in the chamber; 9 - PGG; 10, 11, 18, 19 - cutoff valves; 12 - turbine; 13 - fuel pump; 14 - oxidizer pump; 15 - exhaust duct; 16, 21 - throttles; 17 - regulator of equivalence; 20 - chamber; 22 - feed reduction valve; 23 - relief valve; 24 - gas from ground starting system; 25 - joint; 26 - peroxide pump.

Driving the turbine of the TNA by the vapors of one of the components forming in the cooling system, finds application in connection with the use of hydrogen as the coolant (see Fig. 8.7). As we will see below (section 8.2), the disadvantage of such a method of driving a TNA is the limited efficiency of the vapor, which limits possible magnitude of feed pressure of components, and consequently also the pressure in the chamber. However at comparatively low pressures in the chamber, on the order of 30-50 [atm(abs.)] ($\approx 3-4 \text{ MN/m}^2$), application of this method is fully justified.

Driving the turbine by means of takeoff of gas from the combustion chamber did not become widespread because of difficulties arising in the takeoff of products of combustion from the chamber of the engine. However, according to foreign data work is being conducted on the realization of a such a method of driving the TNA.

Driving the turbine by power combustion products forming in the PAD is used only for starting the TNA.

Basic Elements of a Propulsion System with a Turbopump Assembly

In Fig. 6.3 and 6.4 there are shown generalized model diagrams of propulsion systems having a turbopump feed system with a ZhGG or PGG. The diagrams shown do not belong to any specific engine and are designed to show various methods of feeding the working substance in a gas generator and the basic elements of a system ensuring its normal operation.

Depending upon the purpose of the propulsion system, we can drop the necessity in certain systems or units and other methods of guaranteeing operation of this or that unit of the system can be applied, however, in a propulsion system with a TNA, the following systems must always be provided for:

- a) starting and stopping;
- b) pressurizing the tanks;
- c) guaranteeing assigned operating conditions;
- d) filling and jettisoning of components.

Furthermore, in certain cases it is necessary to anticipate additional systems to ensure the fulfillment of special problems, for example, transition from one operating method to another, operation of the system during breakdown of one of the chambers, control by direction of thrust vector, decrease of aftereffect, etc.

The required operating conditions of each of the systems and their joint work is ensured by the control and adjustment system of ZhRD.

Let us consider briefly the fundamentals of the system mentioned.

Starting and stopping systems

Systems ensuring starting and stopping of ZhRD in general include: a) a system for preparation of the apparatus for starting (blowing through, cooling, feeding of starting components, etc.); b) system of units to ensure starting and stop (starting systems - starters, valves for turning on and cutoff of fuel feed, diaphragms, etc.); c) branched network of various locks ensuring prescribed sequence of operation of units.

The arrangement of the starting and stopping system is determined by the method used for spin-up of the TNA during starting. In different installations the following basic methods of spin-up of the TNA are used.

Spin-up of the TNA by means of a starting solid propellant pressure accumulator of the PAD (cartridge starter).

In this manner, for starting of the TNA cartridges are ignited by electrical spark igniting the solid propellant in the starting PAD 21 (see Fig. 6.3). The products of combustion of the solid propellant from the PAD reach the blades of turbine 7, thanks to which spin-up of the TNA occurs.

The advantage of the method is in the comparative simplicity of the starter and in its reliability. The method is convenient in single-use starting; with a necessity for multiple starting it is practically difficult to use a starting PAD although systems are known in which a starting PAD ensures restarting.

Spin-up of a TNA from a ground starting system. In this way, from ground system 24 (Fig. 6.4b) a compressed gas or the combustion products of a gas generator, is fed which produces spin-up of the TNA.

The advantage of the method is the fact that with it the starting system is not a built-in system of the rocket, i. e., does not increase the mass of the system, but a disadvantage is in the fact that it is useful only during single use. Furthermore, with this method there must be ensured automatic disconnection of the pneumatic system of supplying the working substance from the ground installation to the turbine.

For spin-up of the TNA, in certain cases, use is also made of special starting gas generators (ZhGG or PGG) having their own pressure system of feeding components. The use of starting gas generators is convenient when there is a requirement for multiple starting of the propulsion system.

To ensure multiple starting there are also used systems with special starting tanks. Thus a basic gas generator can serve for starting. An example of such system of multiple starting is shown in the diagram in Fig. 6.5.

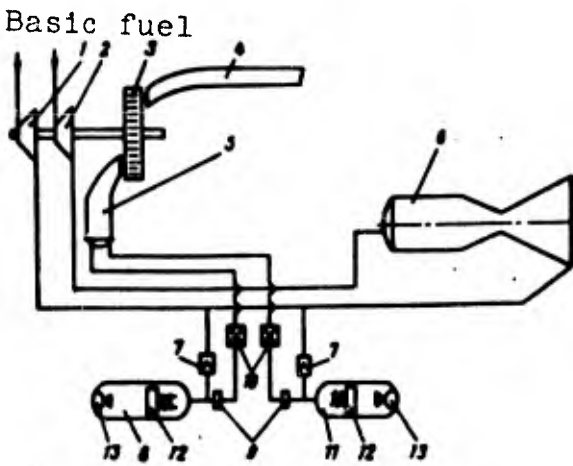


Fig. 6.5. Diagram of a system ensuring multiple starting. 1 - oxidizer pump; 2 - fuel pump; 3 - turbine; 4 - exhaust duct; 5 - ZhGG; 6 - chamber of the engine; 7 - relief valves; 8 - small starting tank of oxidizer; 9 - throttle discs; 10 - cutoff valves; 11 - small starting fuel tank; 12 - piston; 13 - compressed nitrogen bottle.

At the command "Start," into the starting tanks 8 and 11 from bottles 13 compressed nitrogen moves, which presses on pistons 12 fitted with springs. The pistons in turn press on flexible diaphragms inside the starting tanks, displacing a fuel component. Valves 10 open, the components enter the ZhGG 5 and from there the products of combustion reach 3 of the TNA. The turbine rotates the pumps of TNA 1 and 2, which feed the basic components to engine 6 and into the ZhGG. Thus a part of the components is directed into starting tanks 11 and is forced into them until the flexible diaphragms and pistons occupy their initial position. After that, the starting tanks are ready for the next start of the engine. All the enumerated operations after receipt of the command to start are accomplished automatically.

Stopping of the engine is produced by shutting off valves 10.

If there is compressed gas on board the rocket then spin-up of the TNA by compressed gas is possible. In so doing, the compressed gas (for example, helium) is fed from the pressure accumulator to the blades of the turbine.

In propulsion systems of ballistic missiles, spin-up of the TNA can also be produced by means of pressure of a column of liquid in the tanks and inlet pipeline.

A system of forced stopping of the engine should ensure an expedient order of shutting the valves, for the given components and also measures to reduce the aftereffect pulse (see section 5.5). In certain propulsion systems (for example, a ZhRD for antiaircraft guided missiles or certain meteorological rockets) a special shut-off system can not be provided for, so that the engine works until complete depletion of components from the tanks.

Tank Pressurization Systems

Pressurization of tanks is used for safeguard operation of pumps without cavitation and also to provide the necessary stability of the

tank shells. The amount of tank boost pressure is determined by condition of cavitationless operation of the pump, i. e., production of the necessary inlet pressure in pump p_{inlet} .

Pressure of liquid at entrance into the pump p_{inlet} (or head on entrance $H_{\text{inlet}} = p_{\text{inlet}}/\gamma$) is composed of pressure of a column of liquid p_{at} and absolute pressure in the tank above free surface of liquid p_{at} . Considering losses of pressure Δp_{inlet} in the pipelines and fittings located on the way from the tank to the pump, we will obtain

$$p_{\text{inlet}} = p_{\text{at}} + p_{\text{cr}} - \Delta p_{\text{inlet}}; \quad H_{\text{inlet}} = \frac{p_{\text{at}}}{\gamma} + H - \frac{\Delta p_{\text{inlet}}}{\gamma}. \quad (6.1)$$

For a motionless rocket $p_{\text{cr}} = \gamma H_0$, where H_0 — initial height of column of liquid in meters.

For rocket engines such a mutual location of tanks and pumps is characteristic (Fig. 6.6), when the tanks of fuel components are located higher than the engine. For aircraft ZhRD the tanks can be located lower than the pump. In this case, the value of p_{cr} will be negative.

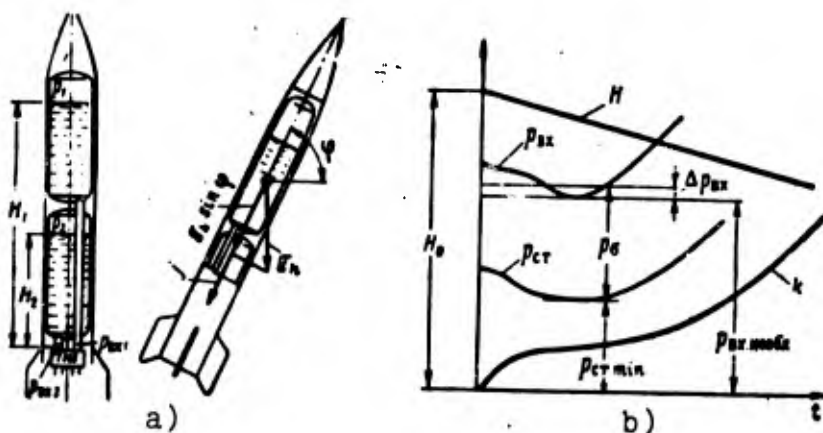


Fig. 6.6. To determine pressure of a column of liquid on entrance to a TNA and the necessary tank pressurization.

For different components the value of p_{cr} varies. During flight of a rocket with an operational engine, the pressure of the column of liquid will be variable. On the one hand, because of depletion of components from the tanks the height of column H decreases; on the other hand, a rocket during operation of the engine always moves with

axial acceleration j . Thus the axis of the rocket can be inclined to the horizon at an angle φ (Fig. 6.6a).

Then the total force having effect on the base of a column of liquid with height H ,

$$p_{cr} = Hg + Hy \sin \varphi.$$

Substituting $\varphi = j/g$, we obtain

$$p_{cr} = Hy \left(\frac{j}{g} + \sin \varphi \right) = Hy(k + \sin \varphi), \quad (6.2)$$

where the value $k = j/g$ bears the name of axial rocket overload.

During the flight of the rocket values H and k are changed approximately as shown in Fig. 6.6b. The law of change of p_{cr} will also be affected by change in time of angle of inclination of rocket axis φ . Pressure of the column of liquid will be minimum after starting the engine, it turns out to be smaller than the pressure at the time of rocket launching. For determination of $p_{cr\min}$ it is necessary to have data about the law of motion of a rocket according to trajectory. If, during calculation of the pump for cavitation value $p_{cr,med}$ is determined, then the necessary pressure in the tank p_0 should be such that at minimum pressure of the column of liquid there will be ensured necessary pressure $p_{cr,med}$, i. e.,

$$p_0 = p_{cr,med} - p_{cr\min} + \Delta p_{cr}. \quad (6.3)$$

Increasing boost pressure of the tank, it is possible to increase permissible number of turns of the pump. However in so doing there is an increase in mass of the tanks and the whole system of pressurization and mass of gas consumed for this purpose. Therefore, an increase in the number of turns of the pump by means of pressure in the tanks is possible only within well-known limits.

Losses of pressure in the main line from tank to pump Δp_{ex} are determined by the usual formulas of flow friction. Usually, the value of boost pressure of tanks is within limits of 2-6 [atm(abs.)] (≈ 0.2 - 0.6 MN/m^2).

The following methods of tank pressurization are used.

Pressurization by gas from the pressure accumulator (see Fig. 6.46). Usually for this purpose helium, nitrogen or air are used. For decrease of the necessary reserve of gas sometimes it is heated before being fed into the tank.

Pressurization by vapors of components (Fig. 6.3). Such a method is rational during operation of an engine on low-boiling components (one or both). In this method the component enters evaporator 15 and from there to the tank.

In a number of cases by means of a liquid gas generator pressurization is rational (unit 10 in Fig. 6.3). In so doing, for prevention of afterburning the ZhGG operates with a surplus of component found in the pressurized tank.

Tanks of a ZhRD of rockets, the active flight of which takes place in the atmosphere (for example, antiaircraft guided missiles) can be pressurized by means of impact pressure of air.

With low-boiling components, pressurization of tanks can be produced also by vapors of the actual component found in the tank. Such systems are called self-generating.

Systems for Guaranteeing Required Operating Conditions of an Engine

The required operating conditions of an engine are ensured by various kinds of regulators.

One of the basic ones is a regulator of change of thrust (or pressure in the combustion chamber) according to assigned conditions

of flight of rocket, and another is a regulator (stabilizer) of correlation of flow rates of components into the chamber and into the ZhGG. The stabilizer of correlation of flow rates of components into the combustion chamber serves to maintain the assigned operating method of the combustion chamber, and also assigned temperature limits of the products of combustion forming in the gas generator.

Sometimes, for maintaining constant thrust a regulator of pressure constancy is set in the combustion chamber.

To ensure prescribed flow friction of the different main lines of the feed system, and consequently also the prescribed (at a given pressure) flow rate of components during flow through the system throttle washers (jets) will be selected (see for example, throttles 8, 13, 23, 25 in Fig. 6.3).

6.3. Thrust and Specific Thrust of a Propulsion System

In operating on an open circuit thrust of propulsion system $P_{x,y}$, is composed of two components: thrust P , created by the chambers of the engine and additional thrust ΔP_{TNA} appearing due to outflow from nozzles of the TNA of the working substance of the TNA drive, i. e.,

$$P_{x,y} = P + \Delta P_{TNA}. \quad (6.4)$$

The value of the addition of thrust created by the nozzles is very small and usually composes 0.5-1.5% of engine thrust.

Specific thrust of the propulsion system $P_{y,x,y}$ is defined as thrust of the system divided by full flow rate of components entering the combustion chamber G and expended on drive of the TNA ΔG_{TNA} . i. e.,

$$P_{y,x,y} = \frac{P_{x,y}}{G + \Delta G_{TNA}}. \quad (6.5)$$

Although in certain cases exhaust gases from the TNA are used for operating the steering nozzles (Fig. 6.7), specific thrust of a propulsion system operating on an open circuit is always smaller than

specific thrust of the chambers of the engine, due to less effective use of components expended on drive of the TNA. The fact is, that temperature and pressure of the working substance in the nozzles is considerably lower than in the combustion chamber. Accordingly, the degree of utilization of working substance (i. e., specific thrust of nozzles or steering nozzles) in obtaining of additional thrust ΔP is much lower than in the combustion chamber of a ZhRD.

Thus, although the nozzles give a certain additional thrust ΔP_{TNA} , flow rates in producing this thrust are disproportionately great. Moreover, depending on feed pressure and perfection of the TNA, loss of specific thrust composes 2-3% of the specific thrust of the engine.

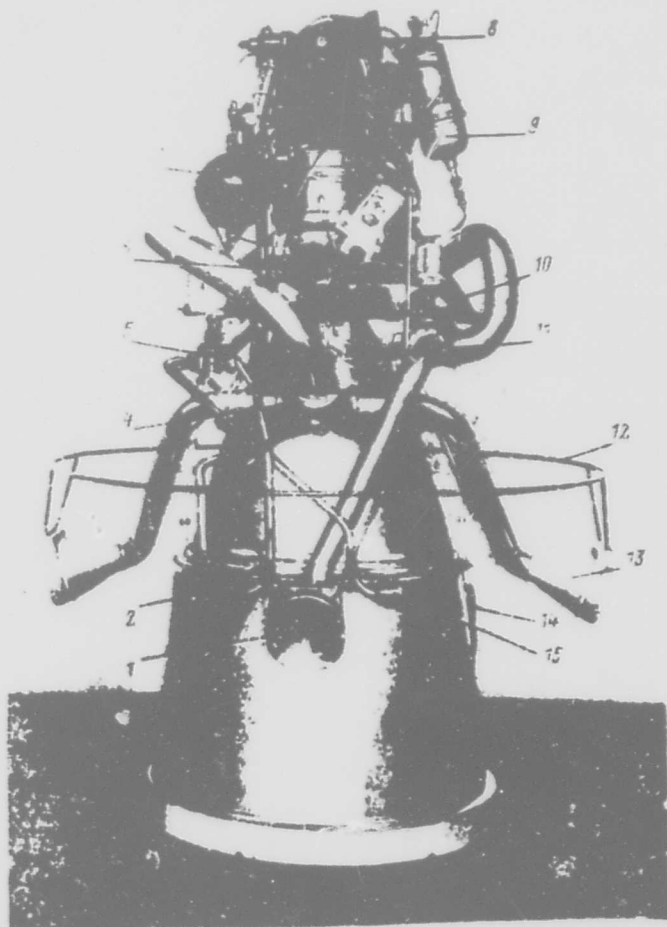


Fig. 6.7. ZhRD RD-119 "Cosmos." 1 - pitch control nozzle; 2, 15 - roll control nozzles; 3, 13 - yaw control nozzles; 4, 5, 11 - gas-distributors with electric drives; 6 - chamber; 7 - cylinders for compressed air; 8 - TNA; 9 - PGG; 10 - frame; 12 - assembly ring of steering system; 14 - detachable plug.

Limits of Pressure in a Chamber Operating on an Open Circuit

Let us examine how specific thrust of a propulsion system is changed with increase of pressure in the combustion chamber (Fig. 6.8). If, with fixed pressure per section p_2 , pressure in the combustion chamber p_1 is increased, then specific thrust of the chamber of the engine P_{ys} according to the equation of characteristic (1.28) will grow according to curve 1. With growth of p_1 necessary feed pressure will grow in the chamber: correspondingly the necessary power of the TNA and flow rate of the working substance for driving the turbine will grow. According to curve 1, with high pressures in the combustion chamber, the increase of specific thrust with growth of pressure is small. At the same time, flow rate of working substance on the drive of the turbine of the TNA will grow proportionally with pressure in the chamber (see equation 8.51, 8.55). Since growth of specific thrust of the engine is small, beginning with some pressure $p_{2\text{opt}}$, loss of specific thrust of the propulsion system $\Delta P_{ys\text{ max}}$ because of flow rate of component on the drive of the TNA will be higher than its increase because of augmentation of thrust of the engine. It is obvious that there is no point in further increasing the pressure in the combustion chamber.

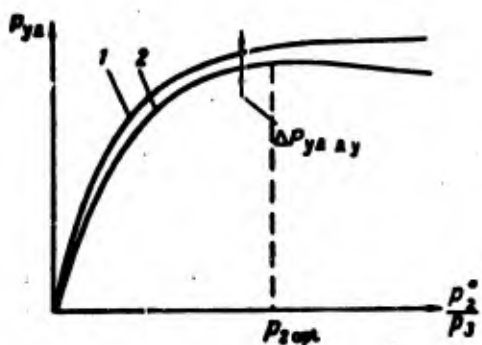


Fig. 6.8. Change of P_{ys} of an open circuit propulsion system with growth of pressure in the chamber.

The value of $p_{2\text{opt}}$ depends on improvement of operation of the TNA assembly on the whole, and also on the form of throttle characteristics of a given engine. Actual values of $p_{2\text{opt}}$ are within limits of 100-150 absolute atmospheres ($\approx 10-15 \text{ MN/m}^2$). As the efficiency of pumps and

turbine are improved $p_{2\text{opt}}$ is increased, however, even at pressures less than $p_{2\text{opt}}$ strong there is a increase in the advantage of systems operating on a closed circuit (see Chap. VIII). Therefore even with a greatly improved TNA it is not always expedient to have a propulsion system with high pressure in the combustion chamber, operating on an open circuit.

6.4. Fuel Tanks

Depending upon method of feeding the components two basic types of tanks are distinguished.

Pressure tanks, i. e., tanks which during operation of a ZhRD are under high feed pressure of components. Such tanks are used in pressurized feed systems.

Non-pressurized tanks, i. e., tanks not under high pressure during operation of a ZhRD. Such tanks are used with feed systems with a TNA. Pressure in non-pressurized tanks does not exceed 3-6 [atm(abs.)], and is determined by conditions of guaranteeing the stability of the tanks and cavitationless operation of the pumps.

Since the tanks compose in their dimensions the biggest part of a rocket, they are frequently used as a supporting member of the rocket structure, absorbing forces having an effect on it. Such tanks are called supporting tanks.

In designing tanks they strive to ensure the following basic requirements.

1. Tanks of any design have to be as light as possible. With a decrease of mass of the tanks the mass of the rocket decreases and its technical characteristics are improved (for example, flying range for the given dimensions). This requirement is especially important to consider in designing a ZhRD with pressure tanks, since their mass always amounts to a large part of the structural mass of the whole rocket.

Construction of tanks is facilitated by using durable and light materials, and also by selecting the most rational form for the tanks.

2. Tanks must possess stability against corrosion. This requirement has special importance in the operation of a ZhRD using aggressive components, and in the case where prolonged storage of components in the tanks is necessary.

3. Tanks must be simple to manufacture and convenient in operation.

Relative Position and Shape of Tanks

In Fig. 6.9 there are different diagrams of tank arrangement. The relative position of fuel and oxidizer tanks is usually determined by conditions of centering of the rocket. In certain cases in the distribution of tanks there is also considered the requirement for creating the necessary inlet head in the TNA to ensure operation of the pumps without cavitation.

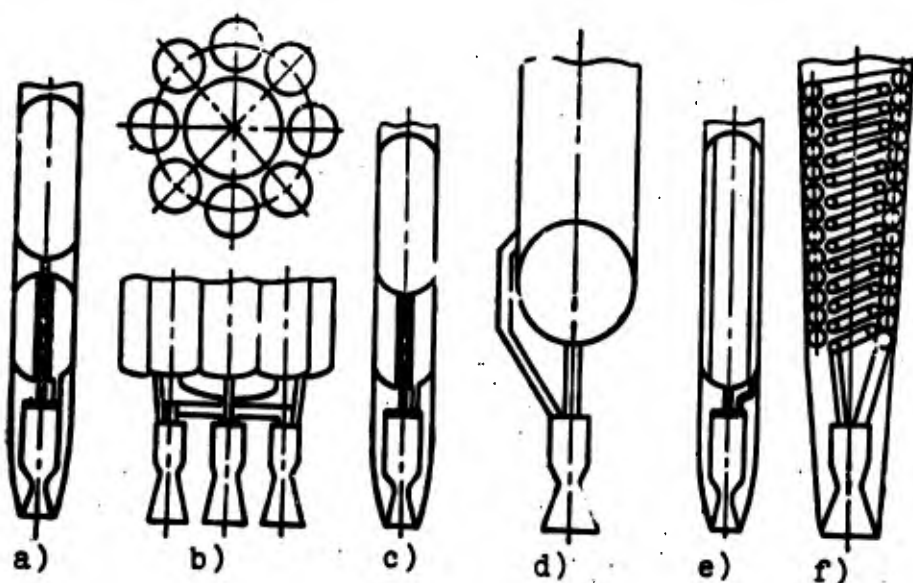


Fig. 6.9. Diagrams of tank location:
a) - separate;
b) - united;
c) - concentric;
d) - spiral tanks.

The most widely-used is the diagram of separate location of fuel and oxidizer tanks. In this way tanks can be located consecutively (Fig. 6.9a) and in the form of a cluster (Fig. 6.9b). Location of tanks in the form of a cluster may be expedient in propulsion

systems with very great thrust and when using multichamber installations. Use is also made of the united construction of tanks (Fig. 9c, d) which in certain cases permits decreasing the overall dimensions of the tank part of the rocket. There are known examples of concentric location of tanks (Fig. 6.9e). An example of installations with concentric location of tanks is that of the ZhRD of the antiaircraft guided missile "oerlikon" and the ZhRD of the "Typhoon" surface-to-air rocket [25]. Concentric location does not cause a gain in mass and in the given installations it was used due to conditions of preserving the position of center of mass. Such a diagram did not achieve wide practical application.

In Fig. 6.9f, there is an example of a diagram of spiral position of tanks [25].

The most wide-spread shape for tanks is cylindrical. This shape for tanks permits obtaining a tank of great volume with comparatively small cross section. From the point of view of least surface of tank and its mass, and expedient shape is spherical. Pressure tanks of spherical form possess the best strength properties, in consequence of which their use frequently is expedient in small thrust systems with a pressure feed system. Spherical tanks also find application in engines of great thrust, when gain in mass due to shape of tank is essential. Such tanks are convenient also when there is necessity of reducing heat exchange. For example, when liquid hydrogen is put into them. An example of application of a spherical tank is shown in Fig. 9.5.

Along with tanks of cylindrical and spherical shape, in certain cases, according to conditions of arrangement of the whole rocket application of lenticular and toroidal tanks is expedient.

Besides the examined simple shapes of tanks more complicated ones are possible. Thus, for the purpose of best use of rocket volume use is made of so-called buried designs (see Fig. 9.31), in which the chamber of the engine is, as it were, "buried" in the tank volume.

Internal Arrangement of Tanks and Diagrams of Extracting Devices

To ensure reliable operation of the propulsion system and convenience in exploitation, in the design of tanks a whole series of units and devices are provided for as, for example, to ensure filling and draining of components for maintaining assigned level of the component (when using low-boiling components), for damping oscillations of the level of components in tanks during maneuver, for funnel damping, and others. In a number of cases in the construction of tanks special hatches are provided for inspection and repair of tanks, tunnel tubes for distribution of main feed lines of the second component, pipelines for tapping of component vapors, and for pressurizing the tanks. Large capacity tanks of ballistic missiles frequently have a frame made from stringers and frames or internal ribs to ensure sufficient rigidity and strength of construction. In Fig. 6.10 there is a schematic representation of the S-2 rocket propulsion system, on which is represented a number of elements of internal system of tanks of united construction.

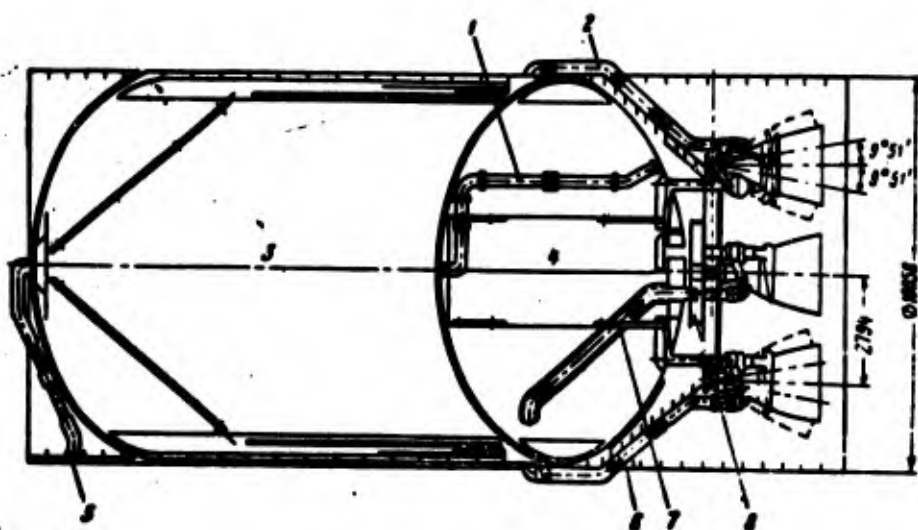


Fig. 6.10. Diagram of an S-2 rocket: 1 - pipeline for tapping of oxidizer vapors; 2 - pipeline for feeding combustible into peripheral engine; 3 - fuel tank (liquid hydrogen); 4 - oxidizer tank (liquid oxygen); 5 - pipeline for tapping fuel vapors; 6 - filler for filling and jettisoning of fuel; 7 - pipeline for feeding combustible to the central engine; 8 - frame for bracing the central engine.

The most important element of a tank is the device to ensure continuous feeding of fuel components from the tanks to the chamber of the engine, since interruption in fuel feed can lead to disturbance of the operating system.

Continuity in feeding components into the chamber of the engine can be disrupted, first, due to temporary uncovering of the extracting device as a result of the action of inertial forces during maneuver of the rocket and secondly, due to information of a funnel on the surface of the component at the place of its entrance into the extracting device. Causes of formation of a funnel are the increased rates of movement of component at the entrance to the extracting device as compared to its speeds on the periphery, and also irregularity of speeds of the component along the axis of the tank (due to the blocking of the volume of the tank by different fittings), in consequence of which the component can rotate around the entrance axis, promoting a more intense funnel-shaped formation. Formation of funnels on the surface of the component is possible also due to action of the stream of entering gas with a pressure feed system or during pressurization of the tanks.

Special requirements for extracting devices are presented during operation of a propulsion system under conditions of weightlessness. As theoretical and experimental investigations show, under conditions of weightlessness the location of liquid in the tank depends mainly on the relationship between value of surface tension of the liquid at the gas-liquid boundary and the value of cohesive forces of the liquid with the wall. If the first predominates (as, for example, for mercury), the liquid strives to separate from the wall and, taking spheric form, to float in the tank. If however, as in case of liquid or hydrogen, cohesion with the walls predominates, the liquid strives to moisten the entire internal surface of the tank, and a gas phase turns out to be in the central part of the tank surrounded by liquid. In both cases there can occur uncovering of the extracting device and disruption of the uninterrupted feeding.

In Fig. 6.11 there are diagrams of different devices which are used to ensure uninterrupted feed of components.

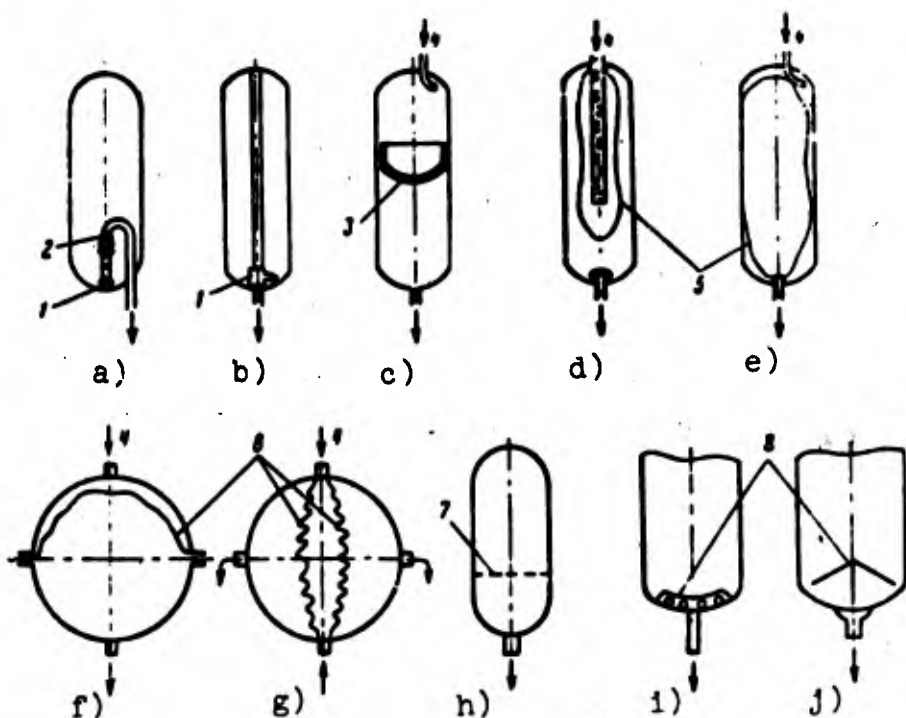


Fig. 6.11. Diagrams of extracting devices for feeding of components: a) fluctuating extractor; b) swiveling extractor; c) piston pressurizing; d, e, f, g) feeding by means of elastic bags or diaphragms; h) tank with a screen-type shield; i, j) extracting devices with funnel dampers; 1 - extractor; 2 - bellows; 3 - piston; 4 - gas feed; 5 - elastic bag; 6 - diaphragm; 7 - screen-type shield; 8 - funnel damper.

Devices, of the type represented in Fig. 6.11a, b, have fluctuating or swiveling extractor, travelling together with the volume of components. Ribs on the end of the extractor promote entrainment of inducer after the volume of liquid, and also there are funnel dampers, disrupting rotation of the liquid. Such extracting devices are the most rational with operation of a ZhRD under conditions of the appearance of lateral or negative inertial forces during maneuver of the rocket (for example, guided antiaircraft missiles).

The devices represented in diagrams of Fig. 6.11c, d, e, f, g, prevent entrance of gas into the feed system by means of an elastic or metallic shell separating the liquid component from the gas. Such devices can be used in operation of a system with a ZhRD under conditions of weightlessness, and also during the appearance of negative or lateral inertial forces. In the operation of a propulsion system under conditions assuming no sharp maneuver of the rocket (for example, on a ballistic missile), to ensure uninterrupted feeding of the component frequently installation of funnel damping devices of type of shown in Fig. 6.11h, i, is sufficient.

Calculation of Tank Volume

Full free volume of a tank V is composed of the following component volumes:

$$V = V_{\text{pert}} + V_{\text{res}} + V_{\text{ull}}, \quad (6.6)$$

where V_{pert} - calculation volume of the tank; V_{res} - volume of guaranteed reserve of component; V_{ull} - volume of ullage.

In determining the geometric dimensions of tank volume it is necessary to consider obstruction of tank from within by pipelines, extractors, and tunnel tubes. Let us consider determination of the components of volume.

Calculation volume of necessary quantity of component V_{pert} . Since flow rate per second G_{nom} and time of operation of a ZhRD are known,

$$V_{\text{pert}} = \frac{G_{\text{nom}}\tau}{\gamma}, \quad (6.7)$$

where γ - density of component in kg/m^3 ; τ - time of operation of the engine from moment of breakaway of the rocket from launcher to moment of shut down of the engine in s.

Volume of guaranteed reserve of component V_{res} . Guaranteed reserve includes the quantity of component expended for operation on the starting or launching device from the moment of beginning operation

up to the moment of take off of the rocket, and the quantity of component necessary to ensure reliable operation of a ZhRD in the last period of engine operation.

Combustion duration of a ZhRD on the launcher is determined basically by the starting system of the engine. With gun starting this time is short and composes tenths of a second; with step starting it increases to several seconds; therefore during step starting of an engine a large reserve is needed.

Guaranteed reserve is necessary also for compensation of possible deviations of actual flow rate per second of component from that calculated.

Taking into account the above-indicated factors, depending upon method of starting of the engine and maneuverability of the rocket, the value of V_{mp} can be accepted as being within 2-5% of V_{pacv} .

Volume of ullage V_{max} . Ullage is necessary so that with an increase in temperature of the component during the storage of a filled rocket excessive increase of pressure in tanks will not occur. With a pressure feed system, ullage is also a damper, softening the starting process. Moreover, ullage is necessary in order to ensure space in case of release of gases dissolved in the component or its products of decomposition.

Volume of ullage is determined proceeding from the condition that during the greatest operation temperature assigned by technical conditions, T_{max} pressure in the tanks will not exceed the given p_{6max} . Value of pressure p_{6max} is determined by construction of the rocket tanks and the characteristics of the hydraulic feed system. With pressurized feed the value of p_{6max} must not exceed bursting pressure of the membranes, since otherwise spontaneous starting can occur. With pump feed (unpressurized tanks), value of p_{6max} is determined by boost pressure of the tanks. Usually, the value p_{6max} is considered as equal to 5-10 [atm(abs.)] ($\approx 0.5-1 \text{ MN/m}^2$).

Knowing p_{max} , value of ullage V_{max} is determined from the following considerations.

In filling of tanks, the equation of state of gases in ullage takes the form

$$p_0 V_{\text{max}} = GRT_0. \quad (6.8)$$

where p_0 and T_0 – pressure and ambient temperature during filling; G – mass of gas.

With increase of temperature up to T_{max} , pressure in ullage increases, volume of ullage thus will decrease to value ΔV_{max} by means of temperature increase of component volume in the tank V_{vessel} :

$$\Delta V_{\text{max}} = V_{\text{vessel}} \beta (T_{\text{max}} - T_0). \quad (6.9)$$

where β – expansion coefficient of component (Table 6.1).

Table 6.1. Values of expansion coefficient for different liquid at 15°C .

Liquid	$\beta \cdot 10^4$	Liquid	$\beta \cdot 10^4$
Nitric acid 100%	12.4	Sulfuric acid	5
Aniline	2.58	Turpentine	9.4
Benzine	12.4	100% ethyl alcohol	10.4
Kerosene	9+10	50% ethyl alcohol	7.4
Methyl alcohol	12.2		
Hydrogen peroxide	10.7		

Equation of state of gases in ullage

$$p_{\text{max}} (V_{\text{max}} - \Delta V_{\text{max}}) = GRT_{\text{max}}. \quad (6.10)$$

Substituting in this expression values G and V_{max} from equations (6.8) and (6.9), we obtain

$$p_{\text{max}} [V_{\text{max}} - V_{\text{vessel}} \beta (T_{\text{max}} - T_0)] = \frac{p_0 V_{\text{max}}}{RT_0} RT_{\text{max}}.$$

whence, after reductions and conversion we obtain

$$V_{\text{max}} = \frac{V_{\text{const}} \delta (T_{\text{max}} - T_0)}{1 - \frac{\rho V_{\text{max}}}{\rho_0 \delta T_0}}. \quad (6.11)$$

6.5. Feed System Equipment

Equipment of the feed system ensuring normal operation and prescribed operating conditions of propulsion system includes cutoff and regulating valves of different forms, intake relay, tank filling and emptying devices, throttle washers, and pipelines.

The equipment of each propulsion system has its own characteristics determined by the purpose of the system and the special requirements presented to it. From a wide variety of different constructions of units of the equipment we will examine examples of some of them.

Starting and Shut-Off Valves and Devices

The purpose of starting and shut-off valves – to control the starting and shutting off of the propulsion system. The force, necessary for opening or shutting of a valve can be created by means of a pneumatic or hydraulic system, an electromagnet, or a cartridge.

In Fig. 6.12a, there is shown a pneumatic valve. Valve cone 5 with gasket 6 is pressed against body 4. Valve 7 is pressed against the valve cone by spring 3 and pressure of the component. The valve is opened with feed on piston 2 of controlling pressure through pipe connection 1. Leakage of controlling gas is prevented by packing 10, and drainage of gas from the cavity under the piston occurs through an opening in the body. Packing 9 prevents leakage of the component into the cavity under the piston. The valve is closed under the action of spring 3 during drop in pressure of controlling gas in the cavity above piston 2.

In Fig. 6.12b, there is shown a pyrotechnic shut-off valve. With the triggering of a cartridge set in pipe connection 13, powder gases break through membrane 12 and press upon the shank of valve 7.

Under pressure of gas, pin 11 will be cut, the valve shifts forward and is jammed in valve seat 5, covering the cross section.

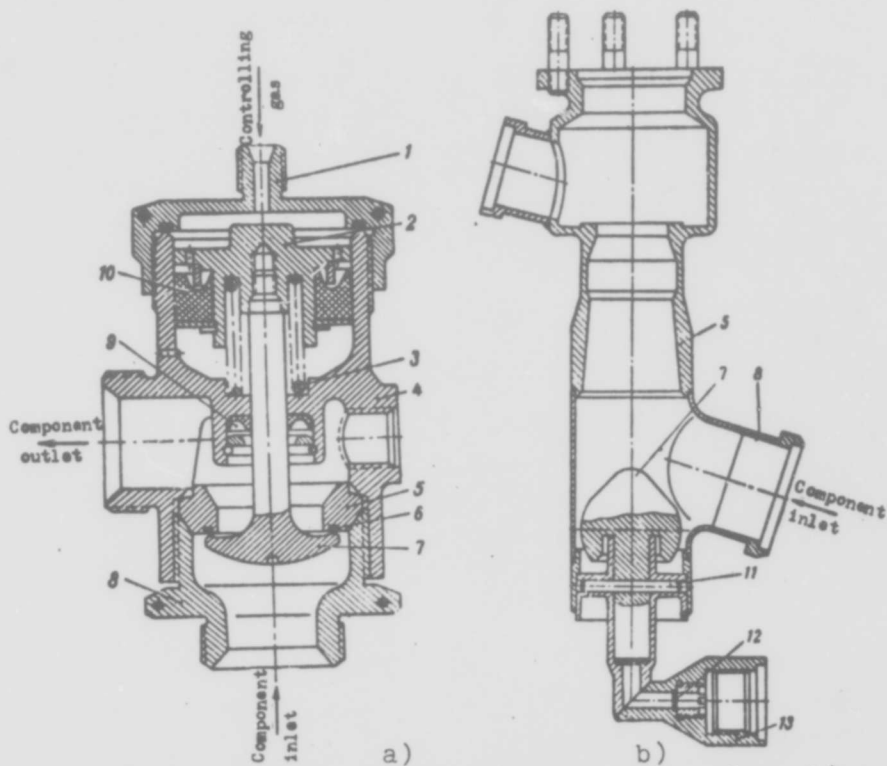


Fig. 6.12. Cutoff valves: a) pneumatic valve; b) pyrotechnic valve: 1 - pipe connection; 2 - piston; 3 - spring; 4 - body; 5 - valve cone; 6 - valve cone gasket; 7 - valve; 8 - inlet pipe connection; 9, 10 - packing; 11 - pin; 12 - membrane; 13 - pipe connection for cartridge.

In Fig. 6.13 there is shown a pyrotechnic valve of a high pressure gas feed. With the triggering of the cartridge set in pipe connection 10, powder gases press on piston 7. The shoulder of rod 4, pressed between body 2 and inlet pipe connection 1, will be cut, the rod shifts and is jammed in the body, opening the gas access in cutlet pipe connection 3.

In the feed systems of a ZhRD there are also encountered dual or triple valves, in which one piston opens two or three valves on lines of different components or on parallel lines of one component.

Transmission of motion from piston to valves in this case is produced by means of rocking levers.

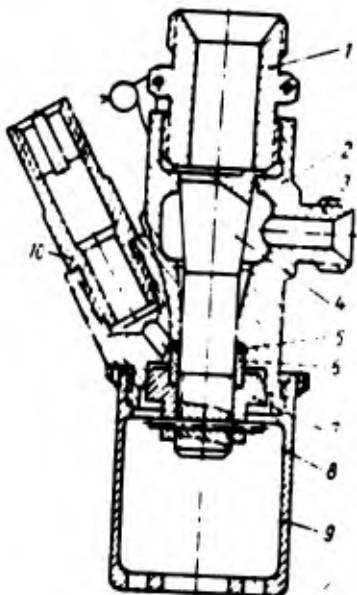


Fig. 6.13. Pyrotechnic valve: 1 - inlet pipe connection; 2 - body; 3 - output pipe connection; 4 - rod; 5, 6 - packing; 7 - piston; 8 - pin; 9 - bucket; 10 - pipe connection for cartridge.

In Fig. 6.14 there is shown an example of a cutoff control valve with electromagnetic drive. Such valves are frequently called PKEDD (electrical remote action pneumatic valve) or simply EPK (electro-pneumatic valve). It consists of a body into which is screwed an inlet pipe connection 1 supplying the appropriate component to the valve. Pressure of the component together with force of spring 2 lifts lower valve 3 upwards. In so doing, packing belt 4 of the valve is seated on the valve seat and blocks the outlet of the component. Simultaneously, by means of rod 5 upper valve 7 rises which joins outlet pipe connection 6 and the systems of pipelines beyond it with the atmosphere through drainage hole 8. For turning on the supply of component, the current flows in the winding of the coil of electromagnet 9. Thus armature 10 is attracted to yoke 11, and through rod 12 force is relayed to upper valve 7, which, being lowered onto its seat disconnects the component feed from drainage hole 8. Simultaneously, by means of rod 5, lower valve 3 is lowered and opens the access of component in the outlet pipe connection, and then in the corresponding main line. Turning off of the electromagnet coil

returns the valve to its initial position. Usually such an electro-magnetic valve with drainage is used as a flow valve of gas for control of other valves by servopistons.

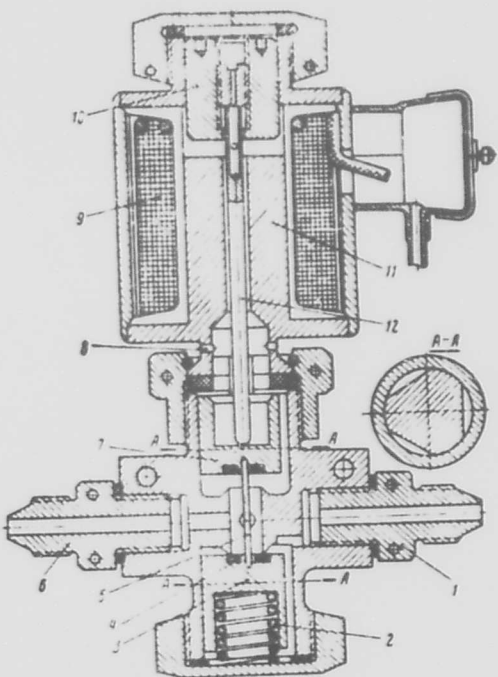


Fig. 6.14. Shut-off valve with electromagnetic drive: 1 - inlet pipe connection; 2 - spring; 3 - lower valve; 4 - packing belt; 5 - rod; 6 - outlet pipe connection; 7 - upper valve; 8 - drainage; 9 - electromagnet; 10 - armature; 11 - yoke of electromagnet; 12 - rod.

In single-time propulsion systems various kinds of membrane devices are used as shut-off units. In this way, access of component to the chamber of the engine is opened after breaking of the membrane. Membranes are divided into free and forced breakthrough. Breaking of a free breakthrough membrane occurs after achievement of a specified pressure in the pipeline.

In Fig. 6.15a there is shown a free breakthrough membrane with annular weakening of section in the form of an incision. Under high pressures the membrane tears precisely along this incision, since here there is the least membrane resistance. After breaking of the membrane along the incision, its lobe bends aside and opens a passage for liquid. In Fig. 6.15b, there is shown such membrane with a

cruciform incision. Under action of pressure, the membrane tears along the incision and is bent aside in the form of lobes.

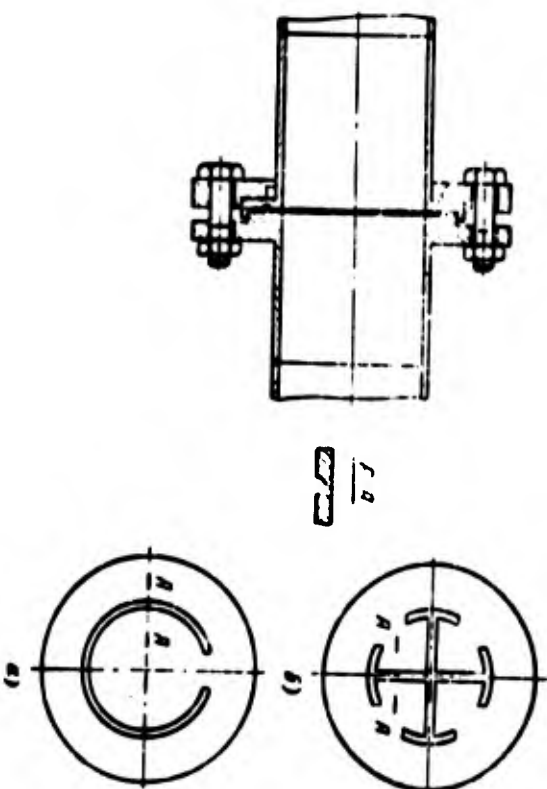


Fig. 6.15. Breaking membranes of free breakthrough.

A membrane usually will be selected for a required bursting pressure since the force, tearing the thin material of the membrane, to a considerable measure depends on the allowance for the thickness of the incision. In membrane closing devices of the forced breakthrough type, breaking of the membrane is produced by means of a special knife arrangement or blasting cartridge. Membrane devices of the forced breakthrough type are considerably more complicated than free breakthrough both to manufacture and to use. However, their great advantage is their operation at the exactly assigned moment.

In Fig. 6.16 there is an example of a membrane valve for opening the access of a component to the engine at the instant that operation begins. The valve works on pressure of gases proceeding the rough pipe connection 4 into the cavity above diaphragm 5, which, under pressure of the gas flexes and forces knife 7 to move. Knife 7 will

cut pins 6 and will cut through membrane 8 along the designated perimeter. Under pressure of the component the membrane bends aside and opens access for the component.

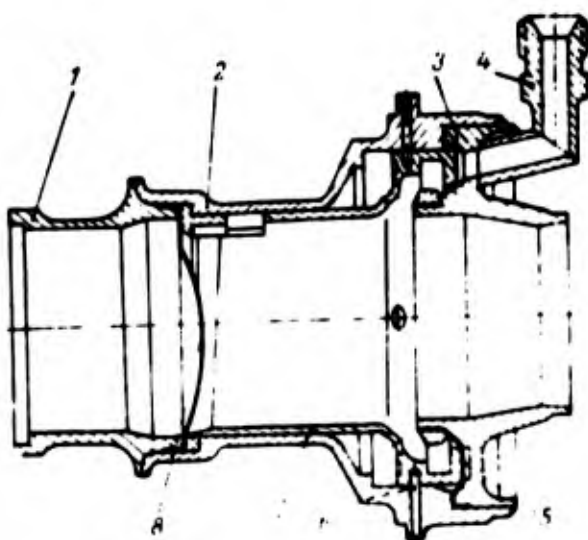


Fig. 6.16. Membrane valve:
1 - membrane block; 2 - body; 3 - cover; 4 - connecting pipe; 5 - diaphragm; 6 - pin; 7 - knife; 8 - membrane.

Regulating Valves and Throttle Washers. Relay

As we noted above, supporting the assigned operating conditions of the system is ensured with the help various kinds of throttles and regulating valves.

The essence of action of regulating valves consists in changing the value of throttle section between valve and valve seat during disturbance of feed conditons of the component or upon the arrival of the appropriate command.

In Fig. 6.17 there is an example of a constant pressure regulator for feeding a component. The component enters valve via pipe connection 7, passes through section between valve 9 and valve cone 8, enters outlet cavity 11, whence it goes according to designation. Pressure of component in cavity 11 is determined by the value of command pressure passed by pipe connection 1 into bellows cavity 4. Pressure of component from cavity 11 through drilling 10 is transmitted to cavity 5. Spring 2, bellows 4, and area of the valve are selected in such a way that with an increase or decrease in pressure of component in

cavity 11 the relationship of forces having an effect on valve 9 changes. In this way, the throttle section between valve and seat 8 respectively decreases, and in cavity 11 the assigned pressure is established.

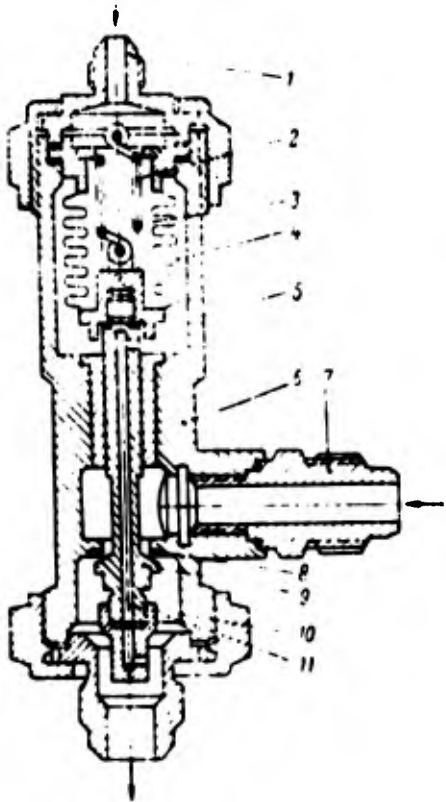


Fig. 6.17. Feed pressure regulator
1 - pipe connection for entrance of command gas; 2 - spring; 3 - bellows cavity; 4 - bellows; 5 - cavity; 6 - body; 7 - inlet pipe connection; 8 - valve seat; 9 - valve; 10 - drilling; 11 - outlet cavity.

In Fig. 6.22c there is an example of a setting of a shift throttle washer (jet), utilized to ensure the assigned flow friction of the main line.

In Fig. 6.18 is a pressure relay. It serves for switching on the electric circuits upon attainment of defined pressure in the serviced main line or volume, and for reverse switching of the circuit upon reduction of pressure to the assigned limit.

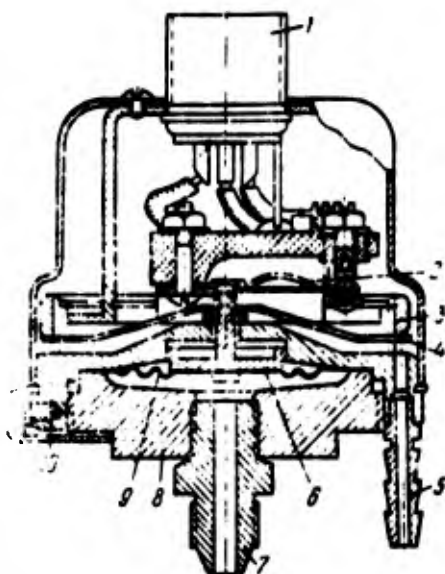


Fig. 6.18. Pressure relay: 1 - electrical wire lead; 2 - switch; 3 - threaded regulating ring; 4 - adjustable spring; 5 - drainage; 6 - plunger; 7 - pressure pipe connection; 8 - base of pressure of receiver; 9 - membrane; 10 - body.

Relay pressure consists of a pressure receiver and a high speed switch. Membrane 9 serve as sensing devices, and reinforced adjustable spring 4 sensing pressure, pressed along the perimeter by the base of pressure receiver 8 to body 10. Under the action of pressure proceeding under the membrane (when it reaches a given value) it is deflected and by plunger 6 located on it presses on the spring of switch 2 which is moved to the upper contact. With reduction of pressure, the membrane releases switch 2 and it drops again to the lower contact. Moving of switch 2 leads to the closing of those or other electric circuits. Adjustment of instrument to a given value of operating pressure is achieved by changing the deflection of spring 4 by means of threaded ring 3. In Fig. 6.19 there are examples of check valves, filling and discharging plugs.

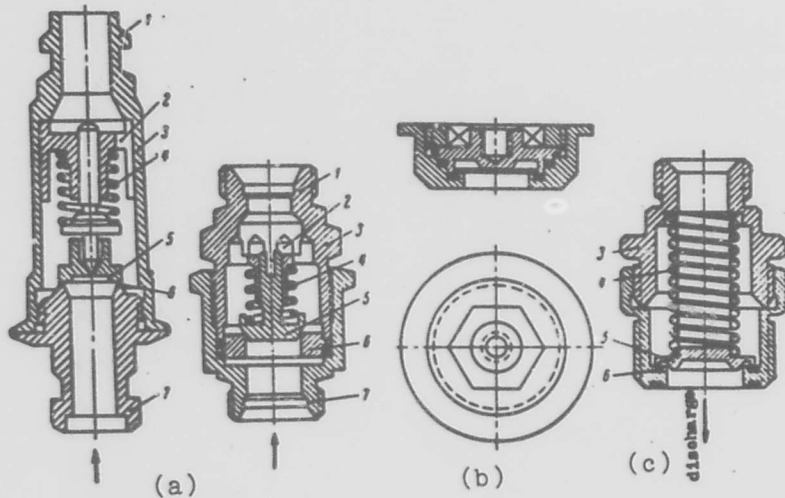


Fig. 6.19. Check valves (a); filling; (b) and discharge; (c) plugs:
 1 - outlet pipe connection; 2 - openings in the thrust flange; 3 - body; 4 - spring; 5 - valve disk; 6 - valve seat; inlet pipe connection.

Pipelines

For feeding components and for controlling valves of the feed systems of pipelines of different dimensions and construction are used.

Sections of pipelines for feeding components are selected based on the permissible rate of component through the pipes. Usually the rate of a liquid is on the order of 5-30 m/s. At high rates there are considerable increases in hydraulic losses proportional to the square of the velocity. At slow speeds losses decrease, but dimensions of pipelines increase considerably. Therefore in pipelines for feed of components to the TNA, where for prevention of cavitation it is important to maintain pressure of components on inlet to pumps, lesser velocities are used.

For feed of components frequently use is made of flexible hoses, the application of which simplifies installation and also allows shift of the unit to which pipelines adjoint. As flexible hoses there can be used flexible-braided and metallic (stretch) hoses. The base of the flexible-braided hoses in most cases is rubber. For aggressive components special bases are used (for example, teflon). Hoses consist of elastic tube, strengthened by woven or metallic braiding.

Depending upon operating pressure single, double, and even triple braiding is used.

In Fig. 6.20 there is a metallic flexible hose with a corrugated internal tube (bellows) enclosed in metallic braiding. Bellows and braiding are made from stainless steel, and also from carbon steel, bronze, nickel, and titanium alloy.

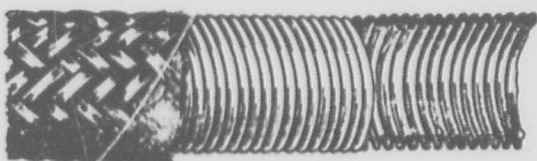


Fig. 6.20. Metallic (bellows) hose with braiding.

In Fig. 6.21 different methods are shown for coupling flexible-braided and bellows hoses. In Fig. 6.22a hoses are coupled by means of a clamp clip 1 and nipple 2, the shank of which is cone-shaped. The clamp clip has on its end a screw thread of large pitch 4. Hose 3 is screwed in the clip up to a stop, beyond which there is screwed into the clip nipple 2 which packs the connection, by pressing the hose by conical shank to clip 2. In Fig. 6.21b packing of the hose is ensured by rolling clip 1 into profile nipple 2. In Fig. 6.21c there is shown a hose coupling between conical surface of clip 1 and nipple 2. In Fig. 6.21d a method for coupling a bellows hose is shown. In the tubular shank with windows of pipe connection 7 is set the end of the hose with preliminary soldered on section of coupling by corrugation and braiding. After that inserted the set end of the hose is soldered along the perimeter of the windows.

In Fig. 6.22 there are shown different types of couplings of pipelines. With small diameters of pipelines wide use is made of nipple couplings of pipelines with expansion (Fig. 6.22a). In Fig. 6.22b there is shown a nipple (spherical) connection with soldered or welded nipples. Airtightness of connection is thus ensured by the contact of the spherical surface of the nipple with the conical surface of the pipe connection. Couplings by means of bellows (Fig. 6.22d) and flanged joint (Fig. 6.22e) are used with large diameters

of pipelines. The use of a bellows coupling or bellows inserts on pipelines permits compensating for unfavorable combination of tolerances in the measured circuit, and also temperature expansion of pipes and parts of the article.

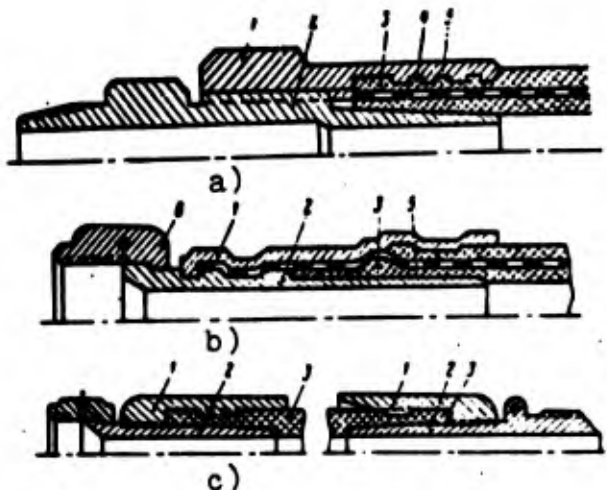


Fig. 6.21. Methods of coupling flexible-braided and bellows flexible hoses: a, b, c) flexible-braided hoses; d) bellows hose; 1 - clamp clip; 2 - nipple; 3 - hose; 4 - screw thread; 5 - internal braiding; 6 - sleeve nut; 7 - shank of pipe connection with windows.

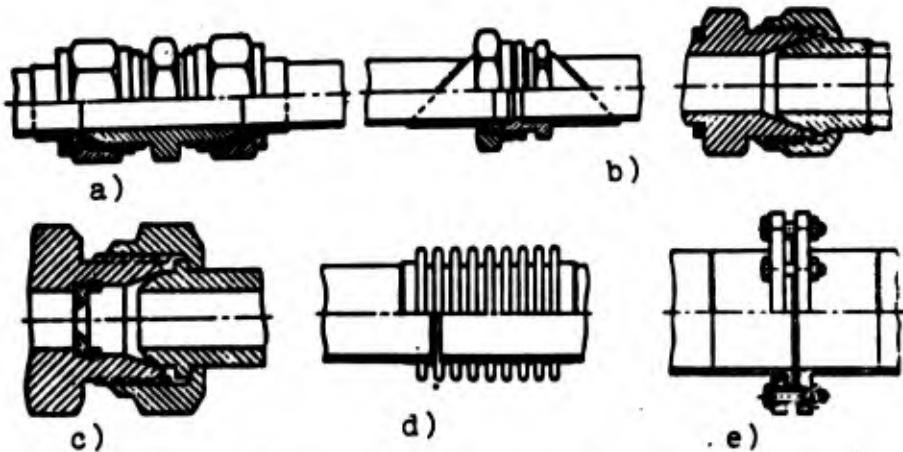
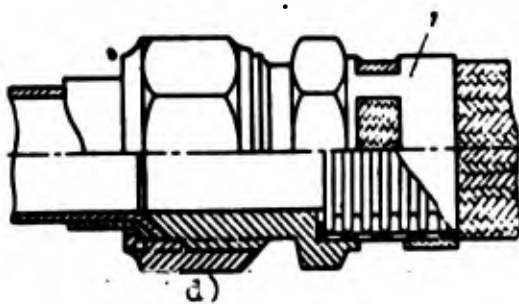


Fig. 6.22. Methods of coupling pipelines: a) nipple coupling with expansion of pipes; b) coupling with soldered or welded nipples; c) coupling with installation of a throttle washer; d) coupling by means of bellows; e) flanged coupling.

6.6. Determination of Feed Pressure and Hydraulic Characteristics of the Feed System

Necessary feed pressure of components p_{feed} is composed of pressure in combustion chamber p_2 and hydraulic losses of pressure in the feed system of the component, i. e., on the way from the pumps of the TNA or tanks (in a pressure feed system) to the combustion chamber. In general (neglecting the pressure of the column of liquid and the action of inertial forces)

$$p_{\text{feed}} = p_2 + \Delta p_{\text{inj}} + \Delta p_{\text{coolant}} + \Delta p_{\text{pipes}} + \Delta p_{\text{valves}} + \Delta p_{\text{throttles}} \quad (6.12)$$

where Δp_{inj} ; $\Delta p_{\text{coolant}}$; Δp_{pipes} ; Δp_{valves} ; $\Delta p_{\text{throttles}}$ — losses of pressure respectively in injectors, coolant passage, pipelines, valves, and throttles. The sum $(\Delta p_{\text{inj}} + \Delta p_{\text{coolant}} + \Delta p_{\text{pipes}} + \Delta p_{\text{valves}} + \Delta p_{\text{throttles}})$ constitutes hydraulic losses of pressure of a component in the feed system. Calculation of hydraulic losses in the feed system of a ZhRD is possible only with known or assigned dimensions of coolant passage of the chamber, circuit of the feed system, dimensions and form of pipelines, and also the type and number of valves and other local flow frictions: elbows, branching, headers, and so forth.

Loss of pressure in injectors Δp_{inj} is known from calculation of the injectors (see Chap. III). Let us consider method of determining the remaining component hydraulic losses.

Losses of Pressure in the Coolant Passage of the Engine Chamber

In the coolant passage two forms of losses take place:

Loss by friction $\Delta p_{\text{friction}}$ appearing as a result of the friction of the liquid on the wall of the channel.

Local losses Δp_{local} induced by local resistances to motion of the component (fastenings, stampings, turns, inlet and outlet of the collector, beginning and termination of ribs, smooth and sudden

narrowing and expansions of the coolant passage, etc.). Thus,

$$\Delta p_{\text{tot}} = \Delta p_{\text{ext. fr}} + \Delta p_{\text{ext. n.}} \quad (6.13)$$

In cooling the chamber with a low-boiling component (for example, hydrogen) frequently it is necessary to consider also reduction of static pressure in the flow by means of acceleration of the cooling gas Δp_e (sometimes this value is called losses of pressure due to gas acceleration).

Since the dimensions of the coolant passage and temperature of the coolant are variable along the length of the chamber, calculation of losses due to friction in the coolant passage is usually conducted by sections. In selection of sections it is convenient to use the division of the chamber already accepted earlier during calculation of cooling. For each section all the rated values (geometric dimensions, velocity of coolant, etc.) are averaged.

Determining loss due to friction on each section $\Delta p_{\text{ext. fr}, i}$, full value of losses due to friction in the coolant passage is found as the sum of losses on sections, i. e., $\Delta p_{\text{ext. fr}} = \sum \Delta p_{\text{ext. fr}, i}$.

All further computations are given for calculation of one section of a system in which all parameters are averaged.

Losses due to friction are calculated by the formula

$$\Delta p_{\text{ext. fr}, i} = \lambda \frac{l}{d_e} \gamma \frac{v^2}{2g}, \quad (6.14)$$

where l - length of section of coolant passage; d_e - equivalent (hydraulic) diameter of the coolant duct for a given section; γ - coolant density; v - coolant velocity; λ - dimensionless friction loss factor.

As can be seen, the problem is reduced to determination of d_e and coefficient λ in formula (6.14).

Equivalent diameter is defined as relation of quadruplicated area of useful cross section to perimeter of section II:

$$d_e = \frac{4A_e}{P} \quad (6.15)$$

Coefficient of friction λ depends on character of flow and form of the duct. Character of flow is determined by Reynolds number Re , and form of duct - form factor ω . For laminar flows, i. e., where $Re < 2320$

$$\lambda = \frac{64}{Re} \omega \quad (6.16)$$

Thus the form factor ω for round ducts is equal to unity, for annular slot - 1.5, and for right angled channels with ratio of sides b/a has the following values:

b/a	0	0.1	0.2	0.3	0.4	0.5	0.7	1.0
*	1.50	1.32	1.25	1.10	1.03	0.97	0.91	0.90

For turbulent flows when $2320 < Re < 10^5$

$$\lambda = \frac{0.3164}{\sqrt[4]{Re}} \omega \quad (6.17)$$

When $Re > 4000$, coefficient of friction λ can also be determined by the formula [119]

$$\lambda = \frac{1}{(1.81 \lg Re - 1.64)^2} \quad (6.18)$$

Form factor ω during turbulent flow for round and right angled ducts with $0.5 < b/a < 2$ is equal to unity, for an annular slot - 1.5. Re number is calculated by the formula

$$Re = d_e \omega / v \quad (6.19)$$

where v - kinetic viscosity in m/s.

For a more convenient determination of Re number we will convert expression (6.19). Since

$$w = \frac{G}{f_x}, \quad (6.20)$$

$$v = \frac{F}{\rho} = \frac{M}{V}, \quad (6.21)$$

then, substituting the expressions (6.15), (6.20) and (6.21) in formula (6.19), we will obtain

$$Re = \frac{d_x w}{v} = \frac{4 f_x G V}{\Pi f_x \rho g \mu} = \frac{4 G}{\Pi g \mu}, \quad (6.22)$$

where G – flow rate of liquid coolant.

For certain forms of coolant passages the formula (6.22) can be reduced to a more convenient form.

For a slot duct, considering $d_{cp} \approx d_{oxn}$, we obtain

$$Re = \frac{4G}{\Pi g \mu} = \frac{2G}{d_{oxn} g \mu}. \quad (6.23)$$

For a coolant passage with ribbing and can-type chambers we consider that the passage constitutes a system of identical ducts linked in parallel. Resistance of the whole tract is equal to the resistance of one of the ducts.

Thus, in the case of longitudinal milled ribs and for tubes of right angled section

$$Re = \frac{4G_t}{\Pi g \mu} = \frac{2G_t}{(a + s_{oxn}) g \mu}, \quad (6.24)$$

where $G_t = G/z$ – flow rate in one of z ducts. At other forms of ribbed channel (for example, with corrugations)

$$Re = \frac{4G_t}{\Pi g \mu}. \quad (6.25)$$

In case of screw ducts, the coolant passage also is composed of a number of identical ducts linked in parallel, the number of which equals the number of turns of the screw thread, and the resistance of the whole passage also equals the resistance of one of the ducts. The Re value is determined by the same formula (6.24), as in the case of a slot duct with longitudinal stiffening ribs. Coefficient of friction for a screw duct

$$\lambda_{\text{duct}} = \lambda. \quad (6.26)$$

Coefficient of friction λ is calculated by the usual formulas, and coefficient

$$\beta = 1 + 3.5 \frac{d}{d_{\text{duct}}}. \quad (6.27)$$

where d_{duct} — diameter of helix in the calculated section.

Length of the screw duct on a given section

$$L_{\text{duct}} = \frac{L_t}{\sin \gamma_{\text{cp}}}. \quad (6.28)$$

where L_t — length of a given section; γ_{cp} — angle of ascent of helix on a given section.

All the above-mentioned expressions do not consider the presence of heat exchange in the coolant passage by virtue of which loss due to friction during flow of the liquid coolant will be somewhat less.

Local losses are defined as the sum of losses induced by local resistances in the coolant passage:

where

$$\Delta P_{\text{local}} = \sum \Delta P_{\text{local},i}$$

$$\Delta P_{\text{local},i} = \xi_i \frac{v^2}{2g}. \quad (6.29)$$

Here ξ — coefficient of local resistance, determined for each particular case according to manuals of hydraulics [118], [119]. In the presence

stumpings and in certain other cases which are specific for a ZhRD, for determining ; it is possible to use [89], [121]. With complicated configurations of the passage, when reference data are lacking the most reliable method of determining drag coefficient is by experimental pouring through of an element of the passage and determining the necessary coefficients by its results.

Decrease of static pressure in the passage due to acceleration of the coolant during cooling by gaseous hydrogen Δp_w is determined by the Bernoulli equation. Disregarding difference of heights and pressure losses in the examined section, it is possible to write

$$\frac{p_1}{\gamma_1} + \frac{v_1^2}{2g} = \frac{p_2}{\gamma_2} + \frac{v_2^2}{2g},$$

whence, considering for the given section $\gamma_1 = \gamma_2 = \gamma$,

$$\Delta p_w = (p_1 - p_2) = \frac{\gamma}{2g} (v_2^2 - v_1^2). \quad (6.30)$$

Hydraulic Losses in Pipelines and Equipment

In pipelines, pressure losses are the same as in the coolant passage; they are composed of losses due to friction on the wall of the pipeline and local losses, i. e.,

$$\Delta p_{tot} = \Delta p_{fr} + \Delta p_{loc}. \quad (6.31)$$

Losses due to friction in pipelines are determined just as in the coolant passage, by formula (6.14):

$$\Delta p_{fr} = \lambda \frac{l}{d_p} \gamma \frac{v^2}{2g},$$

where the coefficient of friction, depending upon conditions of flow is determined by the formulas (6.16)-(6.18).

Local losses in pipelines are determined as the sum losses of pressure due to different causes (bending of the pipe, inlet and outlet of the pipe, sudden or smooth expansion or constriction of flow, merging and separation of flows, etc.), i. e., $\Delta p_{loc} = \sum \Delta p_{loc i}$.

The value of local losses in each case is determined by formula (6.29):

$$\Delta p_w = \frac{1}{2} \gamma \frac{w^2}{g},$$

where ξ - drag coefficient determined in reference to each case of losses.

Losses in valves and throttles (Δp_{vn} and Δp_{vt}) are calculated also by formula (6.29). The problem thus is reduced to determination of loss factor ξ . In connection with the great variety of forms of valves (or various kinds of regulators) it is impossible to give a universal recommendation for all types. Usually the value of ξ for valves of regulating devices and throttles is estimated according to results of pour through of similar designs.

Hydraulic Characteristic of the System

The Hydraulic characteristic of the feed system we will call the dependence of necessary feed pressure (or head) on flow rate of components.

In accordance with equation (6.12) necessary feed pressure

$$p_{\text{nos}} = p_i + \Delta p_0 + \sum \Delta p_i,$$

where Δp_i - hydraulic losses in the system due to various causes.

During a change in flow rate of components, pressure in the chamber p_i , in first approximation will be changed directly proportionally to the flow rate, and change of sum $\Delta p_0 + \sum \Delta p_i$ can be taken as proportional to the square of the flow rate. Summing the value p_i and $\Delta p_0 + \sum \Delta p_i$ for different flow rates, we will obtain the hydraulic characteristic $p_{\text{nos}} = f(G)$ (Fig. 6.23a).

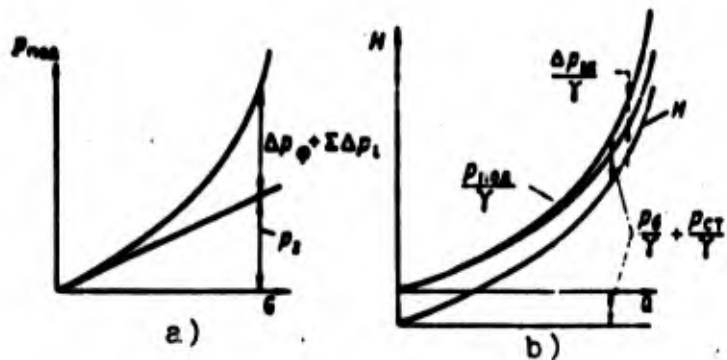


Fig. 6.23. Hydraulic characteristics of the feed system.

Value of required pressure, created by the pump of a ZhRD is defined as difference feed pressure and pump inlet pressure, i. e.,

$$H = \frac{P_g}{\gamma} - \frac{P_{in}}{\gamma} - \frac{P_{ct}}{\gamma}. \quad (6.32)$$

According to equation (6.1)

$$\frac{P_{ct}}{\gamma} = \frac{P_1}{\gamma} + \frac{P_{ct}}{\gamma} - \frac{\Delta P_{M1}}{\gamma},$$

whence

$$H = \frac{P_{req}}{\gamma} - \left(\frac{P_1}{\gamma} + \frac{P_{ct}}{\gamma} \right) + \frac{\Delta P_{M1}}{\gamma}. \quad (6.33)$$

Value $(P_1/\gamma) + (P_{ct}/\gamma)$ does not depend on flow rate of the component. Value of pressure losses in the inlet main line $\Delta P_{M1}/\gamma$ is proportional to the square of the flow rate. Summing all the components of the right side of equation (6.33), we obtain the hydraulic characteristic of change of required pressure of pumps depending upon flow rate $H=f(Q)$ (Fig. 6.23b).

6.7. Systems of Control and Adjustment of a ZhRD

General Information

According to the problems facing a control system, it is possible to distinguish two basic groups of systems¹.

1. Systems ensuring starting and shut-off of the propulsion system.

2. Systems ensuring maintenance of assigned operating conditions of the chamber of the engine and the propulsion system.

Devices of the first group of systems to a considerable degree are determined by the method selected for starting and shut-off of the propulsion system (see section 5.4). Basic requirements for this group of devices - guarantee of reliability of starting and shut-off, guarantee of prescribed time of arrival at the method and time of full cessation of operation of the system during possible change in temperature of units and operating conditions of the propulsion system. Thus, an important characteristic of operation of a system is the time of arrival at conditions during starting of the system. For the engines of ballistic missiles this time amounts to less than 2-3 seconds. For engines of guided antiaircraft missiles and antimissile missiles time of arrival at conditions should be still shorter.

Basic requirements for devices of the second group of control systems - guarantee of reliable operation of the engine under prescribed conditions, maintenance of constant or assigned conditions of thrust and ratio of components. Depending upon the purpose of the ZhRD, rigidity of these requirements is different. Tentatively one may assume that for engines of ballistic missiles, the control system should maintain prescribed thrust to within accuracy of 2%, ratio of flow rates of components into the chamber - with an accuracy of 1.5% and in a gas generator - up to 2%, boost pressure of tanks - with an accuracy of 3%. For engines of guided antiaircraft rockets the required accuracy of maintenance of thrust - to 2%, ratio of flow rates of components into the combustion chamber and into the gas generator - to 2.5-3%, and boost pressure - 3.5-4%. These requirements are approximate and in each concrete case can be changed substantially.

Let us consider basic methods of thrust control of the engine and certain possible circuits for control of the operation of the whole propulsion system.

Methods of Thrust Control

Thrust control of a ZhRD is necessary both for maintaining constancy of thrust during change in operating conditions of the propulsion system and also for changing thrust for the purpose of maintaining prescribed flight conditions of the rocket.

Possible methods of thrust control can be obtained from consideration of thrust equation (1.12): $P = K f_{np} p_2$.

We see that thrust can be changed effecting $K f_{np}$, or p_2 ; according to equation (1.13) with a given fuel (i. e., n_m) it is possible to change thrust coefficient K by only changing the ratio f_2/f_{np} . However, in practice, to produce a design allowing a change of f_2/f_{np} is difficult.

A second possible method of thrust control - changing the area of critical throat section f_{np} , which is possible, first, placing in the critical section a profiled bullet 1 (Fig. 6.24). By shifting the bullet along the axis of the chamber, we can increase or decrease f_{np} . In so doing the possibility is ensured of deep adjustment (i. e., a large range of change of thrust). The main disadvantage of this method - in considerable complication of construction, in the first place due to difficulty in providing cooling of the mobile bullet. Therefore such method of adjustment of f_{np} up to now has not obtained wide use.

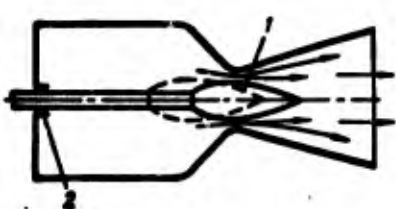


Fig. 6.24. Diagram of change of f_{np} by a profiled bullet. 1 - bullet; 2 - bullet packing.

It is possible also to change f_{np} by cutoff of one or several chambers of a multichamber ZhRD. Thus preservation of the operating characteristic of each chamber is ensured. Such a method permits changing thrust in any range. A disadvantage lies in the "stepness"

of the change of thrust. Furthermore, in this way we lose out in mass, since with a decrease of thrust the turned off chamber becomes ballast.

However, due to the possibility of changing the thrust of the propulsion system within wide limits, this method finds application in a number of cases (for example, in an aircraft ZhRD).

Basically, the most widely used, method of thrust control is change of pressure in chamber p_2 by means of changing the flow rate of components. This method makes it possible to regulate thrust in a wide range of changes by 3-5 times. In Table 6.2 different methods are given for thrust control by means of changing the pressure in the chamber.

Table 6.2. Methods of thrust control by changing the pressure in the combustion chamber.

Methods of adjustment	Characteristics of the adjustment method
1. Change in number of revolutions of TNA: a) change in flow rate of the working substance to the turbine at constant temperature. b) change in temperature of the working substance by changing the ratio of flow rates of components.	Quick reaction; Impairment of operating characteristics of propulsion system due to operation of the TNA at partial load conditions. Method, "a" is more acceptable with an open circuit; method "b" - with a closed circuit.
2. Throttling of flow rate of components into the combustion chamber.	Quick reaction. Possible both with pressurized feed and with feed from TNA. In the first case, superfluous pressure in tanks, i. e., superfluous mass. With supply from TNA - unproductive TNA power input.
3. Cutoff of part of the injectors.	Analogous to condition 2. Danger of burnout of head appears.
4. Change in pressure drop at the injectors.	Analogous to condition 2.

Table 6.2. (Cont'd)

Methods of adjustment	Characteristics of the adjustment method
5. Diversion of part of the flow of components.	Quick reaction. Superfluous expenditure of power of the TNA for circulation of component.
6. Change of pressure in tanks with pressure feed.	Very slow process. It is necessary to bleed pressure from the tanks. Superfluous safety factor of tanks, i. e., superfluous mass.
7. Change in ratio of flow rates of components into the combustion chamber.	Quick reaction. Impairment of operating characteristics of the combustion chamber.

With a necessity of changing thrust in a range up to 10-15% the most widespread method of thrust control is by means of changing the number of revolutions of the TNA. As an example, in Fig. 6.25 there is shown a typical thrust control circuit of a ballistic missile to ensure the prescribed conditions of flight of the rocket.

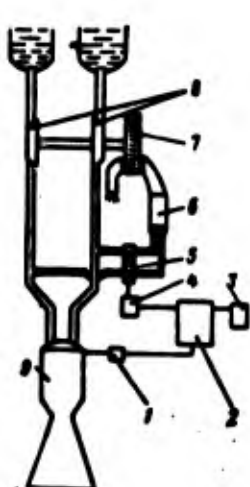


Fig. 6.25. Diagram for thrust regulation of a ZhRD to ensure prescribed flight conditions of a rocket. 1 - pressure pickup; 2 - computer; 3 - source of energy; 4 - drive; 5 - throttle regulators; 6 - ZhGG; 7 - turbine; 8 - pumps; 9 - chamber.

The arriving signal is pressure in chamber p_1 (since thrust is proportional to pressure). From pressure pickup 1 the signal enters the monitoring computer 2, where actual flight conditions of the

rocket are compared with those prescribed. According to the existing mismatch of flight conditions the necessary change of pressure in chamber (i. e., thrust) is determined. A signal from device 2 reaches the throttle regulating valve (or valves) in the system of feeding components to the gas generator. Flow rate (or ratio of expenditures) of components into the ZhGG 6 is changed, change accordingly is made in feed working substance to turbine 7 of the TNA, there is a change in number of revolutions of pumps 8 and in fuel feed to combustion chamber 9. In conformity with change of fuel feed pressure is changed in chamber and of thrust of a ZhRD.

Besides the methods examined a small change of thrust can also be effected by choking or diverting part of the fuel consumption (Table 6.2, para. 2 and 5).

Possibility of changing thrust in a wide range is hampered in the first place by the fact that during change of flow rate of components pressure drop on injectors is sharply changed, proportional to the square of the flow rate. Due to this, on systems of greatest thrust a considerable increase of feed pressure is necessary. For maintenance of constant feed pressure, in certain cases, part of the injectors are disconnected (para. 3).

Furthermore, difficulties with guaranteeing cooling of engine in conditions of least thrust appear, since, with a decrease of fuel consumption and slow rate of coolant decreases accordingly.

Due to the causes mentioned, with a necessity of change of thrust in wide limits, frequently it is more expedient to use a multichamber installation.

Possible Circuits for Maintaining Assigned Operating Conditions of a System

To ensure assigned operating conditions of a propulsion system and to achieve the required law of change of speed of a rocket according to time of flight it is necessary to regulate, besides thrust of the system, still a whole series of parameters (oxidant-fuel ratio,

entering the chamber, and in ZhGG, pressurization of tanks, operation of steering motons, etc.).

In the propulsion systems of ballistic missiles, one of the basic systems is a control system by oxidant-fuel ratio. Its purpose - to maintain the flow ratio within set limits and to ensure simultaneous output of tanks of both components. The fact is, that due to the action of acceleration on the feed system and, connected with this, the pressure differences on entrance to the pump, and also due to the change in density of components during change in their temperature and possible instability of the characteristics of the pumps, actual flow rates of components differ from nominal (calculation). This can lead to a deviation of the oxidant-fuel ratio from that calculated, and to nonsimultaneous emptying of tanks, i. e., to incomplete use of components.

These systems are usually founded either on measurement of levels of components in tanks, or on measurement of flow rate per second (Fig. 6.26a, b).

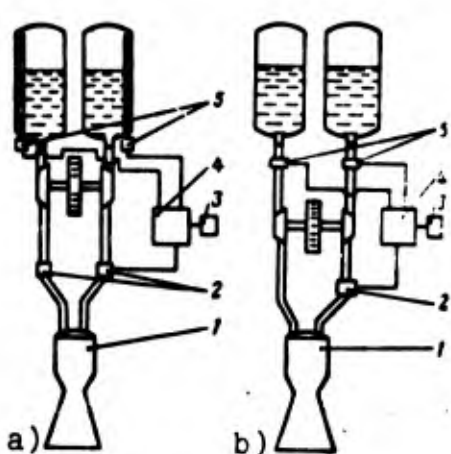


Fig. 6.26. Diagrams of systems for control by oxidant-fuel ratio. a) system with measurement of levels of components in tanks. b) system with flowmeters.
1 - chamber; 2 - throttle regulators;
3 - source of energy;
4 - computer; 5 - transducer of level of fuel in tanks; 6 - flowmeters.

In Fig. 6.26a there is an example of a system of emptying tanks (SOB) based on measurement of levels of components in the tanks. Transducers of fuel level in tanks 5 give a signal regarding the output of the component to the computer system 4. From the system signals reach the throttle regulators 2, which, throttling the flow

rate of one or another component, ensure the prescribed ratio of expenditures of components and simultaneous emptying of the tanks.

To ensure simultaneous emptying of tanks it is usually more expedient to have the throttle expenditure regulator system only on the feed line of one of the components as is shown in the diagram of Fig. 6.26b. In this way expenditure of one of the components by means of throttle regulator 2 "is tuned" to the flow rate of the second component.

During operation of the propulsion system, to ensure the prescribed operating conditions, simultaneously several parameters are regulated (first of all, thrust and oxidant-fuel ratio entering the chamber).

In Fig. 6.27a examples are given of simplified diagrams of control of propulsion system operation. In diagram 6.27a there is shown a system ensuring the maintenance of prescribed thrust conditions and simultaneous emptying of the tanks. In this way, change in flow rate of components into the chamber can be ensured both by changing the feed of the TNA by means of influencing expenditure of components in gas generator 8, and also by direct influence on throttle regulator 5 (shown by the dotted line). For exact maintenance of oxidant-fuel ratio sometimes there is set a regulator (stabilizer) of oxidant-fuel ratio (RSK) 11. In Fig. 6.27b there is shown a system of maintaining given thrust values and oxidant-fuel ratio.

With the ZhRD system on the smaller and more maneuverable rockets, in which simultaneous emptying of tanks does not play so great a role as in ballistic missiles (for example, guided antiaircraft missiles, torpedos, etc.) the necessity for a special system of emptying tanks is reduced. In this case, for maintenance of the oxidant-fuel ratio it is sufficient to have a system for stabilizing the oxidant-fuel ratio.

With a gas generator operating on basic components, for supporting the prescribed oxidant-fuel ratio entering the gas generator,

sometimes there is also set a stabilizer 12 of the oxidant-fuel ratio in the gas generator, throttling flow rate in the ZhGG of one of the components in accordance with the flow rate of the second component (Fig. 6.27c).

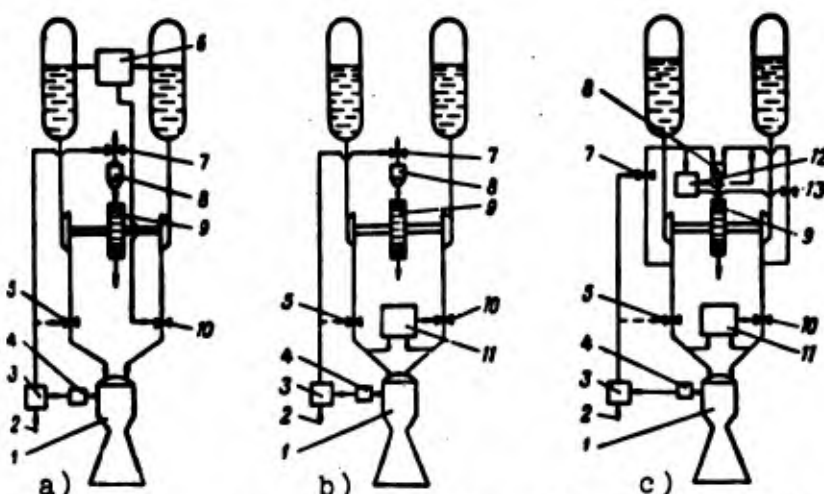


Fig. 6.27. Simplified control circuits of a ZhRD. 1 - chamber; 2 - command from the ground; 3 - computer; 4 - pressure transducer; 5 - flow rate throttle regulator; 6 - tank emptying system; 7 - fuel feed control in a ZhGG (or PGG); 8 - ZhGG (or PGG); 9 - turbine; 10 - throttle regulator; 11 - stabilizer of the chamber; 12 - stabilizer of ZhGG; 13 - throttle of the ZhGG stabilizer.

Changing Direction of a Thrust Vector

In Fig. 6.28 different methods are shown for changing the direction of a thrust vector.

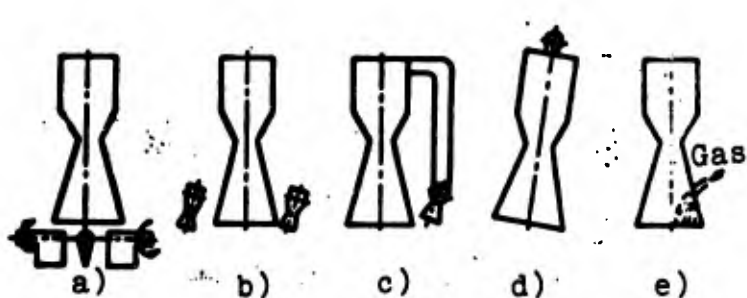


Fig. 6.28. Methods of changing the direction of a thrust vector. a) jet vanes; b) thrust chambers. [Translator's note: Russian term literally reads: "steering engines"]. c) gas from the TNA; d) gimbal suspension; e) blowing gas.

Changing the direction of a thrust vector by means of jet vanes (Fig. 6.28a) was even proposed by D. E. Tsiolkovskiy and was successfully used on a number of rockets. A disadvantage of the method - in comparatively great thrust losses since the jet vanes are constantly in the jet stream.

Use has been found for the following methods of changing the direction of a thrust vector shown in Fig. 6.28b, c. d. A disadvantage of these methods - in the necessity for a special drive for turning the thrust chamber or the actual chamber. Furthermore, use of thrust chambers requires a special feed system.

Control by direction of a thrust vector by means of blowing gas into the supercritical part of the nozzle (Fig. 6.28e) is convenient in the fact that it does not require a special drive for turning the chamber. In the case of using a nozzle with a central body, direction of thrust vector can be changed by changing fuel flow rate on separate sections of the annular combustion chamber. When using a cluster engine, direction of thrust vector can be changed also by means of mismatch of thrusts of separate chambers of the cluster engine.

6.8. Examples of Systems Carried Out with Turbopump Feed

We shall consider some examples of actual propulsion systems. In them there is provided specific presentation about methods and order of starting and shutting off of ZhRD, about methods of driving a TNA, pressurizing tanks multiple starting, and also about the operation and arrangement of the propulsion system on the whole.

Propulsion System of the Second Stage Carrier Rocket "Cosmos"

In Fig. 6.7 there is shown the ZhRD RD-119 "Cosmos," the most highly developed in respect to specific thrust of any known ZhRD of the oxygen class with a high-boiling fuel. (developed in 1958-62 by the organization created as a part of GDL [Translators note: possibly stands for] [25]. Its data is as follows.

Propulsion system - open circuit. Drive of TNA from PGG, working on NDMG; spin-up of TNA (starting) from a starting pyrostarter. Engine has system of steering nozzles 1, 2, 3, 13, 15. Steering system is designed for the control and orientation of second stage of the control and orientation of second stage of the "Cosmos" rocket by means of redistribution of products of combustion by means of distributors 4, 5, 11. Thrust of the propulsion system is regulated.

Propulsion System of the First Stage of the Space Rocket "Vostok"

In Fig. 6.29 there is shown the ZhRD RD-107 "Vostok" – the first oxygen class engine in the world, using hydrocarbon fuel (developed in 1954-57 in the organization which developed the ZhRD "Cosmos").

The ZhRD "Vostok" was used as the power plant on the first stage of a number of rockets for sending spacecraft into circumterrestrial orbit and to the nearest planets of the solar system (for example, spaceship "Vostok-1"). Its data is as follows.

Fuel.....	liquid oxygen + hydro-carbon fuel
Thrust in a vacuum.....	102 r (1 MN)
Specific thrust in a vacuum.....	$314 \text{ kgf}\cdot\text{s/kg}$ ($3070 \text{ N} \times \text{s/kg}$)
Expansion ratio.....	$p_0/p_\infty = 1/150$
Pressure in chamber.....	60 [atm(abs.)]

Propulsion system - open circuit. Drive of TNA from PGG, working on hydrogen peroxide. TNA has 4 pumps (oxidizer, combustible, hydrogen peroxide, and liquid nitrogen utilized for pressurizing tanks). Gasification of liquid nitrogen is produced in heat exchanger 8, heated by steam gas from the TNA. Internal cooling of chamber - by fuel passed through injectors on the head; ignition is pyrotechnic;

starting is staged through preliminary stage or thrust; control by thrust vector by means of a steering ZhRD 1. Thrust is regulated by changing the flow rate of hydrogen peroxide to the TNA.

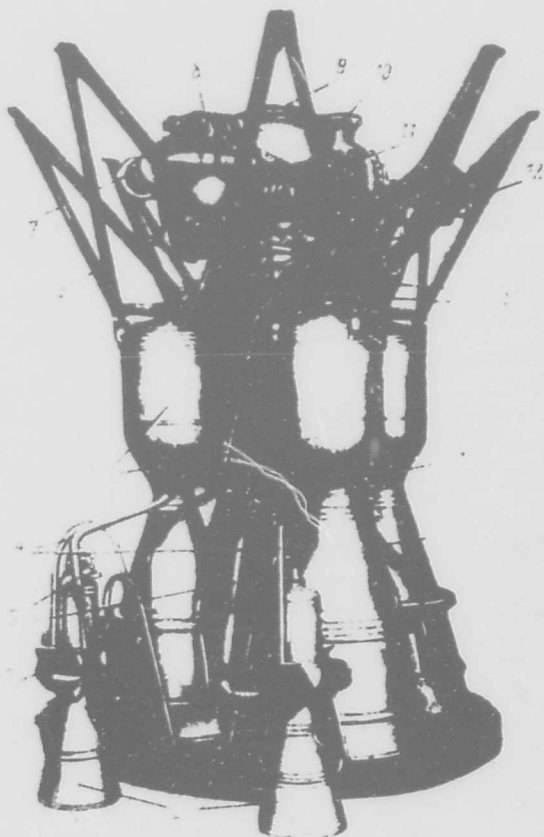


Fig. 6.29. ZhRD RD-107 "Vostok."
1 - steering ZhRD; 2 - node of pumping and feed of oxidizer; 3 - pipelines of oxidizer of steering ZhRD; 4 - mock-up brackets; 5 - basic chambers of the engine (4 pieces); 6 - power frame; 7 - PGG; 8 - body of heat exchanger on the turbine; 9 - inlet duct of oxidizer pump; 10 - inlet duct of fuel pump; 11 - transducer of pressure in the chamber; 12 - main oxidizer valve; 13 - oxidizer pipelines; 14 - main fuel valve; 15 - fuel pipelines.

Propulsion System of the First Stage of a Three-Stage Rocket

In Fig. 6.30 a diagram shows the feed system and a view of the RZ-2 propulsion system, consisting of a two-chamber engine. Its basic data is as follows.

Fuel..... liquid oxygen + kerosene

Thrust of the propulsion system.....~134 r (1.31 MN)

Thrust of one chamber P:

- at sea level.....62.145 r (0.6 MN)

- at the end of boost phase($H=75 \text{ km}$). 76.2 r (0.75 MN)

Specific thrust P_{sp} :

- at sea level..... $245 \text{ kgf}\cdot\text{s}/\text{kg}$ ($2403 \text{ N} \times \text{s/kg}$)

- at the end of boost phase($H=75 \text{ km}$). $289 \text{ kgf}\cdot\text{s}/\text{kg}$
(~ $2835 \text{ N}\cdot\text{s/kg}$)

Oxidant-fuel ratio:

- at sea level.....2.16

- at the end of boost phase².....2.45

Pressure in combustion chamber.....38.25 [atm(abs.)]
(3.75 MN/m^2)

Feed.....turbopump

Drive of TNA.....from restoring ZhGG,
working on basic components with a ratio
 $\nu=0.351$

Feed pressure:

oxygen.....52.94 [atm(abs.)]
(5.19 MN/m^2)

Kerosene.....55.38 [atm(abs.)]
(5.43 MN/m^2)

Combustion duration of ZhRD.....160 s

Certain parameters characterizing operation of the chamber of the engine and TNA are given in section 5.1 and 7.4.

To ensure strict starting sequence there is an electropneumatic system with blockings allowing switching on of the next unit only after the entering of the impulse indicating that the preceding unit has fulfilled its functions. The pneumatic part of the system is assembled on the engine, and the electric part consists of ground relay block, connected with box relay on the engine. The working substance of the pneumatic system (gaseous nitrogen at a pressure of 52.2 [atm(abs.)] (5.12 MN/m^2) is kept in six bottles mounted on the

rocket. Before beginning the starting, the rocket engines are connected to priming fuel tanks (see Fig. 6.30) located on the ground unit. After pushing the "start" button the ground and on board systems of automation goes into action and starting of the propulsion system is conducted in the following order.

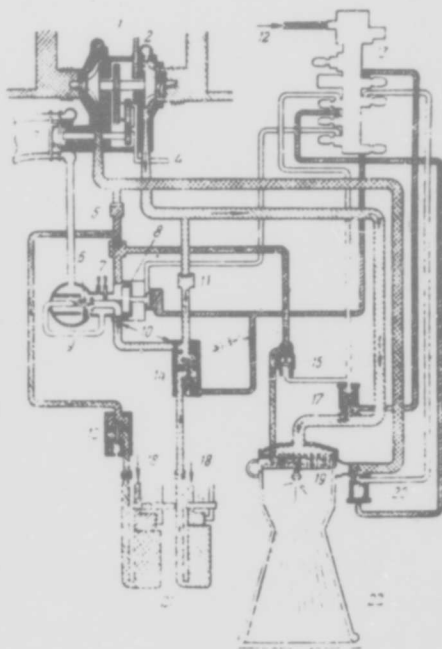


Fig. 6.30. Feed system and view of ZhRD of the RZ-2 rocket. 1 - pumps; 2 - drainage; 3 - turbine; 4 - lubrication feed; 5 - check valve; 6 - igniter; 7 - drainage; 8 - valve ZhGG; 9 - ZhGG; 10 - throttle (jet); 11 - check valve; 12 - high pressure nitrogen from on-board system; 13 - distributor of nitrogen feed; 14 - liquid oxygen filling and check valves; 15 - feed valve of starting fuel; 16 - kerosene filling and check valves; 17 - main oxygen valve; 18 - feed of nitrogen from ground system; 19 - igniter; 20 - main kerosene valve; 21 - ground tanks of fuel and oxidizer; 22 - chamber; 23 - wire contact.

From the ground system via tubes 18 nitrogen is supplied for blowing starting tanks 21 and the tanks with lubrication for the reducing valve. In the combustion chamber pyrotechnic igniter 19 ignites and after burnout the electrical contact in it by means of a electropneumatic connection the main oxygen valve 17 and flow valve

for starting fuel 15 are opened. Oxygen under pressure of static pressure in tank of the propulsion system and kerosene under boost pressure in starting tank 21 enter the combustion chamber where they ignite from igniter 19. The resulting flame destroys wire indicator of ignition 23 set an outlet from the chamber. Thereupon, ZhGG igniter 6 closes; the contact in the igniter burns out and the command is given to open the main kerosene cutoff valve 20. ZhGG valve 8 is opened, the components enter the ZhGG, and the products of combustion -- from the ZhGG to turbine 3. As a result, spin-up of the TNA occurs, and the pumps begin to pass the component through the main valves into the combustion chamber.

When outlet pressure from the pumps exceeds feed pressure from the starting tanks, check valves 5 and 11 are opened and into the ZhGG the component from the on board feed system begins to move. Thereupon the valves of the ground starting system 14 and 16 will be closed.

Time of reaching conditions of full thrust from moment of beginning starting amounts to 4 s.

The engine will be disconnected from the control system by the flight of the rocket. In this way ZhGG valve 8 and main oxygen valve 17 are closed, and after 0.2 s kerosene valve 20 is closed.

Propulsion System of an Intercontinental Long-Range Ballistic Missile [BRDD]

In Fig. 6.31 there is an assembly diagram of the propulsion system of an intercontinental BRDD. It consists of five ZhRD with thrust (on the ground) of 68 r (0.67 MN), a sustainer with thrust of 27.2 r (0.267 MN) and two steering engines with thrust of 450 kgf (4415 N). During the start all five engines work. The starting ZhRD works 145 s, after which the block of boosters is dropped together with the five tanks and further motion of the rocket is carried out by the sustainer and the steering ZhRD. Time of operation of the sustainer is 300 s. A rocket of this type is sometimes called one-and-a half stage, since the boosters of the first stage and the

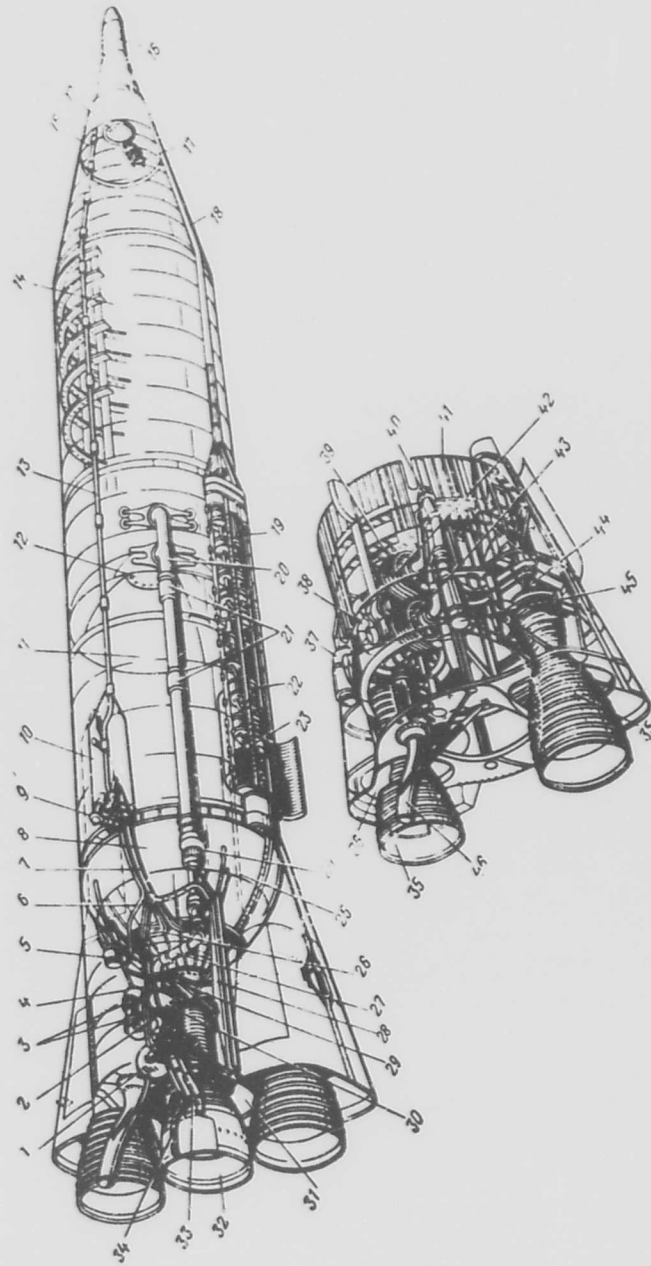


Fig. 6.31. Assembly diagram of the propulsion system of a BRDD and the jettisonable block engines of the "Atlas" rocket. 1 - tank of liquid helium, fitted with a jacket with liquid nitrogen (a total of 6 tanks); 2 - turbine of TNA of the sustainer ZhRD; 3 - bellows; 4 - fuel supply pipeline; 5 - removable connection of the fuel supply pipeline; 6, 7 - pipelines supplying oxidizer and combustible to the control ZhRD; 8 - lower bulkhead of fuel tank; 9 - control ZhRD; 10 - fairing of the control ZhRD; 11 - fuel tank (kerosene); 12 - hatch cover; 13 - pipeline for pressurizing the oxidizer tank with helium; 14 - oxidizer tank (oxygen); 15 - upper bulkhead of oxidizer tank; 16 - nose cone; 17 - vent valve of oxidizer tank; 18 - cable cover; 19 - recessed antenna; 20 - pipeline for supplying and filling the oxidizer; 21 - bellows; 22, 23 - compartments with instrumentation; 24 - separable connection with pipeline for supplying and filling of oxidizer; 25 - pipeline for pressurizing of fuel tank with helium; 26 - hydraulic and other connections for controlling the ZhRD; 27 - pipeline for supplying oxidizer; 28 - rails for dropping the booster ZhRD; 29, 30 - pumps for oxidizer and fuel; 31 - fireproof shield; 32 - sustainer ZhRD; 33 - heat exchanger on the exhaust duct of the TNA for preheating helium; 34 - drainage tube of the TNA; 35 - starting ZhRD; 36 - asbestos heat insulation; 37 - tank filler neck; 38 - fuel pipeline; 39 - ZhGG (recovery); 40 - separation coupling; 41 - booster engine skirt; 42, 43 - pumps for fuel and oxidizer; 44 - main fuel valve; 45 - oxidizer valve; 46 - TNA exhaust duct.

sustainer begin to operate simultaneously. All five ZhRD have a gimbal thrust pad. The steering engines after exact adjustment of velocity vector and turning off of the justainer ZhRD ensure roll control.

Tanks of the propulsion system - supporting. Their ridigity is ensured by a set of frames and stringers, and also pressurization of the tanks with helium. Capacity of the upper tank of oxygen is 71 m^3 , capacity of the lower, kerosene, tank- 44m^3 . Location of units of propulsion system is shown in Fig. 6.30.

Propulsion System of a First Stage Carrier Rocket

In Fig. 6.32 and 6.33 there are shown assembly diagrams of the propulsion system of first stage carrier rocket "Saturn," consisting of a cluster of eight H-1 engines. Basic data on the system is as follows.

Fuel.....	liquid oxygen + ker-
	osene
Thrust of propulsion system.....	680 r (6.67 MN)
Thrust of one chamber at sea level.	85 r (0.83 MN)
Specific thrust at sea level.....	255 kgf.s/kg (2500 N.s/kg)
Expansion ratio of nozzle.....	$t_s/t_{k_p}=8$
Combustion duration.....	$110-150 \text{ s}$

Drive of the TNA - from the reducing ZhGG operating on basic components. The four internal engines are fixed at an angle of 3° to the axis of the rocket. The four external (rotatable) engines are secured in a gimbal thrust pad at an angle of 6° to the axis of the rocket and can be deflected to an angle of 7° for change in direction of thrust vector of the system. Each engine has its own TNA rigidly joined with the chamber of the engine. With such an installation of the TNA on a turning chamber the flexible section of the main lines of components is the section between the tanks and the TNA. This facilitates turning chamber, since pressure of a component on a given section always remains comparatively small.

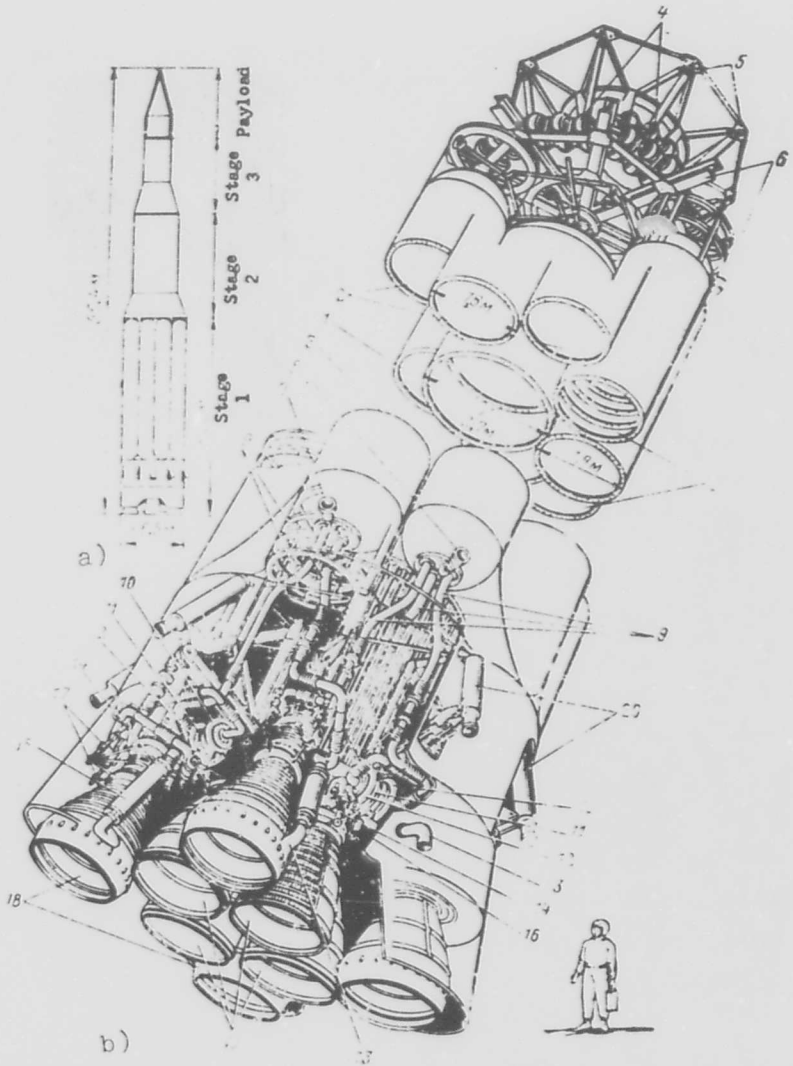


Fig. 6.32. Assembly diagram of the propulsion system of first stage of the carrier rocket "Saturn." a) general outline of the rocket; b) assembly diagram of first, booster stage of the rocket; 1 - central tank with oxidizer; 2 - external tanks with oxidizer; 3 - tanks for fuel; 4 - bottles with helium; 5 - mounting lugs of the second stage; 6 - lower part of frame under first and second stage; 7 - fuel filler neck; 8 - oxidizer filler neck; 9 - pipelines for supplying oxidizer; 10 - oxidizer pump; 11 - turbine of TNA; 12 - fuel pump; 13 - exhaust of turbine of TNA; 14 - powder pressure accumulator for starting the turbine of the TNA; 15 - heat exchanger; 16 - tank with lubrication for TNA; 17 - hydraulic drives for rotating combustion chambers; 18 - rotating combustion chambers; 19 - internal fixed combustion chambers; 20 - retrorockets of the return system.

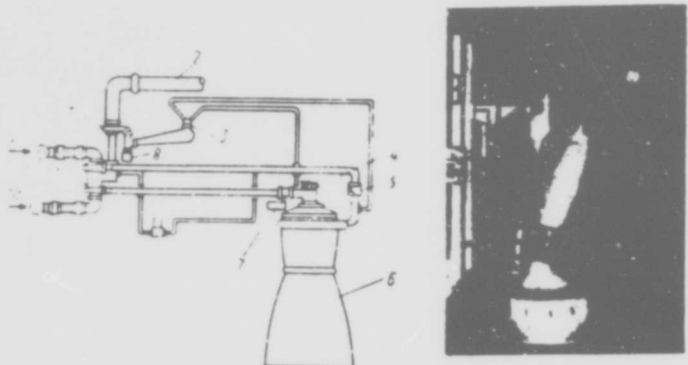


Fig. 6.33. Diagram of feed system and mock-up of the N-1 engine of a "Saturn" rocket." 1 - turbine; 2 - exhaust duct; 3 - ZhGG; 4 - gimbal thrust pad of the engine; 5 - main fuel valve; 6 - chamber; 7 - main oxidizer valve; 8 - starting PAD; 9 - fuel feed; 10 - oxidizer feed; 11 - TNA;

On the outboard engines are set heat exchangers 15, in which oxygen is heated which is utilized for pressurizing the tank oxidizer. For pressurizing the tanks of fuel helium is used which is passed from bottle 4. Propulsion system is started from one command which is given immediately after termination of filling. To avoid a one-sided load or strong blow during simultaneous switching on of all eight chambers engine they are switched on in symmetric pairs at intervals of 0.25-0.4 s.

Starting of an individual engine takes place in the following order (Fig. 6.33 and 6.34). At the "Start" signal the charge of the starting PAD (starter) 8 ignites, hot products of combustion of the PAD reach the turbine wheel of the TNA and begin its spin-up. After achieving the necessary outlet pressure from the TNA main oxygen valve 7 is opened, and there also begins supply of starting fuel to the combustion chamber through a special belt of injectors which will form an ignition flame with the liquid oxygen. After the starting combustible the basic fuel - kerosene reaches the chamber. After opening of main valves 5 and 7 by feed pressure, part of the fuel from the basic main lines enters ZhGG 3 and further operation of the TNA occurs from the ZhGG working on basic components. Fuel feed to the ZhGG is regulated by two plate valves compressed by springs.

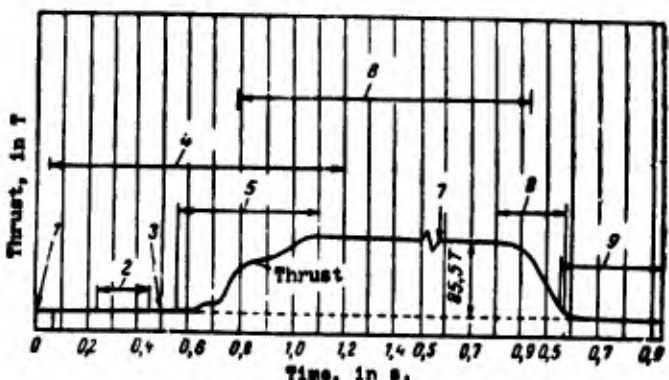


Fig. 6.34. Diagram of starting and shut-off of an N-1 ZhRD of a "Saturn."
 1 - signal to start; 2 - main oxygen valve is opened; 3 - injection of igniter fuel; 4 - solid fuel starting gas generator operates; 5 - main fuel flow valve is opened; 6 - main gas generator of the engine operates; 7 - signal for shutting off the engine; 8 - main oxygen valve is closed; 9 - main fuel flow valve is closed.

Total outlet time of the engine per schedule is 1.5 s. Character of thrust buildup during starting is shown in Fig. 6.34.

To shut off the engine, a signal reaches the pyrocharge, after the explosion of which the oxygen valve is closed, supply of components to the ZhGG ceases, the TNA ceases to pass fuel and all remaining valves are closed under action of springs due to drop in pressure.

In the propulsion system provision is made for the possibility of operational refusal of two engines out of eight (one of them controlling). Refusal of one engine is permissible immediately after start, a second one, after 60 s. In this way, the fuel system automatically switches supply from the non-operating engine to the working one.

Aircraft Liquid Fuel Rocket Engine

In Fig. 6.35 there is a diagram of the feed system of a liquid rocket engine, XRL-99 which is the sustainer of the X-15 aircraft and having the following basic data.

Engine.....multiple starting with controllable thrust in a range of 100-30%
 Fuel.....liquid oxygen + liquid ammonia; oxidant-fuel component ratio ~ 1.25

Thrust:

- on the ground.....22.7 τ (0.22 MN)
- at an altitude of 30 km.....25.8 τ (0.25 MN)

Specific thrust at an altitude of 30 km.....276 kgf·s/kg (2740 N \times s/kg)

Pressure in chamber.....42 [atm(abs.)] (4.12 MN/m²)

Drive of TNA.....from the PGG working on 90% H₂O₂

Combustion duration of engine for one flight (determined by capacity of tanks).....120 s

Lifetime of the engine.....1 h

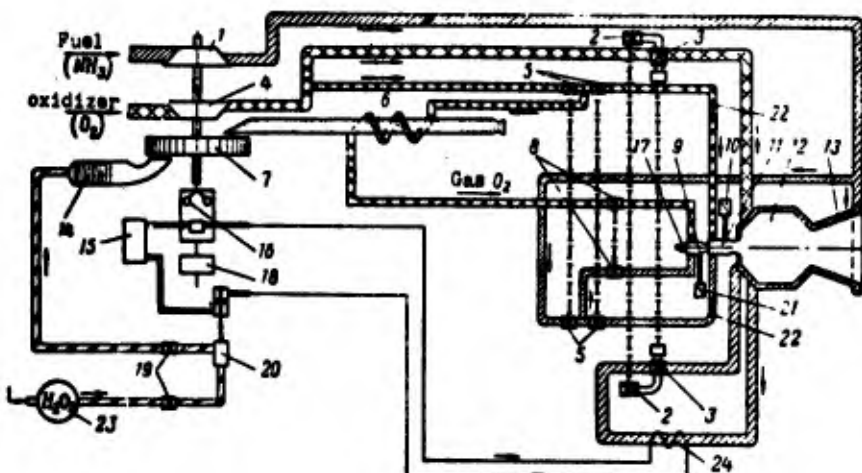


Fig. 6.35. Feed system of an aircraft ZhRD.
 1 - fuel pump; 2 - flow-through valves; 3 - main cutoff valves; 4 - oxidizer pump; 5 - cutoff valves of starting chamber 11; 6 - evaporator; 7 - turbine; 8 - cutoff valves of starting chamber; 9 - starting chamber of first stage stage; 10 - relay; 11 - starting chamber of second stage; 12 - engine chamber; 13 - coolant passage; 14 - PGG; 15 - hydraulic drive power supply; 16 - speed regulator; 17 - spark igniter plug; 18 - servodrive; 19 - peroxide cutoff valves; 20 - peroxide feed adjuster; 21 - relay; 22 - Venturi tube; 23 - 90% hydrogen peroxide unit; 24 - heat exchanger of the hydraulic system.

To ensure increased requirements for reliability and safety of operation of a ZhRD provided by the propulsion system of the engine on piloted aircraft a two-stage system of starting with help of starting chambers of first and second steps (9 and 11) is provided. Components in the starting chamber of the first stage ignite from spark plug 17, and in the starting chamber of the second stage and in the main chamber 12 – from the flame proceeding respectively from chambers 9 and 11. Starting launching and stopping of the propulsion system are produced in the following order.

Before the beginning of starting, by means of valves 2 there are produced pour-through of the TNA and basic main lines of fuel feed for the purpose of guaranteeing the operating temperature conditions of the metallic parts of the TNA, the main lines, and the valves. Then, there is switched on the blowing of the combustion chamber with helium. Starting of the engine is carried out by opening the hydrogen peroxide regulating and cutoff valves 19 and 20 entering the PGG 14 where, passing through the assembly of catalyzing grids (35 grids, covered with silver, located alternately between 36 grids made of stainless steel), it is decomposed. The steam gas mixture reaches turbine 7 and sets in rotating the pumps of fuel 1 and oxidizer 4 located on the same shaft with the turbine. The pumps feed fuel into the main line to shut-off valves 3 and 5 which are still closed for supply of components, but open for pouring through.

Shut-off valves 8 are opened and the components enter the starting chamber of the first stage 9. In so doing, the oxidizer passes through evaporator 6, as a consequence of which it enters chamber 9 in a gaseous state. This ensures great reliability during first ignition, since it prevents accumulation of a large quantity of fuel. After ignition in the starting chamber 9, on a signal from relay 21 there are opened the cutoff valves 5 of the starting chamber of the second stage 11. After the beginning of operation of the starting chamber on a signal from relay 10 the main valves of the components 3 are opened. The components enter the engine chamber 12 where they ignite from the constant flame jet coming out of the starting chamber.

Shut off of the engine is produced upon receipt of a command to shut off the main valves. Fuel feed ceases and blowing of chamber 12 by helium is turned on. Starting chambers still operate 0.5-1 s to promote the burning of residual components of fuel displaced by the helium from the main lines into the chamber. After cessation of burning in chamber 12 the valves of the starting system are closed and their blowing with helium is switched on. After blowing of the engine with helium and its complete purification from remainders of fuel, the engine is ready for a new start. The number of possible repeated starts is limited by the supply of helium for blowing (usually 4-5). The sequence of operations of switching on and shutting off of the engine is ensured by an automatic device, controlling the functioning of each stage and after that switching on the next operation.

Thrust is regulated by changing the flow rate of hydrogen peroxide to the TNA by means of regulating (throttle) valve 20.

Comparison of the Systems Presented

Comparison of first systems with systems of later development shows that requirements both for a ZhRD and as to the power plant of aircraft have sharply increased. This is in connection with the accuracy of observance of parameters of the propulsion system, its economy, and reliability. Improved fuels are being used, which sharply increase the thrusts, created by the separate chambers and the propulsion system on the whole. In spite of this, there is a tendency to simplification of propulsion systems and their elements.

Simplification of propulsion systems occurs both by the application of simpler and more rational circuits, and also by means of improvement in the designs of the separate units.

It is possible to note several basic trends in simplification of elements of the propulsion system, first of all pertaining to starting the system. The complicated electropneumatic systems (for example, in the A-4 propulsion system which was examined in detail in [25] have been replaced by simpler and more reliable system. Improvement in the

design) of fuel valves permits simplifying their control system. For example, in the N-1 propulsion system, valves are opened in a defined sequence automatically, without a special electropneumatic control system. Starting of the propulsion system is also simplified for application of a powder pressure accumulator or head in the fuel tanks for spin-up of the TNA.

The various kinds regulating servosystems have been simplified by unification of several functions into one servosystem.

In a number of cases, much simplification has been attained by means of using the basic components to drive the TNA. This permits saving the installation of a third component (for example, hydrogen peroxide), with all the systems to ensure its storage and supply.

Furthermore, toward simplification of elements of the structure of the propulsion system a more rational diagram for location of pipelines and valves, application of flexible hoses, soldered nodes improved methods of bracing the engine and methods of ignition in the combustion chamber of a ZhRD have been performed.

Footnotes

¹For a detailed analysis of questions of automatic adjustment of ZhRD see [125].

²Increase of v at the end of booster phase occurs, first, due to unequal change of level of liquid in tanks and, secondly, from increase of acceleration from 1 g at start to 10 g at the end of boost phase ($H = 75$ km).

CHAPTER VII

TURBOPUMP UNITS

Basic unit of the system of pump feed of components is the turbopump assembly (TNA). Main elements of the turbopump assembly are pumps, feeding components at prescribed pressure; turbine, driving the pumps, and gas generator (liquid-gas generator [ZhGG]) or steam-gas generator [PGG]), in which the working substance of the turbine is obtained.

Designing the turbopump assembly involves designing these elements, and also auxiliary devices (discharges, ducts, etc), their general arrangement and determination of characteristics of joint operation.

The procedure of designing the pumps and turbines of the turbopump assembly does not differ in principle from conventional methods of designing centrifugal pumps and aviation turbines, but should consider peculiarities of operating conditions and arrangement of the propulsion system of liquid-fuel rocket engines [ZhRD].

Questions of theory and designing of the units and subassemblies of the TNA are discussed in detail in [132], [134], [136], [137], [138], [139], therefore we will examine only the basic questions and specific peculiarities of the selection of basic parameters when designing separate units and the TNA on the whole, and also certain characteristics of the TNA.

7.1. Pumps for Feeding Components to ZhRD

Pumps are divided into the following fundamentally different types: displacement, vane and jet.

Displacement pumps supply liquid, displacing it with some other solid, as for example, plunger, piston, gear and revolving pumps.

In vane pumps the energy necessary for increase of liquid pressure is imparted by vanes of the revolving wheel. Vane pumps include centrifugal and axial pumps.

Diagram of a jet (injector) pump is shown on Fig. 7.1. Here the component enters head 2. From nozzle 1 emanates gas (or liquid) of high energy, which attracts the component and pumps it through the head to the cavity of increased pressure. Increase of pressure is determined by energy of the stream emanating from the central nozzle. Advantage of jet pumps is in their structural simplicity and the absence of revolving parts. However, the efficiency of these pumps is low and to provide feed they require driving a greater quantity of gas than the TNA. Jet pumps have not yet found application in ZhRD as basic pumps, although recently the possibility of their use has been considered [13].

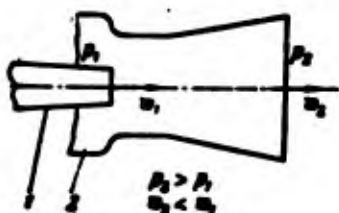


Fig. 7.1. Diagram of jet pump:
1 - nozzle; 2 - head.

In the TNA of ZhRD centrifugal pumps are usually applied as basic. In certain cases for preventing cavitation in the TNA there are installed additional axial (screw) or jet prepumps. With high volumetric flow rates the application of axial pumps as basic is possible.

Basic advantages, determining the preferential use of these types of pumps in ZhRD, are:

- provision of high feed pressures and productivity at small overall dimensions and mass;
- possibility of operating on aggressive and low-boiling components;
- possibility of operating with high r/min and convenience of use of a turbine for their drive.

Diagrams of Centrifugal Pumps

Figure 7.2 shows a diagram of a single-stage centrifugal pump. Liquid is fed to revolving wheel 2 through inlet duct 1. In the wheel of the pump liquid moves along a channel formed by walls of the wheel and vanes 3. Force exerted from the wheel vanes on the liquid causes it to move so that the reserve of energy per unit of mass of liquid is increased. In this case there occurs increase of both potential energy (static pressure) and kinetic energy of the liquid (its absolute velocity). Upon exiting the wheel the liquid enters diffuser 4, where its absolute velocity decreases and pressure additionally increases. The simplest diffuser consists of smooth disks, making up its walls and is called vaneless. Vaned diffuser has stator blades 5 (shown on Fig. 7.2 by dotted line), which promote faster suppression of the flow velocity. Passing the diffuser, the liquid enters spiral channel (volute) 6, the purpose of which is to collect the liquid exiting the wheel, and also to reduce its velocity. Liquid is fed to the network through the delivery duct.

In order to decrease overflow of liquid from the high-pressure cavity (diffuser, volute) to the low pressure region, in the pump there are made seals 7.

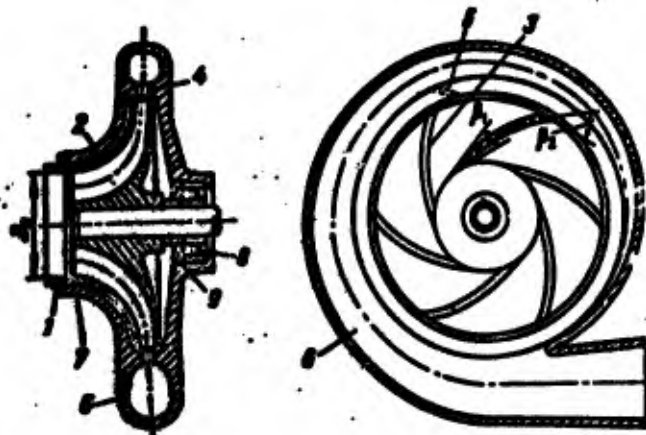


Fig. 7.2. Diagram of centrifugal pump: 1 - inlet duct; 2 - pump wheel; 3 - vanes; 4 - diffuser; 5 - diffuser vanes; 6 - collector or volute; 7 - front seal; 8 - shaft bearing; 9 - bearing seal.

Centrifugal pumps are made with axial, spiral and double inlet, and are made single- and multistage. The selection of axial or spiral inlet (Fig. 7.3a, b) is determined primarily by conditions of arrangement of the TJA and propulsion system. Double inlet (Fig. 7.3c) is made with high flow rates for deceleration at the inlet and thereby for improvement of anticavitation properties of the pump. Multistage pumps (Fig. 7.3d) are applied with the necessity of obtaining especially great pressure heads.

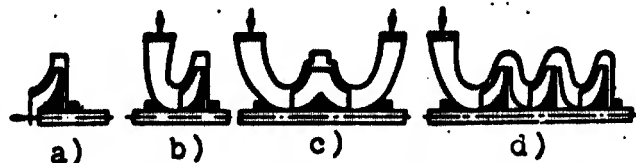


Fig. 7.3. Diagrams of centrifugal pumps: a) with axial inlet; b) with spiral inlet; c) with two-sided inlet; d) multistage pump.

Basic Values Characterizing Pump Operation

For calculation of a pump and appraisal of its basic properties following values are the most important.

1. Volumetric flow rate of liquid through the pump Q . It is determined from the flow rate of component (G_r or G_o) found in thermal calculation by relationship

$$Q = \frac{G}{\gamma}. \quad (7.1)$$

where γ - density of component.

2. Pressure head of pump. Pressure head, created by the pump, is determined by the necessary feed pressure p_{nec} by formula (6.12). From this pressure it is necessary to subtract liquid pressure at the pump inlet. Thus, pressure drop, created by the pump,

$$\Delta p_n = p_{nec} - p_{in}. \quad (7.2)$$

Pressure head of pump H is usually expressed in meters of column of fed liquid:

$$H = \frac{\Delta p_n}{\gamma} = \frac{p_{nec} - p_{in}}{\gamma} \text{ m.} \quad (7.3)$$

3. Pump efficiency. Losses in the pump and its total efficiency are characterized by three efficiencies - volumetric η_o , hydraulic η_h and mechanical η_m .

Volumetric efficiency η_o determines the quantity of liquid overflowing from the high-pressure cavity back to the low-pressure cavity, and leakages of liquid from the high-pressure cavity through seals. Thus

$$\eta_o = \frac{Q}{Q_o}. \quad (7.4)$$

where Q_0 - volumetric flow rate of liquid through the pump wheel.

Value of n_0 depends on the pump construction and feed pressures. For pumps of ZhRD $n_0 = 0.9-0.95$.

Hydraulic efficiency η_r characterizes the amount of hydraulic losses in the pump. These losses are composed of losses connected with separation and impact of flow at the inlet to the wheel, diffuser, volute and outlet duct Δh_{rA} , and losses on friction of liquid against walls of channels Δh_{rp} , i.e.,

$$\Delta h_r = \Delta h_{rA} + \Delta h_{rp}. \quad (7.5)$$

Hydraulic efficiency η_r is the ratio of real pressure H_r , created by the pump, to theoretical pressure H_r , i.e.,

$$\eta_r = \frac{H_r}{H_t}. \quad (7.6)$$

For pumps of ZhRD $\eta_r = 0.7-0.9$. Product of $\eta_r \cdot \eta_o = \eta_{ra}$ is called internal efficiency.

Mechanical efficiency η_m characterizes power losses on friction in bearings, seals, and also losses on friction appearing with rotation of the pump wheel in liquid (disk friction). The amount of mechanical losses strongly differs depending upon the pump design. For pumps of ZhRD $\eta_m = 0.85-0.98$.

Total efficiency of pump

$$\eta_e = \eta_r \eta_o \eta_m. \quad (7.7)$$

Total efficiency determines the portion of useful expenditures of power N_e , i.e.,

$$\eta_e = \frac{N_e}{N_a}. \quad (7.8)$$

For pumps of ZhRD $\eta_s \sim 0.5 - 0.85$.

4. Effective power

$$N_e = \frac{QH\gamma}{75} \text{ hp} \quad (7.9)$$

Required power, expended for driving the pump N_m , will be greater than effective power because of losses and in accordance with formula (7.8) is equal to

$$N_m = \frac{QH\gamma}{75\eta_m} = \frac{Q(p_{out} - p_{in})}{75\gamma\eta_m} \quad (7.10)$$

(pressures p_{out} and p_{in} in kgf/m^2)

5. Specific speed of pump n_s — number of revolutions of a standard pump, geometrically similar to a natural pump, with the same hydraulic and volumetric efficiency, but with pressure head 1 m and effective power 1 horsepower. In general

$$n_s = \sqrt{\frac{1}{75}} \times \frac{\sqrt{Q}}{H^{1/4}}. \quad (7.11)$$

If the standard pump operates on water,

$$n_s = 3.65 n \frac{\sqrt{Q}}{H^{1/4}}.$$

Value of n_s characterizes the shape of the pump wheel (Fig. 7.4). Actually, at given r/min n the value of n_s corresponds to high flow rates Q and lower pressure heads H . Increase of Q and decrease of H leads to increase of the flow cross-section area of the wheel channel (width) and to decrease of the outlet diameter of the wheel D_2 . Thus, at high values of n_s the wheel channel will be short and wide. With decrease of n_s the channel narrows, and ratio D_2/D_1 is increased.

Pumps of ZhRD, as a rule, have relatively low flow rates Q and high pressure heads H , i.e., small value of n_s (usually less than 100).

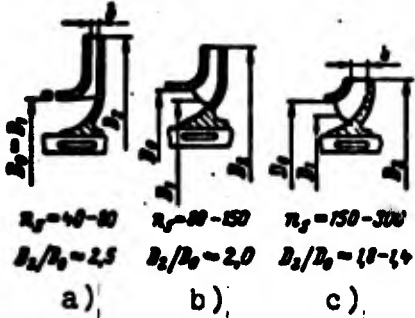


Fig. 7.4. Shape of pump wheel depending upon n_s : a) low-speed wheel; b) normal wheel; c) high-speed wheel.

Velocity Plan at Wheel Inlet and Arrangement of Vanes

Component enters the inlet part of the wheel at a speed of

$$c_0 = \frac{Q_0}{\frac{\pi}{4}(D_0^2 - d_{in}^2)}. \quad (7.12)$$

where D_0 and d_{in} — external diameter of inlet and hub diameter of pump wheel (see Fig. 7.5).

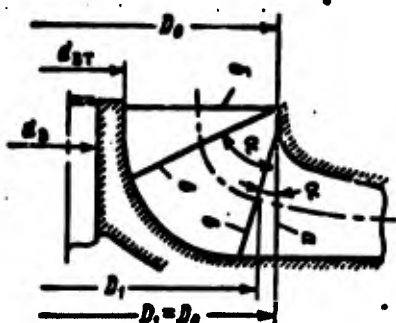


Fig. 7.5. Inlet part of the pump wheel: a) edge is parallel to the pump axis; b) vane edge of double camber; c) edge is inclined at angle α .

During calculations it is usually considered that c_0 is directed along the axis of the pump, not considering a possible twist of flow (for example, in a screw prepump).

Meridian velocity component, at which the liquid enters the vanes, in general

$$c_m = \frac{Q_0}{F_1}. \quad (7.13)$$

where F_1 - area of flow cross-section, area which is the surface of revolution generatrix of which is normal to the meridian velocity component (see Fig. 7.12).

Taking into account obstruction (constraint) of flow cross-section area by vanes

$$F_1 = \pi D_1 b_1 \psi_1, \quad (7.14)$$

where D_1 - average diameter of vane edge inlet; b_1 - width of inlet (Fig. 7.5); $\psi_1 < 1$ - coefficient of constraint of flow of cross-sectional area by vanes.

According to the diagram on Fig. 7.6

$$\psi_1 = \frac{t - s_1}{t} = 1 - \frac{s_1 z}{\pi D_1 \sin \beta_M}, \quad (7.15)$$

where s_1 - vane thickness; z - number of vanes; t - pitch between vanes; β_M - inlet vane angle.

Value of ψ_1 depends to a great degree on dimensions of the pump. For big pumps of ZhRD $\psi_1 = 0.85-0.9$.

Vane edge can be parallel to the axis of the wheel or located at certain angle α . It is simpler to make vanes, the edges of which are parallel to the pump axis and the vanes start where the turn of liquid is basically already completed. In this case the diameter of the vane inlet edge D_1 is frequently made equal to the inlet diameter of the wheel D_0 (see Fig. 7.5).

However, with such arrangement of edges the inlet part of the wheel is not used for imparting energy of the liquid. Sometimes the vanes are made longer and made in the inlet part of the wheel. A wheel with such vanes possesses the best anticavitation qualities. To provide smooth entry of liquid over the entire edge, the vane should have an intricate-shaped surface of double camber.

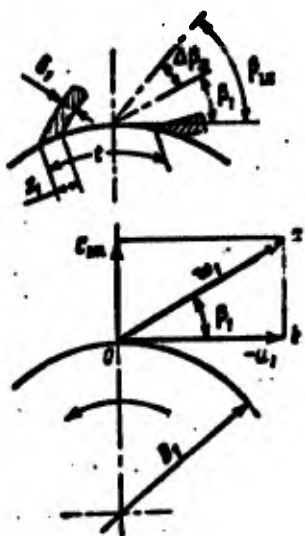


Fig. 7.6. Velocity plan at wheel inlet.

Entering the wheel, the liquid obtains a certain velocity with respect to the wheel which is called relative velocity w . At any point of the wheel it is composed of the meridian velocity of liquid c_m and peripheral velocity of a given point of the wheel, taken with the opposite sign, i.e., $-u$. It is necessary to take peripheral velocity with the "minus" sign, since if one were to represent the wheel as motionless, then to the liquid flowing to the wheel it is necessary to impart angular velocity, equal to the angular velocity of rotation of the wheel. Consequently, each point of the liquid in relative motion obtains peripheral velocity $-u$. Thus, for example, at the vane inlet the liquid in relation to the wheel will obtain velocity

$$-u_1 = -\frac{\pi D_1 n}{60}. \quad (7.16)$$

The value of relative inlet velocity can be calculated by equation

$$w_1 = \sqrt{c_{in}^2 + u_1^2}. \quad (7.17)$$

Its direction is determined by the value of angle θ_1 , which is computed from negative direction of peripheral velocity.

$$\operatorname{tg} \lambda = \frac{c_{lm}}{u_1}. \quad (7.18)$$

On Fig. 7.6 there is represented the velocity plan at the vane inlet. It is represented in the form of velocity triangle Oab and therefore is often called the velocity triangle.

So that the flow would enter the wheel without shock, i.e., with minimum losses, there is necessary conformity of the relative flow rate and shape of the channel, formed by wheel vanes. As operational experience of pumps has shown the wheel works better if the inlet vane angle β_{1a} is somewhat larger than angle β_1 .

Thus, at the wheel inlet the vane is turned opposite the direction of rotation at angle β_{1a} in such a manner that the angle of attack of the inlet edges of the vane $\Delta\beta_a$ is positive:

$$\Delta\beta_a = (\beta_{1a} - \beta_1) > 0,$$

where value $\Delta\beta_a = 5-15^\circ$. If the inlet edge has a large slope, different points of this edge have different peripheral velocity u , and accordingly angle β_{1a} will be different. The pressure drop during flow around the inlet edge of the wheel is proportional to the square of relative velocity w_1 . For prevention of cavitation it is desirable that w_1 be as small as possible.

According to expression (7.17), w_1 depends on the value of c_{lm} and u_1 . In turn, according to equalities (7.13) and (7.16), with increase of the diameter of wheel inlet D_0 , and consequently D_1 , meridian velocity c_{lm} is decreased and peripheral velocity u_1 , conversely, is increased (Fig. 7.7). Obviously there can be found the most advantageous inlet diameter D_0^* , at which velocity w_1 will be the least.

Investigation of conditions at which the pressure drop during entry on blades will be minimum gives an expression for determination

of the equivalent inlet diameter, known as the 1-st formula of S. S. Rudnev:

$$D_{in} = k_0 \cdot 10^3 \sqrt{\frac{Q_2}{\pi}} \text{ mm}, \quad (7.19)$$

where $D_{in} = \sqrt{D_0^2 - d_{in}^2}$;

$$k_0 = 5 \dots 6.$$

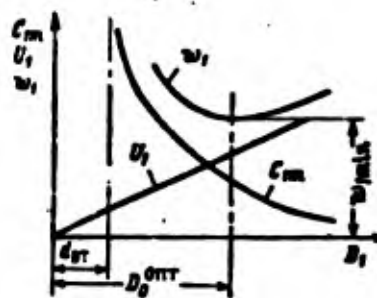


Fig. 7.7. Change of velocity w_1 depending upon the wheel inlet diameter.

Velocity Plan at the Wheel Outlet

Let us examine the velocity plan at the wheel outlet (Fig. 7.8), where the liquid flow has a specific speed w_2 relative to the wheel along the channel formed by vanes. This velocity can be calculated by using the equation of flow rate of liquid along the wheel channel. Axis of the channel, and consequently the axis of flow, if it coincides with the channel, relative to the wheel has direction determined by the vane angle at the wheel outlet β_2 , computed from the negative direction of peripheral velocity in the direction of rotation of the wheel.

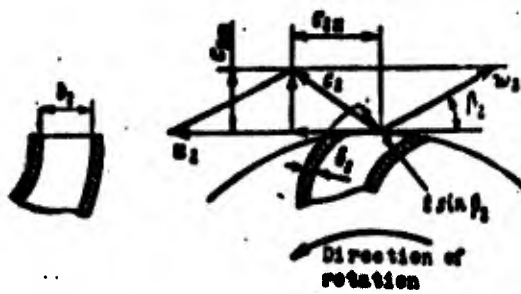


Fig. 7.8. Velocity plan at wheel outlet.

The cross-sectional area of this channel is equal to the product of the wheel width b_2 by the second dimension of the section of channel, perpendicular to the axis of flow and equal to $t \sin \beta_2$.

For the entire wheel the outlet section comprises $\pi b_2 t \sin \beta_2$, but since $t_2 = \pi D_2$, then it will be equal to $\pi D_2 b_2 \sin \beta_2$.

Therefore, taking into account outlet constraint, relative velocity

$$w_2 = \frac{Q_0}{\pi D_2 b_2 \sin \beta_2} : \quad (7.20)$$

where ψ_2 — coefficient of flow constraint by vanes at the outlet.

Thus, just as for the wheel inlet,

$$\eta = 1 - \frac{\psi_2}{\pi D_2 b_2 \sin \beta_2}, \quad (7.21)$$

where δ_2 — vane thickness at the wheel outlet.

The value of coefficient of constraint at outlet ψ_2 is 0.93-0.97. Direction of velocity w_2 approximately coincides with the direction of the channel axis, i.e., with exit blade angle β_2 .

Besides relative velocity w_2 , flow at the wheel exit has also velocity of following, equal to the peripheral velocity of the wheel at exit u_2 . The flow will keep this velocity by inertia

after exiting the wheel. Absolute exit velocity of flow c_2 will be equal to the geometric sum of these two velocities.

In the calculation of pumps projections of absolute velocity c_2 on the direction of peripheral velocity, so-called peripheral component of absolute velocity c_{2u} and on the direction of radius of wheel - meridian component of absolute velocity c_{2m} , play an essential role.

Meridien velocity taking into account constraint of flow by vanes at the exit

$$c_{2m} = w_2 \sin \beta_2 = \frac{Q_0}{\pi D_2 A_2 c_2}. \quad (7.22)$$

Pump wheels are usually designed so that velocity c_{2m} is approximately equal to or somewhat less than velocity c_{1m} .

Peripheral component of absolute velocity c_{2u} can be calculated by proceeding from the fact that the projection of resultant velocity to some direction is equal to the sum of projections of its components in the same direction. Projection of flow velocity of following u_2 in the direction of the tangent is equal to its own value, and projection of relative velocity

$$-w_2 \cos \beta_2 = -\frac{c_{2u}}{c_2}.$$

whence in accordance with vebocity plan on Fig. 7.8 there is obtained relationship

$$c_{2u} = u_2 - \frac{c_{2m}}{c_2}. \quad (7.23)$$

Theoretical Pressure Head Created by the Pump

Theoretical pressure head, created by a centifugal pump, can be calculated by Euler equation:

$$H_{t\infty} = \frac{u_2 c_{2u\infty} - u_1 c_{1u}}{\rho}, \quad (7.24)$$

where $H_{t\infty}$ - pressure head of column of liquid in m, created by the wheel with infinite number of vanes; c_{1u} - peripheral component of absolute inlet flow velocity.

Since twist of flow at the inlet in the direction of peripheral velocity (i.e., velocity c_{1u}) will decrease the pressure head created by the pump, all other conditions be equal, then when designing usual wheels we try to provide radial supply of liquid to the wheel in such a manner that c_{1u} is equal to zero. Then formula (7.24) will be converted into the basic calculation equation of the pump:

$$H_{t\infty} = \frac{u_2 c_{2u\infty}}{\rho}. \quad (7.25)$$

This pressure head is composed of increase of static pressure in liquid and increase of dynamic pressure due to increase of its absolute velocity.

Since $u_2 = \pi D_2 n / 60$, and the value of $c_{2u\infty}$ is proportional to u_2 , then theoretical pressure head, created by the pump, will depend on the square of peripheral velocity, i.e.,

$$H_{t\infty} = k_s \frac{u_2^2}{\rho} = k_s \left(\frac{\pi D_2 n}{60} \right)^2. \quad (7.26)$$

where $k_s < 1$ - coefficient determined by construction of the pump.

Formula (7.26) shows that at prescribed wheel dimensions the pressure head is proportional to the square of r/min, and with prescribed r/min the pressure head is proportional to the square of the wheel diameter.

Using Euler formula in the form of (7.24) or (7.25), it is necessary to place real values of velocity c_{2u} in it, which have a stream of liquid exiting the wheel. According to the velocity plan at the wheel exit let us assume that flow along the wheel completely follows the profile of the vanes. However, such a position is possible only theoretically, namely, when on the wheel there would be placed an infinitely large number of infinitely thin vanes. With a finite number of vanes only streams directly adjacent to the leading (according to the travel of the wheel) surface of the vane follow the profile of the vane. Streams farther away from the vane have wheel exit angle smaller than angle β_2 , at angle of untwist of stream $\Delta\beta_2$ (Fig. 7.9). For this reason (see Fig. 7.8) with the same value of w_2 velocities c_{2u} for these streams become smaller, and the pressure head, calculated by formula (7.24), is also decreased in remote streams.



Fig. 7.9. Angle of untwist

With equalization of pressure head of separate streams the overall theoretical pressure head H_v , created by a wheel with finite number of vanes, will be smaller than the pressure head which a wheel with an infinitely large number of vanes $H_{v\infty}$ would create. The connection among these pressure heads is determined by relationship

$$H_v = \frac{H_{v\infty}}{1+p}, \quad (7.27)$$

where the value of p considers lowering of pressure head due to the finite number of vanes; the greater the lowering of pressure head; the higher is p .

Value of p can be calculated by approximate formula

$$p = 2 \frac{\psi}{\pi} \frac{1}{1 - \left(\frac{D_1}{D_2}\right)^2}. \quad (7.28)$$

Value of p and consequently, lowering of pressure head will be greater, the smaller the number of vanes z and the shorter the channel between vanes (the greater the ratio of D_1/D_2). Value of ψ considers the quality of treatment of the wheel and the magnitude of vane exit angle; it is computed for wheels of centrifugal pumps by relationship

$$\psi = (0.55 - 0.68) + 0.6 \sin \beta_2. \quad (7.29)$$

Lowering of pressure head created by the wheel at the expense of finite number of vanes, does not cause increase of the necessary work or power consumed for rotation of the wheel. This occurs because if the wheel does not completely twist the flow, then energy, corresponding to untwisting, is not removed by flow from the wheel. Thus, lowering of pressure head due to finite number of vanes requires only a change of dimensions of wheel or increase of r/min (increase of u_2), but does not lead to loss of work and does not have to be considered in wheel efficiencies.

As can be seen from formula (7.25), theoretical pressure head of the wheel depends on the type of velocity plan at the pump exit, the type of velocity plan is determined to a considerable degree by the value of angle β_2 .

Cavitation

Cavitation, or cold boiling, is the appearance of breaks or vacuums, filled with liquid vapors, in the liquid flow in the zone of minimum pressure.

In general, according to Bernoulli equation in the absence of losses the total head of liquid

$$\frac{P}{\gamma} = \frac{P_0}{\gamma} + \frac{V^2}{2g}$$

whence static pressure in the flow

$$P = P_0 - \frac{V^2}{2g}$$

At high flow velocities the static pressure can become less than the pressure of saturated vapors P_s and then the start of boiling liquid occurs, i.e., cavitation appears.

In the wheel of a centrifugal pump the most dangerous with respect to cavitation is the inlet section of the liquid on vanes of the wheel, where total pressure of liquid is minimum (pump as yet did not impart energy to the liquid), and absolute and relative flow rates are great.

High relative velocities at the vane inlet promote the formation of cavities of lowered pressure on the rear of the vane (Fig. 7.10), i.e., promote the appearance of cavitation. Furthermore, nonuniform field of absolute velocities during approach to the vane causes an additional pressure drop in streams, where the velocity will be greater than average.

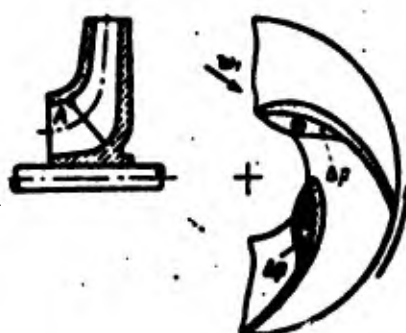


Fig. 7.10. Region of reduced pressure during flow around pump vanes.

The least pressure at vane inlet p_{\min} can be defined as the difference of static wheel inlet pressure p_{∞} and the value of additional pressure drop Δp_{loss} due to the formation of zones of lowered pressure and the irregularity of absolute velocities, i.e.,

$$p_{\min} = p_{\infty} - \Delta p_{\text{loss}} \quad (7.30)$$

Condition of cavitationless operation

$$p_{\infty} - \Delta p_{\text{loss}} = p_{\min} > p_s$$

or

$$p_{\infty} - p_s > \Delta p_{\text{loss}} \quad (7.31)$$

Value $(p_{\infty} - p_s)$ characterizes the pressure head, which can still be used for increase of the flow rate without the appearance of cavitation and is called the cavitation margin.

Other things being equal, increase of r/min of the pump n and flow rate Q_0 leads to increase of the relative and absolute flow velocities [(7.13), (7.16)], and consequently, to increase of the danger of appearance of cavitation. With rise of n and Q_0 cavitation appears on vanes at lower inlet pressures.

Cavitation disturbs the normal pump operation by two causes.

First, due to the fact that part of the volume fed by the pump turns out to be filled with liquid vapors, there occur a pressure drop and decrease of the flow rate of fed liquid.

Secondly, with impact of liquid, having vapor pockets in its mass, in the region of higher pressures the vapor is condensed and filling of the volume of vapor pockets by liquid occurs at a high rate (up to 1500-1800 m/s), which leads to water hammer phenomenon at the moment of filling of volume. The totality of directed water hammers to the focal point of the hemisphere of vapor volumes, located on the surface of vanes, leads to erosion destruction of the metal.

Since cavitation erosion is developed gradually, in view of the small duration of operation of ZhRD pumps it is not dangerous; however, cavitation is impermissible in pumps of ZhRD because of the pressure drop and decrease of volumetric flow rate.

Change of pressure head with the appearance of cavitation is characterized by so-called cavitation characteristics.

There are distinguished stalling characteristics (Fig. 7.11a, b), i.e., the dependence of the pressure head H_H on inlet pressure p_{in} (or value of $p_{in} - p_s$), and cavitation characteristics, expressing the dependence of ultimate inlet pressure $p_{in, \text{cav}}$, below which cavitation starts, on the number of revolutions n and flow rate Q . Stalling characteristics are obtained by results of testing pumps at a prescribed flow rate and number of revolutions.

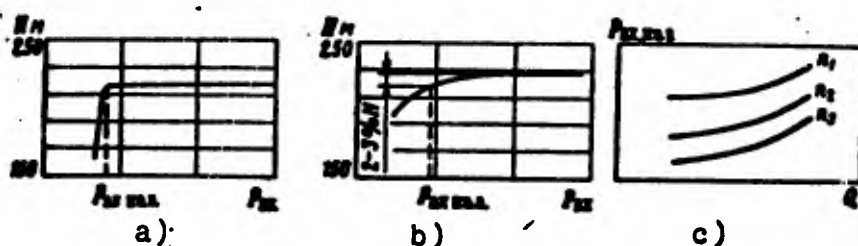


Fig. 7.11. Cavitation characteristics: a, b) stalling characteristics; c) cavitation characteristics $p_{in, \text{cav}} = f(n, Q)$.

Ultimate inlet pressure $p_{in, \text{cav}}$, below which cavitation starts, is defined as pressure at which the pressure head drop is 2-3%. On the basis of a series of conducted tests there are constructed cavitation characteristics $p_{in, \text{cav}} = f(n, Q)$ (Fig. 7.11c). Cavitation properties of a pump are reliably established only experimentally.

During calculation of pumps one of the basic problems is determination of the maximum permissible pump revolutions with respect to cavitation conditions at a prescribed inlet pressure and

flow rate. Proceeding from condition of cavitationless operation (7.31)

$$P_{in} - P_s > \Delta P_{sat}$$

and conducting analysis of the value of components ΔP_{sat} [139], [25], we will obtain the calculation formula for determining the maximum permissible revolutions of the pump (S. S. Rudnev formula):

$$n_{max} = c_{np} \frac{1}{\sqrt{Q_0}} \left(\frac{H_{in} - H_s}{10} \right)^{\frac{3}{4}}. \quad (7.32)$$

Here c_{np} - critical coefficient of cavitation, which is determined experimentally and characterized the cavitation qualities of the pump, i.e., degree of predisposition of the pump to cavitation with lowering of P_{in} . Coefficient c_{np} was offered for the first time by S. S. Rudnev, therefore it is often called Rudnev coefficient. For usual pumps $c_{np} = 800-1100$. For wheels with high anticavitation properties, having special shapes and vanes of special profile, c_{np} can reach 2000-2200. With the application of axial or screw prepumps, which is one of the basic measures of cavitation, value of c_{np} is increased to 3000-3100. Data indicate that with the help of prepumps it is possible to increase c_{np} to values 3500-4000 [139]. Screw prepumps not only increases the pressure of liquid, but also creates twist of flow, decreasing the relative inlet velocity of the liquid. Screw conveyers are usually double or triple; the pressure head of the screw conveyer makes up 3-20% of the overall pressure head.¹

Cavitation can be prevented also by tank pressurization to 2-6 [atm(abs.)] ($\approx 0.2-0.6 \text{ MN/m}^2$) in order to accordingly increase the pump inlet pressure.

Anticavitation properties of pumps depend on structural shapes (number and length of vanes, angle of attack, application of double

inlet, application of oversized wheels), and also on thermodynamic properties of the component to be fed [139], [141].

7.2. Calculation and Characteristics of ZhRD Pumps

Order of Calculation

Initial data for calculation of ZhRD pump are: flow rate of component, volumetric - $Q \text{ m}^3/\text{s}$ or mass - $G \text{ kg/s}$; necessary pump head $H \text{ m}$ and pump inlet pressure p_{ax} . Engineering calculation of the pump should give its following basic parameters; - basic dimensions d_m , D_0 , D_1 , b_1 , D_2 , b_2 ; - shape of wheel in meridian section, number and profile of vanes, dimensions of volute; - power and efficiency; - characteristics.

The pump can be calculated in the following order.

1. Let us select the number of revolutions of the pump $n \text{ r/min}$. It can be assigned; then from calculation for cavitation it is necessary to find inlet pressure p_{ax} , assuring cavitationless operation. If the number of revolutions must be determined, then it is found from calculation for cavitation by formula (7.32). If several pumps are placed on one shaft, then the r/min of the shaft is determined by the least calculated number of revolutions.
2. By formula (7.11) let us determine specific speed n_s .
3. Let us preliminarily assign values of efficiency $\eta_0 = 0.9-0.95$ when $n_s = 30-130$ (large η_0 corresponds to large n_s); $\eta_r = 0.7-0.9$ and $\eta_u = 0.85-0.98$. Let us preliminarily estimate $\eta_u = \eta_0 \eta_r \eta_u$.
4. In the first approximation let us find required power of the pump (7.10):

$$N_p = \frac{Q \cdot H \cdot \gamma}{75 n_m} \text{ hp}$$

5. Torque on shaft

$$M_{sp} = 71620 \frac{\text{N}}{\text{m}} \text{ kgf}\cdot\text{cm},$$

we find the shaft diameter from calculation for torsion:

$$d_s = \sqrt{\frac{M_{sp}}{0.2\tau_s}} \text{ cm}$$

where τ_s kgf/cm² – permissible torsional stress.

If the shaft diameter is obtained unconstructively small, it is increased accordingly.

6. From structural considerations we find hub diameter

$$d_{sr} = (1.1 - 1.3)d_s$$

7. Real volumetric flow rate of component through the wheel

$$Q_0 = \frac{q}{k_0} \text{ m}^3/\text{s}.$$

8. Let us determine dimensions of wheel inlet. By formula (7.19) we find the equivalent diameter and inlet diameter

$$D_{le} = k_0 \cdot 10^3 \sqrt{\frac{Q_0}{n}} \text{ mm.}$$

where $k_0 = 5-6$;

$$D_0 = \sqrt{D_{le}^2 + d_{sr}^2}$$

Diameter of circumference D_1 , on which the vane edge is located, is taken equal to D_0 or somewhat smaller (the latter usually in the absence of a prepump).

9. Speed of liquid at inlet (7.12)

$$c_0 = \frac{Q_0}{\frac{\pi}{4} (D_0^2 - d_{sr}^2)} = \frac{Q_0}{\frac{\pi}{4} D_{le}^2} \text{ m/s.}$$

10. We determine the width of the wheel inlet b_1 . For improvement of ant cavitation properties the inlet is made widened; accordingly we find width b_1 from condition

$$1.2 < \frac{4\pi D_1 b_1}{\pi D_1^2} < 2.5.$$

whence

$$b_1 = (0.375 - 0.625) \frac{D_1^2}{4\pi D_1}.$$

11. Knowing D_1 and b , we determine peripheral velocity u_1 and meridional velocity c_{1m} . According to equation (7.16)

$$u_1 = \frac{\pi D_1 n}{60}.$$

In accordance with equations (7.13) and (7.14)

$$c_{1m} = \frac{Q_0}{\pi D_1 b_1 \psi_1}. \quad (7.33)$$

Let us prescribe coefficient of constraint ψ_1 (0.85-0.9). After determination of ψ_1 ; z and β_{1z} the value of ψ_1 is corrected by formula (7.15).

12. We find the inlet vane angle from the velocity triangle (see Fig. 7.6): $\operatorname{tg} \beta_1 = c_{1m}/u$. Vane angle β_{1z} is determined in accordance with equality (7.19): $\beta_{1z} = \beta_1 + \Delta\beta_z$, where $\Delta\beta_z = 5-15^\circ$. At small angles of β_1 we take large values of $\Delta\beta_z$, since small β_{1z} leads to an unfavorable shape of the vane channel (long narrow channel). Usually β_{1z} is within limits of $12-22^\circ$. Having determined β_{1z} , assigning the vane thickness $\delta_1 = 3-5$ mm, by formula (7.15) we correct the value of ψ_1 . We select the number of vanes z preliminarily, by analogy with other constructions; we further check the correctness of selection by equality (7.35). If the inlet edge of the vane is not parallel to the axis of rotation, but has a large angle of slope, then various points of the edge have various values of u_1 and it is necessary to determine angle β_{1z} for several points.

13. We determine parameters at the wheel exit in two procedures: at first approximately, and then the obtained values are refined.

For a rough determination of diameter D_2 we find the approximate value of peripheral velocity by formula (7.26), considering $H_v \approx H_{\text{vis}}$:

$$H_v = k_n \frac{u_2^2}{g}.$$

where in accordance with equality (7.6) $H_v = H/\eta_r$.

Coefficient k_n during practical calculations can be taken equal to 0.5. By the found value of u_2 we find the approximate value of wheel diameter:

$$D_2' = \frac{60u_2}{\pi n}. \quad (7.34)$$

Let us assign the value of exit angle of flow from the wheel, i.e., the vane angle β_2 . For usual pumps β_2 is taken equal to 15-60° (for hydrogen pumps up to 90°). Pumps with large values of specific speed n_s have smaller values of β_2 . In separate cases, at very high pressures and small densities of components, it is possible to take the value of β_2 on the order of 40-60°.

By the found preliminary values of D_2' and β_2 we check the correctness of the number of blades z selected in para. 12:

$$z = 6.5 \frac{D_2 + D_1}{(\omega_2 - \omega_1)} \sin \frac{\beta_2 + \alpha}{2}. \quad (7.35)$$

Usually $z = 6-12$.

Let us assign c_m . In the first approximation $c_{m0} \approx c_{im}$. By formula (7.22) we find the width of the wheel at b_2 . In this case ψ_2 is determined preliminarily by equation (7.21). From structural

considerations the value of b_2 is taken not less than 4-5 mm; besides there is allowed decrease of c_{2m} to value $c_{2m} \approx 0.5c_{1m}$.

Let us refine the obtained preliminary values. For this, by formula (7.27) we determine $H_{1m} = H_1(1+p)$, where we find p by formula (7.28).

We determine the refined value of u_2 . In accordance with Fig. 7.8 formula (7.25) is copied in the form

$$H_{1m} = \frac{g c_{2m}}{\varepsilon} = \frac{u_2}{\varepsilon} \left(u_2 - \frac{c_{2m}}{u_2 b_2} \right).$$

whence

$$u_2 = \frac{c_{2m}}{2 u_2 b_2} + \sqrt{\left(\frac{c_{2m}}{2 u_2 b_2} \right)^2 + g H_{1m}}. \quad (7.36)$$

Having determined u_2 , by formula (7.34) we find the refined value of D_2 . If divergence of D_2 from D'_2 is over 5%, calculation is conducted again, using the value of D_2 as initial.

14. We profile the wheel in the meridian section. For this let us prescribe the form of the center line of the wheel. Usually the form of the center line is taken analogous to the center line of the wheel of a similar pump. The form of center line is determined to a known degree by the value of specific speed n_s (see Fig. 7.4).

Width of meridian section at inlet and exit is known, since b_1 and b_2 are known. We determine the change of meridian velocity c_m along the section of the wheel. In this case we consider along the section velocity c_m is changed smoothly (usually along a straight line) from velocity c_{1m} to velocity c_{2m} (Fig. 7.12).

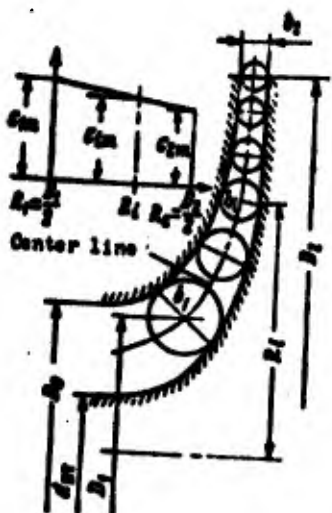


Fig. 7.12. Construction of meridian section of pump wheel.

Width of section b_1 on arbitrary radius R_1 is determined by a formula analogous to expression (7.33) (disregarding constraint of the section by vanes):

$$c_{lm} = \frac{Q_0}{2\pi R_1 b_1}.$$

Having determined several values of b_1 at various R_1 , let us profile the lateral walls of the channel as envelopes of circumferences with radii $b_1/2$ with centers on the center line.

15. Proceeding from obtained values of D_1 , b_{lm} , D_2 and s_2 , let us profile the vanes.

16. We select the type of diffuser (if it is necessary).

17. Let us determine the dimensions and profile the volute of the pump.

18. Let us profile the inlet and exhaust ducts of the pump.

19. Let us determine amounts of hydraulic losses and find the exact value of η . At large divergence of obtained value of η with prescribed we correct the calculation.²

Characteristics of Pumps

Operation of the pump in the feed system of ZhRD is characterized by head H , flow rate Q , number of revolutions n and efficiency of pump η . With assigned Q and η the power and pressure head are connected simply by equation (7.10):

$$N_s = \frac{H Q \eta}{n \eta_m}.$$

Characteristics in the form of dependencies of pressure, efficiency and power on the flow rate received the most propagation in practice.

Let us consider dependence $H = f(Q)$, called pressure characteristic.

With an infinite number of vanes according to equation (7.25)

$$H_{\infty} = \frac{\beta_2 \sinh \beta_2}{\beta_2} Q_{\infty}$$

In accordance with expressions (7.23) and (7.22) and considering that with an infinite number of vanes $\psi_2 = 1$, we obtain

$$H_{\infty} = \frac{\beta_2^2}{\beta_2} - \frac{\beta_2 \sinh \beta_2}{\beta_2 D_2 A_2} Q_{\infty} \quad (7.37)$$

i.e., equation of straight line. The slope of $H_{\infty} = f(Q)$ depends on the value of β_2 . When $\beta_2 < 90^\circ$ (vanes are bent back) we obtain "incident" characteristic (Fig. 7.13).

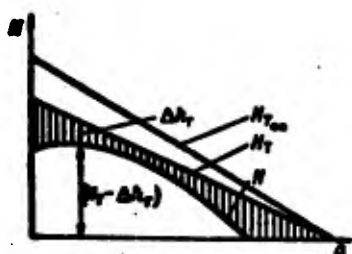


Fig. 7.13. Pressure characteristics at constant r/min .

With a finite number of vanes according to formula (7.27)

$$H_r = \frac{H_n}{1+p}.$$

Considering that p does not depend on the flow rate, we obtain characteristic $H_r=f(Q)$ in the form of a straight line, ordinates of which are reduced $(1+p)$ times.

For obtaining the real pressure characteristic it is necessary to subtract hydraulic losses Δh_r from H_r . According to expression (7.5) $\Delta h_r = \Delta h_{r,n} + h_{r,p}$. Friction losses $\Delta h_{r,p}$ increase in proportion to the square of flow rate (Fig. 7.14). Losses on separation and impact $\Delta h_{r,n}$ appear due to noncorrespondence of the direction of flow to the direction of the channels. With decrease of flow rate, and also at very high flow rates the value of $\Delta h_{r,n}$ increases. Minimum of hydraulic losses (usually corresponds to rated conditions) does not coincide with minimum $\Delta h_{r,n}$.



Fig. 7.14. Dependence of hydraulic losses on the flow rate.

Having determined the difference of $(H_r - \Delta h_r)$ at various pressure heads, we obtain the real pressure characteristic at prescribed number of revolutions $H = f(Q)$ (see Fig. 7.13).

Let us examine the character of change of $\eta_r=f(Q)$ (Fig. 7.15a). According to design conditions, the highest efficiency occurs under rated conditions (point C). With flow rate equal to zero (point A), and with pressure head equal to zero (point B), the efficiency is obviously equal to zero. From the graph of $\eta_r=f(Q)$ we see that there are always two conditions (points a and b), when efficiency is identical (at flow rates greater and less than calculated).

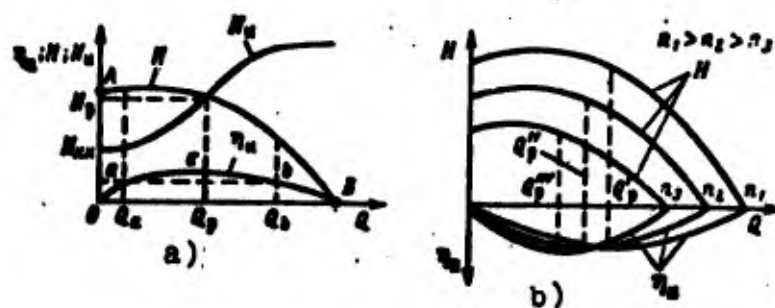


Fig. 7.15. Characteristics of pumps $\eta = f(Q)$; $N = f(Q)$; $H = f(Q)$: a) when $n = \text{const}$; b) at various r/min .

Dependence $N_n = f(Q)$ at known characteristics $H = f(Q)$ and $\eta_n = f(Q)$ can be obtained by formula (7.10). When $Q = 0$ considerable power is expended on driving the pump.

The above-examined characteristics are obtained at constant r/min . In the practice of application of pumps it is necessary to have characteristics at different r/min .

They are represented by a family of curves (Fig. 7.15b). This family of curves is obtained the most reliably by experimental means, however, having dependence $H = f(Q)$ at one r/min , it is possible to recalculate it to other r/min on the basis of the similitude theory, according to which for conditions with similar velocity triangles (similar conditions)

$$\eta_n = \eta_r \eta_0 = \text{const}; \quad (7.38)$$

$$\frac{Q_1}{Q_2} = \frac{n_1}{n_2}; \quad \frac{H_1}{H_2} = \left(\frac{n_1}{n_2}\right)^2. \quad (7.39)$$

Excluding n from formulas (7.39), for similar conditions at $\eta_{\text{sim}} = \text{const}$ we obtain

$$\frac{H_1}{Q_1^2} = \frac{H_2}{Q_2^2} = \frac{H}{Q^2} = \text{const}. \quad (7.40)$$

In coordinates $H-Q$ the lines of similar conditions are expressed by parabolas (Fig. 7.16). By transposing along the line of similar

conditions it is possible by formulas (7.39) to compute the pressure characteristic at any r/min . Lines of similar conditions are lines of constant internal efficiency η_{int} . As experiments show, lines of constant total efficiency do not always coincide with lines of constant internal efficiency. Because of the presence of mechanical losses at low r/min , when a portion of mechanical losses grows and, consequently, η_{int} decreases, drop of total efficiency η_t occurs faster. This graphically indicates the intersection of curves of constant internal efficiency by lines of constant total efficiency at small Q and H .

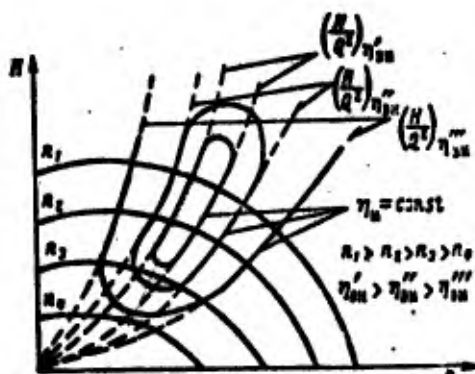


Fig. 7.16. Grid of pressure characteristics and lines of equal efficiency.

In the region of large Q and H as a result of lowering of efficiency because of the appearance of cavitation phenomena there also occurs closure of lines of constant efficiency. As a result, lines of constant efficiency η_t have the form of closed curves (solid lines on Fig. 7.16).

In practice for characteristic of pump operation at various r/min there is sometimes used not a grid of characteristics, but a universal characteristic.

For similar conditions in accordance with expression (7.39)

$$\frac{Q_1}{n_1} = \frac{Q_2}{n_2} = \frac{Q}{n} = \text{const}; \quad \frac{H_1}{n_1^2} = \frac{H_2}{n_2^2} = \frac{H}{n^2} = \text{const.} \quad (7.41)$$

Dependence $H/n^2 = f(Q/n)$ gives the connection between H and Q for all r/min and therefore is called universal characteristic (Fig. 7.17).

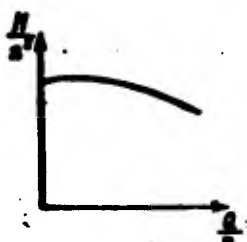


Fig. 7.17. Universal characteristic.

Joint Operation of Pump and Feed System of ZhRD

Operating point A of pump (Fig. 7.13) is found as the point of intersection of pressure characteristic with hydraulic characteristic of system $H = f(Q)$, determined by equation (6.33). As can be seen, at point A there is provided stable pump operation, since with random increase of flow rate to Q' the power of the pump will be insufficient and, conversely, with random decrease of the flow rate to Q'' the excess power of the pump will again ensure increase of the flow rate to Q_p .

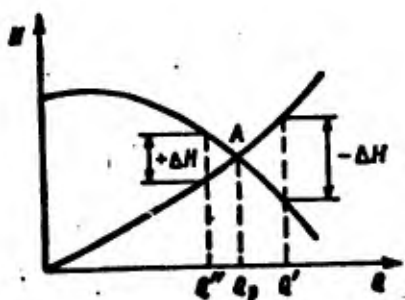


Fig. 7.18. Determination of operating point of pump.

Let us examine the change of pump operation with basic methods of flow control: a) choking, b) diversion, c) change of r/min .

With decrease of flow rate from Q_p to Q'_p by choking (Fig. 7.19a) the required pressure head is defined as the sum of resistance of the system (curve 1) and additional resistance of the throttle and the operating point will shift to point A' (curve 2). Introduction of throttle resistance will require increase of pressure head and thereby increase of pump power N_s . Required power is increased more because during pump operation at partial load condition its efficiency deteriorates. Thus, during choking we have an unproductive expenditure of power.

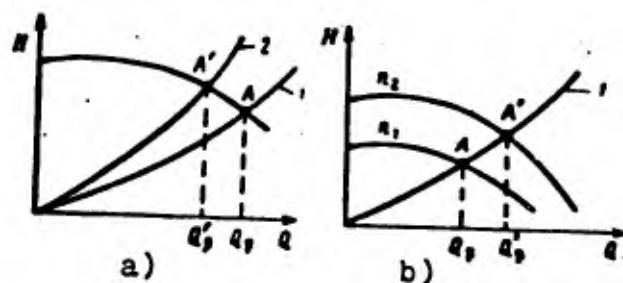


Fig. 7.19. Shift of operating point: a) during choking; b) with decrease of r/min .

Smaller unproductive expenditures occur with change of the flow rate by "diverting" part of the component (Fig. 7.20). In this case the operating point remains constant and an unproductive expenditure of power occurs only for the supply of unnecessary (bypassed) component.

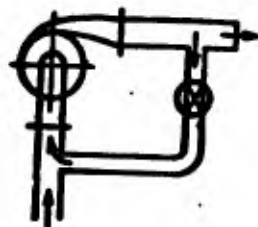


Fig. 7.20. Diagram of change of the flow rate by diversion.

For changing the flow rate we often use change of the pump r/min . The operating point shifts along the characteristic of the

system. With increase of r/min from n_1 to n_2 the operating point will shift from point A to point A' (see Fig. 7.19b). Pump head H and required power will be increased accordingly. In this case there is no unproductive expenditure of power, but a system is necessary which provides decrease of r/min of the pump (usually the r/min are increased or decreased by corresponding increase or decrease of the amount of working substance fed to the turbine).

Let us determine the relationship of change of required power with change of r/min. It is possible to consider that the characteristic of system is changed along a parabola, i.e., that $H = \text{const} \cdot Q^2$. Then according to equation (7.39) the operation conditions of the pump will be similar with change of the r/min. If we consider $\eta_p = \text{const}$, then in accordance with formula (7.38) $\eta_{\text{req}} = \eta_p \eta_M = \text{const}$.

By comparing expressions (7.39) and (7.10) for similar conditions, it is possible to express the dependence of required power on r/min in the form

$$N_{\text{req}} = Cn^2. \quad (7.42)$$

where C – constant coefficient.

Curve of dependence $N_{\text{req}} = f(n)$ is shown on Fig. 7.21.



Fig. 7.21.
Dependence
 $N_{\text{req}} = f(n)$.

7.3. TNA Turbines

Classification of Turbines

One of the basic elements of the TNA is the gas turbine. In the turbine the potential energy of combustion products from the gas generator or vapors of collant will be converted into mechanical work of the turbine. Conversion of gas energy occurs in the motionless nozzle ring of the turbine and on vanes of the turbine wheel. An elementary diagram of the turbine is shown on Fig. 7.22. With expansion of gas in the nozzle ring the gas velocity increases from inlet velocity c_0 to exit velocity c_1 . At this velocity c_1 the gas enters the vanes of the turbine wheel, having peripheral velocity

$$u = \frac{\pi D n}{60} \text{ m/s.} \quad (7.43)$$

Relative vane inlet velocity w_1 is composed of absolute velocity c_1 and peripheral velocity u at a given point, taken with opposite sign. In the vane channel the gas changes its direction and emerges at velocity w_2 . Due to a turn of the jet and in certain cases (reaction turbine) its acceleration there appears force of action on vanes P , revolving the turbine. By combining relative velocity w_2 with peripheral u , we find the absolute exit velocity of gas from vanes of the wheel c_2 . Peripheral force affecting the vanes P_u , can be determined by the theorem of momentum, by projecting velocity vectors of flow c_1 and c_2 and force of action of gas on vanes P in circumferential direction:

$$P_u = \frac{\sigma}{\epsilon} (c_{2u} - c_{1u}). \quad (7.44)$$

The amount of available work, i.e., highest possible turbine work without losses, is determined by adiabatic lapse rate κ_a (heat drop) from parameters of gas in retarded state at the turbine inlet ($p_m^*; T_m^*$) to outlet pressure p_{mn} (Fig. 7.23):

$$L_a = \frac{\kappa_a}{A} = \frac{k}{k-1} R T_m^* \left[1 - \left(\frac{p_{mn}}{p_m^*} \right)^{\frac{k-1}{k}} \right]. \quad (7.45)$$

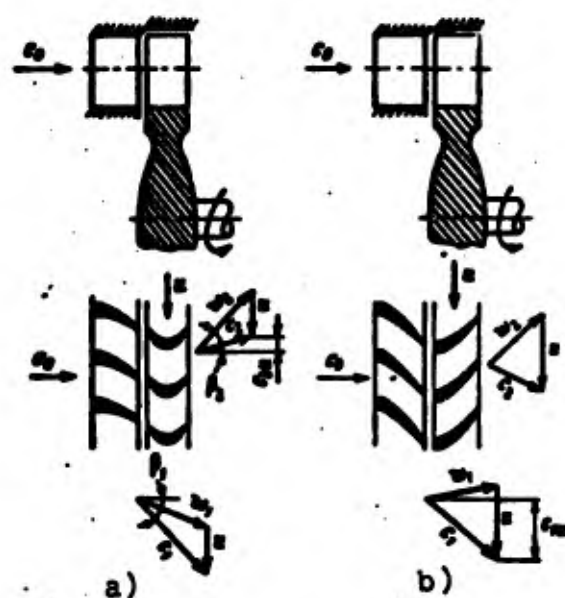


Fig. 7.22. Elementary diagram and velocity triangles of the turbine: a) action; b) reaction.

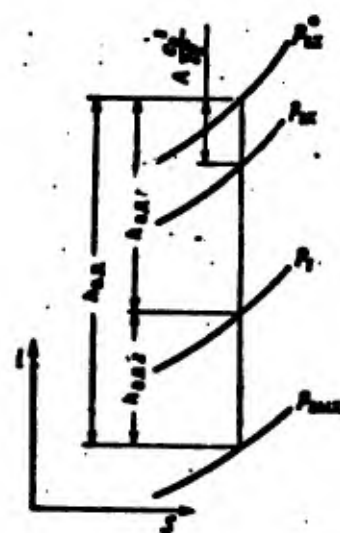


Fig. 7.23. Adiabatic expansion of gas in the stage.

During analysis of work of turbines there is used the idea of adiabatic velocity (Fig. 7.23)

$$c_a = \sqrt{\frac{2g}{A} h_{st}} - 91.5 \sqrt{A_{st}}. \quad (7.46)$$

In the action stage disregarding losses $c_{a1} = c_1$. Kinetic energy $c_a^2/2g$ is equivalent to adiabatic lapse rate in the stage.

According to different criteria turbines are divided into action and reaction, axial-flow, radial-flow and tangential-flow, single-stage and multistage. Furthermore, we distinguish velocity stage turbines and expansion turbines, partial and unpartial, single-shaft and two-shaft.

Separation into active and reaction turbines is produced by the method of distribution of pressure drops in the turbine stage.

In action turbines the whole drop of pressure, arriving at the stage, is in the nozzle ring, and on the rotor blades of the turbine wheel there is no pressure drop. In the vane channel of the wheel the flow is turned and reactive force acts on the blades. Thus, part of the energy of gases is transmitted to the rotor and the absolute velocity of gas is reduced. If we disregard losses, relative velocity w remains constant, i.e., $w_1 = w_2$. In reaction turbines the overall pressure drop is divided in the nozzle ring and rotor blades. Due to expansion of gas on the rotor blades the relative velocity w increases, i.e., $w_2 > w_1$. The ratio of adiabatic lapse rate, occurring on rotor blades, to total heat drop on the stage is called the degree of reaction:

$$\epsilon = \frac{h_{st}}{h_{st}}. \quad (7.47)$$

Separation into axial, radial and tangential turbines is produced with respect to the direction of gas flow (Fig. 7.24).

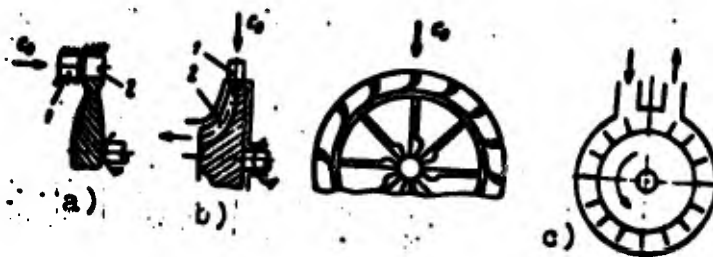


Fig. 7.24. Types of turbine: a) axial-flow; b) radial-flow centripetal; c) tangential-flow: 1 - nozzle ring; 2 - blades.

Axial-flow turbines are turbines in which the direction of flow in the meridian section is parallel (or almost parallel) to the turbine axis.

Radial-flow turbines in which the direction of flow in the meridian section is perpendicular to the turbine axis. Depending upon the direction of gas flow we distinguish centripetal (direction of flow from periphery to center) and centrifugal (direction of flow from center to periphery) turbines.

Because of large friction surfaces and additional turns of gas at small w/c_{∞} the efficiency of a radial turbine is less than that of an axial-flow turbine. However, in small-sized turbines the difference in efficiency of a centripetal radial-flow turbine and axial-flow turbine is small. Radial-flow turbine can be regulated by turning the blades of the nozzle ring. In certain cases the application of a radial turbine simplifies the arrangement of the TNA.

Tangential turbines are those in which gas moves along the circumference in a plane perpendicular to the turbine axis, and due to friction drags the turbine blades.

According to the number of stages we distinguish single-stage and multistage turbines (Fig. 7.25).

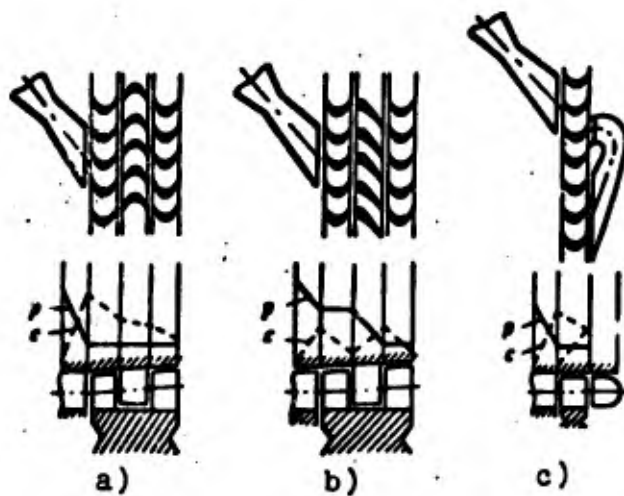


Fig. 7.25. Multistage turbines:
a) with velocity stages; b) with
pressure stages; c) with rotation
of gas.

In a multistage turbine the gas after exiting the blades of the wheel enters the turning apparatus (nozzle ring) and again joins the wheel in the second row of rotor blades. The number of stages can be two, three and more. The application of multistage turbines permits using a large heat drop, although installation of the stages is connected with additional hydraulic losses, as a consequence of which the maximum value of efficiency of a multi-stage turbine is less than the efficiency of a single-stage (see Fig. 7.30). However as we will see below, with open circuit the turbines of the turbopump assembly at small values of u/c_{∞} , therefore, in the TNA in a number of cases for increase of efficiency of more than two stages gives an insignificant work gain.

We distinguish multistage turbines with velocity stages and with pressure stages. In the first the pressure drop operates in the nozzle ring of the first stage, and the obtained kinetic energy is gradually used on other stages. In a turbine with pressure stages in each stage there operates a specific pressure drop. Velocity stage turbines have lower efficiency, however, with

stages, first of all, there is required a smaller amount of stages for use of the prescribed heat drop (at identical peripheral velocity); secondly, during operation of the entire heat drop in the nozzle ring of the first stage the temperature of gas entering subsequent stages is lowered more essentially; thirdly, axial forces are less.

On the whole, velocity stage turbines are simpler and are expedient in comparatively small ZhRD. In engines of large thrusts with open circuit, when the effectiveness of the TNA plays an essential role, the application of expansion turbines is possible.

A variety of the multistage velocity stage turbine is a turbine with rotation of gas feed (Fig. 7.25c). In these turbines the gas enters the turning channel from the rotor blades of the wheel, where the direction of flow is changed, and it is again feed to the rotor wheel. Such a turbine has large losses, but then the rotor wheel has one rim. There is known the application of a turbine with rotation of flow in a "Walter" ZhRD [25].

According to the degree of utilization of the flow cross-sectional area of the nozzle ring we distinguish partial-flow and unpartial-flow turbines. Turbines in which the nozzle channels are only on part of the circumference are called partial flow. The ratio of working arc of the nozzle ring a_p to the entire circumference is called the degree of partiality:

$$\epsilon = \frac{a_p}{2\pi D}$$

Partiality causes additional losses. However, at low gas flow rates (which frequently occur in ZhRD) the application of partiality permits obtaining a turbine of sufficient diameter (to provide u) with blades of acceptable length. In the final analysis, in a number of cases the improvement of turbine efficiency due to increase of u and increase of length of blades is obtained greater than its drop due to partiality losses. Furthermore, at a prescribed

gas temperature the temperature of the blades of a partial-flow turbine is lower.

According to the number of shafts we distinguish single-shaft and double-shaft turbines. A diagram of a double-shaft turbine is shown on Fig. 7.26. The application of a double shaft turbine in the TNA of a ZhRD can turn out to be expedient because of the considerable difference in maximum allowable r/min of fuel and oxidizer pumps (see Table 7.1). However, the application of double-shaft turbines in the TNA can lead to complication of starting and control of the engine and complicates the construction of the TNA on the whole.

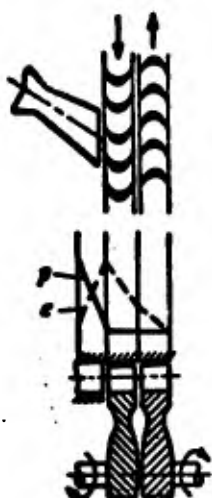


Fig. 7.26. Double-shaft turbine.

Basic Parameters of TNA Turbines

Calculation of turbines of the TNA does not differ in principle from calculation of aviation gas turbines and is discussed in detail in [132], [134], [136]. Let us consider the specific character of evaluation and selection of basic parameters of turbine operation in reference to the TNA.

Required turbine power N_t is determined generally as the sum of required powers of pumps of oxidizer N_{ox} , fuel N_{fu} , and accessories

N_{turb} , driven by the turbine:

$$N_t = N_{\text{a.e.}} + N_{\text{a.r.}} + N_{\text{turb.}} \quad (7.48)$$

In the absence of accessories

$$N_t = N_{\text{a.e.}} + N_{\text{a.r.}} \quad (7.49)$$

In accordance with expression (7.10)

$$N_t = \frac{\Delta p_e G_e}{75 \gamma_e \eta_{\text{me}}} + \frac{\Delta p_r G_r}{75 \gamma_r \eta_{\text{mr}}} \quad (7.50)$$

If we assume $\Delta p_e = \Delta p_r = \Delta p$ and consider $\eta_{\text{me}} = \eta_{\text{mr}} = \eta_{\text{m}}$,

$$N_t = \frac{\Delta p G}{75 \gamma_r \eta_m} \quad (7.51)$$

where $G = G_e + G_r$; γ_r - fuel density,

$$\gamma_r = \frac{1 + v}{\frac{1}{\gamma_e} + \frac{1}{\gamma_r}} \quad (7.52)$$

Required power of turbine per ton of thrust N_t/P can be approximately determined by formula (7.51):

$$\frac{N_t}{P} = \frac{\Delta p G}{75 \gamma_r \eta_m P_{\text{f},1} G} = \frac{\Delta p}{75 \gamma_r \eta_m P_{\text{f},1}} \quad (7.53)$$

Figure 7.27 lists the approximate calculation of relationship $N_t/P = f(p_2)$. We see that for tentative appraisals it is possible to assume

$$\left| \frac{N_t}{P} \right| \text{ hp/T}_{\text{th}} = |p_2| \text{ kgf/cm}^2 \quad (7.54)$$

Turbine power (available)

$$N_t = \frac{L_m \eta_r}{75} \cdot G_r \quad (7.55)$$

where G_t — flow rate of working substance through the turbine;
 η_t — turbine efficiency.

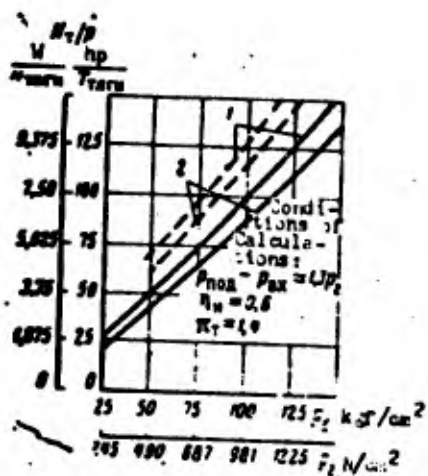


Fig. 7.27. Dependence
 1 — $O_2 +$ kerosene; 2 — $HNO_3 +$
 + kerosene; — open circuit;
 ----- closed circuit.

Expansion ratio of gas in the turbine

$$\pi_t = \frac{P_{t2}}{P_{t1}}. \quad (7.56)$$

In accordance with equality (7.55) an increase of expansion ratio, increasing L_{av} , leads to an increase of available turbine power. However, at high values of π_t the growth of L_{av} and N_T with further increase of π_t is insignificant. Therefore, with open circuit the expansion ratio is taken within limits of 15-40.

In the TNA of systems operating by a closed circuit the gas expansion ratio on the turbine is determined by coordinating the available turbine power and the required power of the pumps (see Chap. VIII). Usually for closed circuits π_t is within limits of 1.3-1.8.

Depending upon the value of π_t the turbine can operate at both subsonic, i.e., at subsonic speeds in the blading, and at supersonic speeds, i.e., at supersonic speeds in the blading. Supersonic turbines are characteristic for the TNA of open circuits. In the TNA of closed circuits the turbines are usually subsonic although

at magnitudes of pressures in the chamber close to maximum (see section 8.1), an increase of pressure ratio $p_{\text{ex}}^*/p_{\text{exz}}$ to supersonic is possible.

Turbine exit pressure (back pressure) p_{exz} at prescribed expansion ratio π , determines the turbine inlet pressure and its decrease leads to reduction of the mass of the TNA. Thus, it is desirable to always have the smallest possible p_{exz} .

In closed-circuit TNA turbines of p_{exz} is defined as the sum of pressure in the chamber p_2 and the amount of losses of pressure on the section from the turbine to the combustion chamber Δp_2 :

$$p_{\text{exz}} = p_2 + \Delta p_2. \quad (7.57)$$

In open-circuit TNA turbines it is desirable to have the lowest possible pressure p_{exz} . However, it is not always expedient to take p_{exz} equal to ambient pressure p_∞ since with change of flight altitude the exit pressure will be changed and consequently also the TNA operating conditions. To ensure constancy of TNA operating conditions at the end of the exhaust pipe there is sometimes placed an adapter with a supersonic Laval nozzle. In this case the value of p_{exz} is set from the following considerations. If we provide simply a supercritical pressure drop, then p_{exz} should be $(\frac{\kappa+1}{2})^{\frac{1}{\kappa}}$ times greater than p_∞ , i.e., approximately 1.7-1.9 times. However, if we consider that the adapter with Laval nozzle can operate under conditions of overexpansion, i.e., with adapter exit pressures equal to (0.3-0.4) p_∞ pressure p_{exz} can be reduced and taken approximately equal to $1.3 p_\infty$.

Thus, the use of overexpansion in the exhaust adapter permits a 40-50% reduction of pressure p_{exz} necessary to ensure constant operating conditions of the TNA. In certain cases for obtaining constant and sufficiently small values of p_{exz} the exhaust gases from the TNA are directed to the flow at the nozzle section.

Temperature of gas entering the turbine T_{in} is selected by proceeding from the strength possibilities of the turbine elements. Depending upon conditions and time of operation, and also material of blades, T_{in} is taken within limits of 750-1200°K. In certain cases during short-duration operation T_{in} is increased.

Number of revolutions of the turbine n is most frequently determined by the maximum permissible number of revolutions of pump with respect to conditions of cavitation (see section 7.1). Moreover, in a single-shaft TNA (see Fig. 7.40) the turbine r/min is limited by the r/min of the oxidizer pump. With a reduction gear circuit of the TNA the selection of turbine r/min is determined by conditions of economic operation of the turbine with sufficiently small dimensions.

Efficiency and Selection of w/c_{in} Turbines of the TNA

Losses of work in the turbine are composed of the following types of losses:

- a) hydraulic losses in the nozzle ring L_c ;
- b) hydraulic losses during flow of gas in the rotor wheel L_s ;
- c) with exit velocity L_{smax} ;
- d) disk friction and windage losses L_w ;
- e) due to leakages of gas through seals and radial clearances of the rotor and nozzle blades (the latter - in multistage turbines) L_m ;
- f) mechanical losses L_m .

The amount of hydraulic losses L_c and L_s characterizes the degree of perfection of the turbine blading and is estimated by adiabatic

(blade) efficiency

$$\eta_{\text{bl}} = \frac{L_m - (L_t + L_s)}{L_m} \quad (7.58)$$

The essence of losses with exit velocity L_{exit} involves the fact that gas after exiting the rotor blades of the turbine possesses a specific terminal velocity c_2 , and consequently, kinetic energy, i.e.,

$$L_{\text{exit}} = \frac{c_2^2}{2g} \quad (7.59)$$

By subtracting the sum of hydraulic losses $L_t + L_s$ and losses with exit velocity from available work L_m we determine work on the blades, or circumferential work of the turbine:

$$L_b = L_m - (L_t + L_s + L_{\text{exit}}) \quad (7.60)$$

The ratio of circumferential work to available is called circumferential efficiency:

$$\eta_c = \frac{L_b}{L_m} \quad (7.61)$$

Losses on disk friction (disk losses) are friction of the lateral surfaces of the disk. Windage losses appear only in partial-flow turbines. At a small degree of partiality (0.2-0.3) the amount of losses can be 20-30%. These losses are characteristic for partial-flow turbines of the TNA assembly of installations operating on an open circuit. In the absence of partiality ($\epsilon = 1$) there are no windage losses. It is necessary to consider that the amount of losses due to partiality essentially depends on the structure of the nozzle ring. Use of the nozzle ring, assembled one sector (Fig. 7.28a) is more effective than the symmetric location on the circumference of the wheel of several sectors (Fig. 7.28b).

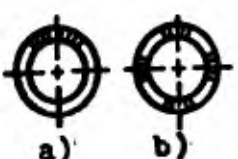


Fig. 7.28. Location of nozzle ring in partial-flow turbine: a) rational; b) irrational.

Leakage losses primarily depend on the value of radial clearance δ between blades and the body, and in multistage turbines — still on the clearance between the nozzle blades and disk. With long blades the relative value of clearance δ/i (where i — height of the blade) is small and losses are also small. With short blades, which is characteristic for TMA turbines, δ/i is comparatively great and losses become appreciable.

By subtracting windage and disk losses and also leakage losses from circumferential work, we obtain the internal work of the turbine:

$$L_i = L_a - (L_w + L_{le}). \quad (7.62)$$

Ratio of internal work to available is called internal efficiency:

$$\eta_i = \frac{L_i}{L_a}. \quad (7.63)$$

By subtracting mechanical friction losses in bearings and seals from internal work, we obtain effective work of the turbine L_e .

$$L_e = L_i - L_m. \quad (7.64)$$

Ratio of effective work to internal is called mechanical efficiency:

$$\eta_m = \frac{L_e}{L_i}. \quad (7.65)$$

Ratio of effective work to available is called effective efficiency or simply efficiency of the turbine η_t :

$$\eta_t = \frac{L_e}{L_a}. \quad (7.66)$$

It is obvious that

$$\eta_t = \eta_i \cdot \eta_m. \quad (7.67)$$

The value of η_u is usually equal to 0.95-0.99. The value of η_r for TNA turbines of open circuit is within limits of 0.3-0.7 (see Table 7.2). For TNA turbines of installations operating on a closed circuit, η_r is increased due to increase of u/c_{ax} .

Dependence of efficiency on u/c_{ax} and selection of peripheral velocity. Of all the losses, those with exit velocity are basic. In accordance with equality (7.59) these losses are less, the lower the absolute exit velocity c_2 . In turn, velocity c_2 depends on peripheral velocity u , worked by heat drop, i.e., velocity c_{ax} (or in a particular case for action turbine velocity c_1), and degree of reaction ρ .

Investigation of the change of circumferential efficiency of the turbine η_u shows that η_u primarily depends on relationship u/c_{ax} (or u/c_1 for action turbine). Typical form of dependence $\eta_u=f(u/c_{ax})$ is shown on Fig. 7.29. When $u/c_{ax}=0$, i.e., with a motionless turbine, obviously η_u is also equal to zero. The value of η_u grows as u/c_{ax} increases and at some value of u/c_{ax} the value of η_u reaches maximum. With further increase of u/c_{ax} , η_u decreases mainly because of the growth of losses with rise of exit velocity. Fig. 7.29 lists coefficients of hydraulic losses in the nozzle ring ξ_c and on rotor blades ξ_r . Value of ξ_c is determined only by work of the nozzle ring and does not depend on u/c_{ax} . Hydraulic losses on blades are increased with decrease of u/c_{ax} .

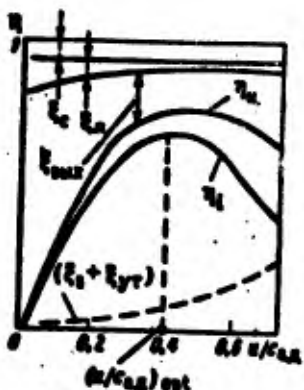


Fig. 7.29. Balance of energies in the turbine depending upon

It is possible to show [134] that relative windage and friction losses ξ_w and losses on leakage ξ_l are proportional $(u/c_{\infty})^n$, where $n > 1$. On Fig. 7.9 by a dotted line there are plotted relative losses $(\xi_w + \xi_l)$. By subtracting the relative losses from η_u we find the value of internal efficiency:

$$\eta_i = \eta_u - (\xi_w + \xi_l). \quad (7.68)$$

For a multistage turbine the value of $(u/c_{\infty})_{opt}$, corresponding to maximum value of efficiency, shifts to the left more, the greater the number of stages (Fig. 7.30a). Although maximum value of efficiency decreases with this, at small values of $(u/c_{\infty})_{opt}$ the value of efficiency of a multistage turbine is higher. Therefore, at small u/c_{∞} the application of double-stage turbines is often rational.

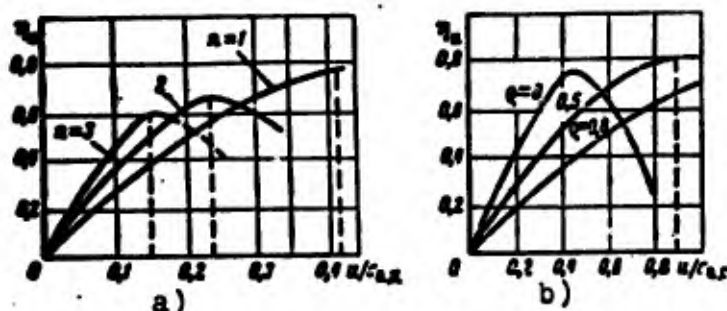


Fig. 7.30. Effect of the number of stages (a) and degree of reaction (b) on efficiency.

With increase of the degree of reaction of turbine ρ the value of $(u/c_{\infty})_{opt}$, corresponding to maximum of efficiency is increased (Fig. 7.30b); furthermore, characteristic $\eta_u = f(u/c_{\infty})$ are more mildly sloping, which is sometimes very important. In the TNA of installations with closed circuit, having small pressure drop and, as a result, small values of c_{∞} , i.e., comparatively high values of (u/c_{∞}) , the application of reaction turbines is often rational.

The value of peripheral velocity u depends on the number of revolutions of the turbine and diameter of the wheel. The number of revolutions of the turbine is often limited by the allowable number of revolutions of pumps. Increase of u due to increase of the wheel diameter leads to increase of dimensions and mass of the TNA. Furthermore, at low flow rates of gas the increase of diameter will entail a decrease of the degree of partiality, i.e., increase of losses. Considering the shown considerations and strength requirements, the value of peripheral velocities in turbines of the TNA is taken within limits of 250-350 m/s.

In TNA turbines of installations with open circuit due to a large pressure drop on the turbine π_t , the heat drop (i.e., value of c_{ax}) is very considerable. Thus, for a single-stage action turbine the value of $c_i = \varphi c_{ax}$ reaches 1000-1400 m/s. Due to this, values of w/c_{ax} at which the turbine works are small and within limits of 0.1-0.3 (see Table 7.2). In turbines of installations with closed circuit the pressure drops π_t are small and c_{ax} is considerably less. Therefore, the values of w/c_{ax} for them comprise a value on the order of 0.4-0.6.

Types of TNA Turbines

Specific character of operating conditions of the turbine in a TNA and requirements for the TNA, as the most important unit of the propulsion system, determine the types of turbines which it is rational to use at different schemes of propulsion systems of ZhRD.

In the TNA of liquid propellant rocket engines there are mainly applied axial-flow action turbines. These turbines are simpler in construction and are sufficiently reliable in operation. For the TNA of liquid-propellant rocket engines, operating on an open circuit, the application of partial-flow action turbines is characteristic. The point is that with an open circuit for decrease of losses of components on driving the TNA we try to

decrease the flow rate of working substance to the turbine (this is attained by increase of pressure drop π). Due to small flow rates it is expedient to make the turbine partial-flow. The presence of partiality is responsible for the application of action turbines, since in reaction turbines due to pressure drop on the wheel blades there would appear large losses because of overflow of gas into the channels not streamlined by flow. Furthermore, at small u/c_{∞} (which is characteristic for turbines of the TNA of open circuits) lowering of the degree of reaction leads to increase of efficiency.

In the TNA of open-circuit engines we use both single- and double-stage turbines, more often with velocity stages. In the TNA of liquid propellant rocket engines with closed circuit there are basically used axial-flow single-stage turbines. The application of several stages in this case is inexpedient because of the small heat drop. With a closed circuit due to high values of u/c_{∞} along with action turbines there can be used turbines with small reactance. From convenience of arrangement with a closed circuit the application of radial-flow turbines is possible.

If for spin-up of the TNA there are applied special turbines, operating from a combustion turbine starter, then they are usually made axial-flow single-stage, partial.

Characteristics of Turbines

Dependence of the change of some operating parameter of the turbine (power, torque, efficiency, etc.) from the turbine operating conditions (number of revolutions, gas flow rate, etc.) is called the turbine characteristic.

We distinguish normal characteristics, i.e., relationship between absolute operating parameters, and universal, i.e., relationship between complexes of operating parameters of the turbine. The construction of different characteristics is examined in detail in [132], [134].

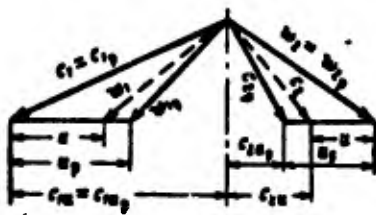


Fig. 7.31. Change of velocity triangles with change of r/min.

For analysis of the joint operation of turbine and pumps let us examine the characteristic of change of turbine power depending upon the number of revolutions $N_r = f(n)$. For simplicity let us assume that at constant pressure drop π , the flow rate of gas, degree of reaction and gas velocity w_2 do not depend on the number of revolutions n . Let us examine the change of velocity triangles with change of r/min (Fig. 7.31). As initial let us take velocity triangles during operation at rated conditions. From Fig. 7.31 it is clear that if

$$c_1 = c_{1s} = \text{const}; \quad w_2 = w_{2s} = \text{const};$$

then

$$c_{1s} = c_{1s_p} = \text{const}; \quad c_{2s} = c_{2s_p} + u_s - u. \quad (7.69)$$

Having placed the value of c_{2s} , obtained in expression (7.69), in formula (7.44), we obtain

$$P_s = \frac{\sigma}{\epsilon} (c_{1s_p} + c_{2s_p} + u_s - u).$$

Torque of turbine

$$M_s = P_s \frac{D}{2} = \frac{\sigma}{\epsilon} (c_{1s_p} + c_{2s_p} + u_s - u) \frac{D}{2}. \quad (7.70)$$

When $u = 0$ we obtain the value of maximum torque $M_{s_{\max}}$:

$$M_{s_{\max}} = \frac{\sigma}{\epsilon} (c_{1s_p} + c_{2s_p} + u_s) \frac{D}{2}. \quad (7.71)$$

Since in expression (7.70) all values, except velocity u , do not depend on the number of revolutions, dependence $M_u = f(n)$ is expressed by a straight line. Consequently,

$$M_u = M_{u,\max} - (M_{u,\max} - M'_{u,p}) \frac{n}{n_p}. \quad (7.72)$$

Having designated

$$\mu = \frac{M_{u,\max}}{M'_{u,p}}, \quad (7.73)$$

we obtain

$$M_u = M'_{u,p} \left[\mu - (\mu - 1) \frac{n}{n_p} \right]. \quad (7.74)$$

Turbine power

$$N_t = \frac{M_u n}{78.2}. \quad (7.75)$$

Having placed equality (7.74) in expression (7.75), we obtain characteristic of change of power respect to the number of revolutions at constant gas flow rate

$$N_t = N'_{t,p} \frac{n}{n_p} \left[\mu - (\mu - 1) \frac{n}{n_p} \right]. \quad (7.76)$$

This characteristic is expressed by a parabola and is represented on Fig. 7.32. At different gas flow rates we obtain a family of characteristics. Equating the first derivative dN_t/dn , to zero we find the number of revolutions n , corresponding to peak power $N_{t,\max}$ and the value of $N_{t,\max}$:

$$n = n_p \frac{\mu}{2(\mu - 1)}; \quad N_{t,\max} = N'_{t,p} \frac{\mu^2}{4(\mu - 1)}. \quad (7.77)$$

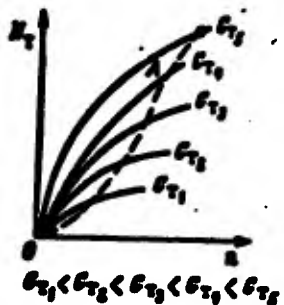


FIG. 7.32. Characteristics $N_r=f(n)$.

7.4. Joint Operation of Turbine and Pumps

Characteristic of joint operation of pumps and turbine is primarily determined by the method of feeding working substance to the turbine - independently of the TNA or pumps, actuated by the TNA.

The first method is usually applied when driving the TNA from a PGG having its own pressurized feed (see, for example, rocket A-4). In this case the supply of component to PGG does not depend on operation of the TNA. In the second case components are fed to PGG or ZhGG by pumps of the TNA. In this case feed already depends on the operating conditions of the TNA. Let us consider the joint course of characteristics $N = f(n)$ and starting of the TNA in each of the indicated cases.

Joint Operation of Turbine and Pumps with Independent Feed of Working Substance

With independent feed the parameters of working substance p_m^*, T_m^*, G_r remain constant and do not depend on TNA operation. According to equation (7.76) the characteristic of turbine $N_r=f(n)$ will pass as is shown on Fig. 7.33. Pumps of the TNA are connected with the feed system, having its own hydraulic characteristic. For each of the pumps according to expression (7.42) $N_p=C_p n^3$. Obviously, the dependence of required power of all the pumps can be expressed as

$$\Sigma N_p = C \cdot n^3. \quad (7.78)$$

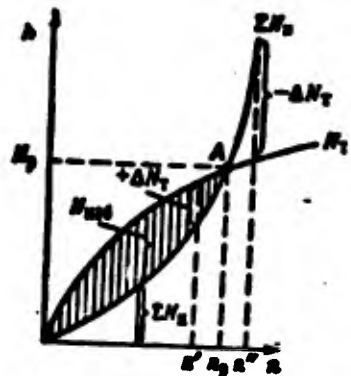


Fig. 7.33. Characteristics of joint operation of turbine and pumps with independent supply of working substance.

Combined graph of characteristics of pumps and turbine is shown on Fig. 7.33. Point A – operating point, where

$$\Sigma N_s = N_r. \quad (7.79)$$

With change of the number of revolutions from 0 to n_p (spin-up of TNA) we have an excess of turbine power (shaded region), i.e.,

$$N_r - \Sigma N_s + N_{ss}. \quad (7.80)$$

When $n = n_p$ power $N_{ss} = 0$. Stability of operation of the TNA at operating conditions (point A) is determined by the magnitude of the angle between characteristics of pumps and turbine. With such a course of characteristics, as is shown on Fig. 7.33, at point A the operating conditions of the TNA will be stable, since with random probable deviation of the number of revolutions from calculated we obtain excess $+ \Delta N_r$ (when $n' < n_p$) or deficiency $- \Delta N_r$ (when $n' > n_p$) of available power, and the system is returned to the operating point. Thus, stable operating condition

$$\frac{dN_s}{dn} > \frac{dN_r}{dn}. \quad (7.81)$$

Stability margin is determined by the value of ΔN_r with deviation from operating conditions, i.e., value of the angle between characteristics (Fig. 7.34). At a small angle between characteristics

(shown on dotted line) is small and there can occur scattering of values of N and n of operating conditions (floating conditions). The greater the angle between characteristics, the stabler the conditions.



Fig. 7.34. For appraisal of stability of operating conditions.

Spin-Up of TNA with Independent Supply of Working Substance

Let us determine the spin-up time of the TNA to working r/min.

In formula (7.80) power ΣN_s is expended on the flow through of components; excess of power N_{ss} goes for spin-up of the TNA, i.e.,

$$N_{ss} = N_r - \Sigma N_s. \quad (7.82)$$

If J — moment of inertia of TNA rotor and adjacent masses of liquid, and ω — angular velocity of rotation of the rotor, then

$$N_{ss} = J \frac{d\omega}{dt}. \quad (7.83)$$

By placing the expression for N_{ss} in equality (7.82) and integrating, we find the spin-up time of the TNA to arrival at operating conditions

$$\tau_p = \int_0^{\omega} \frac{J \omega}{N_r - \Sigma N_s} d\omega. \quad (7.84)$$

We usually determine τ_p by numerical integration. The smaller J is and the greater is N_{max} , the faster the spin-up of the TNA occurs. From this point of view the adjacent masses of liquid must be smaller. However, if we produce spin-up of pumps without the adjacent masses (i.e., without components) and then switch on the supply of components to pumps a severe water hammer will be obtained, which can destroy the TNA. Therefore, we frequently start spin-up of the TNA and filling of pumps simultaneously, obtaining with this some gain in the time of arrival at conditions.

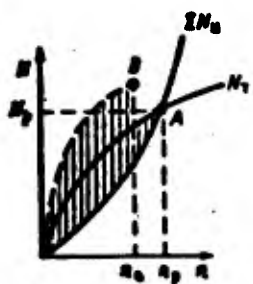


Fig. 7.35. Reduction of time of arrival at conditions by increase of the flow rate of working substance.

For decrease of the time of arrival at conditions up to a specific number of revolutions n_* (Fig. 7.35) it is possible to feed a high flow rate to the turbine, which will ensure a large excess of power N_{max} during arrival at conditions. Upon achievement of number of revolutions n_* (point B) the flow rate of working substance is decreased to nominal.

In the TNA of powerful ZhRD, having large revolving masses, the time of arrival at conditions τ_p can reach considerable values. However, large values of τ_p signify superfluous fuel consumption; furthermore, for a number of rockets (upper stages of space rockets, surface-to-air rockets, etc.) it is desirable to have the smallest possible τ_p . Usually values of τ_p reach several seconds (for H-1 engine $\tau_p \approx 1.2$ s).

Joint Operation of Turbine and Pumps with Dependent Supply of Working Substance

With dependent feed to the PGG or ZhGG the components enter the gas generator from pumps of the TNA. In this case as the

number of revolutions of the TNA increase from 0 to n_p , the flow rate of components to the gas generator increases from zero to the calculated flow rate. Accordingly pressure in the gas generator is increased to calculated. If the ratio of components in ZhGG ω_{MP} remains constant (or if the gas generator is single-component - PGG), then the temperature in the gas generator can be considered constant.

As the flow rate of the working substance increases the available turbine power will increase along curve OA (see Fig. 7.32) to calculated (point A). Under all conditions at numbers of revolutions smaller than calculated, characteristic $N_t=f(n)$ will pass below the characteristic at constant flow rate, first, due to decrease of the flow rate, and, secondly, due to a sharp increase of losses during operation at partial load conditions with decreased flow rates of working substance.

Characteristics of joint operation of pumps and turbine for two possible cases are shown in Fig. 7.36. In the first case (Fig. 7.36a) the curve of available power $N_t=f(n)$ in the entire range of revolutions from 0 to n_p will pass above the curve of required power $\Sigma N_s=f(n)$. This case does not differ in principle from spin-up of the pump with independent feed of working substance. However, excess power of turbine N_{ex} will be considerably less (shaded region), as a consequence of which the time of arrival at conditions will increase sharply. During operation of TNA with dependent feed the second case can often be encountered, when at the beginning of spin-up the available power is less than the required (Fig. 7.36b) $N_t < N_s$, i.e., up to the point for spin-up of the TNA an outside influence from a special starting device is necessary. Characteristic of available power intersects the characteristic of required power twice (at points B and A). At point B the conditions are unstable. With displacement to the right of point B the TNA will gain revolutions; with displacement to the left the TNA will subside; at point A the operating conditions are stable.

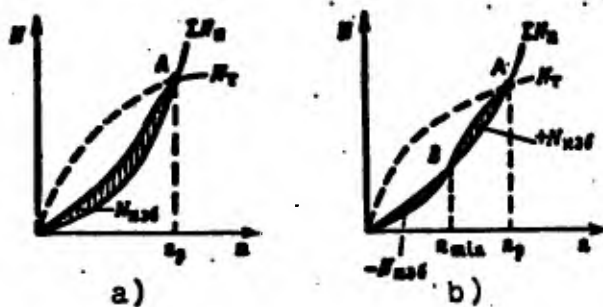


Fig. 7.36. Characteristics of joint operation of turbine and pumps with dependent feeding of working substance.

Spin-Up of TNA with Dependent Feed of Working Substance

With dependent feed of working substance the problem of spin-up of the TNA is reduced to "bringing" the TNA to conditions with n/min greater than n_{\min} (point B) with the help of a starting device (starter). As we noted earlier (section 6.2), for spin-up there can be used starters with solid fuel pressure accumulator (PAD), with compressed gas and with PGG, having independent feed. In certain cases the excess available power during spin-up is created due to head in the fuel tanks and pressure head of column of components.

Characteristics of joint operation of turbine and pumps during starting with the aid of a starter are shown on Fig. 7.37. The starting device is calculated from the condition of providing $n_{\text{spin}} = (1.1+1.2)n_{\min}$. The spin-up time to n_{spin} is determined by a condition analogous to condition (7.84):

$$\tau_{\text{spin}} = \int_{n_{\min}}^{n_{\text{spin}}} \frac{J_n}{N_{\text{spin}} - \Sigma N_n} dn. \quad (7.85)$$

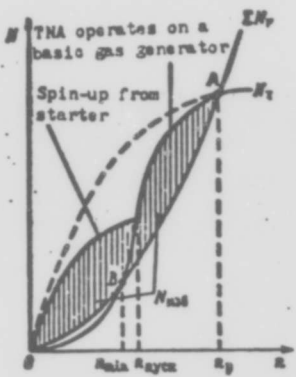


Fig. 7.37. Characteristics of TNA during starting by a starting device.

The more powerful the starting device, the smaller is τ_{sync} , and the greater its mass, which it is especially necessary to consider if the device is placed on a rocket. Thanks to high reliability ($\approx 99.8\%$), starters with PAD received wide propagation. On Fig. 7.38 there is shown the PAD for engine H-1. In the PAD are three propellant assembly of installations with closed circuit, during selection of the type of starting device and arrangement of the TNA one should consider that in the case of use of a starter with PAD the combustion products of FAD, as a rule, have a negative oxygen balance. Therefore, if the ZhGG is oxidizing, then to avoid the danger of a sudden temporary rise of temperature during burning of combustion products of ZhGG and solid fuel gases a starting turbine is more expedient.

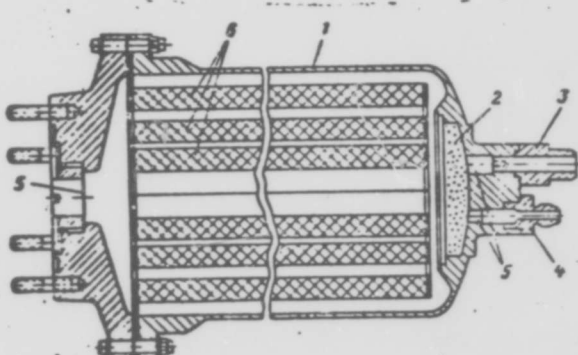


Fig. 7.38. Starting PAD of H-1 engine:
 1 - body; 2 - igniter;
 3 - primer; 4 - pressure pickup; 5 -
 breaking membranes; 6 - propellant charges.

Arrangement of TNA

The construction and operating characteristics of the TNA are determined to a considerable degree by the accepted diagram of its arrangement and also the type of basic units, i.e., pumps and turbines.

According to the layout diagram we distinguish single-shaft (without reduction gear), reduction gear and separate TNA.

The most wide-spread are single-shaft TNA (Fig. 7.39A). They are simpler in construction and more reliable in operation. However, a disadvantage of them is the difficulty (and sometimes impossibility) of provision of operation of pumps and turbine at parameters (efficiency, number of revolutions) close to optimum.

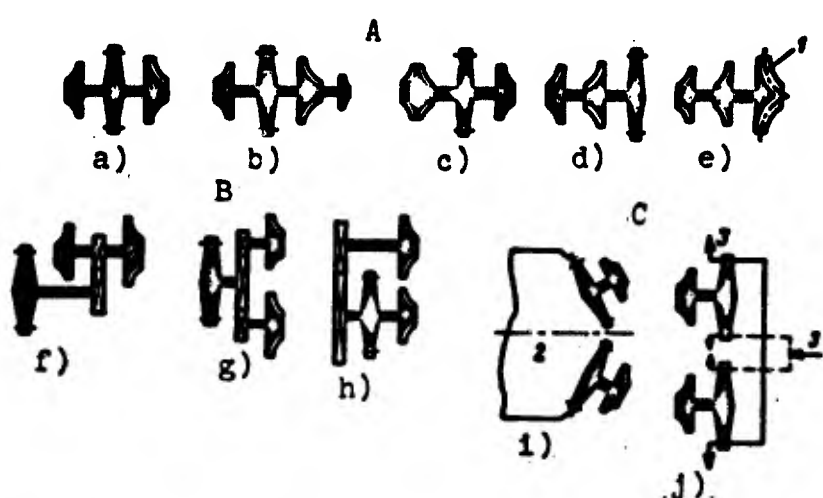


Fig. 7.39. Diagrams of arrangement of TNA:
a) single-shaft TNA; b) reduction gear TNA;
c) separate arrangement; 1 - radial-flow
turbine; 2 - combustion chamber; 3 - working
substance.

The point is that with single-shaft arrangement the numbers of revolutions of the turbine and all the pumps are identical. The highest possible number of shaft revolutions is limited to the lowest of the maximum permissible revolutions n_{\max} of pumps, placed

on the shaft. In turn, according to equality (7.32)

$$n_{\max} = \frac{c_{\text{sp}}}{\sqrt{Q}} \left(\frac{P_{\text{ex}} - P_0}{107} \right)^{\frac{1}{2}}.$$

If for a qualitative appraisal we take values $(P_{\text{ex}} - P_0)$ and c_{sp} of fuel and oxidizer pumps approximately equal, then the ratio of maximum permissible revolutions of fuel and oxidizer pumps

$$\frac{n_{\max, T}}{n_{\max, p}} = \sqrt{\frac{T_0}{T_r}} \sqrt{\frac{c_{\text{sp}, T}}{c_{\text{sp}, p}}}.$$
 (7.86)

Data calculated by formula (7.86) for certain fuels are represented in Table 7.1, from which it is clear that n_{\max} of fuel and oxidizer pumps differ by several times. There is an especially great difference of n_{\max} for hydrogen engines. Thus, by determining the number of revolutions of a single-shaft TNA depending on n_{\max} of the pump, allowing a lower number of revolutions, we underestimate the revolutions of the turbine, placing it in operating conditions that are considerably worse than optimum. It is true that by application of special measures, protecting from cavitation (pressurization of tanks, installation of prepumps, etc.), it is possible to somewhat increase the value of n_{\max} , but not so much that the turbine of a single-shaft TNA would operate in the most advantageous conditions. Moreover, turbines of single-shaft TNA of propulsion systems of open circuits operate under more difficult conditions.

Due to the shown cases under certain conditions the arrangement of a TNA with reduction gear or a separate arrangement can be more advantageous. Reduction gear TNA (Fig. 7.39B and 7.40) have a transmission, lowering the revolutions of the pump (one or several) as compared to the turbine revolutions. In this case each unit (turbine and pumps) works at optimum revolutions, which gives a definite gain in their efficiency. However, such TNA are considerably more complicated and heavier. Frequently they require special lubrication and cooling of the reduction gear.

Table 7.1

Components	γ	α	v_0	$\frac{n_{max}}{n_{max0}}$
Kerosene	0.83			
Liquid oxygen	1.11			
Kerosene	0.83			
Nitric acid	1.51			
Liquid hydrogen	0.07			
Liquid oxygen	1.14			
Liquid oxygen	0.07			
Liquid fluorine	1.51			

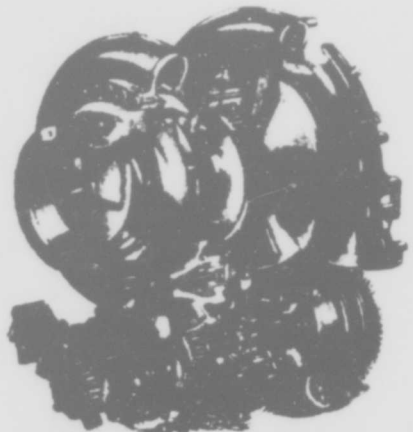


Fig. 7.40. Reduction gear TMA of RZ-2 engine.

Diagrams of separate arrangement of the TMA are presented on Fig. 7.39C. Here each pump is driven by its own turbine, which permits operating the turbine at more favorable conditions and can be expedient in hydrogen engines, when the difference in n_{max} of oxidizer and fuel pumps is especially great. Furthermore, with such an arrangement the problems of fuel feed to the TMA and component feed control are solved more easily. A deficiency of the separate arrangement is the fact that two turbines are installed

with it. Separate arrangement of the TNA is apparently inevitable in closed circuit propulsion systems of the "gas + gas" type (see section 8.3). An example of ZhRD with separate arrangement of the TNA can be RL-20P propulsion system (see Fig. 8.5).

In a single-shaft TNA the turbine can be located between the pumps (see Fig. 7.39a, b, c) and overhung (see Figs. 7.39d, e, 7.42 and 7.43).

Overhung location of the turbine is expedient in propulsion systems with closed circuit, since it facilitates the feed of combustion products from the turbine to the chamber of the engine. In installations with open circuit the place of location of the turbine is often determined by the convenience of distribution of units of the installation (ZhGG, evaporator, pipeline of components, etc.). With a single-shaft TNA the overhung location of the turbine imposes raised requirements for seals of the closely located fuel and oxidizer pumps (especially with hypergolic components).

The TNA can have two, three and more pumps. The additional pumps are for fuel feed to the PGG (see Fig. 6.4b), and also for fuel feed to ZhGG in installations of closed circuit of the type shown on Fig. 8.3. Sometimes the TNA are also used for driving the accessories (electrical generators, regulators, etc.).

Arrangement of TNA in the Propulsion System

Figure 7.41 lists possible schemes of joint arrangement of the TNA and engine chamber.

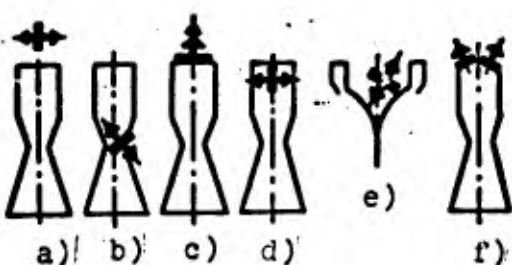


Fig. 7.41. Diagrams of arrangement of TNA relative to engine chambers.

During arrangement of the TNA, besides compactness for the purpose of decreasing dimensions and mass of the entire installation, it is necessary to provide as far as possible the straightest path of fuel from the tanks to pumps (for decrease of pressure losses), convenient feed of working substance to the turbine and removal of gases from it. In engines with closed circuit it is desirable that the gas line for feeding high-temperature gases from the turbine to the chamber head be as short as possible, and the velocity of gases in it do not exceed 150-200 m/s. Furthermore, during operation of the TNA one should consider the appearance of torque, imparted to the rocket, which can require additional compensation. With a rotating engine chamber it is better to fasten the TNA to the chamber; in this case flexible hoses for fuel feed are not under pressure, that increases the reliability of the flexible hose and decreases the force necessary for turning the chamber.

Basic Parameters and Examples of Completed TNA

Table 7.2 lists data of completed TNA. These data permit judging the order of values of efficiency of pumps and turbines, specific speed of the pumps and revolutions of the pumps and turbines of ZhRD. From the table there is also seen the tendency to increase of efficiency of pumps and, especially, efficiency of turbines.

Construction of the TNA of A-4 and "Walter" engines is examined in sufficient detail in [25].

On Fig 7.42 there is shown the TNA of the aircraft ZhRD ZRL-99 (see diagram on Fig. 6.35). The TNA feeds the fuel component: oxygen + ammonia. Basic data of the TNA are given in Table 7.2. Drive of the TNA is independent from the PGG, operating on 90% hydrogen peroxide. Turbine 5, action, with two velocity stages, is overhung. The oxidizer pump 13 has prepump 15; inlet to the pump is axial. Fuel 9 pump is made with double inlet. Control system of the ZhRD permits reducing thrust to 30% of nominal value by changing the revolutions of the TNA. In turn, the revolutions of the TNA are regulated by changing the flow rate of hydrogen peroxide from the PGG to the turbine.

Table 7.2. Parameters of Completed MA.

Engine	Components	Pump						Turbines						Note					
		Flow rate Q $\frac{\text{kg}}{\text{s}}$	P_{in} $\frac{\text{kN}}{\text{cm}^2}$	P_{out} $\frac{\text{kN}}{\text{cm}^2}$	η $\frac{\text{min}}{\text{min}}$	N_a	Type of gas generator	σ $\frac{\text{kg}}{\text{kg}}$	P_{in} $\frac{\text{kN}}{\text{cm}^2}$	P_{out} $\frac{\text{kN}}{\text{cm}^2}$	η $\frac{\text{min}}{\text{min}}$	effi- ciency η_p	N_t						
A-4	Oxygen 75% ethyl alcohol	68.2 55.4	2.8 1.3	0.273 0.128	18.2 21.9	1.78 2.15	3800 3800	0.44 0.35	193 272	142 200	PCC on H ₂ O ₂	2.13 0.32	26.32, 581, 750, 17 2.751, 750, 17	650 750	3800 1720	0.1 0.16	0.32 0.31	453 90	Turbo- double- stage; partial; $\epsilon=0.4$
"Malkin (aircraft)	Hydrogen peroxide Methyl alcohol • hydrazine- hydrate	60.6 2.4	0.3 0.3	-0.03 -0.03	42 42	4.12 4.12	17200 17200	— —	— —	— —	PCC on H ₂ O ₂	0.38- 0.32	2.751, 750, 17 750	650 750	1720 1720	0.16 0.16	0.31 0.31	90 90	Turbo- single-stage with burning of TSS
XM-90 (aircraft)	Oxygen Ammonia	52.9 42.3	15.2 19	1.49 1.87	69.1 81.1	6.80 7.93	12990 12990	0.75 0.68	445 759	327 5558	PUG on H ₂ O ₂	3.38 90%	— —	2.8 2.8	0.27 0.27	900 12900	— —	0.5 0.5	— —
RZ-2	Oxygen Kerosene	174.6 80.7	4.64 2.95	0.455 0.29	52.94 55.33	5.19 5.43	5990 5990	0.41 0.41	2400 1720	1767 1255	PUG on kerosene $\eta=0.351$	4.54 —	— —	— —	— —	923 29300	— —	0.65 0.65	4200, 3130 TMA reduc- tion gear; turbo- double- stage
H-1	Oxygen Kerosene	205.3 90.7	($P_{\text{out}} - P_{\text{in}}$) $= 57.8 \text{ kN/cm}^2$ ($5.67 \cdot \text{MN/m}^2$)	0.75	5940	0.75	1650	1350	2400 on O ₂ + kero- sene	— —	31,33,07	— —	— —	— —	— —	2800 29300	— —	0.88 0.88	2975, 2190

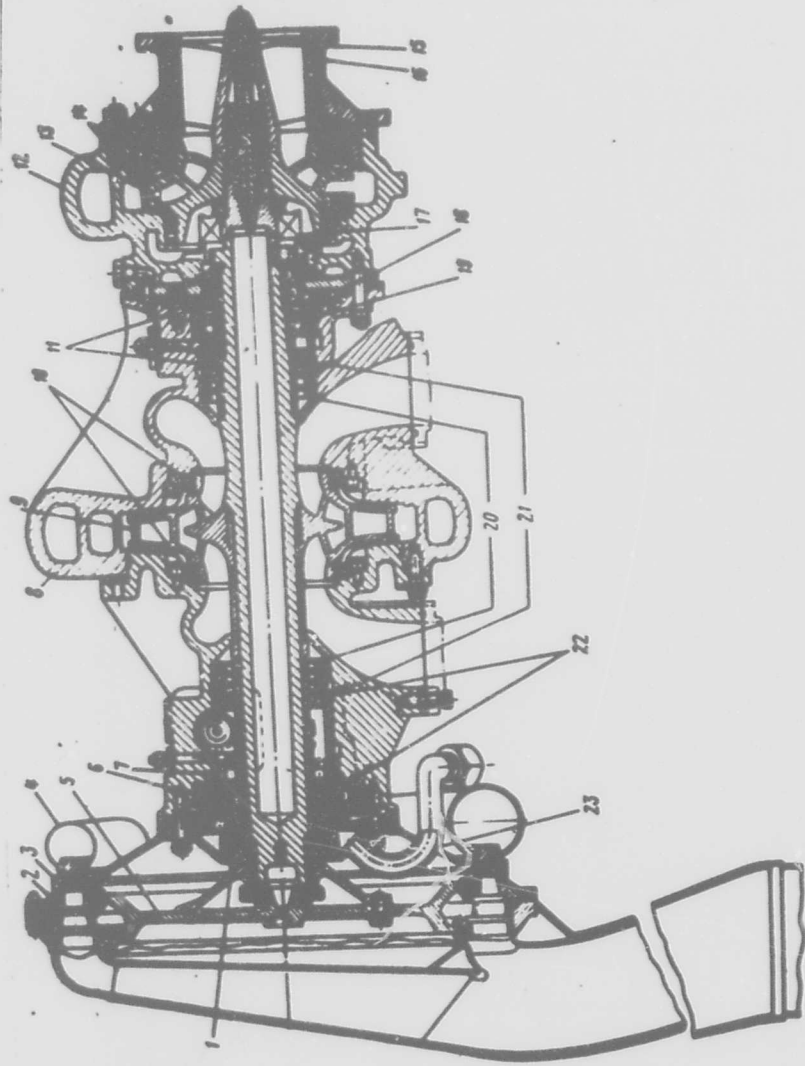


FIG. 7.42. TMA of a ZhRD: 1 - packing; 2 - body of turbine; 3 - nozzle unit; 4 - turbine inlet collector; 5 - turbine disk; 6 - bearing thrust ring; 7 - bearing; 8 - fuel-pump diffuser; 9 - fuel-pump impeller; 10 - fuel-pump packing; 11 - packing; 12 - oxidizer-pump diffuser; 13 - oxidizer pump impeller; 14 - oxidizer-pump; 15 - pre-pump; 16 - pre-pump body; 17 - packing; 18 - bearing thrust ring; 19 - bearing; 20 - fuel-pump packing; 21 - fuel and oil drains; 22 - packing; 23 - steam drain.

On Fig. 7.43 there is shown the TNA of RD-107 engine. TNA feeds fuel to the chamber, and also hydrogen peroxide for the gas generator and liquid nitrogen for pressurization of tanks.

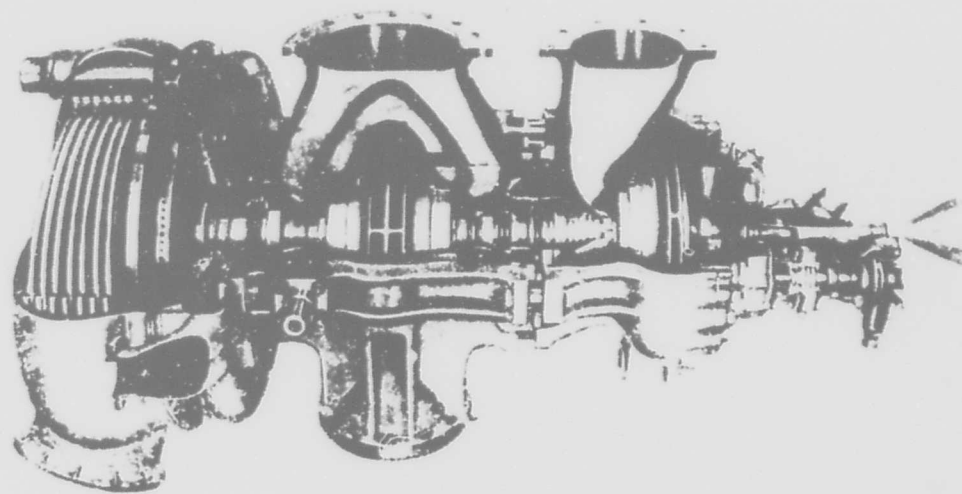


Fig. 7.43. Turbopump assembly of the RD-107 engine.

7.5. Gas Generators

Classification and Basic Parameters

The basic assignment of the gas generator is the obtaining of working substance of given temperature and quantity for driving the TNA. Furthermore, gas generators can be used as pressure accumulators for forced fuel feed (solid-propellant [PAD] and liquid-propellant [ZhAD] hot-gas generators), for pressurization tank, and for driving auxiliary systems. Gas generators can work on

liquid and solid fuel. Those of solid-fuel type (PAD) are usually applied for starting the TNA or as pressure accumulators for forced fuel feed [9.6]. For driving the TNA liquid fuel gas generators.

According to the number of components utilized for production of the working substance, we distinguish one-, two-, and three-component gas generators.

In the one-component gas generator the working substance is formed as a result of decomposition of fuel. They are usually called steam generators (PGG).

In two-component gas generators the working substance is obtained as a result of combustion of fuel and oxidizer. In three-component gas generators in order to lower temperature or for improvement of values of PT of the working substance a third component is used. Two- and three-component gas generators are usually called liquid gas generators ZhGG (Fig. 7.44). Conditions of the application of the PGG or ZhGG are examined in section 6.2. The basic operating parameters of the gas generator are temperature of working substance, value of RT and flow rate of working substance G_{xx} .

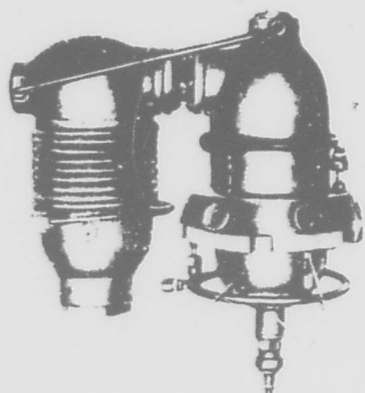


Fig. 7.44. External appearance of a ZhGG working on HNO_3 + kerosene (1937). 1 - starter cartridge; 2 - chamber; 3 - oxidizer injector; 4 - water injector; 5 - injector of fuel; 6 - chamber of additional evaporation.

The temperature of the working substance which the gas generator must provide is determined by the maximum permissible blade temperature and is 750-1200°K. The value of RT of the working substance characterizes its efficiency and depends on the components used and their relationship. The flow rate of the working substance through the gas generator is determined from the condition of providing necessary power of the TNA.

In propulsion systems with closed circuit of "gas + liquid" type total flow rate of components through the ZhGG is determined in the end by the temperature of the working substance, since all of one of the components in the ZhRD is fed to the ZhGG and its flow rate through the ZhGG is equal to that the chamber of the engine, while the flow rate of the second is so selected that the temperature of the working substance is equal to that assigned. With the closed "gas + gas" circuit flow rates of components through each ZhGG are determined from condition of providing rated temperature of working substance. Calculation of flow rates is given in section 8.3.

In propulsion systems with open circuit the flow rate of components through the gas generator is determined on the basis of the condition of providing necessary power of the TNA.

Knowing the necessary power of the turbine of the TNA to ensure fuel feed, we can determine the necessary flow rate of working substance produced by the gas generator from formula (7.55):

$$G_w = \frac{N_t}{L_{w\eta}} \quad (7.87)$$

Let us examine the operation and arrangement of different types of liquid-fuel gas generators

Steam Generators (PGG)

In the PGG the working substance is formed as a result of decomposition of monopropellant. In Table 7.3 are given certain fuels for the PGG.

Table 7.3.

Fuel	T°K	RT kgf·m/kgf	RT J/kg	n
Hydrogen peroxide, 100% concentration	1270	48,000	471,000	1.35
Isopropyl nitrate	1260	64,000	628,000	1.15
Hydrazine	867	68,000	668,000	1.37
Ethylene oxide	1200	56,000	55,000	1.17
UDMH	—	—	—	—

Most widely used in the PGG is hydrogen peroxide of different concentrations. The decomposition of hydrogen peroxide in the PGG occurs under the influence of a catalyst. As catalyst are used both liquids (aqueous solutions of the permanganates Na^+MnO_4 , KMnO_4) and different types of solid catalysts. As solid catalysts are applied grains of some porous substance, in the pores of which is precipitated catalyst (for the most part the same KMnO_4) or catalyzing mats. In Fig. 7.45 are shown diagrams of PGG is working on hydrogen peroxide and using liquid or solid catalyst. Wide use has been made of the PGG with solid catalyst.

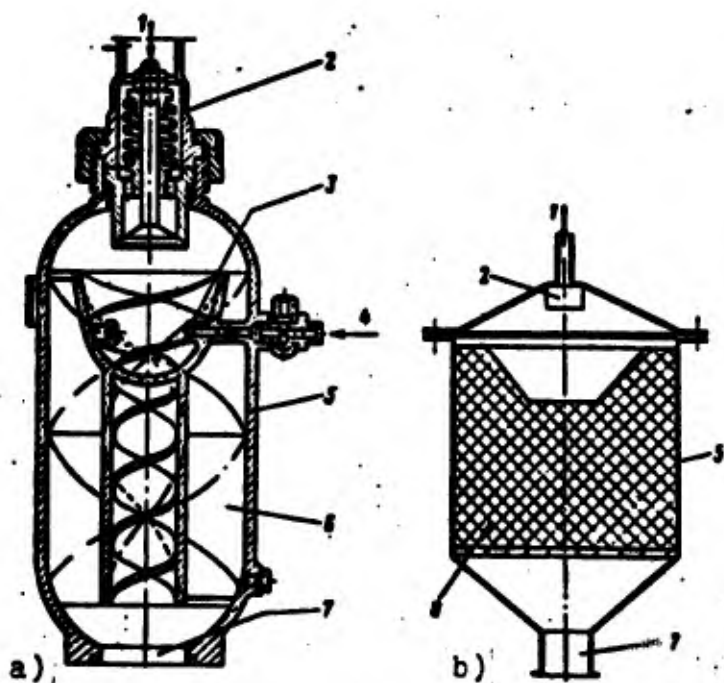


Fig. 7.45. Hydrogen peroxide PGG is: a) with liquid catalyst; b) with solid catalyst;
 1 - peroxide inlet;
 2 - hydrogen peroxide injector;
 3 - catalyst injector;
 4 - catalyst inlet;
 5 - body;
 6 - worm;
 7 - steam collection and discharge pipe;
 8 - catalyst.

Temperature and composition of steam produced by way of decomposition of hydrogen peroxide is determined wholly (if we ignore certain incompleteness of decomposition of peroxide and thermal losses) by concentration of the peroxide entering the reactor.

In calculating the composition of steam we should assume that at those low temperatures which prevail in the PGG reactor dissociation of products of decomposition is absent and steam consists of water vapor and free oxygen (we will disregard the catalyst content and the products of decomposition). One gram molecule of peroxide (34 g) upon decomposition gives 1 gram molecule of water (18 g) and 1/2 gram molecule of oxygen (16 g). The relative contents of water vapor and oxygen depends on the concentration of the peroxide. If we designate the concentration of peroxide by σ_0 , the composition of the steam will be the following.

The quantity of water vapor in 1 kg of the products of decomposition of peroxide

$$g_{H_2O} = (1 - \sigma_0) + \frac{18}{34} \sigma_0 \text{ kg H}_2\text{O/kg of steam} \quad (7.88)$$

oxygen content

$$\sigma_0 = \sigma_0 \frac{16}{34} \text{ kg O}_2/\text{kg of steam} \quad (7.89)$$

(With the use of liquid catalyst the value of σ_0 should include the quantity of water in the permanganate solution). Knowing the composition of the peroxide and the theoretical temperature of the steam, we find from the condition of equality of total heat contents of peroxide with concentration σ_0 and products of decomposition:

$$I_{H_2O,0} = [g_{H_2O}/\sigma_0 + \sigma_0/I_{O,0}] \cdot h \quad (7.90)$$

where I_{H_2O} and $I_{O,0}$ - total heat content of H_2O and O_2 at assigned temperature - are determined from tables; I_{H_2O} - total heat content

of H_2O_2 . For peroxide with concentration σ_0

$$I_{H_2O_2} = \sigma_0 / I_{H_2O_2} + (1 - \sigma_0) / I_{H_2O_{the}} + (1 - \sigma_0) \Delta I_{perox} \quad (7.91)$$

where ΔI_{perox} — heat of dissolution of water in H_2O_2 :

$$\Delta I_{perox} = -11 \text{ kcal/kg } H_2O (-46 \cdot 10^3 \text{ J/kg } H_2O).$$

Solving (usually graphically) equation (7.90), we determine temperature. In Fig. 7.46 are given data on calculation of composition and theoretical temperature of steam [5]. The true temperature of steam will be less because of losses of heat connected with incomplete decomposition of peroxide and because of cooling of steam in the reactor and lines and is 0.92-0.95 of the theoretical value.

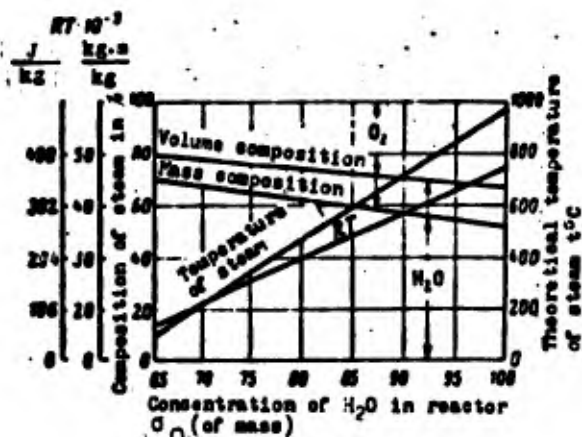


Fig. 7.46. Composition, theoretical temperature, and RT of steam obtained through decomposition of hydrogen peroxide of different concentrations.

In determining the dimensions of a PGG reactor working on liquid catalyst it is possible to assume that in 1 l of volume at a pressure of 20-30 kg/cm² ($\approx 2-3 \text{ MN/m}^2$) it is possible with good degree of fullness to decompose in 1 s 1 kg of 30% peroxide. The flow rate of liquid catalyst is 7-8% of that of peroxide.

Calculation of dimensions of the reactor using solid catalyst is based on determination of mass and dimensions of the catalyst packet. For this calculation two quantities are used. The first is allowed specific consumption of peroxide, in kg/s, which 1 kg of solid catalyst can decompose. This quantity we will designate

$$s \frac{\text{kg/s H}_2\text{O}}{\text{kg kat.}}$$

The second quantity is the total resource of catalyst s kg H_2O_2 per 1 kg of catalyst, by which is understood the total quantity of peroxide, in kg, which can be decomposed by 1 kg of catalyst for the entire time of its work.

Using these values, we can easily determine the mass of the catalyst packet

$$G_{\text{cat.}} = \frac{G_{\text{H}_2\text{O}_2}}{s} \text{ kg.} \quad (7.92)$$

The found mass is checked for total resource in the following way. Total consumption of peroxide in the entire time of operation of an engine τ should be less than the total resource of the given quantity of catalyst:

$$G_{\text{H}_2\text{O}_2} \tau < G_{\text{cat.}} s. \quad (7.93)$$

Values of s and s depend on the applied catalyst.

With smaller resources s the value of s can be increased considerably. This is explained by the fact that with increase of specific consumption of peroxide due to high speeds of motion of peroxide and steam through the catalyst packet depletion of the catalyst is increased.

The volume of the catalyst packet $V_{\text{cat.}}$ is found from the bulk density of the catalyst $\gamma_{\text{cat.}}$:

$$V_{\text{cat.}} = \frac{G_{\text{cat.}}}{\gamma_{\text{cat.}}} \quad (7.94)$$

Liquid Gas Generators (ZhGG)

The advantage of the ZhGG as compared to the PGG consists in the possibility of use for operating the ZhGG of the basic components on which the ZhRD operates. The ZhGG makes it possible to control the total consumption of working substance and relationship of flow rates of oxidizer and fuel (i.e., temperature of working substance). In a propulsion system with closed circuit in the ZhGG a considerable part of the processes of conversion of the engine's fuel to products of combustion takes place. In most practical cases the ZhGG works on the basic components of the ZhRD (Fig. 7.47).

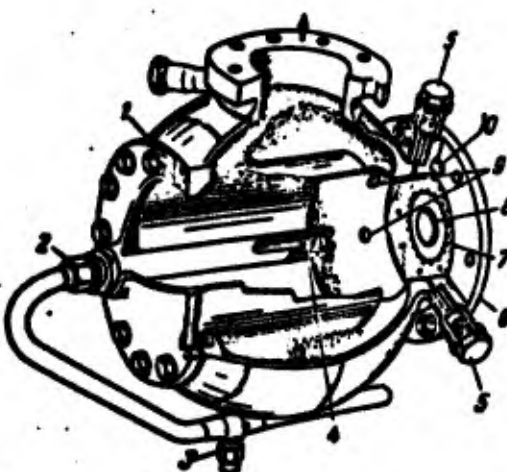


Fig. 7.47. ZhGG for the RZ-2 engine: 1 - packing; 2 - fuel feed (~10%); 3 - drain cock; 4 - swirler; 5 - pipe connection for measurements; 6 - head; 7 - fuel injectors; 8 - oxidizer injectors; 9 - ignition hole; 10 - packing.

Chief characteristic and distinction of the ZhGG from a combustion chamber consists in the fact that the ZhGG works with "displaced" α , i.e., with a coefficient of excess oxidant $\alpha \gg 1$ or with $\alpha \ll 1$. In both cases the relationship between components is determined from the condition of providing required temperature of working substance.

The ZhGG working with $\alpha \gg 1$ is called oxidizing or simply "acid," while that with $\alpha \ll 1$ is called reducing or "sweet".

Selection of type of ZhGG (oxidizing or reducing) is determined by its assignment, applied components, and the circuit of the propulsion system.

With a closed circuit propulsion system of "gas + liquid" type selection of oxidizing or reducing ZhGG is determined in the end by the efficiency of the working substance passed through the turbine, i.e., by the product $(GRT)_n$.

With an open circuit for production of working substance of rated temperature it is possible to use a ZhGG with $\alpha \gg 1$ or $\alpha \ll 1$ in equal measure. Final selection of oxidizing or reducing ZhGG in this case is determined by the applied components and the specific character of operation of units of the propulsion system (design, materials, and assignment).

An example is shown in Fig. 7.48 of the theoretical dependence of change of T and RT and of the rate of change of temperature $\partial T/\partial \ln \alpha$ for $O_2 +$ kerosene fuel over a wide range of change of α .

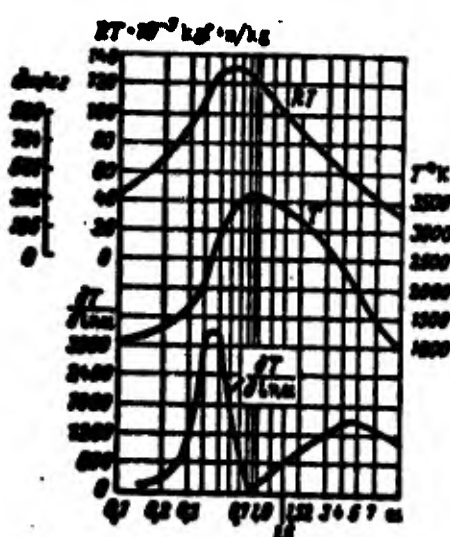


Fig. 7.48. Dependence of T , RT , and $\partial T/\partial \ln \alpha$ on α for $O_2 +$ kerosene fuel at $p = 40$ kg/cm^2 (3.92 MIL/m^2).

Analyzing these graphs, we see that, for example, at a temperature of working substance of 1500°K RT for the reducing ZhGG is twice that of the oxidizing type and the rate of change of temperature $\Delta T/\Delta \ln a$ is somewhat less, which frequently is more favorable for operation of the propulsion system. However, in the reducing ZhGG deposition of soot and coke formation are possible, which is a negative factor. The engines of the "Atlas," "Blue Streak," and "Saturn" missiles, working on $O_2 +$ kerosene fuel, contain reducing ZhGG's.

When a ZhGG is used to pressurize tanks, the type of generator is determined by conditions of prevention of burning in the tanks. For the oxidizer tank, naturally, an oxidizing ZhGG is applied, and for the fuel tank one of reducing type issued.

According to the method of organization of the process of obtaining working substance, we distinguish ZhGG is with single-stage and two-stage fuel feed (one-zone and two-zone).

With single-stage feed (Fig. 7.49a) all fuel passes through the head and in the chamber of the ZhGG combustion with assigned relationship of components takes place. Such ZhGG is useful for highly volatile and inflammable fuels. With two-stage feed (Fig. 7.49b) part of the fuel (oxidizer when $a \gg 1$, fuel when $a \ll 1$, or water) is fed through special injectors or a belt of injectors, placed at a certain distance from the head. Such fuel-feed circuit can be rational when there is great displacement of the relationship of components from stoichiometric or when water is supplied. In this case fuel with relationship closer to stoichiometric is fed through the head, which ensures reliable ignition and combustion with formation of combustion products of high temperature. For lowering the temperature of the gases additional fuel is fed through the belt of injectors. Complicated processes of evaporation, decomposition, and in certain cases burning of additional injected component take place here. The process is especially complicated with additional injection of

hydrocarbon fuel, which can bring about deposition of soot and coke formation.

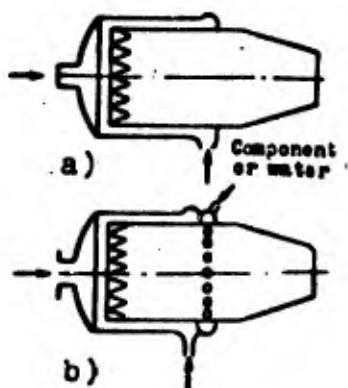


Fig. 7.49. ZhGG arrangements:
a) with single-stage fuel feed;
b) with two-stage fuel feed.

As it is known, the thermodynamic properties of the working substance ballast (third component) is added. This component can be added either through a separate belt or from the head.

Peculiarities of Processes in and Designing of the ZhGG

Owing to the great surplus of one of the components and the necessity of providing comparatively low temperature of working substance, the following peculiarities of organization of the process of formation of the working substance in the ZhGG are characteristic.

1. With great displacement of the coefficient of excess oxidant the relationship of components becomes close to the limits of inflammability and ignition involves application of two-stage fuel feed. With fuel feed from the head only in certain cases it is necessary to provide a reliably ignited kernel, which is attained by proper placement of injectors.
2. Temperature and chemical irregularity of composition of gases. Owing to the large surplus of one of the components and low temperatures, part of the excess component can be evaporated and not enter into reaction. Here heating of this part of the gases

is due only to heat removal from the products of combustion of the reacting part of the fuel.

3. Partial nonequilibrium of the process. Because of low temperatures, chemical reactions develop slower than, for example, in the chamber of ZhRD. As a result of this, the composition of the combustion products does not succeed to follow temperature and equilibrium is not established. The degree of nonequilibrium with two-stage fuel feed is especially great when injection of the cold additional portion of fuel (or water) causes partial "freezing" of the composition of the products of combustion.

4. With use of fuel components having complex molecule, because of the comparatively low temperatures in the chamber of the ZhGG formation of combustion products with molecular structure is possible, but when there is a large surplus of hydrocarbon fuel, in addition to the appearance in the combustion products of complex molecules (for example, CH_4 , and C_2H_2), precipitation of carbon in solid phase, in the form of soot is possible.

With surplus of the component with simpler molecule (for example, oxygen in O_2 + kerosene fuels) the last peculiarity vanishes.

As a result of the peculiarities of organization and development of process in the ZhGG, exact calculation of operational parameters of the ZhGG is more complicated than calculation of parameters in the combustion chamber of the ZhRD.

In a number of cases the ZhGG can be designed with the use of empirical coefficients, making it possible to correct data in accordance with type of ZhGG and applied fuel.

Let us consider simplified schemes for analyzing the ZhGG for three cases of its operation [14], [25]:

- with surplus of oxidizer;

- with surplus of hydrocarbon fuel;
- with water injection.

Analysis for surplus of oxidizer. In this case it is possible to start from the assumption that combustion is complete and dissociation is absent. Then the products of combustion of four-element fuel will consist of CO_2 ; H_2O ; N_2 and O_2 .

Mass fractions of components of combustion products

$$\left. \begin{aligned} \varepsilon_{\text{CO}_2} &= \frac{11}{3} \text{C}_r; \quad \varepsilon_{\text{H}_2\text{O}} = 9\text{H}_r; \quad \varepsilon_{\text{N}_2} = \text{N}_r; \\ \varepsilon_{\text{O}_2} &= \text{O}_r - \frac{8}{3} \text{C}_r - 8\text{H}_r. \end{aligned} \right\} \quad (7.95)$$

Naturally

$$\varepsilon_{\text{CO}_2} + \varepsilon_{\text{H}_2\text{O}} + \varepsilon_{\text{N}_2} + \varepsilon_{\text{O}_2} = 1. \quad (7.96)$$

The temperature of the obtained combustion products is determined, as usual, from the condition of equality of total heat content of fuel and products of combustion:

$$I_{\text{av}} = I_{\text{av},c} \quad (7.97)$$

where

$$I_{\text{av},c} = \sum I_{\text{av},i} \varepsilon_i = I_{\text{av},\text{CO}_2} \varepsilon_{\text{CO}_2} + I_{\text{av},\text{H}_2\text{O}} \varepsilon_{\text{H}_2\text{O}} + I_{\text{av},\text{N}_2} \varepsilon_{\text{N}_2} + I_{\text{av},\text{O}_2} \varepsilon_{\text{O}_2}. \quad (7.98)$$

Here I_{av} is total heat content of components of combustion products; and is given in tables [14], [25]. If the calculated temperature is found to differ from that assigned for the ZHOD, it is necessary to change the composition of the fuel, for the new fuel to determine the composition of the products of combustion and I_{av} and, solving equation (7.97), to find the new temperature.

Analysis with surplus of hydrocarbon fuel. In this case calculation is complicated by the fact that in the products of combustion the appearance of solid carbon (soot) and hydrocarbons, in the first place CH_4 , and those of type C_2H_2 ; C_2H_4 , etc., is possible. The presence of gaseous hydrocarbons leads to the appearance of additional equation for equilibrium constants:

$$\frac{P_{\text{CH}_4}}{P_{\text{H}_2}} = K^I; \quad \frac{P_{\text{C}_2\text{H}_2}}{P_{\text{H}_2}} = K^{II}; \quad \frac{P_{\text{C}_2\text{H}_4}}{P_{\text{H}_2}} = K^{III}. \quad (7.99)$$

The presence of carbon is allowed for by the equation for equilibrium constant

$$\frac{P_{\text{CO}_2}}{P_{\text{CO}}} = K^{IV}. \quad (7.100)$$

Let us examine the order of calculation by an example of three-element fuel (H, C, O). Designating by n the mass fraction of solid carbon and assuming that for three-element fuel the composition of remaining combustion products is characterized by partial pressures P_{CO} ; $P_{\text{H}_2\text{O}}$; P_{H_2} ; P_{CH_4} (hydrocarbons of C_nH_m type will be disregarded), we can record the system of equations determining composition in the following form:

balance equations

$$\left. \begin{aligned} \frac{\text{C}_{\text{r}-n}}{\text{O}_{\text{r}}} &= \frac{12}{16} \frac{P_{\text{CO}} + P_{\text{CO}_2} + P_{\text{CH}_4}}{2P_{\text{CO}_2} + P_{\text{CO}} + P_{\text{H}_2\text{O}}}; \\ \frac{\text{H}_{\text{r}}}{\text{O}_{\text{r}}} &= \frac{1}{16} \frac{2P_{\text{H}_2} + 2P_{\text{H}_2\text{O}} + 4P_{\text{CH}_4}}{2P_{\text{CO}_2} + P_{\text{CO}} + P_{\text{H}_2\text{O}}}; \end{aligned} \right\} \quad (7.101)$$

equations for equilibrium constants

$$\frac{P_{\text{CO}}P_{\text{H}_2\text{O}}}{P_{\text{CO}}P_{\text{H}_2}} = K_{\text{H}}; \quad \frac{P_{\text{CH}_4}}{P_{\text{H}_2}} = K^I; \quad \frac{P_{\text{CO}_2}}{P_{\text{CO}}} = K^{IV}; \quad (7.102)$$

equation for equality of the sum of partial pressures to pressure in the ZhCG

$$P_{\text{atm}} = \sum P_i. \quad (7.103)$$

Solving equations jointly (7.101)-(7.103) jointly for rated temperature and pressure, we determine the composition of the products of combustion.

We determine the temperature of the obtained combustion products by solving equation (7.97):

$$I_{\text{av}} = (I_{\text{comb}})_v$$

where

$$I_{\text{comb}} = \frac{1-\eta}{\sum \mu_i p_i} \sum I_{\text{av},i} p_i + \frac{\eta}{\mu_C} I_C,$$
(7.104)

μ_C and I_C - molecular weight and enthalpy of solid carbon.

For the obtained combustion products entropy is determined by the equation

$$S = \frac{1-\eta}{\sum \mu_i p_i} \sum (S_{\text{av}} - AR \ln p_i) p_i + \frac{\eta S_C}{\mu_C},$$
(7.105)

where S_C - entropy of solid carbon.

Analysis with water injection. Calculation is reduced to determination of the necessary quantity of water for lowering the temperature of the products of combustion of fuel fed to the ZhGG to assigned level. Temperature T^I and composition of the products of combustion obtained in the first zone of the ZhGG are determined by usual methods of calculation.

We will assume that the injection of water into the hot products of combustion results in their abrupt cooling to assigned temperature T_{mix} and that the composition of the combustion products is not changed (i.e., "freezing" occurs). Here the water is evaporated and the water vapor is heated to T_{mix} .

The decrease of total heat content of the combustion products will be equal to

$$\Delta I_{\text{comb}} = I_{\text{comb}}^{\text{I}} - I_{\text{comb}}^{\text{ext}}. \quad (7.106)$$

where $I_{\text{comb}}^{\text{I}}$ and $I_{\text{comb}}^{\text{ext}}$ - total heat content of the products of combustion of ZhGC fuel in the first zone with identical ("frozen") composition at temperatures T^{I} and T_{ext} .

$$I_{\text{comb}}^{\text{I}} = \frac{1}{\sum p_i p_i} \sum I_i^{\text{I}} p_i = I_{\text{v}}; I_{\text{comb}}^{\text{ext}} = \frac{1}{\sum p_i p_i} \sum I_i^{\text{ext}} p_i. \quad (7.107)$$

In accordance with the law of conservation of energy a decrease of total heat content of the combustion products ΔI_{comb} goes to an increase of heat content of the water converted to vapor:

$$\Delta I_{\text{v.a.v}} = \Delta I_{\text{H}_2\text{O}}. \quad (7.108)$$

Designating by σ the quantity of water used for cooling 1 kg of the products of combustion, we determine

$$\Delta I_{\text{H}_2\text{O}} = \sigma (I_{\text{H}_2\text{O}}^{\text{ext}} - I_{\text{H}_2\text{O}}^{\text{I}}). \quad (7.109)$$

where $I_{\text{H}_2\text{O}}^{\text{I}}$ - total heat content of liquid water at the supply temperature. Substituting expressions (7.106) and (7.108) in equality (7.109), we find σ :

$$\sigma = \frac{I_{\text{comb}}^{\text{I}} - I_{\text{comb}}^{\text{ext}}}{I_{\text{H}_2\text{O}}^{\text{ext}} - I_{\text{H}_2\text{O}}^{\text{I}}}. \quad (7.110)$$

The gas constant of the obtained mixture of water vapor and the products of combustion is determined by the expression

$$R_{\text{av}} = \xi_{\text{H}_2\text{O}} R_{\text{H}_2\text{O}} + \xi_{\text{v}} R_{\text{v}}. \quad (7.111)$$

where $\xi_{\text{H}_2\text{O}}$ and $\xi_{\text{a.c.}}$ - mass fractions of the vapors of injected water and the products of combustion in the mixture:

$$\xi_{\text{H}_2\text{O}} = \frac{1}{1+\alpha}; \quad \xi_{\text{a.c.}} = \frac{\alpha}{1+\alpha}. \quad (7.112)$$

The given scheme of calculation can be used also for calculation of composition and temperature of the working substance of the two-component ZhGG with two-stage injection if the assumption is applied about total "freezing" of the products of combustion formed prior to injection and it is considered that the additional portion of the component is only evaporated, without participating in the reaction. It is obvious that, depending upon the applied fuel and the type of ZhGG ($\alpha \ll 1$ or $\alpha \gg 1$), the validity of such assumptions will differ. These assumptions are more acceptable when there is additional injection of components with simple molecule.

The volume of the ZhGG, if there are no experimental data, can be determined analogously to that of the combustion chamber of the ZhRD in accordance with conditional time of stay (3.3). Here, considering the lower temperatures and peculiarities of organization of the process in the ZhGG, we must take the conditional time of stay in the ZhGG as 1.5-3 times greater than for the combustion chamber of a ZhRD working on the same fuel.

Footnotes

¹Operation and calculation of axial screw prepumps are examined in detail in [139].

²Designing of sections and determination of parameters, shown in section 1.2 are examined in [25], [139], [140].

C H A P T E R VIII

CLOSED-CIRCUIT PROPULSION SYSTEMS

A propulsion system with closed circuit is one in which the working substance from the turbine enters combustion chamber, where it is burned with optimum relationship of fuel and oxidizing elements. Here losses of thrust characteristic for open-circuit propulsion system and caused by inefficient consumption of components driving the turbine are absent - the specific thrust of the propulsion system with closed circuit is equal to the specific thrust of the engine.

Thus in propulsion systems with closed circuit more complete use for creation of thrust is made of the chemical energy of all the fuel available aboard the rocket.

Earlier (section 6.3) it was shown that for a propulsion system with open circuit increasing the pressure in the chamber above 100-150 [atm(abs.)] ($\approx 10-15 \text{ MN/m}^2$) is inefficient, since the increase of feed pressure necessary for this requires a corresponding increase in power of the TVA. Here the fuel consumed in driving the TVA ΔG_{TVA} increases so much that the gain in specific thrust of the propulsion system due to the increase of p_2/p_3 is not obtained [see formula (6.5) and Fig. 6.8].

Thus the application of the closed circuit not only increases the specific thrust of the propulsion system as compared to the

P_m of the system with open circuit but also makes it possible to further increase P_m as a result of the increase of pressure in the chamber.

Depending upon the state in which components are fed to the combustion chamber, we distinguish two types of closed circuits for propulsion systems: "gas + liquid" and "gas + gas". With the "gas + liquid" arrangement (Fig. 8.1) one of the components, oxidizer or fuel, goes completely to the ZhGG, where it burns with part of the second component (with $\alpha \gg 1$ respectively). The formed gaseous products of combustion with great surplus of oxidizing or fuel elements drive the turbine of the TMA and then through the gas duct enter the combustion chamber. The second component enters the combustion chamber in liquid form. A variety of the closed circuit of "gas + liquid" type is shown in Fig. 8.7. This is used in the RL-10 engine, working on oxygen and hydrogen. There is no special ZhGG here. The hydrogen is gasified in the coolant passage, is fed to the turbine of the TMA and from there into the combustion chamber. Oxygen enters the combustion chamber from the pump in liquid form.

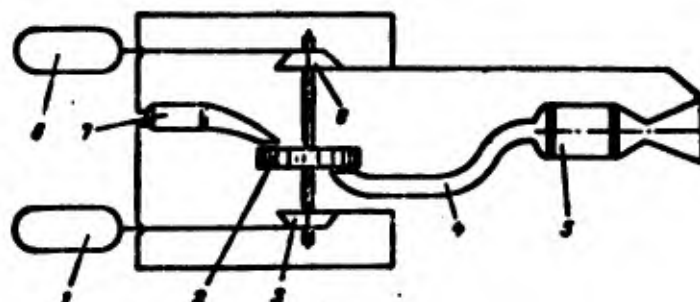


Fig. 8.1. Propulsion systems with closed circuit of "gas + liquid" type:
1 - oxidizer tank; 2 - turbine; 3 - oxidizer pump; 4 - feed of products of combustion from TMA to chamber; 5 - engine chamber; 6 - fuel tank; 7 - ZhGG; 8 - fuel pump.

With the "gas + gas" circuit (see Fig. 8.10) both components enter two ZhGG's (one with $a \gg 1$). From the ZhGG the combustion products are used to drive the turbines of the TNA and then enter the combustion chamber, where they are burned with assigned relationship of fuel and oxidizer.

8.1. "Gas + Liquid" Closed Circuit

Simplified closed circuits of "gas + liquid" type are shown in Figs. 8.1 and 8.3.

For definitiveness we have taken a circuit working with an oxidizing gas generator (that working with reducing ZhGG is analogous). During operation of the system the oxidizer pump 3 feeds all the oxidizer from tank 1 to the ZhGG 7. Fuel from pump 8 goes in two directions: that part of the fuel necessary for formation of the working substance to drive the turbine enters ZhGG 7, while the other, main part of the fuel goes immediately to combustion chamber 5. The working substance with surplus oxidizer formed in ZhGG 7 goes to turbine 2 and then through gas duct 4 to combustion chamber 5.

Thus the components of fuel enter the combustion chamber in both liquid form and in the form of gaseous products of combustion at a temperature of 600-300°C with large surplus of oxidizer (whence the name "gas + liquid"). Let us analyze the operation of a system working in accordance with the circuit represented in Fig. 8.1.

Determination of Operational Parameters of Basic Units

The fundamental equation, making it possible for assigned pressure in the combustion chamber to determine pressure in the ZhFF necessary for driving the TNA, and consequently the necessary feed pressure (sometimes called the pressure at which the circuit

is closed), is the equation for the balance of powers consumed by the pumps and developed by the turbine:

$$N_t = \sum N_p. \quad (8.1)$$

According to equations (7.10) and (7.55), for the examined system (see Fig. 8.1)

$$N_p = \frac{G_{\text{m}}}{\eta} \frac{k}{k-1} RT_{\infty}^{\circ} \left[1 - \left(\frac{P_{\text{out}}}{P_{\text{in}}} \right)^{\frac{k-1}{k}} \right]; \quad (8.2)$$

$$\sum N_p = \frac{G_o (P_{\text{out},o} - P_{\text{in},o})}{\eta_o \eta_{\text{pump}}} + \frac{G_f (P_{\text{out},f} - P_{\text{in},f})}{\eta_f \eta_{\text{pump}}}. \quad (8.3)$$

Substituting expressions (8.2) and (8.3) in equation (8.1) we obtain

$$\frac{G_{\text{m}}}{\eta} \frac{k}{k-1} RT_{\infty}^{\circ} \left[1 - \left(\frac{P_{\text{out}}}{P_{\text{in}}} \right)^{\frac{k-1}{k}} \right] = \frac{G_o (P_{\text{out},o} - P_{\text{in},o})}{\eta_o \eta_{\text{pump}}} + \frac{G_f (P_{\text{out},f} - P_{\text{in},f})}{\eta_f \eta_{\text{pump}}}. \quad (8.4)$$

where G_{m} — flow rate of working substance through turbine — obviously, equal to that of components through the ZhGG; k — adiabatic index of products of combustion of the ZhGG (usually $k = 1.2-1.3$); η_o ; η_{pump} ; η_{pump} — effective efficiency of turbine and efficiency of oxidizer and fuel pumps; $P_{\text{out},o}$; $P_{\text{in},o}$ — feed pressure of components by pumps; $P_{\text{out},f}$; $P_{\text{in},f}$ — pressure of oxidizer and fuel at pump inlet; RT_{∞}° — gas constant and stagnation temperature of working substance at turbine inlet.

We will consider them equal to the gas constant and exit temperature from the ZhGG, i.e.,

$$RT_{\infty}^{\circ} = (RT)_{\text{exit}}. \quad (8.5)$$

With the closed circuit pressure P_{out} is determined by chamber pressure, i.e.,

$$P_{\text{mz}} = P_2 + \Delta P_2 \quad (8.6)$$

where ΔP_2 - losses of pressure of combustion products on the way from turbine to combustion chamber.

The turbine inlet pressure can be considered equal to the pressure in the ZhGG:

$$\dot{P}_2 = P_{\text{mz}} \quad (8.7)$$

Pressure drop in the turbine, taking into account relationships (8.6) and (8.7), is

$$\alpha_t = \frac{\dot{P}_2}{P_{\text{mz}}} = \frac{P_{\text{mz}}}{P_2 + \Delta P_2} \quad (8.8)$$

Feed pressure of pumps P_{mzo} and P_{man} is obviously higher than the pressure in the ZhGG by the value of hydraulic losses of pressure of the component on the way from the pump to the combustion chamber of the ZhGG, i.e., in general

$$P_{\text{mz}} = P_{\text{mzr}} + \Delta P_{\text{mzr}} = \alpha_t (P_2 + \Delta P_2) + \Delta P_{\text{mzr}} \quad (8.9)$$

where ΔP_{mzr} - losses of pressure of component in lines, valves, regulators on the way from pump to ZhGG and also in the ducts and injectors of the ZhGG.

Substituting expressions (8.5)-(8.9) in formula (8.4) we obtain an expanded expression for determination of α_t or pressure in the ZhGG for assigned pressure in the combustion chamber:

$$\begin{aligned} \frac{C_{\text{mz}}}{2} \frac{1}{k-1} (RT)_{\text{mzr}} \left(1 - \frac{1}{\alpha_t^k} \right) = & 0 \cdot \frac{\alpha_t (P_2 + \Delta P_2) + \Delta P_{\text{mzr}} - P_{\text{mzo}}}{2k C_{\text{mzo}}} + \\ & + 0 \cdot \frac{\alpha_t (P_2 + \Delta P_2) + \Delta P_{\text{mzr}} - P_{\text{mzr}}}{2k C_{\text{mzr}}} \end{aligned} \quad (8.10)$$

For solution of this equation we assign or are given from analysis of the engine chamber and ZhGG flow rates of components G_a , G_h , G_v , and values of k and $(RT)_{\text{air}}$ in dependence upon pressure in the ZhGG. Assigning values of efficiency η_{turb} , η_{pump} and η_{air} , estimating values of Δp_1 , p_{air} , p_{air} , Δp_{turb} and Δp_{pump} , we solve equation (8.10) and determine the drop in the turbine π_t and pressure in the ZhGG, p_{ZhGG} for selected combustion-chamber pressure p_2 .

Equation (3.10) is conveniently solved by assigning a number of values of π_t . Having determined for each π_t the value of $\pi_t(p_2 + \Delta p_2) - p_{\text{ZhGG}}$, we plot curves of dependence of right and left parts of the equation on π_t , i.e., graphs of available turbine power $N_t = f(\pi_t)$ and required pump power $N_p = f(\pi_t)$. The point of crossing of the curves gives us the computed values of π_t , and power of the TMA N_p , for which the circuit is closed (Fig. 8.2).

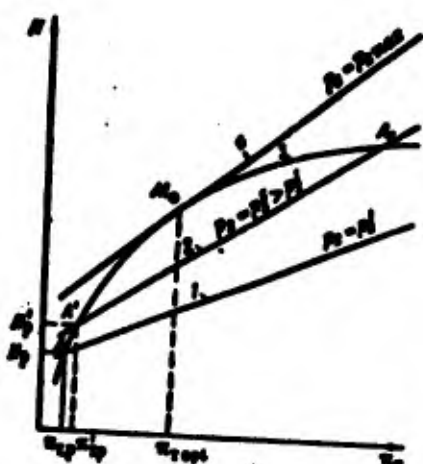


Fig. 8.2. Dependences of available turbine power N_t and required pump power N_p on π_t and chamber pressure p_2 :
1, 2, 4 - required power; 3 - available power.

Influence of Combustion-Chamber Pressure on Operational Parameters of the System

Let us examine the influence of an increase in pressure in the combustion chamber p_2 on the operating parameters of the supply system. For definitiveness here and subsequently the entire analysis of operation of the propulsion systems with closed circuit

will be conducted with constant total flow rate of fuel through the combustion chamber. Here change of pressure in the combustion chamber is attained only by changing the value of A_p . It is obvious that the character of interconnection in operation of units of the supply system will not be changed with other fuel flow rates.

With increase of p_2 necessary feed pressure increases, i.e., power consumed by pumps increases. The power of the turbine N_t , necessary to drive the pumps must be increased accordingly. From equation (8.2) we see that for assigned efficiency η_t an increase in turbine power can be attained by increasing flow rate G_t , the value of $(RT)_{min}$ and pressure drop in the turbine x_t . However, the value of $(RT)_{min}$ for a given fuel is determined by the highest temperature of working substance allowed by the blade and with assigned components remains practically constant. It is also possible to consider k , the adiabatic index of the products of combustion of the ZhGG, constant. Flow rate of working substance G_t for this circuit is also constant, since one of the components wholly enters the ZhGG, and the value of the relationship of components v_{min} is determined by the allowed temperature of working substance and for the given type of ZhGG (oxidizing or reducing) remains constant.

Thus with increase of pressure p_2 for an increase of turbine power it is necessary to increase the drop in the turbine x_t . Here available turbine power N_t is changed in accordance with curve 3 of Fig. 8.2. Power consumed by the pumps, in accordance with equality (8.3) and taking into account expression (8.9), with increase of p_2 will be changed in accordance with curve 2, corresponding to new pressure in chamber. Point A' of the intersection of curve 2 with the curve of available power $N_t=f(x_t)$ gives values of pressure drop x_{t_p}' and power of the TMA N_p' for the new pressure in the chamber.

With further increase of pressure in the chamber the power of the TJA and drop in the turbine α_{tj} will increase accordingly. However, as one can see from Fig. 8.2, increase of p_2 is possible only to a defined value $p_{2 \text{ max}}$, at which curve of required power $N_r = f(\alpha_r)$ is tangent to curve of available power $N_v = f(\alpha_v)$ (point M_o).

With pressure in the chamber greater than $p_{2 \text{ max}}$ the necessary pump feed pressure increases so much that the required pump power becomes higher than the available power of the turbine for given components, turbine efficiency η_t and outlet pressure. It is possible by continuing to increase the drop in the turbine and with the given components to obtain still higher power, but this requires a decrease of outlet pressure and chamber pressure p_2 (point A_1). It is obvious that such operating conditions of the system are inefficient, since all of the additional turbine power due to the increase of α_r is expended only on increase of feed pressure. Pressure in combustion chamber p_2 , and consequently the thrust of the propulsion system remain the same as under conditions corresponding to A' , i.e., lower than for conditions with pressure $p_{2 \text{ max}}$.

Thus with the closed-circuit propulsion system there is a maximum possible pressure in the combustion chamber $p_{2 \text{ max}}$. The value of this pressure is determined by the properties of the working substance: $(RT)_{\text{ref}}$, k , efficiency of pumps and turbine, losses in ducts, and type of ZhGG applied (oxidizing or reducing).

Determination of $p_{2 \text{ max}}$

The value of $p_{2 \text{ max}}$ and values of corresponding pressure drop α_{tj} and power of the TJA for engines of closed-circuit "gas + liquid" type can be determined analytically by applying a number of simplifying assumptions. It was noted above that with assigned components for the circuit adopted flow rate to the turbine G_t , the value of $(RT)_{\text{ref}}$ and the adiabatic index of the products of combustion of the ZhGG remain practically constant. For simplicity

of analysis we will consider, furthermore, that efficiency of fuel and oxidizer pumps, losses of pressure Δp_{pump} in fuel and oxidizer lines, and inlet pressure to pumps are equal and do not depend on the operational parameters of the system, i.e.,

$$\left. \begin{array}{l} \eta_{\text{pump}} = \eta_{\text{pump,f}} = \eta_{\text{pump,o}} = \text{const}; \\ \Delta p_{\text{pump,f}} = \Delta p_{\text{pump,r}} = \Delta p_{\text{pump}} = \text{const}; \\ \rho_{\text{pump,f}} = \rho_{\text{pump,r}} = \rho_{\text{pump}} = \text{const}. \end{array} \right\} \quad (8.11)$$

We will consider also that losses Δp_2 do not depend on operational parameters. Then equation (8.10) can be recorded:

$$A = \frac{\rho_1}{Q_s} \frac{R}{g-1} (RT)_{\text{inlet}} \left(1 - \frac{1}{\frac{\rho_1}{\rho_2}} \right) - \frac{\Delta p_{\text{pump}} + \Delta p_2 - \rho_{\text{pump}} g}{\rho_1} Q_s. \quad (8.12)$$

where

$$Q_s = \frac{\rho_1}{\rho_2} + \frac{\rho_1}{\rho_2}. \quad (8.13)$$

Hence

$$A = \frac{\rho_1}{Q_s} \frac{R}{g-1} (RT)_{\text{inlet}} \frac{1}{\rho_2} \left(1 - \frac{1}{\frac{\rho_1}{\rho_2}} \right) - \frac{\Delta p_{\text{pump}} + \Delta p_2 - \rho_{\text{pump}} g}{\rho_1}. \quad (8.14)$$

Relation ρ_1/Q_s will be called reduced density and will be designated by γ_{inlet} . Obviously, for the oxidizing ZhGG

$$\gamma_{\text{inlet}} = \frac{\rho_1(\rho_{\text{inlet}}+1)\gamma_r\gamma_f}{\rho_{\text{inlet}}(\gamma_r+\gamma_f)}. \quad (8.15)$$

For the reducing ZhGG

$$\gamma_{\text{inlet}} = \frac{(\rho_{\text{inlet}}+1)\gamma_r\gamma_f}{(\gamma_r+\gamma_f)}. \quad (8.16)$$

Designating the constant factor in equation (8.14)

$$A = \frac{\rho_1}{Q_s} \gamma_{\text{inlet}} \frac{R}{g-1} (RT)_{\text{inlet}} - \gamma_{\text{inlet}} \rho_1 \frac{R}{g-1} (RT)_{\text{inlet}}. \quad (8.17)$$

we obtain after transposing

$$P_2 = (A - \Delta P_{\text{min}} + P_{\text{ch.m}}) \frac{1}{x_t} - \frac{A}{x_t^{\frac{2b-1}{b}}} - \Delta P_2 \quad (8.18)$$

Here P_2 depends only on pressure drop x_t . For determination of $P_2 \text{ max}$ derivative dP_2/dx_t is equated to zero:

$$\frac{dP_2}{dx_t} = - \frac{(A - \Delta P_{\text{min}} + P_{\text{ch.m}})}{x_t^2} + A^{\frac{2b-1}{b}} \frac{1}{x_t^{\frac{2b-1}{b}}} = 0.$$

Hence we find the value of the pressure drop corresponding to the highest possible chamber pressure:

$$x_{t,\text{max}} = \left(\frac{A}{A - \Delta P_{\text{min}} + P_{\text{ch.m}}} \frac{2b-1}{b} \right)^{\frac{b}{b-1}}. \quad (8.19)$$

Knowing $x_{t,\text{max}}$ from equation (8.19) we find the value of $P_2 \text{ max}$:

$$P_{2,\text{max}} = (A - \Delta P_{\text{min}} + P_{\text{ch.m}}) \frac{1}{x_{t,\text{max}}} - \frac{A}{x_{t,\text{max}}^{\frac{2b-1}{b}}} - \Delta P_2. \quad (8.20)$$

Equations (8.19) and (8.20) make it possible with known (or assigned) operational parameters of the TMA (η_w ; η_t ; G_t ; $(RT)_{\text{min}}$; Q_s) to determine $P_2 \text{ max}$ and $x_{t,\text{max}}$ directly without plotting graphs of the type presented on Fig. 8.2.

From joint consideration of equations (8.20) and (8.17) it follows that the value of $P_2 \text{ max}$ in considerable degree depends on perfection of operation of pumps and turbine (η_w and η_t), properties of working substance [k and $(RT)_{\text{min}}$], and on the true value of $(RT)_{\text{min}}$, i.e., on quality of operation of the ZhGG.

The value of $P_2 \text{ max}$ can also be increased by changing the circuit of the propulsion system. In Fig. 8.3 is given a variant

of the closed-circuit system of "gas + liquid" type. With this circuit for supplying fuel to the ZhGG additional pump 9 is used. Here, obviously, the feed pressure of main fuel pump 8 will be lower than that of pumps 3 and 9. This leads to a decrease of power consumed by the pumps, which in turn makes it possible to decrease the pressure in the ZhGG with simultaneous increase of the highest possible pressure p_2 max.

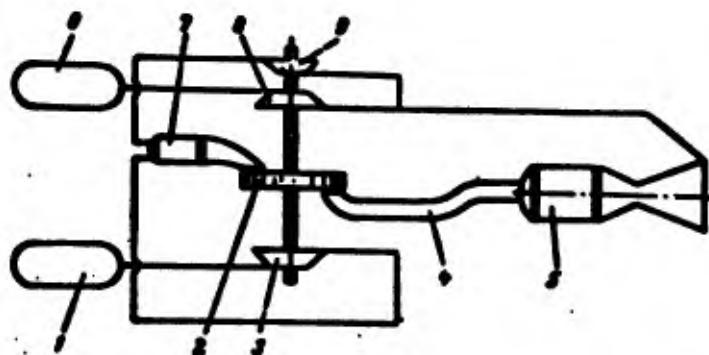


Fig. 8.3. Propulsion system with closed circuit of "gas + liquid" type with additional pump for fuel feed to the ZhGG: 1 - oxidizer tank; 2 - turbine; 3 - oxidizer pump; 4 - supply of combustion products from TMA to chamber; 5 - engine chamber; 6 - fuel tank; 7 - ZhGG; 8 - main fuel pump; 9 - additional fuel pump.

The circuit of Fig. 8.3 is also frequently more efficient when $p_2 < p_{2 \text{ max}}$, since with the use of the additional pump the circuit is closed at lower supply pressures. This, in turn leads to improvement of the weight characteristics of the system, while introduction of the additional pump can lead to complication of the system and lowering of reliability.

Capabilities of Closed Circuits of "Gas + Liquid" Type with Oxidizing and Reducing ZhGG's

The above examined closed-circuit of "gas + liquid" type for definitiveness had an oxidizing ZhGG (since that with reducing

ZhGG has analogous form, obviously, the entire above analysis remains valid for case of the reducing ZhGG).

However, for identical chamber pressure the basic operational parameters of the ZhGG and T!IA with application of oxidizing or reducing gas generator differ greatly. The fact is that for fuels used in the ZhRD the relationship of components v is usually greater than unity, i.e., the flow rate of oxidizer is greater than that of fuel. Since with the closed "gas + liquid" circuit one of the components most frequently goes completely to the ZhGG, the flow rate of working substance to the turbine with the oxidizing ZhGG is always higher than with the reducing ZhGG. Since for the majority of fuels (with the exception of those using hydrogen) the increase of $(RT)_{mn}$ in the reducing ZhGG as a result of an increase in the gas constant of the combustion products is comparatively small, decisive influence on available turbine power is rendered by an increase of flow rate Q_0 .

In Fig. 8.4 are shown typical graphs of change of available turbine power $N_t=f(x_r)$ with application of oxidizing and reducing ZhGG's working on fuel having $v > 1$, from which it is clear that with the use of the oxidizing ZhGG for the same chamber pressure the value of x_r and consequently of the pressure in the ZhGG and feed pressure for which the circuit is closed are lower. Tentative calculations show that the propulsion system operating on fuel using nitrogen oxides as oxidizer, with chamber pressure of 100 [atm(abs.)] ($\approx 10 \text{ MN/m}^2$) and with oxidizing ZhGG is closed at a pressure in the ZhGG of 140-180 [atm(abs.)] ($\approx 14-18 \text{ MN/m}^2$), while with a reducing ZhGG the circuit is closed at a ZhGG pressure of 180-230 [atm(abs.)] ($\approx 18-26 \text{ MN/m}^2$).

The application of oxidizing or reducing ZhGG's also influences the value of $p_2 \text{ max}$. In Fig. 8.4 points x_o and x_p at which the curves of required power $N_r=f(x_r)$ are tangent to the curves of available turbine power $N_t=f(x_r)$, determine the highest permissible pressure in the combustion chamber for oxidizing or reducing ZhGG's in an engine with $v > 1$.

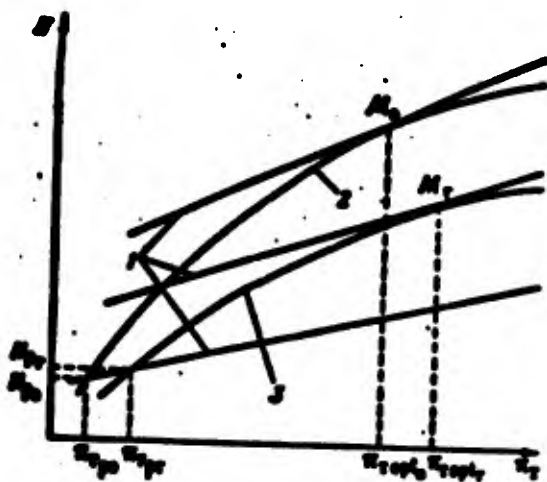


Fig. 8.4. Change of available turbine power $N_t/(n)$ with oxidizing and reducing ZhGG's working on usual (not hydrogen) fuel: 1 - required power; 2 - N_t with oxidizing ZhGG; 3 - N_t with reducing ZhGG.

However, in certain practical cases it can be more efficient to use the reducing ZhGG for $v > 1$ also. The fact is that blades of the turbine working on reducing gas allow higher temperature of working substance than those of the turbine working on the oxidizing gas. Due to this the difference in pressures at which the circuit is closed with oxidizing or reducing ZhGG's decreases, and in selecting the type of ZhGG (oxidizing or reducing) questions of convenience of control, layouts, reliability, etc., can be decisive.

In engines using hydrogen as fuel, in connection with the very considerable increase in the gas constant of the combustion when $a \ll 1$ decisive influence on the value of available turbine power is rendered by an increase of $(RT)_{\text{avr}}$. Therefore for hydrogen ZhRD with closed circuit it is more efficient to use the reducing ZhGG.

At present combustion-chamber pressure is still considerably below maximum possible values. The basic cause of the fact that with an increase of pressure p_2 the feed pressure for which the circuit is closed increases in proportion to the product $x_1 p_2$. Because to this, lines and units of the supply system have to work at very high pressures, which leads to considerable increase in mass of the propulsion system and lowering of its operational reliability.

As one of the examples of a system with closed circuit and reducing ZhGG, in Fig. 8.5 are shown a diagram and mock-up of the proposed RL-20P engine, working with a closed circuit of "gas + liquid" type on oxygen + hydrogen fuel. Chamber pressure is 210 [atm(abs.)] (20.6 MN/m^2), thrust is 120 T (1.18 MN). Expected specific thrust is about $430 \text{ kg}\cdot\text{s/kg}$ ($\approx 4300 \text{ N}\cdot\text{s/kg}$). Here ZhGG 4 is the precombustion chamber for the engine chamber. The ZhGG is fed 90% of the hydrogen and 15% of the oxygen of the total amount of each component to the chamber. The remaining oxygen is fed through injectors, placed on radial flanges 2. The remaining 10% of the liquid hydrogen is used for external cooling of nozzle 1 and is then fed through porous wall 7 into the combustion chamber. A near-wall layer for internal cooling is formed here.

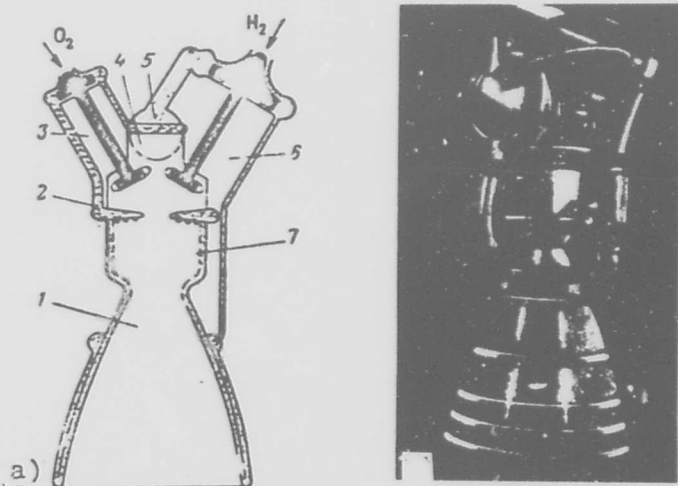


Fig. 8.5. Diagram and mock-up of the RL-20P engine, working on $O_2 + H_2$ fuel with closed circuit of "gas + liquid" type: a) diagram of engine; b) mock-up; 1 - nozzle; 2 - flange with injectors of liquid O_2 ; 3 - TNA for liquid O_2 ; 4 - ZhGG; 5 - liquid H_2 ; 6 - TNA for liquid H_2 ; 7 - porous wall.

**Example of calculation of basic parameters
of the closed supply system**

The propulsion system of a ZhRD works on a fuel of 30% HNO_3 and 20% N_2O_4 + Tonka 250 with a closed circuit of "gas + liquid" type, represented in Fig. 8.1, with oxidizing or reducing ZhGG.

Given:

parameters of TNA and ZhGG:

$$\eta_T = 0.4; \eta_{T,0} = \eta_{T,r} = 0.65; \delta = 1.2;$$

density of components:

$$\rho_0 = 1500 \text{ kg/m}^3; \rho_r = 845 \text{ kg/m}^3;$$

flow rates of components: $G_0 = 160 \text{ kg/s}; a_r = 40 \text{ kg/s.}$

From conditions of highest permissible temperature of working substance ZhGG's operate with the following relationships: $v_{max}=20$; oxidizing ZhGG, $v_{max}=0.6$.

Here, taking losses into account, the true value of $(RT)_{max}$ is considered identical for both ZhGG's (RT for the oxidizing ZhGG is less than for the reducing type):

$$(RT)_{max} = 50 \cdot 10^3 \text{ kg} \cdot \text{m/kg} (490 \cdot 10^3 \text{ J/kg}).$$

We consider that all shown values remain constant with change of operating conditions of ZhGG and TNA.

It is necessary to determine for operation of the system with oxidizing or reducing ZhGG: pressure drop in the turbine π , power of the TNA N_{TNA} , pressure in the ZhGG and feed pressure for $p_2 = 90$ [atm(abs.)] (8.83 MN/m^2); the highest possible combustion-chamber pressure $p_2 \text{ max}$.

Solution 1. We determine or estimate values necessary for calculation:

Flow rates through the turbine:

with oxidizing ZhGG

$$G_t = G_o + G_r = G_o + \frac{G_o}{v_{ext}} = 160 + \frac{160}{20} = 168 \text{ kg/s;}$$

with reducing ZhGG

$$G_t = G_o + G_r - G_o v_{ext} = 160 + 0.6 \cdot 160 = 64 \text{ kg/s.}$$

Pressure losses on the way from the pumps to the chamber of the ZhGG and from turbine to combustion chamber are considered constant under all operating conditions and are estimated as

$$\Delta P_{pump} = \Delta P_{turb} = \Delta P_{ext} = 30 \text{ kg/cm}^2 (2.04 \text{ MPa}),$$

$$\Delta P_t = 15 \text{ kg/cm}^2 (1.02 \text{ MPa}).$$

Feed pressure at pump inlets

$$P_{in} = P_{out} = P_{ext} = 5 \text{ kg/cm}^2 (0.49 \text{ MPa}).$$

Volumetric flow rate of components through combustion chamber

$$Q_s = \frac{G_o}{\rho_o} + \frac{G_r}{\rho_r} = \frac{160}{1500} + \frac{160}{845} = 0.148 \text{ m}^3/\text{s}$$

2. We determine π_2 , N_{20} , P_{20} , P_{ext} for chamber pressure $p_2 = 90$ [atm(abs.)] ($28.83 = 10^5 \text{ N/m}^2$). We find the equation for dependence of turbine power on pressure drop in the turbine π_2 .

With the oxidizing ZhGG

$$N_{20} = \frac{G_o \cdot (RT)_{ext}}{\eta} \cdot \frac{k}{(k-1)} \left(1 - \frac{1}{\pi_2^{k-1}} \right)^{1/(k-1)} =$$

$$= \frac{160 \cdot 0.4 \cdot 30 \cdot 10^3}{75} f(\pi_2) = 44.8 \cdot 10^3 \cdot f(\pi_2).$$

where

$$f(x_0) = \frac{b}{b-1} \left(1 - \frac{1}{x_0^{\frac{b-1}{b}}} \right)$$

is calculated or found in tables of gas-dynamic functions.

With the reducing ZhGG

$$N_{\text{req}} = \frac{G_1 x_0 (R)}{25} \frac{b}{b-1} \left(1 - \frac{1}{x_0^{\frac{b-1}{b}}} \right) -$$
$$= \frac{64 \cdot 0.4 \cdot 30 \cdot 10^3}{25} \cdot f(x_0) = 17 \cdot 10^3 f(x_0).$$

We find the equation for dependence of pump power on x_0 or on pressure in the ZhGG. According to equation (8.12)

$$N_p = \frac{x_0 (\rho_1 + \Delta \rho) + (\Delta p_{\text{ext}} - \Delta p_{\text{int}})}{25 x_0} Q_0 =$$
$$= \frac{x_0 (30 + 15) \cdot 10^4 + (30 - 5) \cdot 10^4}{25 \cdot 0.65} 0.145 = 700 + 3150 \cdot x_0$$

We plot graphs of dependences of required power (N_{req}, N_p) and available power N_p on pressure drop in turbine x_0 (Fig. 8.6). Points of intersection of the curve of required pump power with curves of available power give computed values of x_0 and N_p .

With the oxidizing ZhGG: pressure drop $x_0 = 1.11$; power of TMA $N_{\text{req}} = 4300$ hp (3160 kW).

According to equations (8.8) and (8.9) pressure in the ZhGG:

$$\rho_{\text{ext}} = x_0 (\rho_1 + \Delta \rho) = 1.11 (100 + 5) = 116.5 \text{ (atm (abs.)) (11.45 MPa)}$$

feed pressure:

$$\rho_{\text{int}} = \rho_{\text{ext}} + \Delta p_{\text{int}} = 116.5 + 30 = 146.5 \text{ (atm (abs.)) (14.45 MPa)}$$

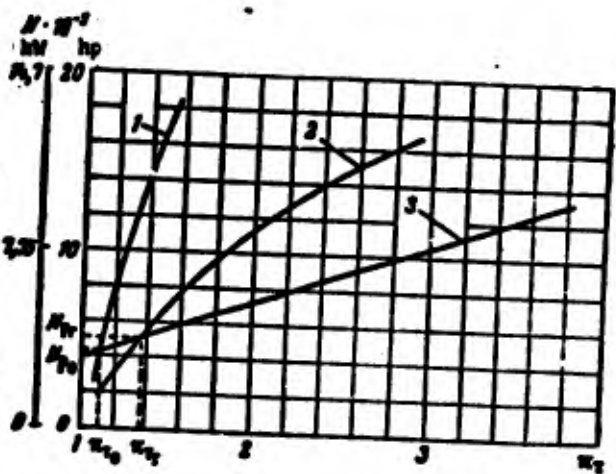


FIG. 8.6. Solution of example
1 - I_{sp} with oxidizing ZhGG; 2 -
 I_{sp} with reducing ZhGG; 3 - I_{sp}
for $p_2 = 90 \text{ kg/cm}^2$ ($\approx 9 \text{ MN/m}^2$).

With reducing ZhGG:

$$A = 1.37; N_{sp} = 5130 \text{ hp} \quad (3770 \text{ kW}); P_{ext} = 1.37(90 + 15) = \\ [\text{atm(abs.)}] (14.12 \text{ MN/m}^2); P_{ext} = 144 + 30 = 174 [\text{atm(abs.)}] (17.1 \text{ MN/m}^2).$$

3. We determine the highest possible pressure in the combustion chamber $p_2 \text{ max}$.

With the oxidizing ZhGG from equations (8.17), (8.18), and (8.20):

$$A = \frac{Q_1}{Q_2} \frac{w_1}{w_2} \frac{k}{k-1} (RT)_{ext} = \frac{108}{0.148} \cdot 0.4 \cdot 0.65 \cdot \frac{1.2}{1.2-1} 30 \cdot 10^3 = \\ = 8630 \cdot 10^4 \text{ kg/m}^2 \quad (867 \text{ MN/m}^2); \\ \pi_{opt} = \left(\frac{A}{A - 4P_{ext} + P_{ext}} \frac{2k-1}{k} \right)^{\frac{1}{k-1}} = \\ = \left[\frac{8630 \cdot 10^4}{8630 \cdot 10^4 - (30 - 5) 10^4} \frac{2 \cdot 1.2 - 1}{1.2} \right]^{\frac{1}{1.2-1}} = 2.55; \\ P_{max} = (A - 4P_{ext} + P_{ext}) \frac{1}{\pi_{opt}} = \frac{A}{\frac{2k-1}{k}} - 4P_2 = \\ = [8630 \cdot 10^4 - (30 - 5) 10^4] \frac{1}{2.55} = \frac{8630 \cdot 10^4}{2.55} - 5 \cdot 10^4 = 485 [\text{atm(abs.)}] (\approx 47.70 \text{ MN/m}^2).$$

Analogously, with the reducing ZhGG:

$$A = 3360 \cdot 10^4 \text{ kg/m}^2 \quad (330 \text{ MN/m}^2); \pi_{opt} = 2.64; \\ P_{max} = 190 [\text{atm(abs.)}] (18.58 \text{ MN/m}^2).$$

8.2. Closed "Gas + Liquid" Circuit Without ZhGG

In Figs. 8.7 and 8.8 are shown closed circuits of "gas + liquid" type and the outward appearance of the propulsion system of the liquid-fuel RL-10 rocket engine, working on oxygen and hydrogen. Liquid hydrogen enters two-stage pump 6, then the coolant passage of the engine chamber 3, whence the gaseous hydrogen formed goes to turbine 5, driving the TIIA, and then into combustion chamber 3. Bypass 7 serves to maintain constancy of operating conditions of the system. Liquid oxygen is fed to the combustion chamber by pump 1. Thus in this system the working substance used to drive the turbine is hydrogen, which is gasified and heated to needed temperature in the coolant passage of the engine chamber. Here the temperature of the "heated" hydrogen can be below zero. With such arrangement of the propulsion system the need for a special ZhGG disappears, which considerably simplifies the entire system. Its deficiency is limited maximum possible combustion-chamber pressure p_2 max.

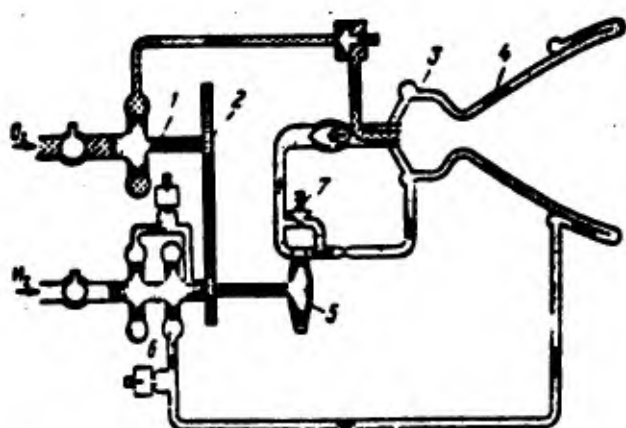


Fig. 8.7. Diagram of the RL-10 propulsion system (closed "gas + liquid" circuit without ZhGG:
1 - pump for liquid O_2 ; 2 - reduction gear; 3 - combustion chamber; 4 - nozzle; 5 - turbine;
6 - two-stage pump for liquid H_2 ; 7 - regulator.

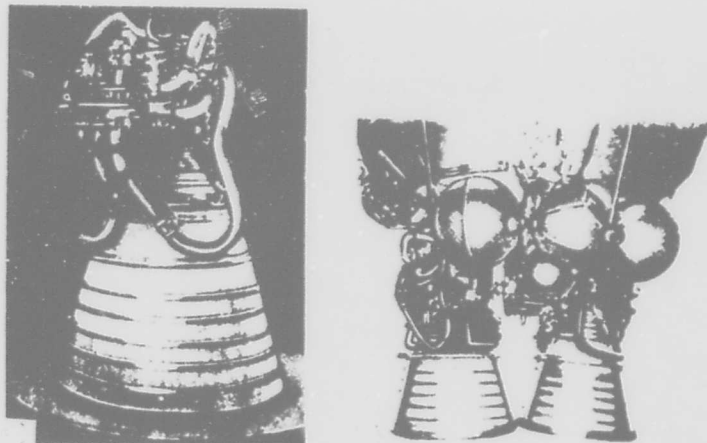


Fig. 8.8. The RL-10 engine: a) assembly; b) in system.

Determination of Basic Parameters

The equation connecting the basic parameters of the combustion chamber and TNA is that for the balance of powers of turbine and pump $N_t = N_p$, which in expanded form is recorded:

$$G_{H_2} \eta_t \frac{k}{k-1} (RT)_{H_2} \left(1 - \frac{1}{\frac{k-1}{k}} \right) = \frac{G_{H_2} (\rho_{noz, H_2} - \rho_{ex, H_2})}{\gamma_{H_2} \eta_{noz, H_2}} + \\ + \frac{G_{O_2} (\rho_{noz, O_2} - \rho_{ex, O_2})}{\gamma_{O_2} \eta_{noz, O_2}}, \quad (8.21)$$

where G_{H_2} — flow rate of hydrogen through the combustion chamber, equal to that of H_2 through the turbine; G_{O_2} — flow rate of oxygen; ρ_{H_2} and ρ_{O_2} — densities of liquid hydrogen and oxygen; $k = 1.4$ — adiabatic index for hydrogen; η — pressure drop in turbine:

$$\eta_t = \frac{\rho_{ex}}{\rho_{max}} = \frac{\rho_{ex}}{\rho_2 + \Delta \rho_2};$$

$P_{\text{max}}; P_{\text{min},0}$ — feed pressures for H_2 and O_2 ; $P_{\text{max}}; P_{\text{inlet}}$ — pump inlet pressures. It is obvious that

$$\begin{aligned} P_{\text{max},0} &= p_2 + \Delta p_2 + \Delta p_{\text{max},0}; \\ P_{\text{min},0} &= p_2^* + \Delta p_{\text{min},0} = \pi_2(p_2 + \Delta p_{\text{inlet}}) + \Delta p_{\text{min},0}. \end{aligned} \quad (8.22)$$

where $\Delta p_{\text{max},0}$ — pressure losses between pump and inlet to the engine chamber; $\Delta p_{\text{min},0}$ — pressure losses between pump and turbine; Δp_{inlet} — pressure losses between inlet to engine chamber and combustion chamber (in the head of the engine chamber); Δp_{inlet} — pressure losses between turbine and combustion chamber.

We will determine the value of the highest possible pressure in the chamber $p_2 \text{ max}$. For simplification we will consider constant and identical the values of pump efficiency and pressure losses and pump inlet pressures:

$$\left. \begin{aligned} \eta_{\text{p},0} &= \eta_{\text{t},0} = \eta_0; \\ \Delta p_{\text{max},0} &= \Delta p_{\text{min},0} = \Delta p_{\text{inlet}}; \\ \Delta p_{\text{inlet}} &= \Delta p_{\text{t}} = \Delta p_2; \\ P_{\text{inlet}} &= P_{\text{min},0} = P_{\text{max},0}. \end{aligned} \right\} \quad (8.23)$$

Then, substituting expressions (8.22) in equation (8.21), after simple transpositions we obtain

$$P_2 = \frac{\frac{1}{\eta_0} (M)_{\text{H}_2} \eta_0 \tau_2 m_2 \tau_{\text{O}_2} \left(1 - \frac{1}{\frac{P_{\text{inlet}}}{P_2}} \right) - (\Delta p_{\text{inlet}} - P_{\text{inlet}}) (\tau_{\text{O}_2} + \tau_{\text{H}_2})}{\tau_{\text{H}_2} + \tau_{\text{O}_2}} - \Delta p_2. \quad (8.24)$$

where

$$\tau = \frac{d_0}{d_2}.$$

Designating

$$\left. \begin{aligned} A &= \frac{\rho}{\gamma - 1} (RT)_{M, \infty, \gamma_0, \gamma_{M, \infty}} \\ B &= (\Delta P_{\text{exit}} - P_{\text{exit}})(\gamma_0 + v\gamma_{M, \infty}) \end{aligned} \right\} \quad (8.25)$$

we obtain:

$$P_2 = \frac{A \left(1 - \frac{1}{\frac{\gamma_0}{\gamma}^{\frac{2}{\gamma-1}}} \right) - B}{(\gamma_0 \gamma_{M, \infty} + v \gamma_{M, \infty})^{\frac{2}{\gamma-1}} - \Delta P_2} \quad (8.26)$$

For determination of $P_{2 \max}$ we take the derivative $dP_2/d\gamma_0$ and equate it to zero:

$$\frac{dP_2}{d\gamma_0} = \frac{\frac{2}{\gamma-1} A}{(\gamma_0 \gamma_{M, \infty} + v \gamma_{M, \infty})^{\frac{2}{\gamma-1}}} - \frac{A \left(1 - \frac{1}{\frac{\gamma_0}{\gamma}^{\frac{2}{\gamma-1}}} \right) - B}{(\gamma_0 \gamma_{M, \infty} + v \gamma_{M, \infty})^{\frac{2}{\gamma-1}}} \gamma_0 = 0,$$

whence we obtain an equation for finding pressure drop γ_{drop} corresponding to the highest possible chamber pressure

$$\gamma_{\text{drop}} = \frac{1}{\frac{\gamma_0}{\gamma}^{\frac{2}{\gamma-1}}} + \frac{B}{\gamma_0} \frac{\frac{2}{\gamma-1}}{\frac{\gamma_0}{\gamma}^{\frac{2}{\gamma-1}}} - \left(1 - \frac{B}{A} \right) \frac{A}{\frac{\gamma_0}{\gamma}^{\frac{2}{\gamma-1}}}$$

or, designating constants

$$A = \frac{B}{\gamma_0} \frac{\frac{2}{\gamma-1}}{\frac{\gamma_0}{\gamma}^{\frac{2}{\gamma-1}}} \quad B = \left(1 - \frac{B}{A} \right) \frac{A}{\frac{\gamma_0}{\gamma}^{\frac{2}{\gamma-1}}}, \quad (8.27)$$

we obtain

$$\frac{1}{\frac{\gamma_0}{\gamma}^{\frac{2}{\gamma-1}}} \left(1 + \frac{B}{\gamma_0} \frac{\frac{2}{\gamma-1}}{\frac{\gamma_0}{\gamma}^{\frac{2}{\gamma-1}}} \right) - B. \quad (8.28)$$

Having computed constants Δ and E , we can easily find the value of π_{opt} graphically or by selection (see example). Knowing π_{opt} from equation (8.26) we find $p_2 \text{ max}$:

$$p_{2 \text{ max}} = \frac{\pi_{\text{opt}} \left(1 - \frac{1}{E} \right) - s}{\pi_{\text{opt}} \gamma_{\text{H}_2} + \gamma_{\text{O}_2} - \Delta p_r} \quad (8.29)$$

Calculations show that the highest possible pressure in the chamber is low, and for true values of pump and turbine efficiency the relationship of components v and temperature of hydrogen at the outlet of the coolant passage it cannot be higher than 40-50 [atm(abs.)], ($\approx 4-5 \text{ MN/m}^2$), i.e., the circuit, similar to that represented in Fig. 3.7, for high pressures in the combustion chamber is not acceptable. For illustration we will examine an example of determination of $p_2 \text{ max}$.

Example of determination of $p_2 \text{ max}$

We will determine the value of the highest possible pressure in the combustion chamber $p_2 \text{ max}$ for a propulsstion system working on oxygen + hydrogen fuel with the circuit represented in Fig. 3.7 for two values of temperature of the hydrogen entering the turbine: 1) $T_{\text{H}_2}^I = -73^\circ\text{C} = 200^\circ\text{K}$ and 2) $T_{\text{H}_2}^{II} = 0^\circ\text{C} = 273^\circ\text{K}$.

Remaining basic operating parameters of the system remain constant.

Relationship of components $v = G_{\text{O}_2}/G_{\text{H}_2} = 4.8$; efficiency of turbine $\eta_t = 0.4$; efficiency of pumps $\eta_p = \eta_{\text{p},\text{O}_2} = \eta_{\text{p},\text{H}_2} = 0.8$. Pressure losses of oxygen between pump and engine chamber $\Delta p_{\text{loss},\text{O}_2}$ and of hydrogen between pump and turbine $\Delta p_{\text{loss},\text{H}_2}$ are equal to

$$\Delta p_{\text{loss},\text{O}_2} = \Delta p_{\text{loss},\text{H}_2} = \Delta p_{\text{loss}} = 20 \text{ kg/cm}^2 (1.96 \text{ MN/m}^2).$$

Pressure losses of hydrogen between turbine and combustion chamber and pressure of oxygen in the head respectively are equal and amount to $\Delta p = 8 \text{ kg/cm}^2 (0.79 \text{ MN/m}^2)$. Pump inlet pressures are identical and equal to $p_{\text{in},O_2} = p_{\text{in},H_2} = p_{\text{atm}} = 8 \text{ kg/cm}^2 (0.49 \text{ MN/m}^2)$.

1) When $T_{H_2}^I = 200^\circ\text{K}$. We determine constants entering in equation (8.28)

$$A = \frac{\gamma_0 \gamma_H}{k-1} (RT)_{H_2} v_{H_2} v_{O_2} = \\ -0.4 \cdot 0.6 \frac{1.4}{1.4-1} (424 \cdot 200) 70 \cdot 1140 = 56.8 \cdot 10^4; \\ B = (\Delta p_{\text{head}} - p_{\text{atm}}) (v_{O_2} - v_{H_2}) = (20 \cdot 10^4 - 5 \cdot 10^4) (1140 + 4.8 \cdot 70) = \\ -2.22 \cdot 10^4; \\ C = \frac{T_{H_2}}{T_{O_2}} \frac{k-1}{2k-1} = \frac{70}{1140} \frac{1.4-1}{2 \cdot 1.4-1} 4.8 = 0.0655; \\ D = \left(1 - \frac{B}{A}\right) \frac{k}{2k-1} = \left(1 - \frac{2.22 \cdot 10^4}{56.8 \cdot 10^4}\right) \frac{1.4}{2 \cdot 1.4-1} = 0.748.$$

Plotting dependence on x_1 of left part of equation (8.28), we find graphically the value of $x_{1,\text{opt}}^I$ (Fig. 8.29): $x_{1,\text{opt}}^I = 2.84$.

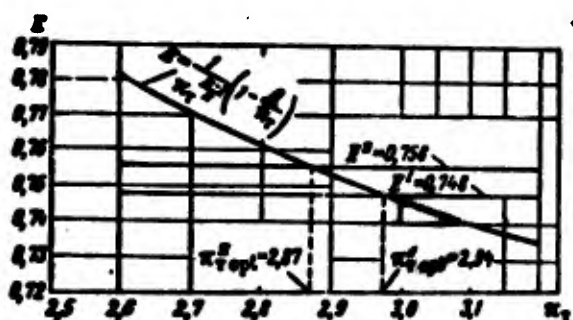


Fig. 8.29. Solution of example.

From equation (8.29) we determine $p_{2,\text{max}}^I$:

$$p_{2,\text{max}}^I = \frac{A \left(1 - \frac{1}{x_{1,\text{opt}}^I}\right) - B}{x_{1,\text{opt}}^I v_{O_2} + v_{H_2}} - \Delta p_2 = \\ 56.8 \cdot 10^4 \left(1 - \frac{1}{2.84 \cdot 1.4}\right) - 2.22 \cdot 10^4 \\ = \frac{2.94 \cdot 1140 + 4.8 \cdot 70}{-8 \cdot 10^4 - 27 \cdot 10^4 \text{ kg/m}^2} = 27 [\text{atm (abs.)}] (2.65 \text{ MN/m}^2).$$

2) When $T_{H_2}^{II} = 0^\circ C = 273^\circ K$.

Performing analogous calculations, we obtain:

$$\eta_{\text{turb}}^{\text{II}} = 2.87; P_{2 \max}^{\text{II}} = 41.8 \text{ atm (4.1 MPa)}$$

Thus an increase in the temperature of hydrogen going to the turbine T_{H_2} of 73° brought about an increase in $P_{2 \max}$ of almost one and a half times. Since the maximum possible value of T_H is determined by conditions of reliable cooling of the engine chamber, the value of the highest chamber pressure $P_{2 \max}$ is dependent upon the organization of cooling. As can be seen from equations (8.25) and (8.29), the value of $P_{2 \max}$ is strongly influenced also by change of efficiency of turbine η_{turb} and pumps η_{pump} .

8.3. Closed "Gas + Gas" Circuit

In Fig. 8.10 is shown a closed circuit for a propulsion system of "gas + gas" type. Fuel and oxidizer from pumps is fed with assigned relationship to the ZhGG's 2 and 3. The gaseous products of combustion in the ZhGG's, with surplus oxidizer and fuel, are used to drive turbines 4 and 10 and then pass through gas ducts 5 and 11 to combustion chamber 6. Thus in a system working with closed "gas + gas" circuit both components are used completely to drive the TJA.

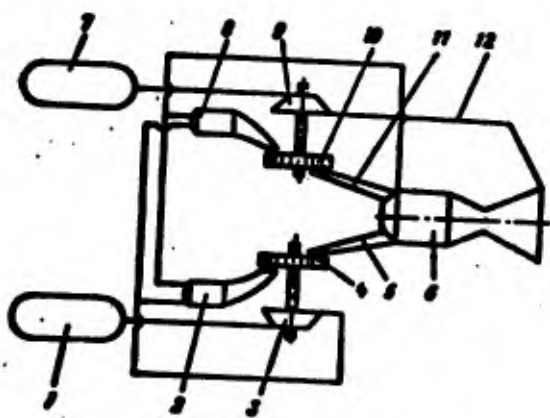


Fig. 8.10. Closed circuit of "gas + gas" type: 1 - oxidizer tank; 2 - oxidizing ZhGG; 3 - oxidizer pump; 4 - turbine; 5 - supply of oxidizing products of combustion from TJA to chamber; 6 - engine chamber; 7 - fuel tank; 8 - reducing ZhGG; 9 - fuel pump; 10 - turbine; 11 - supply of reducing products of combustion to chamber; 12 - supply of fuel for chamber.

Thanks to this assigned pressure in the combustion chamber is ensured at lower supply pressures than with the "gas + liquid" circuit. The gain in feed pressure is especially noticeable when it is necessary to provide high pressures in the combustion chamber.

Determination of Basic Parameters

Initial equations determining for assigned combustion-chamber pressure the basic operational parameters of the TMA and ZhGG will be equations for balance of powers of turbine N_t and pump N_p of fuel and oxidizer TMA:

$$N_{t,e} = N_{p,e}; N_{t,r} = N_{p,r} \quad (3.30)$$

or in expanded form

$$\left. \begin{aligned} \frac{G_{t,e}\eta_{t,e}}{75} \frac{k}{k-1} (RT)_{mrr,e} \left(1 - \frac{1}{\frac{p_{mrr,e}}{p_{mrr,r}}} \right) &= \frac{G_r (p_{mrr,e} - p_{mrr,r})}{75 V_r \eta_{mrr}}; \\ \frac{G_{p,e}\eta_{p,e}}{75} \frac{k}{k-1} (RT)_{mrr,e} \left(1 - \frac{1}{\frac{p_{mrr,e}}{p_{mrr,r}}} \right) &= \frac{G_o (p_{mrr,e} - p_{mrr,r})}{75 V_o \eta_{mrr}}. \end{aligned} \right\} \quad (3.31)$$

It is obvious here that

$$G_o + G_{p,e} = G_r + G_o. \quad (3.32)$$

For certain temperatures of working substance feed to turbines 4 and 10, working respectively on oxidizing and reducing gas, and for certain flow rates of components through the chamber (G_p and G_o), total flow rates ($G_{p,e}$ and $G_{o,e}$) and flow rates of oxidizer ($G_{o,mrr,e}$ and $G_{o,mrr,r}$) and fuel ($G_{p,mrr,e}$ and $G_{p,mrr,r}$) to oxidizing and reducing liquid gas generators are determined simply.

Actually, rated temperatures in the ZhGG are ensured by relationship of components v_{mrr} . Thus for certain temperatures we

know the relationship of components in oxidizing and reducing necessary for a given fuel ZhGG's:

$$v_{\text{ext,e}} = \frac{G_{e,\text{ext,e}}}{G_{r,\text{ext,e}}}; \quad v_{\text{ext,r}} = \frac{G_{r,\text{ext,r}}}{G_{e,\text{ext,r}}}. \quad (8.33)$$

Since all of a component passes through the gas generators, it is obvious that

$$G_e = G_{e,\text{ext,e}} + G_{e,\text{ext,r}}; \quad G_r = G_{r,\text{ext,e}} + G_{r,\text{ext,r}}. \quad (8.34)$$

Solving equations (8.33) and (8.34) jointly, we find flow rates of components in each of the ZhGG's:

$$\left. \begin{aligned} G_{e,\text{ext,e}} &= \frac{G_r v_{\text{ext,e}} - G_r}{v_{\text{ext,e}} - v_{\text{ext,r}}}; & G_{r,\text{ext,e}} &= \frac{G_e - G_r v_{\text{ext,e}}}{v_{\text{ext,e}} - v_{\text{ext,r}}}; \\ G_{e,\text{ext,r}} &= v_{\text{ext,e}} \frac{G_r v_{\text{ext,r}} - G_r}{v_{\text{ext,e}} - v_{\text{ext,r}}}; \\ G_{r,\text{ext,r}} &= v_{\text{ext,r}} \frac{G_e - G_r v_{\text{ext,r}}}{v_{\text{ext,e}} - v_{\text{ext,r}}}. \end{aligned} \right\} \quad (8.35)$$

Hence we find flow rates of working substance to each of the turbines

$$G_{e,e} = G_{\text{ext,e}} = G_{e,\text{ext,e}} + G_{e,\text{ext,r}}; \quad G_{r,e} = G_{\text{ext,r}} = G_{r,\text{ext,e}} + G_{r,\text{ext,r}}. \quad (8.36)$$

Analyzing system of equations (8.3), similar to that conducted above for "gas + liquid" circuits, we obtain equations analogous to (8.19) and (8.20), which permit determining the highest possible combustion-chamber pressure.

Advantages and Deficiencies of Closed-Circuit Systems

Examining different types of closed-circuit systems, we note the basic advantages, deficiencies, and peculiarity of their operation.

The main advantage consists in more complete use of the energy of the fuel available aboard the rocket, since with the closed circuit losses of thrust due to the consumption of components for driving the TMA are absent. The specific thrust of a system with closed circuit is greater than for those with open circuit and is equal to the specific thrust of the engine.

The deficiency of systems with closed circuit is their great complexity as compared to those with open circuits circuits. This complexity is caused, first, by the necessity of supplying from the TMA to the combustion chamber products of combustion of high temperature, and secondly, by the high supply pressures, which with the closed circuit, obviously, are considerably higher than with the open. All of this makes it difficult to ensure high operational reliability of the system.

High feed pressures and high pressures in the ZhGG and in the turbine of the TMA lead also to increase of mass of the supply system. On the whole, in spite of the absence of a separate system for feeding fuel to the TMA and exhaust ducts, the specific weight of the closed-circuit system without tanks will compare with that of systems with open circuits.

However, thanks to gain in specific thrust, the decrease in total mass of the fueled propulsion system can attain 10-20% as a result of the decrease in the necessary reserve of fuel and corresponding decrease in dimensions (and consequently of mass) of tanks. This gain is especially appreciable with high engine thrusts, and therefore the application of assemblies with closed circuit is more expediently in high-thrust propulsion systems. With

low thrust the complication of the system and lowering of its reliability connected with the use of the closed circuit is not always recompensed by the gain in thrust.

Application of closed circuits will give the greatest benefit in propulsion systems high thrust working at high pressure in the combustion chamber, since in this case with the use of the open circuit losses of thrust due to consumption of part of component for driving the TNA would be comparatively high.

An interesting peculiarity of closed-circuit systems is the fact that the efficiencies of pumps and turbine influence only the value of feed pressure and pressure p_2 max and have practically no effect on the specific thrust of the system, since impairment of turbine efficiency η_t or pump efficiency η_p will lead only to increase in required feed pressure, but not to impairment of specific thrust. However values of turbine and pump efficiency in closed-circuit systems are very important, since with impairment of efficiency feed pressure increases with an according increase in mass of the propulsion system. Therefore, with the closed circuit it is also important to ensure economic operation of the TNA.

C H A P T E R IX

PROPELLION SYSTEMS WITH A PRESSURIZED FEED SYSTEM

The basic deficiency of a pressurized system is that with it the tanks are under feed pressure, in consequence of which their mass is very great.

However, the pressure feed systems in their action and design are simpler than turbopump systems; the starting and shutdown of an engine are simpler; there are no complicated units similar to the turbopump assembly [TNA] and no revolving elements, which in certain conditions can also be a considerable advantage.

A gravimetric analysis of propulsion systems with a pressure feed system [152] showed that sometimes with operation at high altitudes the systems with low pressure in the chamber of the 5 [atm(abs)] ($\approx 0.5 \text{ MN/m}^2$) are more rational than systems with a turbopump feed system. The fact is that in operating at high altitude in connection with the insignificantly low ambient pressure, it is possible and at low pressure in the chamber to obtain an expansion ratio of $\delta = \frac{1}{200} - \frac{1}{800}$, which provides quite high specific thrust. With this the specific thrust will decrease somewhat in virtue of a certain decrease in temperature in the combustion chamber, and also dimensions of the engine chamber will increase, since with a decrease in pressure in the chamber with that same thrust (or flow rate according to equations (1.9) and (1.20) the area l_{mp} and area of the section l_0 will be increased accordingly.

For a comparison Fig. 9.1 shows the circuits of an engine with an identical expansion ratio operating at a pressure in the chamber of 4 and 20 [atm(abs)] (0.39 and 1.96 MN/m^2), from which it is clear that with a decrease in pressure the overall dimensions of the chamber considerably increase. However, in connection with low pressure in the chamber the weight characteristics of the propulsion system on the whole remain quite good.

The basic possible regions of the application of propulsion systems with pressurized feed systems: propulsion system of spaceships (for example, engines of the orientation system of the satellite "Mercury"), light rockets of the class "air-to-air", "surface-to-surface" and "air-to-surface." Possible also the application of a pressurized feed in propulsion systems of surface-to-air rockets (Oerlikon) and upper stages of space rockets ("Able Star"). Furthermore, pressurized systems are used as auxiliary systems, for example, for feeding components into a steam-gas generator (PGG) or liquid-gas generator (ZhGG), for supercharging the tanks, etc.

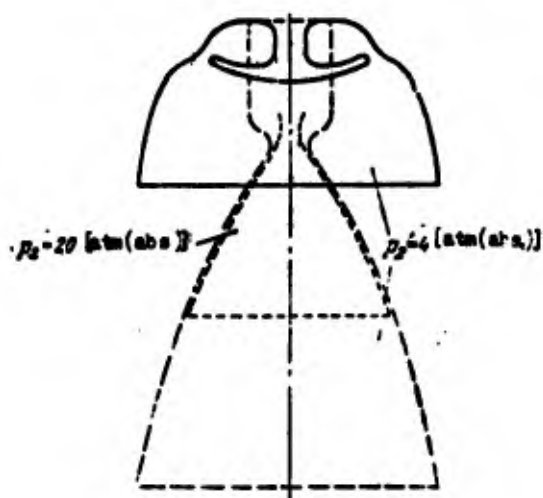


Fig. 9.1. Comparison of circuits of engines having identical thrusts and expansions ratio at different pressures in the chamber.

There are three basic forms of pressurized systems:
gas-pressurized feed systems, which use for displacement nitrogen, air, helium or some other gas; systems with solid fuel pressure accumulator (PAD), which using for displacement products of combustion of powder and systems with a liquid fuel pressure accumulator (ZhAD), which use for displacement products of combustion

of a liquid components. Let us examine each of these systems.

9.1. Gas Cylinder Feed System

A gas cylinder pressurized system is used both as the basic feed system for displacing components in the combustion chamber and for displacing the components in the ZhGG and PGG and for supercharging the tanks. The displacing gas is usually nitrogen, air or helium. The advantage of helium over air and nitrogen is that it has a lower molecular weight and consequently, under identical conditions less density.

In the selection of the displacing gas one should consider that it should not enter into reaction with the component or be easily dissolved in it. It is also necessary to consider that when feeding or pressurizing the tanks with low-boiling components, the temperature of liquefaction of the displacing gas should be lower than the boiling point of the component. Thus, a tank with liquid hydrogen can be pressurized by either hydrogen or helium, since other gases upon contact with the liquid hydrogen will be condensed.

An elementary diagram of a propulsion system with gas cylinder feed system is shown in Fig. 9.2.



Fig. 9.2. Elementary diagram of a gas cylinder feed system:
1 - cylinder with high-pressure gas; 2 - pressure reducer;
3 - fuel tanks; 4 - membrane;
5 - engine change.

Gas under a pressure of 250-300 [atm(abs.)] ($\approx 25-30 \text{ MN/m}^2$) included in cylinder 1 enters into the gas reduction valve 2, where the pressure of the gas drops to the necessary value where it enters into tanks 3, whence the fuel is displaced and through the pipelines enters into the chamber of the engine 5, breaking the membranes installed on the pipeline 4. An exemplary diagram of the use in pressurized feed for pressurizing the tanks is shown on Fig. 6.4.

In the calculation of gas cylinder system the problem is reduced to the determination of the necessary volume of the cylinder and reserve of compressed gas, which serves for the displacement of component or for pressurization.

Change in Temperature of the Displacing Gas

Processes occurring with pressurized feed (see Fig. 9.2) of components and with pressurization of tanks are similar.

High-pressure gas flows out from a cylinder and is throttled in the reduction valve 2 up to a pressure of the feed at which it enters into the tanks. With the outflow of gas from the cylinder 1 the gas remaining there will be expanded and its temperature will drop. As a result of the lowering of the temperature of the gas, to it heat from walls of the cylinder will be fed. But since this heat feed is insignificant, the temperature of the gas in the cylinder in the end drops, i.e., in cylinder 1 there occurs polytropic expansion with the polytropic exponent n smaller than the adiabatic index, i.e., $1 < n < k$.

Using the equation of the polytropic process, it is possible to calculate the final temperature of the gas in the cylinder by expression

$$T_{r.\text{new}} = T_{r.\text{old}} \left(\frac{P_{r.\text{new}}}{P_{r.\text{old}}} \right)^{\frac{n-1}{n}}. \quad (9.1)$$

Designating the quantity $\left(\frac{P_{r.\text{new}}}{P_{r.\text{old}}} \right)^{\frac{n-1}{n}}$ by c_1 , we obtain

$$T_{r.\text{new}} = T_{r.\text{old}} c_1. \quad (9.2)$$

Quantity c_1 depends on the pressure drop $P_{r.\text{new}}/P_{r.\text{old}}$ and polytropic exponent n , which is determined by the intensity of the transmission of heat from the wall of the cylinder to the gas. It is possible

to consider quantity n equal to 1.15-1.33. Table 9.1 gives values of the coefficient c_1 , calculated at the value $n = 1.33$.

Table 9.1.

$\frac{P_{\text{final}}}{P_{\text{initial}}}$	10	7	4	3
$\frac{c_1}{c_2}$	0.85	0.88	0.78	0.82
	0.75	0.80	0.87	0.90

In the process of the outflow of gas from the cylinder, the temperature of it in the cylinder gradually descends from $T_{r,\text{max}}$ to $T_{r,\text{min}}$.

With the throttling of the gas in the reduction valve the temperature of the real gases does not remain constant. In particular, for air and nitrogen it drops, and for helium it is somewhat increased. Furthermore, entering into the tanks, the gas is heated from walls of the tanks.

It is very difficult to consider theoretically all these changes in temperature. For simplification we will not consider changes in temperature of the gas in the process of throttling and heating of it from walls of the tanks. In this case every portion of the gas entering into tank 3 has a temperature equal to the temperature of gas in the cylinder 1 at a given moment. Therefore the first portion of the gas with the starting of the engine enters into the tank at a temperature of $T_{r,\text{max}}$ and the very last portion in the end of operation of the engine — at a temperature $T_{r,\text{min}}$. All these gas portions are mixed in the tank, in consequence of which the average temperature of the gas in the tank will be intermediate between $T_{r,\text{max}}$ and $T_{r,\text{min}}$, i.e.,

$$T_{r,\text{avg}} < T_{r,\text{sp}} < T_{r,\text{min}}$$

We will consider that the gas temperature in the tank at the end of the feed has the magnitude

$$T_{r,\text{avg}} = c_3 T_{r,\text{min}} \quad (9.3)$$

The value of coefficient c_2 is less than unity but larger than the value of c_1 . The tentative values of c_1 and c_2 when $n = 1.53$, depending upon $P_{\text{max}}/P_{\text{min}}$, are given in Table 9.1.

If one were to consider the change in temperature of the gas in the process of throttling, then for nitrogen and air the value of c_2 will decrease as compared to data of Table 9.1, and for helium it will be increased.

Calculation of the Volume of the Cylinder and Gas Reserve

The following initial data serves for calculation of the volume of the cylinder and reserve of gas: the total volume of the tank of fuel and oxidizer V_t , the feed pressure of components or pressurizing the tanks P_f , and also the gas constant R and initial temperature of the gas T_{max} .

The initial pressure of the gas in the cylinder is determined by conditions of filling of the cylinder. The final pressure in the cylinder should be higher than the feed pressure P_f on the magnitude of minimum pressure drop in the reduction valve ΔP_{min} which is necessary to provide normal operation of the reduction valve.

Quantity ΔP_{min} is determined by the design of the reduction valve and depends on the feed pressure or pressurization. At high pressures of the feed, of the order of 30-40 [atm(abs.)] ($\approx 3-4 \text{ MN/m}^2$), quantity $\Delta P_{\text{min}} = (0.25-0.50) P_{\text{max}}$. With pressurization or low pressures of the feed - within 3-10 [atm(abs.)] ($0.3-1 \text{ MN/m}^2$) quantity $\Delta P_{\text{min}} = (2-10) P_{\text{max}}$ (see section 9.4).

Let us examine the state of the emanating gas before the beginning of the feed and at the end of it. Before the beginning of the feed the whole gas is included in the cylinder and according to the equation of state it is possible to write

$$P_{r.mes} V_{res} = G_{res} R T_{r.mes} \quad (9.4)$$

where G_{res} — quantity of gas included in the cylinder.

At the end of the feed the gas is found partially in the cylinder and partially in the tanks. The state of the gas in the cylinder can be expressed by equation

$$P_{r.mes} V_{res} = G_{r.mes} R T_{r.mes}, \quad (9.5)$$

where $P_{r.mes}$, $T_{r.mes}$ and $G_{r.mes}$ — pressure, temperature and mass of the gas which remained in the cylinder toward the end of the feed.

The final pressure in the cylinder $P_{r.mes} = p_0 + \Delta p_{per}$.

The state of the gas in the tanks toward the end of the feed will be determined by equation

$$p_0 V_0 = G_0 R T_{0.mes}. \quad (9.6)$$

where G_0 — quantity of gas proceeding into the tanks toward the end of the feed.

From formula (9.4) we find

$$G_{res} = \frac{P_{r.mes} V_{res}}{R T_{r.mes}}. \quad (9.7)$$

From formula (9.6)

$$G_0 = \frac{p_0 V_0}{R T_{0.mes}}.$$

The quantity of gas in the cylinder and tanks at the end of the operation of the engine is equal to the initial:

$$G_{res} = G_{r.mes} - G_0.$$

whence

$$G_{r.m.s} = G_{res} - G_0 = \frac{P_{r.m.s} V_{res}}{R T_{r.m.s}} - \frac{P_0 V_0}{R T_{0.r.m.s}}. \quad (9.8)$$

Substituting values $P_{r.m.s}$ and $G_{r.m.s}$ into formula (9.5), we will obtain

$$(P_0 + \Delta P_{gas}) V_{res} = \left(\frac{P_{r.m.s} V_{res}}{R T_{r.m.s}} - \frac{P_0 V_0}{R T_{0.r.m.s}} \right) R c_1 T_{r.m.s}. \quad (9.9)$$

Introducing connections indicated above between initial and final temperatures (9.2) and (9.3) and substituting these expressions into formula (9.9), we will obtain

$$(P_0 + \Delta P_{gas}) V_{res} = \left(\frac{P_{r.m.s} V_{res}}{R T_{r.m.s}} - \frac{P_0 V_0}{R c_1 T_{r.m.s}} \right) R c_1 T_{r.m.s}. \quad (9.10)$$

After transformations and reductions we obtain

$$V_{res} = \frac{P_0 V_0 \frac{c_1}{c_2}}{c_1 P_{r.m.s} - (P_0 + \Delta P_{gas})}. \quad (9.11)$$

The volume of the cylinder is directly proportional to the feed pressure and volume of the tanks; it decreases with an increase in initial pressure and does not depend on the gas constant of the applied gas. By knowing the magnitude of the volume of the cylinder V_{res} , we find by formula (9.7) quantity of the necessary reserve of gas

$$G_{res} = V_{res} \frac{P_{r.m.s}}{R T_{r.m.s}}. \quad (9.12)$$

The mass of the gas depends on its properties. With an increase in gas constant it decreases. Therefore, the application, for example, of helium instead of nitrogen or air permits reducing the mass of the reserve of gas by approximately 3.5 times.

Example. Determine the volume of the cylinder for compressed air and the mass of air in a cylinder for a liquid-fuel rocket engine (ZhRD) with a cylinder feed, if the total volume of the tank with fuel is equal to $V_f = 0.209 \text{ m}^3$, and the volume of the tank of

oxidizer $V_o = 0.472 \text{ m}^3$. The feed pressure of the components from the tanks $p_0 = 30 \text{ kgf/cm}^2 (2.94 \text{ MN/m}^2)$. The initial temperature of the gas $T_{r.oxy} = 299^\circ\text{K}$. The pressure in the cylinder is taken equal to $250 \text{ kgf/cm}^2 (24.53 \text{ MN/m}^2)$.

Solution. We determine the total volume of the tanks of fuel and oxidizer

$$V_s = V_r + V_o = 0.209 + 0.472 = 0.681 \text{ m}^3.$$

We assume that the reduction valve provides normal feed with a difference in pressures in the cylinder and tank equal to $\Delta p_{red} = 7 \text{ kgf/cm}^2 (0.67 \text{ MN/m}^2)$.

We find the pressure in the cylinder toward the end of the operation

$$p_{r.end} = p_0 + \Delta p_{red} = 30 + 7 = 37 \text{ kgf/cm}^2 (3.63 \text{ MN/m}^2).$$

The ratio of the initial pressure in the cylinder to the final pressure is equal to

$$\frac{p_{r.end}}{p_{r.oxy}} = \frac{37}{30} = 1.233.$$

From Table 9.1 we find coefficients c_1 and c_2 for this ratio: $c_1 = 0.61$; $c_2 = 0.81$.

By formula (9.11) we find the volume of the cylinder

$$V_{r.oxy} = \frac{p_0 V_s c_1}{c_1 p_{r.end} - (p_0 + \Delta p_{red})} = \frac{30 \cdot 10^4 \cdot 0.681 \cdot 0.61}{0.61 \cdot 250 \cdot 10^4 - (30 \cdot 10^4 + 7 \cdot 10^4)} = 0.156 \text{ m}^3.$$

The mass of gas included in the cylinder is determined by the equation of state:

whence

$$G_{r.oxy} = \frac{p_{r.end} V_{r.oxy}}{R T_{r.oxy}} = \frac{250 \cdot 10^4 \cdot 0.156}{29.3 \cdot 293} = 45.4 \text{ kg.}$$

Selection of Initial Pressure in the Cylinder

The initial pressure in the cylinder P_{init} is selected proceeding from the following considerations. Obviously the greater P_{init} , the less the volume occupied by this cylinder will be, which is very essential if it is necessary to place a spherical cylinder in the design of a rocket of limited dimensions.

It is possible to show that the mass of the spherical cylinder depends little on the initial pressure in it. Actually, the mass of the spherical cylinder Θ_0 with an average diameter d at a density of the material γ_m and thickness of the wall δ will be

$$\Theta_0 = \pi d^2 \gamma_m r_m. \quad (9.13)$$

Since the thickness of the wall of the cylinder

$$d = \frac{\delta}{k}, \quad (9.14)$$

where k - safety factor of strength; σ_u - ultimate tensile strength, that

$$\Theta_0 = \frac{\pi d^2 \rho_m \gamma_m r_m}{4 \sigma_u}. \quad (9.15)$$

Expressing the diameter in terms of volume of the spherical cylinder

$$d = \sqrt{\frac{6V_m}{\pi}},$$

and substituting value d into expression (9.15), we will obtain

$$\Theta_0 = \frac{6\pi \rho_m \gamma_m V_m}{4 \sigma_u} = 1.5 \frac{\rho_m \gamma_m V_m}{\sigma_u}. \quad (9.16)$$

Substituting V_m from expression (9.11), we will obtain

$$\Theta_0 = 1.5 \frac{\gamma_m \rho_m V_0 \frac{\sigma_1}{\sigma_2} P_{\text{max}}}{\sigma_0 (\sigma_1 P_{\text{max}} - (\rho_0 + \Delta \rho_{\text{load}}))}.$$

or

$$\Theta_0 = 1.5 \frac{\Delta p_{\text{gas}} \frac{c_1}{c_2} \frac{V_0}{c_1} \frac{T_0}{c_2}}{\left(c_1 - \frac{p_0 + \Delta p_{\text{gas}}}{p_{\text{max}}} \right) \frac{V_0}{c_1}} \quad (9.17)$$

From formula (9.17) it is clear that at the assigned pressure and volume of the fuel tanks p_0 and V_0 the mass of the cylinder depends only on the difference

$$\left(c_1 - \frac{p_0 + \Delta p_{\text{gas}}}{p_{\text{max}}} \right)$$

and ratio c_1/c_2 . With an increase in p_{max} these values are changed very insignificantly. For example, if

$$p_{\text{max}} = p_0 + \Delta p_{\text{gas}} = 33 + 9 = 42 \text{ [atm(abs.)]} (4.12 \text{ MN/m}^2),$$

that with a change in p_{max} from 280 to 320 [atm(abs.)] (27.4-31.4 MN/m²) quantity Θ_0 will be increased by less than 1%.

Thus, an increase in initial pressure in the cylinder p_{max} essentially does not affect the mass of the cylinder and promotes a decrease in its dimensions.

However, the greatest value of initial pressure in the cylinder is limited by possibilities of servicing means.

The Use of Heating of the Gas

To decrease the necessary reserve of the gas in the cylinder, and, consequently, the mass of the cylinder itself, it is possible to use the heating of the displacing gas. The displacing gas is heated either in the heat exchanger by exhaust gases of the turbopump assembly (see, for example, the diagram on Fig. 6.3) or by heat entering into the wall of the chamber of the engine or by burning solid or liquid fuel in a special generator (Fig. 9.3).

Let us determine approximately the necessary reserve of gas with the heating of it before the entering into tanks up to a

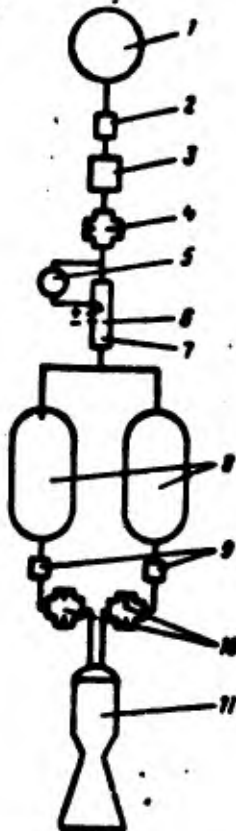


Fig. 9.3. Diagram of a gas cylinder feed system with heating of the gas:
 1 - pressure accumulator; 2 - valve;
 3 - reduction valve; 4 - throttle;
 5 - tank with fuel; 6 - spark plug;
 7 - heating chamber; 8 - tanks;
 9 - valves; 10 - throttles;
 11 - engine chamber.

rated temperature T_{max} . The state of the gas in the tanks can be determined by the equation

$$p_0 V_0 = G_{0,\text{max}} R T_{\text{max}} \quad (9.18)$$

Having compared expressions (9.6) and (9.18), we will obtain

$$G_{0,\text{max}} = G_0 \frac{T_{\text{max}}}{T_{\text{min}}} \quad (9.19)$$

Substituting into equality (9.8) the quantity of gas in the tank equal to $G_{0,\text{max}}$ instead of G_0 , after transformations taking into account expression (9.19) we will obtain

$$V_m = \frac{p_0 V_0 \epsilon_1 \left(\frac{T_{\text{max}}}{T_{\text{min}}} \right)}{\epsilon_1 p_{\text{max}} - (p_0 + \delta p_{\text{min}})} \quad (9.20)$$

If the gas is heated by means of feeding to it a definite constant quantity of heat ΔQ (for example, in a heat exchanger), then approximately, disregarding losses of heat, the temperature of the gas in the tanks at the end of the operation

$$T_{\text{end}} = T_{\text{initial}} + \frac{\Delta Q}{G_{\text{mass}} c_p}. \quad (9.21)$$

With this G_{mass} is determined by formula (9.19), assigning preliminarily the tentative value T_{max} . Determining in the first approximation T_{max} , we correct the value G_{mass} and obtained value T_{max} .

By analyzing formula (9.20), we see that the heating of the displacing gas gives especially high gain at low initial temperatures of the gas in the cylinder. Thus, for example, with the operation of the system according to the circuit of Fig. 9.8 the temperature of the helium in the gas pressure accumulator 3 is very low, since it is inside the tank with liquid hydrogen. Therefore, the heating of the helium even up to 300°K will allow decreasing its reserve by approximately 3-4 times.

9.2 Examples of Propulsion Systems with Gas-Pressurized Feed

There is a large number of propulsion systems with gas-pressurized feed. In the book [25] typical examples are given of the application of pressurized feed in propulsion systems of aircraft accelerators and systems of surface-to-air rockets. Let us examine examples of the application of a gas-pressurized feed system in propulsion systems of upper stages of space rockets and in propulsion systems of spaceships.

Propulsion System of the Second Stage with Gas-Pressurized Feed

Figures 9.4 and 9.5 shows the general form and circuit of the propulsion system of the second stage of the rocket "Able Star" with a gas-pressurized feed system [152]. The engine operates on

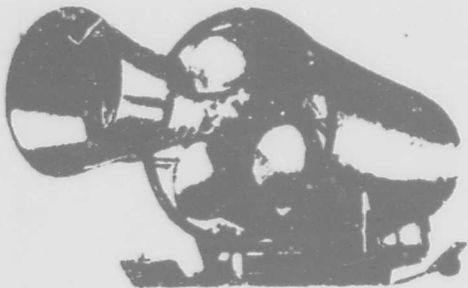


Fig. 9.4. Propulsion system of the second stage of the rocket "Able Star" with pressurized feed.

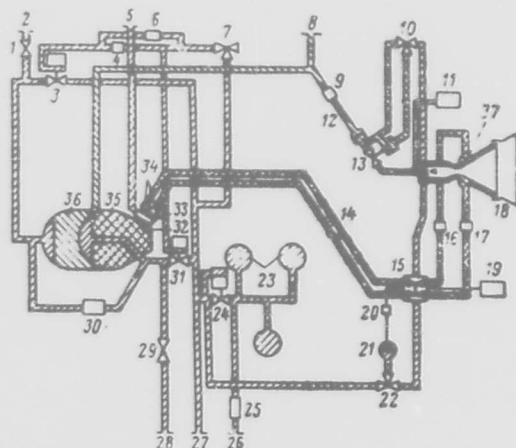


Fig. 9.5. Diagram of the propulsion system of the rocket "Able Star": 1 – vent valve of fuel tank; 2 – vent tube; 3 – closing pneumatic valve; 4 – filter; 5 – line for servicing the tank of the oxidizer; 6 – check valve; 7 – electropneumatic valve; 8 – line for servicing the fuel tank; 9 – fuel flowmeter; 10 – electropneumatic valve for controlling the main fuel valve; 11 – device for measuring pressure in the chamber; 12 – flexible fuel line; 13 – main fuel valve; 14 – flexible oxidizer line; 15 – main oxidizer valve; 16 – flowmeter of the oxidizer; 17 – flow-rate orifice of the oxidizer; 18 – uncooled orifice; 19 – indicator of the opening of the main oxidizer valve; 20 – check valve; 21 – pressure accumulator for opening of the valve 15; 22 – electropneumatic valve for controlling valve 15; 23 – cylinder with helium; 24 – reduction valve; 25 – servicing valve; 26 – line for servicing cylinders with helium; 27 – vent tube of helium; 28 – vent tube of oxidizer tank; 29 – vent valve; 30 – differential pressure relay in fuel and oxidizer tanks; 31 – closing pneumatic valve; 32 – sensor of the quantity of oxidizer in the tank; 33 – filter; 34 – valves; 35 – oxidizer tank; 36 – fuel tank; 37 – collector.

hypergolic fuel - nitric acid + NDMG. As a displacing gas there is used helium, which is under a pressure of 300 kgf/cm^2 (27.4 MN/m^2) in three cylinders 23. The tanks are the carrier type and of combined construction. The system allows multiple starting and shutdown on command from earth.

Basic Data

Fuel.....	$\text{HNO}_3 + \text{НДМГ}$
Thrust in a vacuum	$3590 \pm 100 \text{ kgf}$ ($\approx 35,250 \pm 981 \text{ N}$)
Specific thrust in a vacuum	$278 \text{ kgf}\cdot\text{s/kg}$ ($2730 \text{ N}\cdot\text{s/kg}$)
Thrust coefficient	1.77
Total impulse	$1045 \cdot 10^3 \text{ kgf}\cdot\text{s}$ ($10.25 \cdot 10^6 \text{ N}\cdot\text{s}$)
Pressure in the combustion chamber	$14.5 \pm 0.4 \text{ kgf/cm}^2$ ($1.42 \pm 0.04 \text{ MN/m}^2$)
Fuel consumption	12.9 kg/s
Relationship of components	$\gamma = 23 \pm 0.6$
Complex β	$157 \text{ kgf}\cdot\text{s/kg}$ ($1540 \text{ N}\cdot\text{s/kg}$)
Time of operation	300 s
Given length	1270 mm
Area of throat	140 cm^2
Expansion ratio	40
Pressure on the section	0.0294 kgf/cm^2 (2980 N/m^2)
Mass of propulsion system	4925 kg
Mass of engine chamber	32 kg
Mass of valves	8 kg
Mass of the orifice	4.5 kg
Mass of fuel	3850 kg
Mass of helium	13.3 kg
Volume of cylinder with helium	0.322 m^3

The engine chamber is made of aluminum tubes and is cooled by an oxidizer. The coolant enters into collector 3/, through the tubes goes toward the end of the cooled part of the nozzle and from there through the second system of tubes goes back, cools the nozzle

and combustion chamber and enters into the head (sesquiflow circuit of cooling). The thickness of the tubes is 0.9 mm. To the nozzle there is attached the orifice 18.

With the starting of the engine commands are given for the opening of the electropneumatic valves (EPK) 22 and 7. Through the EPK 22 helium, which is fed into the system from cylinders 23 through the reduction valve 24, enters into the pressure accumulator 21, approaches the main valve of the oxidizer 15 and opens it. With the opening of EPK 7 the pressure of helium is fed to pneumatic valves 3 and 31, through which the helium enters into fuel tanks 35 and 36 for displacing the components. The oxidizer from tank 35 enters into the chamber of the engine with the full opening of the main oxidizer valve 15 there is sent the command for opening the EPK 10, after which the fuel pressure opens the main fuel valve 13, and the fuel enters into the chamber of the engine.

The fuel supply and oxidizer from the tanks into the chamber is regulated so that constant pressure in the combustion chamber of $14.5 \pm 0.4 \text{ kgf/cm}^2$ ($1.42 \pm 0.04 \text{ MN/m}^2$) is maintained.

To shut down the engine, there is sent a command for shutting the EPK 7, 22 and 10, after which main valves 13 and 15 and valves 3 and 31 of the feed of helium into the tanks are closed. To prevent the destruction of the intermediate wall, which divides the capacity of the oxidizer and the fuel, the differential pressure relay 30 is set. When the pressure in one of the tanks becomes higher than in the other, the relay passes the command to the corresponding vent valve (1 or 29), and the pressure in the tanks is balanced. With repeated starting under conditions of zero gravity with the help of the special jet nozzles operating on gaseous nitrogen, little acceleration is imparted to the system so that the fuel shifts to the rear wall of the tanks.

Propulsion System for the Correction
of Speed of a Spaceship

Figure 9.6 shows circuits and external view of a propulsion system for the correction of the speed of the spaceship "Pioneer-VI."

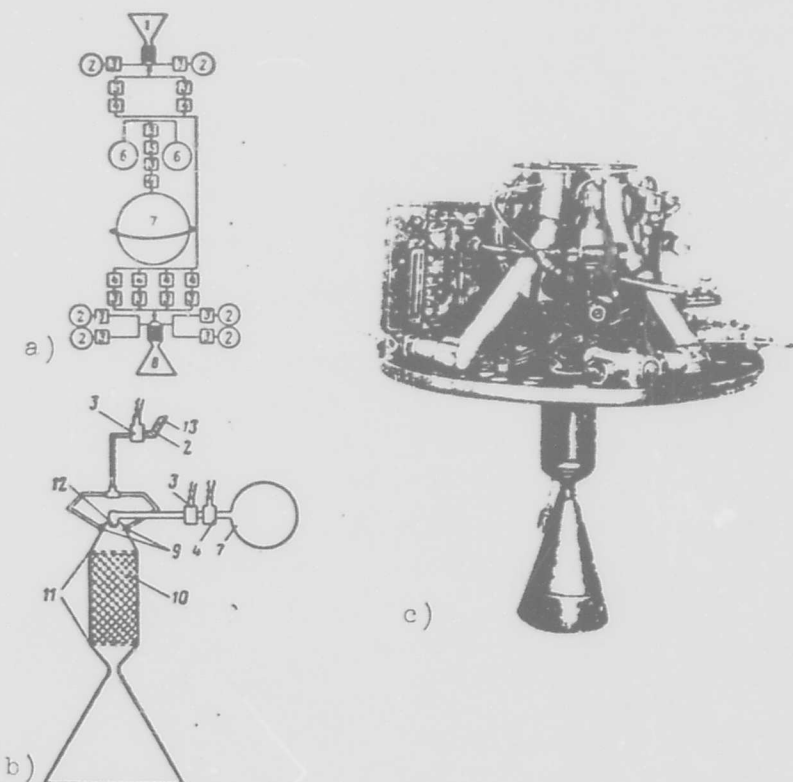


Fig. 9.6. System for the correction of speed of the spaceship: a) circuit of the propulsion system; b) circuit of one of the chambers; c) external view of the propulsion system;
1 - chamber with a nozzle directed along the flight; 2 - tank with nitrogen tetroxide; 3, 4 - pyrotechnic valves; 5 - reduction valve; 6 - pressure accumulator with nitrogen; 7 - tank with hydrazine; 8 - chamber with a nozzle directed opposite the flight; 9 - injectors of the nitrogen tetroxide feed; 10 - catalyst; 11 - nickel grids; 12 - injectors of the hydrazine feed; 13 - compressed gas.

The system has two chambers 1 and 8 which operate on products of the decomposition of hydrazine. The chambers are located along the longitudinal axis of the ship so that the nozzles of the chambers are directed in the opposite directions. The thrust of each chamber is 11.3-7.3 kgf (111-71.6 N) depending upon the boost pressure in the tank with hydrazine; the specific thrust 230 kgf·s/kg, (2260 N·s/kg), and the expansion ratio is 50. The propulsion system should provide four pulses of thrust in the direction of flight and two pulses opposite it. The duration of every pulse is determined by the necessary magnitude of correction. The fuel reserve provides a maximum total impulse in the direction of flight of 3400 kgf·s (33,400 N·s) and opposite the direction, 12,200 kgf·s (119,800 N·s).

The feed system is gas-pressurized. Compressed nitrogen is stored in two spheric pressure accumulators 6 with the initial pressure of 140 kgf/cm² (13.73 MN/m²). With the output of nitrogen the pressure decreases, and into the device determining pulse width there is automatically introduced an appropriate correction. Hydrazine in an amount of ~80 kg is in the sperical tank 7. The initial pressure of the feed from the tank is 28.5 kgf/cm² (2.80 MN/m²). For heating the catalyst 10 upon starting, nitrogen tetroxide is fed into chamber, forming with the hydrazine a spontaneously inflammable mixture. Nitrogen tetroxide is stored in four tanks 2 with a capacity of 8 cm³ each.

The sequence of starting and shutdown with every impulse of thrust consists in the following. By a signal of an airborn guidance system or from a ground station voltage is sent to the single-pass pyrotechnic valves 3 (closed prior to the signal) located on feed lines of nitrogen tetroxide and hydrazine in the chamber. Components with lead of the feed of nitrogen tetroxide of ~50 ms enter into the chamber. After the self-ignition of the mixture the nitrogen tetroxide continues to proceed up to the emptying of the tank in almost ~200 ms. During this time the catalyst 10 is heated up to a temperature ensuring the decomposition of hydrazine. For a turned-off engine the voltage is fed to the single-pass pyrotechnic valve 4

(open before sending the signal), located on the line of hydrazine feed. Every feed line of the component can be used only once.

Propulsion System of a Satellite Orientation System

Figure 9.7 shows a circuit of the propulsion system of the orientation system of the piloted spaceship "Mercury," operating on products of decomposition of hydrogen peroxide. The hydrogen peroxide is displaced by compressed helium from tanks 13 and enters into chambers of decomposition located directly in front of the controlling nozzles. In the chambers, due to the contact with the catalyst, decomposition of the hydrogen peroxide occurs.

On board the satellite there are two autonomous systems. The first system (Fig. 9.7a) is switched on automatically with the help of electrically operated valves connected with sensors of the orientation system. For reasons of fuel economy this system can operate in conditions of high and low thrust. Under conditions of high thrust for pitch and yaw control engines 7 and 8 each operate with a thrust of 11 kgf (108 N) and for roll control - engines 10 with a thrust of 2.7 kgf (26.5 N). In on conditions of low thrust for control on all three axes engines 7, 8 and 10 operate with a thrust of 0.45 kgf (4.41 N). Switching from one regime to the second occurs automatically.

The second system (Fig. 9.7b) can operate in automatic operating conditions and in conditions of manual control. The transfer of the system from one operating regime to the other is carried out by control valve 11, which is controlled by the pilot. When operating in automatic conditions engines 7 and 8 operate with a thrust of 11 kgf (108 N) (for pitch and yaw control) and engines 10 - with a thrust of 2.7 kgf (26.5 N) (for roll control). With manual control the pilot, with the help of throttles, can regulate the thrust of the engines 7 and 8 in a range of 1.8-11 kgf (17.7-108 N) and engines 10 in a range of 0.45-2.7 kgf (4.41-26.5 N).

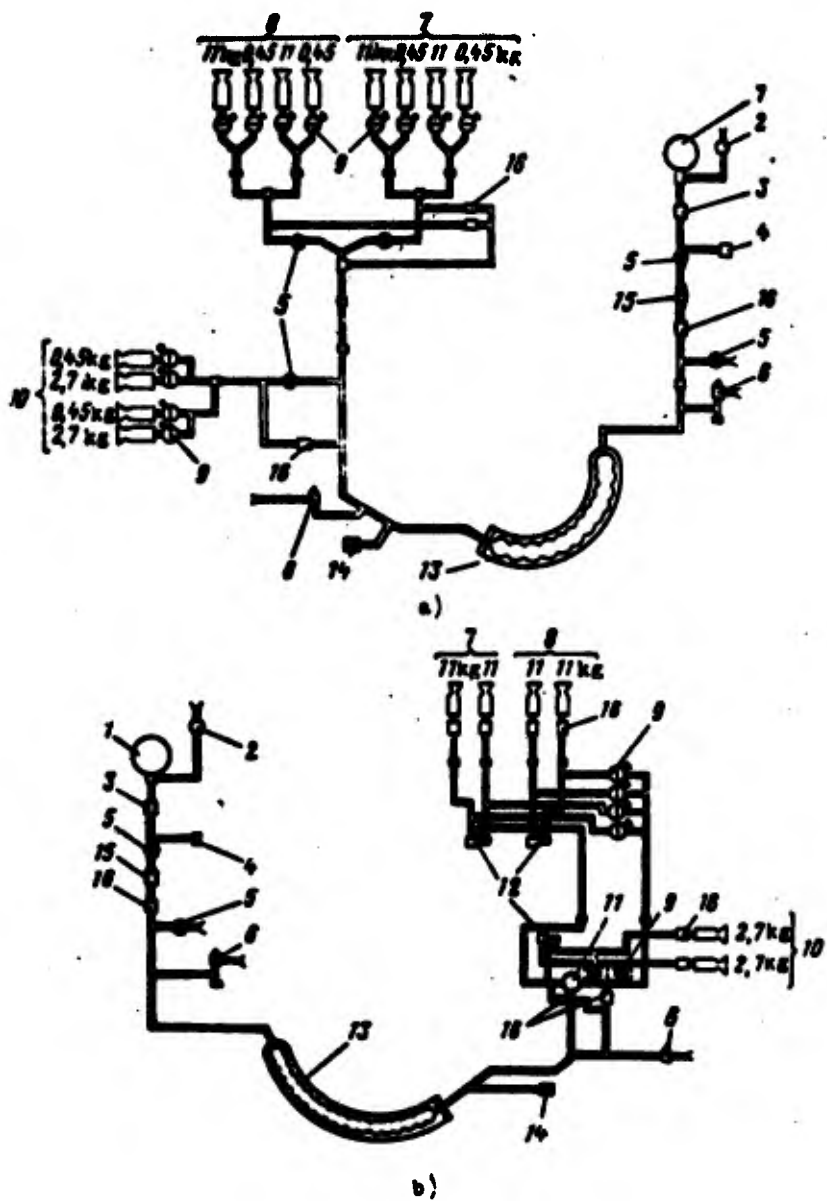


Fig. 9.7. Engines of the orientation system of the piloted satellite "Mercury:" a) with automatic thrust control; b) with automatic and manual thrust control; 1 - cylinder with compressed helium; 2 - valve of servicing the cylinder; 3 - filter; 4 - manometer; 5 - cut-off valves; 6 - safety valves; 7 - engines of pitch control; 8 - engines of yaw control; 9 - electromechanical valves; 10 - engines of roll control; 11 - control valve; 12 - throttles; 13 - tank with hydrogen peroxide; 14 - servicing valve of a tank with hydrogen peroxide; 15 - reduction valve; 16 - check valves.

Propulsion System of the Third Stage with Gas-Pressurized Feed

Figure 9.8 shows a hydropneumatic and constructive diagrams of the propulsion system of the third stage of the rocket "Ofos" [Translator's note: name not verified; could be French] with a gas-pressurized feed system [152]. The displacing of the components is produced by compressed helium, which is stored in a helium pressure accumulator 3. To decrease the reserve of helium the heating of it is produced in a jacket of the combustion chamber (up to 100°K - helium proceeding for the displacement of liquid oxygen, and up to 300°K - helium proceeding for displacement of liquid hydrogen). In the propulsion system an engine with a plate nozzle is used. The time of operation of the engine is up to 400 s.

Basic Data

Fuel.....	fluorine + hydrogen
Thrust in a vacuum.....	3900 kgf (\approx 39,000 N)
Thrust of the control engines in a vacuum.....	2×400 kgf (2×3920 N)
Theoretical specific thrust in a vacuum.....	474 kgf·s/kg (4650 N·s/kg)
Real specific thrust in a vacuum.....	457 kgf·s/kg (448 N·s/kg)
Relationship of the components.....	10
Pressure in the chamber.....	5 kgf/cm ² (0.49 MN/m ²)
Expansion ratio.....	1/800
Volume of fuel tanks.....	6.6 m ³
Volume of helium tank.....	0.03 m ³
Feed pressure in the oxidizer tank.....	7.5 kgf/cm ² (0.73 MN/m ²)
Feed pressure in the fuel tank.....	8.5 kgf/cm ² (0.83 MN/m ²)

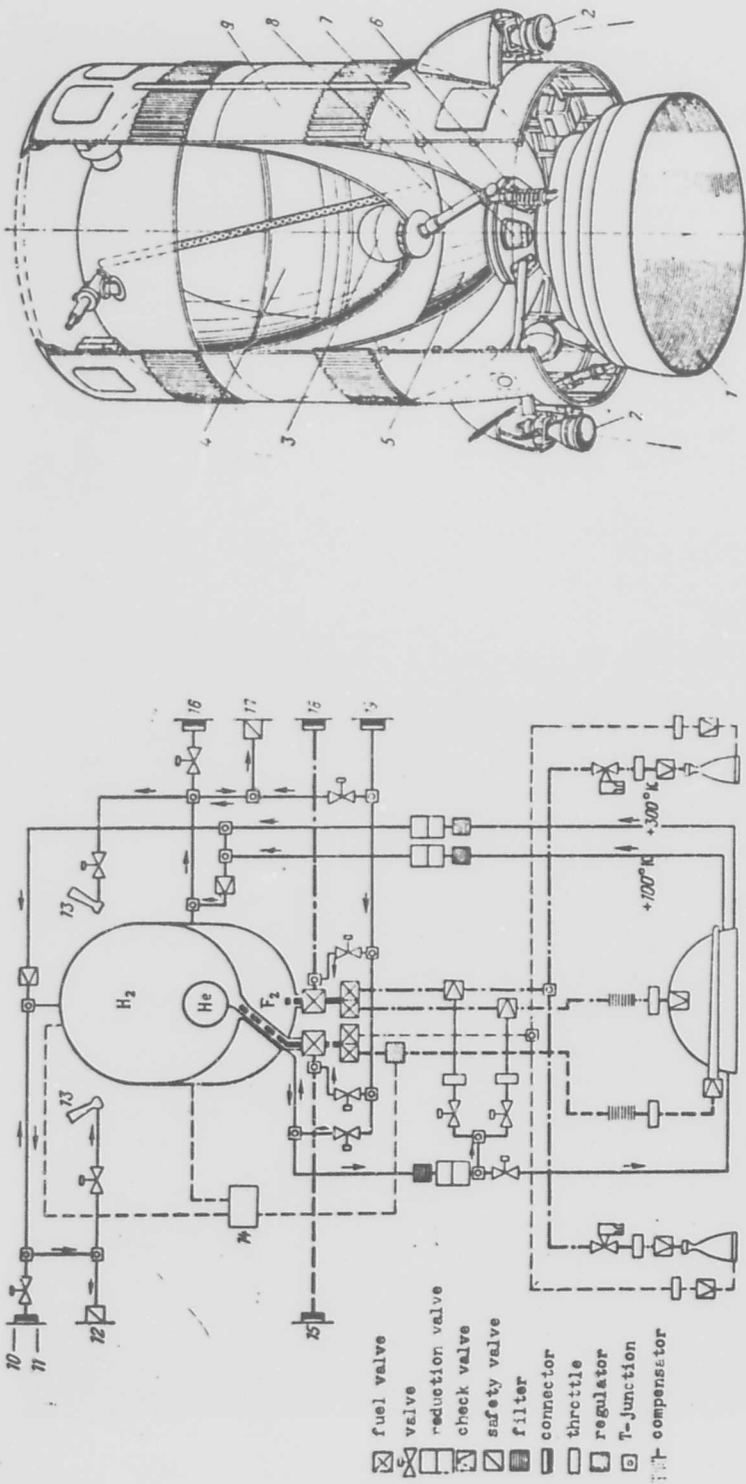


Fig. 9.8. Propulsion system of the third stage of the rocket "Oros": 1 — sustainer liquid-fuel rocket engine; 2 — control liquid-fuel rocket engines; 3 — helium pressure accumulator; 4 — tank with liquid hydrogen; 5 — tank with liquid fluorine; 6 — units of equipment of the control system; 7 — gimbal thrust pad of the sustainer; 8 — hydrogen feed line; 9 — jettisonable housing; 10 — supercharging of H₂; 11 — supercharging of H₂ and He; 12, 13, 14 — safety valves; 15 — venting of H₂; 16 — computing device of the emptying systems; 17 — servicing of H₂; 18 — venting F₂; 19 — servicing of He.

9.3. Reduction Valves of Gas Pressure

Assignment and Classification of Reduction Valves

Pressure reducers serve for lowering the pressure of the gas proceeding from the pressure tanks. In propulsion systems of a liquid-fuel rocket engine pressure reducers are used as reduction feed valves and as reduction valves of pressurization.

Reduction feed valves serve for providing feed of components either directly into the combustion chamber (with a gas-pressurized feed system) or into a gas generator or ZhAD, which, in turn, provide feed of components into the combustion chamber. In this case the reduction valve is one of basic elements of the feed system. The accuracy of the operation of it governs the constancy of the flow rate of components into the chamber of the engine and, consequently, the constancy of operating conditions of the engine chamber. Therefore, the accuracy of operation of these reduction valves have very stringent requirements.

Reduction valves of pressurization serve to provide the pressurization of different elements of the propulsion system and also to feed the units of the control system of the propulsion system. The accuracy of the operation of these reduction valves does not directly affect the operation conditions of the engine chamber, and therefore the accuracy of the operation of these reduction valves have less stringent requirements.

A lowering of the gas pressure in the reduction valve occurs due to the choking (throttling) of the gas during the flow of it from the cavity of high pressure into the cavity of low pressure through a cross section of small area formed by the valve and its seat. The essence of throttling consists in the fact that in the section between the valve and the seat owing to the lowering of the pressure, the gas acquires higher speed, and the energy of the pressure is turned into kinetic energy of the gas. Entering into

the cavity of low pressure, the gas is stagnated; here the kinetic energy of it is lost to friction in numerous addies accompanying the deceleration of the gas. Therefore, with such deceleration of the gas, the pressure of it is not recovered.

For an ideal gas the stagnation temperature all over the flow remains constant, and, consequently, the gas temperature in the cavity of low pressure after deceleration of the gas should be equal to the gas temperature prior to the beginning of throttling. But since the real gas (especially at low temperatures) does not obey the ideal gas laws, then with throttling there occurs a change in temperature. For the majority of gases, including for air and nitrogen, the temperature of the gas drops; and for hydrogen and helium it is increased.

The magnitude of lowering of pressure with throttling is determined by the dimension of the throttling hole between the valve and the seat.

With the operation of the reduction valve, depending on the ratio of outlet pressure p_{out} to the inlet pressure p_{in} two conditions of the flow of gas through the throttling section take place. When

$$\frac{p_{out}}{p_{in}} > \delta_{sp} = \left(\frac{2}{k+1}\right)^{\frac{1}{k-1}}$$

the subcritical outflow of gas takes place. When $\frac{p_{out}}{p_{in}} \leq \delta_{sp}$ there is supercritical gas outflow.

The basic elements of the pressure reducer are:

a) a valve, which provides a change in the throttling section (valve 2 on Fig. 9.9 and 9.10);

b) sensing device loaded on the one hand by the pressure of the reduced gas and on the other hand — by the force of pressure of the spring or controlling gas.

Properties of the reduction valve to a considerable degree are determined by what direction the valve of the reduction valve is opened. According to this criterion the reduction valves are divided into reduction valves of direct and reverse stroke.

In a reduction valve of direct movement (Fig. 9.9a) the valve is opened in the direction of the force appearing owing to the action of the gas of high pressure (along the gas flow).

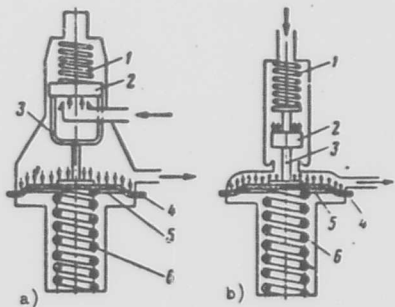


Fig. 9.9. Diagram of reduction valves of direct and reverse movement: a) reduction valve of direct stroke; b) reduction valve of reverse stroke; 1 — closing spring; 2 — valve; 3 — pusher; 4 — membrane; 5 — disk; 6 — main spring.

In the reduction valve of reverse stroke (Fig. 9.9b) the valve is opened opposite the force appearing due to the action of the pressure of high-pressure gas (opposite the flow of the gas).

With respect to the sensing device the reduction valves can be divided into bellows (Fig. 9.10a), membrane (Fig. 9.10b, c and d), plunger or piston (see Fig. 9.13a and b).

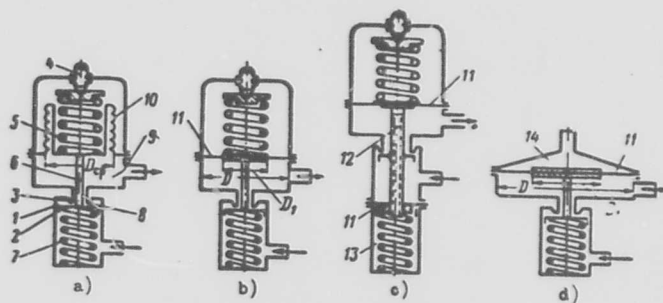


Fig. 9.10. Different diagrams of reduction valves of reverse stroke: 1 — cavity of high pressure; 2 — valve; 3 — valve seat; 4 — regulating screw; 5 — main spring; 6 — rod; 7 — spring; 8 — throttling section; 9 — cavity of low pressure; 10 — bellows; 11 — membrane; 12 — hole (channel); 13 — cavity of low pressure above the valve; 14 — gas cavity of pneumatic drive.

Arrangement and Operation of Reduction Valves

Figure 9.10-9.13 shows diagrams and cross sections of different types of reduction valves.

Reduction valve of reverse stroke. When the reduction valve does not operate, spring 5 (Fig. 9.10a and b, 9.11) is in a free state. The gas of high pressure enters into the cavity of high pressure 1; the force of the pressure of the gas and the force of the action of spring 7 press valve 2 to seat 3, not allowing passage of the gas through the valve. With the compression of the main spring 5 — the reduction valve, by the regulating screw 4 there appears a force which through rod 6 is transmitted to valve 2.

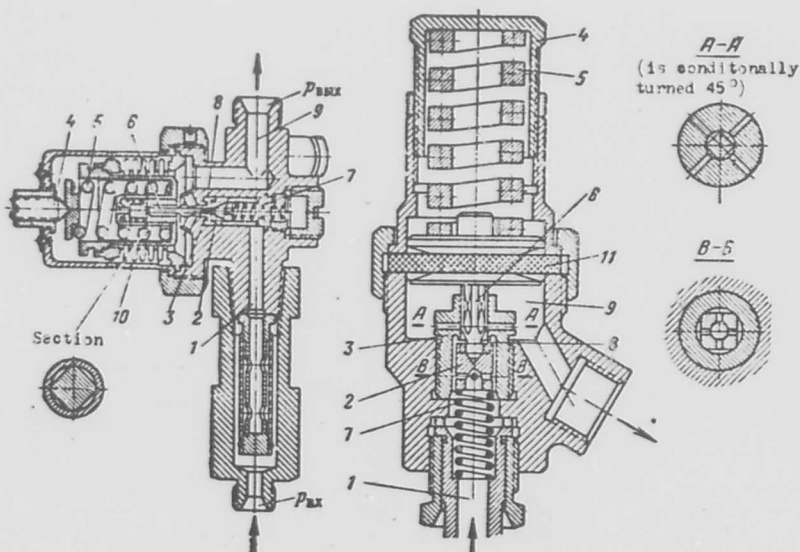


Fig. 9.11. Reduction valves of reverse stroke
(for designations see Fig. 9.10).

The spring is passed down prior to the moment, until the force of pressure of it will become greater than the total force of spring 7, the pressure of the gas in the cavity of high pressure, pressing valve 2 to seat 3, and the pressure of gas in the cavity of low pressure on the working surface F_m (bellows or membrane). Here valve 2 is opened, the gas passes through the throttling section 8, the

pressure of it drops, and the gas enters into the cavity of low pressure 9, whence through the outlet opening it is the direction to the point of destination. The greater the tightening of spring 5, the greater is opened the valve of the reduction valve, the less the gas is throttled, i.e., the greater will be its pressure after the reduction valve.

In the reduction valve shown on Fig. 9.10c and 9.12, the cavity of low pressure 9 by channel 12 in rod 6 is connected with cavity 13, separated from the cavity of high pressure by membrane 11. Thus, forces of pressure of the gas on valve 2 are balanced, i.e., valve 2 of the given reduction valve is completely or partially unloaded from forces of pressure of the gas (completely with the equality of the area of surfaces of membrane 11 and area of surfaces of membrane 11 and area of the valve 2).

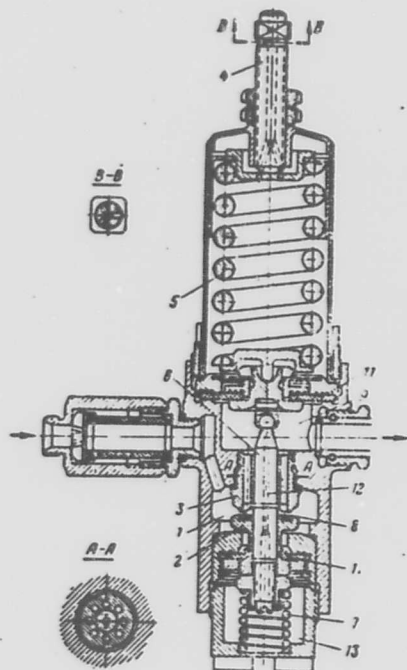


Fig. 9.12. Reduction valve
(see Fig. 9.10 for designations).

The reduction valve not only decreases the gas pressure down to the necessary value, but also is a regulator maintaining the

outlet pressure constant in spite of the fact that the inlet pressure in the reduction valve, i.e., pressure in the cylinder all the time decreases.

Actually, if, for example, the pressure in the cavity of low pressure 9 will increase higher than that assigned, determined by the tightening of the spring 5, then the force acting on the surface F_n becomes so great that it overcomes the force of the spring 5. Then rod 6 together with valve 2 moves upwards, and the cross section is decreased. The entering of the gas into cavity 9 decreases until the pressure in it again becomes equal to that assigned.

If the pressure in cavity 9 becomes lower than that assigned, then the force of pressure on surface F_n acting opposite spring 5 will decrease, and the spring together with rod 6 will move downwards, and together with it valve 2 will move. Due to this the cross section will be increased, the degree of the throttling of the gas will decrease, and the pressure of the gas in cavity 9 is again raised up to that assigned.

Reduction valve of direct stroke. The high-pressure gas enters into cavity (Fig. 9.13). Throttling of the gas occurs in the throttling port 11 between valve 5 and valve seat 4. The gas of lowered pressure enters into the low-pressure cavity 8 and from there goes to the user. In the reduction valve, which operates according to the diagram of Fig. 9.13a, valve 5 is unloaded from a force acting on it on the side of spring 2 and high pressure in cavity 3 by means of the setting of two pistons 6. In cavity 3 and 8 above pistons along channels 10 and 7 there proceeds the gas the pressure of which unloads pistons 6.

In reduction valves operating according to the diagram of Fig. 9.13b, the force acting on valve 5 on the side of spring 2 and pressure of gas in cavity 3 is compensated owing to the pressure on piston 6, which by rod 9 is rigidly joined to valve 5.

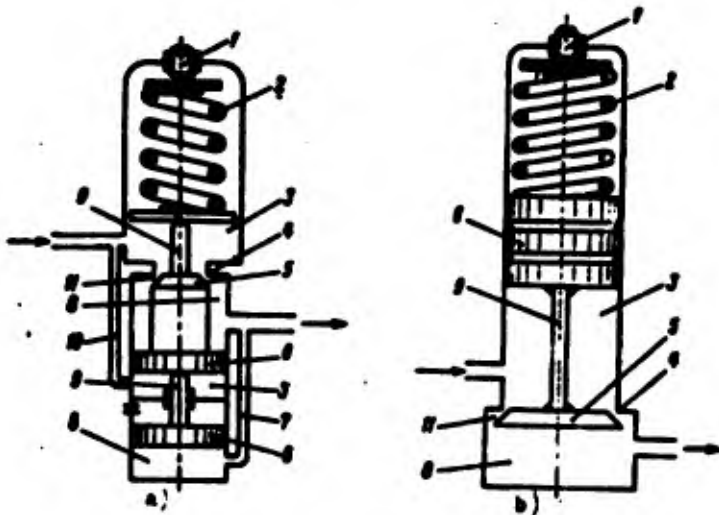


Fig. 9.13. Diagrams of reduction valves of direct stroke: 1 - regulating screw; 2 - main spring; 3 - cavity of high pressure; 4 - valve seat; 5 - valve; 6 - piston (plunger); 7 - channel of low pressure; 8 - low-pressure cavity; 9 - rod; 10 - channel of high pressure; 11 - throttling port.

The distinction of the reduction valve shown on Fig. 9.13a from the reduction valve on Fig. 9.13b is that in the first one cavities of high and low pressure 3 and 8 consist of two parts united, respectively by channels 10 and 7; in the second reduction valve this connection is missing.

The reduction valve of direct stroke operates in the following way. In the case of the excess of pressure in cavity 8 above the assigned and set by means of the appropriate tightening of spring 2 the force on valve 5 acting upwards will increase; here valve 5 is raised and the throttling port will decrease, which will cause a lowering of the outlet pressure up to a given value. In the case of lowering of pressure in cavity 8, valve 5 will be lowered, the throttling port 11 will be increased, and the pressure again will be increased, and the pressure again will be increased to that assigned.

9.4. Characteristics of Reduction Valves

As was shown above, the pressure reducer of gas with its correct arrangement is the regulator of gas pressure at the outlet. But, just as the majority of the regulators, it operates with a certain irregularity, i.e., with a change in inlet pressure into the reduction valve the pressure at the outlet of it changes.

The dependence of outlet pressure p_{out} on inlet pressure into the reduction valve p_{in} is called the characteristic of the reduction valve.

The dependence of outlet pressure from the reduction valve on the inlet pressure in the absence of the flow rate of gas is called the limiting characteristic.¹

Characteristics of a Reduction Valve of Reverse Stroke

In order to determine characteristics of the reduction valve, i.e., to find the dependence of p_{out} on p_{in} , let us formulate the equation of equilibrium of mobile parts of the reduction valve with an open valve (see Fig. 9.10 and 9.11). Forces acting downwards will be considered positive and forces upwards — negative.

With the operation of the reduction valve downwards there acts only the force of spring 5

$$P_{out} = (Q_2 - k_2 h),$$

where Q_2 — force of pressure of spring 5 with a closed valve of the reduction valve in kgf; k_2 — rigidity of spring 5 in kgf/cm (49 N/cm); h — rise of the valve in cm.

The following forces act upwards:

1. The force appearing from the difference in pressure on valve 2:

$$-(P_{\text{hi}} - P_{\text{reduced}}) f_{\text{sw}}$$

where f_{sw} — area of surface of the valve on which acts the force of the difference in pressure of the high-pressure gas and the reduced gas. For the diagram of Fig. 9.14a

$$f_{\text{sw}} = \frac{\pi d_{\text{sw}}^2}{4},$$

where $d_{\text{sw}} = d_{\text{hi}} + \delta$; for the diagram of Fig. 9.14b

$$f_{\text{sw}} = \frac{\pi d_{\text{sp}}^2}{4}; d_{\text{sw}} = d_{\text{sp}}.$$

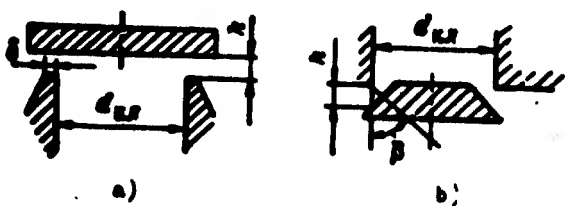


Fig. 9.14. Determination of f_{sw} and f_{sp} .

2. Force of pressure on valve 2 of spring 7 (see Fig. 9.10)

$$-(Q_1 + k_1 h),$$

where Q_1 — force of pressure of spring 7 with a closed valve (force of preliminary tightening) in kgf; k_1 — rigidity of spring 7.

3. Force of pressure of gas in the cavity of low pressure on the membrane or bellows

$$-P_{\text{low}} F_{\text{m}},$$

where F_{m} — surface area of the membrane or bellows.

4. Force acting upwards due to the rigidity of the membrane:

$$-k_m h,$$

where k_m — rigidity of the membrane in kgf/cm.

This force is considered in the installation of rigid metallic membranes. In the case of the installation of "soft" rubber or

plastic membranes, it is more convenient to consider their rigidity by the introduction instead of F the given area of the membrane:

$$F_{\text{spec}} = F_a A_m$$

where a — coefficient considering the rigidity of the membrane (see section 9.5).

With equilibrium of the reduction valve the sum of all these forces is equal to zero, i.e., the equation of equilibrium of the mobile parts of the reduction valve will have the form

$$(Q_2 - k_2 h) - (P_{\text{out}} - P_m) f_m - \\ - (Q_1 + k_1 h) - k_1 h - P_{\text{out}} F_o = 0. \quad (9.22)$$

Denoting

$$k = k_1 + k_2 + k_m \quad (9.23)$$

we will obtain

$$P_{\text{out}} = \frac{1}{F_o - f_m} [(Q_2 - Q_1) - P_m f_m - kh]. \quad (9.24)$$

The magnitude of the rise in valve h is connected with the flow rate of gas flowing through the throttling section of the reduction valve.

The area of the throttling section is equal to

$$f_{\text{spec}} = \pi d_{\text{sp}} h_x \quad (9.25)$$

where h_x is determined depending upon the design of the valve. With the diagram of the valve shown on Fig. 9.14a, $h_x = h$; with the diagram of Fig. 9.14b

$$h_x = h \cos \beta.$$

Subsequently, for simplicity of analysis we will examine the valve of the diagram shown on Fig. 9.14a. In the case of a valve made according to diagram 9.14b, the order of the account does not change.

The flow rate of gas through the reduction valve is equal to

$$G = \mu \rho_{out} f_{spec} v_{out} \quad (9.26)$$

where v_{out} and ρ_{out} - exit velocity and density of gas at the outlet of the throttling section, respectively; μ - discharge (flow) coefficient.

Substituting into expression 9.26 values well-known from gas dynamics $v_{out} = V_{out} \left(\frac{P_{out}}{P_{in}} \right)^{\frac{1}{k}}$, after simple transformations we will obtain the following equations, which determine the flow rate of gas.

With subcritical flow

$$G = \mu \pi d_{sp} A \sqrt{2g \frac{k}{k-1} \frac{P_{in}}{v_{in}} \left[\left(\frac{P_{out}}{P_{in}} \right)^{\frac{1}{k}} - \left(\frac{P_{out}}{P_{in}} \right)^{\frac{k+1}{k}} \right]} \quad (9.27)$$

According to the equation of state the specific volume

$$v_{in} = \frac{RT_{in}}{P_{in}}$$

Substituting into equation (9.27) the expression for specific volume, we will obtain

$$G = \mu \pi d_{sp} A \sqrt{\frac{P_{in}}{RT_{in}}} \sqrt{2g \frac{k}{k-1} \left[\left(\frac{P_{out}}{P_{in}} \right)^{\frac{1}{k}} - \left(\frac{P_{out}}{P_{in}} \right)^{\frac{k+1}{k}} \right]} \quad (9.28)$$

Introducing the notation

$$A_s = \sqrt{2g \frac{k}{k-1} \left[\left(\frac{P_{out}}{P_{in}} \right)^{\frac{1}{k}} - \left(\frac{P_{out}}{P_{in}} \right)^{\frac{k+1}{k}} \right]} \quad (9.29)$$

we obtain

$$0 = \rho d_{sp} k \sqrt{\frac{A_0}{A_k}} - A_k. \quad (9.30)$$

Values of quantity A_k depending upon $\frac{d_{sp}}{A_k}$ when $k = 1.4$ are shown in Fig. 9.15.

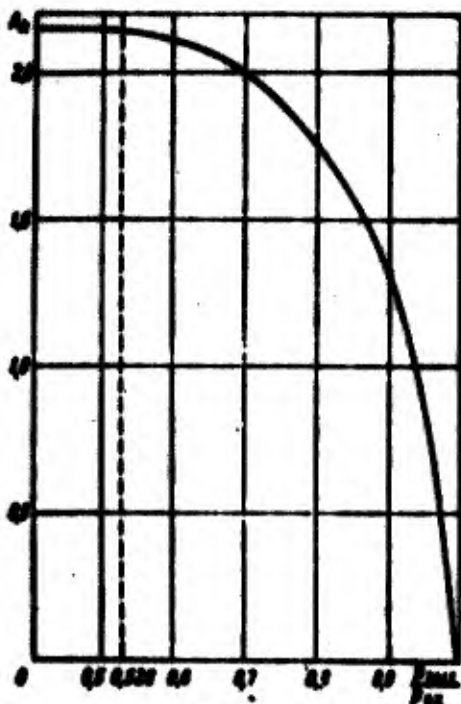


Fig. 9.15. Dependence $A_k = f(\frac{d_{sp}}{A_k})$.

Expression (9.30) can be rewritten in the form of

$$0 = A d_{sp} k \sqrt{\frac{A_0}{A_k}} - A_k. \quad (9.31)$$

where

$$A = \rho \pi A_0. \quad (9.32)$$

Hence

$$k = \frac{0}{A d_{sp} \sqrt{\frac{A_0}{A_k}}} \quad (9.33)$$

With supercritical flow

$$Q = \rho A d_{sp} h \frac{P_1}{\sqrt{RT_{in}}} \times \sqrt{2g \frac{k}{k+1} \left(\frac{2}{k+1}\right)^{\frac{1}{k-1}}}. \quad (9.34)$$

or

$$Q = Ad_{sp} \frac{P_1}{\sqrt{RT_{in}}} h. \quad (9.35)$$

where

$$A = \pi A_s.$$

Here

$$A_s = \sqrt{2g \frac{k}{k+1} \left(\frac{2}{k+1}\right)^{\frac{1}{k-1}}}. \quad (9.36)$$

whence

$$h = \frac{Q}{Ad_{sp} \frac{P_1}{\sqrt{RT_{in}}}}. \quad (9.37)$$

Thus, under any conditions of the outflow of gas through the valve (subcritical or supercritical) movement of the valve is determined by formula

$$h = \frac{Q}{Ad_{sp} \frac{P_1}{\sqrt{RT_{in}}}}. \quad (9.38)$$

With this, however, quantity A_k for the subcritical flow of gas is determined by formula (9.29); with supercritical flow A_k the quantity is constant and is determined by formula (9.36).

Substituting the obtained expression (9.38), which determines h , into equation (9.24), we will obtain the equation of the characteristic of the reduction valve:

$$P_{\text{out}} = \frac{1}{F_n - f_{\text{loss}}} \left(Q_2 - Q_1 - P_{\text{out}} f_{\text{out}} - k \frac{G}{M_n \sqrt{P_{\text{out}}}} \right). \quad (9.39)$$

With the flow of gas through the reduction valve $G \rightarrow 0$, we will obtain the equation of the limiting characteristic:

$$P_{\text{out}} = \frac{1}{F_n - f_{\text{loss}}} (Q_2 - Q_1 - P_{\text{out}} f_{\text{out}}), \quad (9.40)$$

or

$$P_{\text{out}} = \frac{Q_2 - Q_1}{F_n - f_{\text{loss}}} - \frac{P_{\text{out}} f_{\text{out}}}{F_n - f_{\text{loss}}}, \quad (9.41)$$

i.e., the equation of a straight line. The flow of the characteristic is shown on Fig. 9.16. We see that when $G \rightarrow 0$ with a decrease in inlet pressure the outlet pressure somewhat increases. Such a form of limiting characteristic is typical for reduction valves of reverse stroke, and, as we will see further, very frequently takes place in reduction valves of direct stroke.

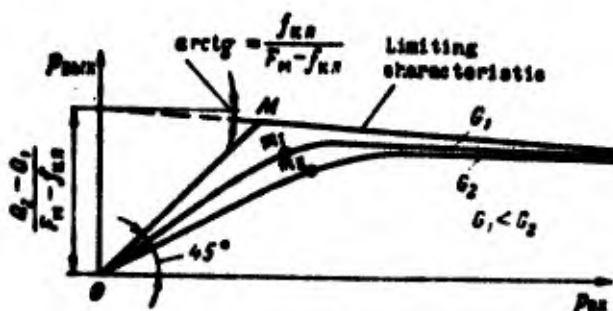


Fig. 9.16. Characteristics of a reduction valve.

It is obvious that the limiting characteristic obtained from expression (9.41) has meaning only up to point M, since from equality (9.41) it follows that the left of M the outlet pressure P_{out} becomes greater than the inlet pressure P_{in} , which is impossible.

Thus, in the case $G \rightarrow 0$ (infinitesimal flow) when $P_{\text{in}} < P_{\text{out}}$, the reduction valve is no longer the regulating element. The valve of the reduction valve is open completely prior to M , and through it there occurs a pressure drop of gas from the cylinder. Since with an infinitesimal flow rate the losses to drag are equal to zero,

then on section OM $p_{\text{max}} = p_{\text{ex}}$, i.e., the limiting characteristic will proceed into the origin of coordinates at an angle of 45° .

Let us examine what form the characteristic of the reduction valve will have at a certain finite flow rate of gas. As can be seen from equation (9.39), with the flow of gas the flow of the characteristic is still affected by a third member of the equation, where the influence of it on the change in p_{max} is opposite to the influence of the second member. With a decrease in $A \frac{p_{\text{ex}}}{\sqrt{RT_m}}$ the influence of the third member is increased, and the characteristic all the more departs from the limiting characteristic.

Thus, just as the limiting characteristic, the characteristic of the reduction valve with the flow of gas obeys equation (9.39) only up to a definite inlet pressure p_{ex} somewhat higher than p_{max} . As can be seen from equations (9.38) and (9.29), at values of p_{ex} close to p_{max} , in connection with the sharp decrease in A for the preservation of the assigned flow G it is necessary to provide great f_{exp} , i.e., large h. The biggest expedient rise of value $h = h_{\text{max}}$ is determined by the condition that there is no meaning in making the area f_{exp} larger than the area of the cross section of value f_{ex} . Consequently, after the opening of the valve prior to h_{max} the reduction valve ceases to be a regulating element (point m on the characteristic). With this in the case of the further gas feed through the reduction valve, the valve of the reduction valve is opened completely and with a decrease in p_{ex} , there is a receptive decrease in p_{max} and flow of gas G. The characteristic of the reduction valve from point m is already the characteristic with variable flow and proceeds into the origin of the coordinates.

Let us determine the magnitude of the biggest expedient rise of the valve h_{max} for the simplest the diagram shown on Fig. 9.14a. Since

$$\begin{aligned} f_{\text{spec}_{\text{max}}} &= f_{\text{ex}} \\ 2d_{\text{cp}}h_{\text{max}} &= \frac{\pi d_{\text{ex}}^2}{4}. \end{aligned} \quad (9.42)$$

Assuming

$$d_{us} \approx d_{sp}$$

we obtain

$$h_{max} = \frac{d_{us}}{4}. \quad (9.43)$$

Similarly, it is possible to obtain magnitude h_{max} for other diagrams of valves.

Substituting h_{max} into expression (9.38), we obtain the expression for the determination of p_{min} , prior to which equation (9.39) is correct.

$$h_{min} = \frac{a}{M_{sp} \frac{p_{min}}{\sqrt{RT_{us}}}}. \quad (9.44)$$

The greater the flow of gas through the reduction valve, the greater (other things being equal) the influence of the third member on the characteristic.

Characteristics of the reduction valve with different flow rates G are as if inscribed into the characteristic when $G \rightarrow 0$. Thus, the meaning of the characteristic when $G \rightarrow 0$ is the fact that it is the limiting characteristic of the family of characteristics of the reduction valve with different flow rates.

Characteristics of a Reduction Valve of Direct Stroke

The equation of equilibrium of mobile parts of a reduction valve (see Fig. 9.13b) is formulated analogous to equation (9.22) and has the form

$$Q - M + A_m (U_m - f_m) - f_m p_{max} = 0. \quad (9.45)$$

where f_m — surface area of the piston (plunger). (A similar equation would be obtained for a reduction valve operating according to the

diagram of Fig. 9.13a).

After simple transformations, taking into account equation (9.38) we obtain the equation of the characteristic

$$P_{\text{ex}} = \frac{1}{f_{\text{ex}}} \left[Q - P_{\text{ex}}(f_{\text{e}} - f_{\text{ex}}) - k \frac{a}{A_{\text{e}} c_p \sqrt{\frac{P_{\text{ex}}}{R T_{\text{ex}}}}} \right]. \quad (9.46)$$

From a comparison of the obtained equation with equation (9.39), it is clear that their structure is identical; however, at the second member of the equation there appeared the factor $(f_{\text{e}} - f_{\text{ex}})$.

Varying the value of the difference in areas of the piston and valve $(f_{\text{e}} - f_{\text{ex}})$, we can ensure the obtaining of the characteristic which approaches most to the desirable one.

Let us examine the flow of limiting characteristic (Fig. 9.17). We obtain the equation of the limiting characteristic from expression (9.46) when $G \rightarrow 0$:

$$P_{\text{ex}} = \frac{1}{f_{\text{ex}}} [Q - P_{\text{ex}}(f_{\text{e}} - f_{\text{ex}})]. \quad (9.47)$$

Depending upon quantity $f_{\text{e}} - f_{\text{ex}}$, the limiting characteristic will have a different slope.

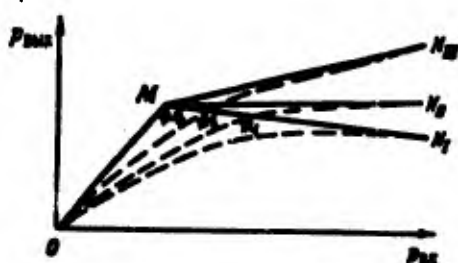


Fig. 9.17. Influence of the difference in areas $(f_{\text{e}} - f_{\text{ex}})$ on the characteristic.

When $f_{\text{e}} > f_{\text{ex}}$ the limiting characteristic will pass along OMN_1 . When $f_{\text{e}} = f_{\text{ex}}$ the second member is equal to zero, and the limiting characteristic on section MN_2 will pass in parallel to the axis of the abscissas. When $f_{\text{e}} < f_{\text{ex}}$ the sign of the influence of the second member will be changed, and the limiting characteristic will pass along OMN_3 . It is obvious that with limiting characteristics OMN_3

and OMN_u the characteristic with any flow rate G will have the incident form $Om_{in}N_m$ or Om_uN_u (i.e. with a decrease in P_{in} the pressure P_{out} also decreases). A greater possibility of the use of gas in a high-pressure cylinder is given by the characteristic of the form Om_iN_i , i.e., it is profitable for us to leave a certain positive difference of the areas ($f_u - f_{in}$).

The characteristic of the reduction valve (9.46), just as the characteristic proceeding from equation (9.39), follows the equation only up to a definite value of P_{out} , corresponding to the full opening of the throttling section. With a further supply of gas we will obtain a characteristic with variable flow (section mO).

Balancing of Reduction Valves

In the example examined above the presence of the piston rigidly joined with the valve as if unloaded the valve from the influence of forces of inlet pressure. Such reduction valves are called balanced.

The analysis conducted above of the reduction valve of direct stroke, operating according to the diagram of Fig. 9.13b shows that balancing improves the flow of the characteristics of the reduction valve. When $f_u = f_{in}$ we have full balancing, however, for the best flow of the characteristic it is advantageous for us to leave a certain instability of the valve. Balancing is used in reduction valves of reverse stroke. An example of a balanced reduction valve of reverse stroke operating according to the diagram of Fig. 9.10c is shown on Fig. 9.12. Balancing of the valve is achieved by the installation of an additional membrane 11 with area f_u and by the connection with the help of channel 12 of the cavity of low pressure with cavity 13. The equation of the characteristic of such a reduction valve has the form

$$P_{out} = \frac{1}{f_u - (f_u - f_{in})} \left[Q_2 - Q_1 - P_{in} (f_{in} - f_u) - k \frac{a}{A \sqrt{\frac{P_{in}}{P_{out}}}} \right]. \quad (9.48)$$

where Q_2 and Q_1 – tightening of the main spring 5 and the spring of valve 7; k – total rigidity of the springs and membranes.

By varying the difference in areas ($I_m - I_n$), we can provide the desirable flow of the limiting and basic characteristics similar to the example examined on Fig. 9.17.

Use of the Gas Reserve in a Cylinder

No matter how successful a reduction valve is designed, it is impossible to obtain such a characteristic of its operation, in which the outlet pressure would remain constant (within the accuracy of operation of the reduction valve) up to the equality pressures at the inlet and outlet.

Always at any $p_{m \min} > p_{m \max}$ the pressure $p_{m \max}$ starts to decrease. Thus, we cannot use the whole reserve of gas in the cylinder. The quantity of underused reserve of gas is determined by the quantity

$$\Delta p_{res} = p_{m \min} - p_{m \max}. \quad (9.49)$$

Quantity Δp_{res} can be determined from the graph of the characteristic of the reduction valve (Fig. 9.18). The less the quantity Δp_{res} , the better the use of the gas reserve from the cylinder.

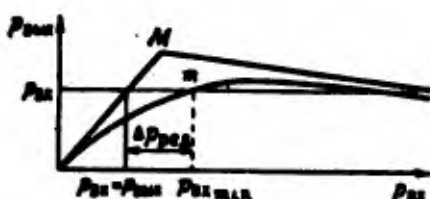


Fig. 9.18. Determination of Δp_{res} .

The ideal characteristic of any reduction valve would be the characteristic on which at the assigned constant flow rate G , independently of the change in inlet pressure P_m there would be ensured a constant outlet pressure $P_{m \max}$. Above it was shown that the flow of the characteristic is influenced by the second and third members of the equation of the characteristic (9.39) or (9.46).

Since with a change in P_{in} these members are changed according to various laws, obviously, it is impossible to obtain a characteristic with constant P_{out} (ideal characteristic), and therefore the problem is to obtain a characteristic as close as possible to the ideal. For this the design elements of the reduction valve (membrane, spring, piston, dimensions of the valves, etc.) must be selected in such a manner so that the change in elastic forces of the action of the springs and membrane (last member of the equation) in the very best manner would compensate the influence of forces of pressure.

Let us examine how the different parameters of operation of the reduction valve influences its characteristic.

Influence of the Change in Inlet Pressure P_{in} on the Change in P_{out}

Let us examine, first, how the change in inlet pressure P_{in} influences the amount of deviation ΔP_{out} from the assigned nominal value P_{out0} , i.e., the quantity

$$\Delta P_{out} = P_{out} - P_{out0}. \quad (9.50)$$

It is obvious that quantity ΔP_{out} determines the quality of our characteristic. The most desirable is the characteristic for which ΔP_{out} is equal to or close to zero.

For this let us write the equation of the characteristic for any fixed value of inlet pressure P_{in0} , at which the outlet pressure is equal to P_{out0} . (Subsequently, for concreteness, we will examine the equation of the characteristic (9.39) as more the general one, although the whole analysis, of course, is correct for the characteristic of any reduction valve).

$$P_{out0} = \frac{1}{f_{in} - f_{out}} \left(Q_2 - Q_1 - P_{in0} f_{in0} - k \frac{\alpha}{A_{out0} \sqrt{R T_{out0}}} \right). \quad (9.51)$$

To determine Δp_{aux} we will subtract term by term equation (9.51) from equation (9.39), and then

$$\Delta p_{\text{aux}} = \frac{1}{F_u - f_{u2}} \left[(p_{u2} - p_u) f_{u2} - \frac{M}{d_{cp}} \left(\frac{1}{A} \frac{f_{u2}}{\sqrt{Kf_{u2}}} - A_0 \frac{f_{u2}}{\sqrt{Kf_{u2}}} \right) \right] \quad (9.52)$$

or

$$\Delta p_{\text{aux}} = \Delta p_{\text{aux}1} - \Delta p_{\text{aux}2}, \quad (9.53)$$

where

$$\Delta p_{\text{aux}1} = \frac{(p_{u2} - p_u) f_{u2}}{F_u - f_{u2}}; \quad (9.54)$$

$$\Delta p_{\text{aux}2} = \frac{M}{d_{cp}} \left(\frac{1}{A} \frac{f_{u2}}{\sqrt{Kf_{u2}}} - A_0 \frac{f_{u2}}{\sqrt{Kf_{u2}}} \right). \quad (9.55)$$

Let us examine the change in Δp_{aux} with a change in p_{u2} .

1. The influence of the change in p_{u2} on $\Delta p_{\text{aux}1}$.

Equation (9.54) is an equation of a straight line. When

$$p_u = p_{u2} \quad \Delta p_{\text{aux}1} = 0;$$

when $p_{u2} = p_{u2 \text{ min}}$

$$\Delta p_{\text{aux}1} = \frac{p_{u2} - p_{u2 \text{ min}}}{F_u - f_{u2}} f_{u2}.$$

The dependence $\Delta p_{\text{aux}1} = f(p_{u2})$ is shown on Fig. 9.19 by the straight line anb.

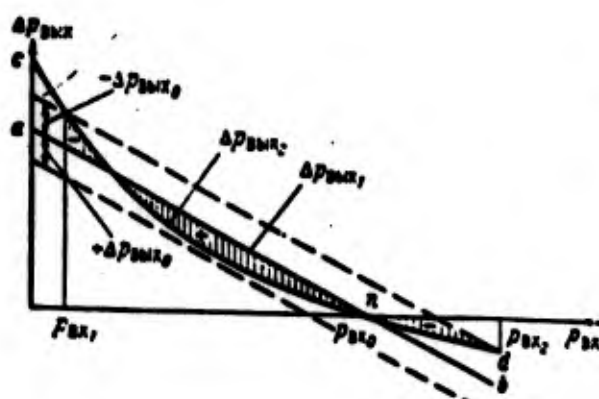


Fig. 9.19. Influence of the change in p_{u2} on Δp_{aux} .

2. The influence of the change in P_{in} on Δp_{out} .

When $P_{in} = P_{in0}$

$$\Delta p_{out} = 0;$$

when $P_{in} = P_{in\max}$

$$\Delta p_{out} = \frac{M}{d_{eq}} \left(\frac{1}{A \sqrt{\frac{P_{in0}}{RT_{in0}}}} - \frac{1}{A_0 \sqrt{\frac{P_{in0}}{RT_{in0}}}} \right);$$

when $P_{in} \rightarrow \infty$

$$\Delta p_{out} \rightarrow \frac{M}{d_{eq}} \frac{1}{A_0 \sqrt{\frac{P_{in0}}{RT_{in0}}}}.$$

The dependence $\Delta p_{out} = f(P_{in})$ is shown on Fig. 9.19 by the curve *end*. Since in equation (9.53) signs of the influence of Δp_{in1} and Δp_{in2} on quantity Δp_{out} are opposite, then it is obvious that the shaded region between lines *end* and *anb* is in the corresponding scale the diagram of the change in $\Delta p_{out} = \Delta p_{out1} - \Delta p_{out2}$. The outlet pressure from the reduction valve P_{out} is assigned with a definite allowance Δp_{out0} for the deviation from that assigned:

$$P_{out} = P_{out0} \pm \Delta p_{out0}. \quad (9.56)$$

Quantity Δp_{out0} is determined by the assigned requirements for operation of the reduction valve. The given magnitude of the allowance for the deviation of P_{out} from P_{out0} for the given reduction valve determines the largest P_{in1} and least P_{in2} of inlet pressure at which the operation of the reduction valve satisfies the presented requirements. For the reduction valve of direct stroke, which operates according to the diagram of Fig. 9.13.

$$\Delta p_{out} = \frac{1}{f_{in}} \left[(P_{in0} - P_{in}) (f_n - f_m) - \frac{M}{d_{eq}} \left(\frac{1}{A \sqrt{\frac{P_{in}}{RT_{in}}}} - \frac{1}{A_0 \sqrt{\frac{P_{in0}}{RT_{in0}}}} \right) \right]. \quad (9.57)$$

An analysis of this equation, similar to the aforementioned analysis of equation (9.54), shows that in this case the influence of p_{ex} on Δp_{out} is expressed by the graph of Fig. 9.19, only in a different scale.

Influence of the Surface Area of the Sensing Device (Membrane, Bellows, Plunger)

For a reduction valve operating according to the diagram of Fig. 9.10, this influence is obvious: the greater the quantity F_w , other things being equal, the less the values of quantity Δp_{out} (9.52). Thus, an increase in F_w increases the accuracy of operation of the reduction valve or at the assigned accuracy increases the permissible range of pressures of gas ($p_{\text{ex}} - p_{\text{out}}$), at which the reduction valve provides the assigned outlet pressure, i.e., improves the use of the reserve of gas in the cylinder. For reduction valves operating according to the diagram of Fig. 9.13, the influence of the area of the piston or plunger is expressed in the difference $(f_w - f_{w0})$ in equation (9.57).

Influence of Dimensions of the Valve of the Reduction Valve

For reduction valves operating according to the diagram of Fig. 9.10, the influence of the change in f_{w0} on quantity $(F_w - f_{w0})$ in equation 9.52 can be disregarded, since for such diagrams $f_{w0} \ll F_w$. The influence of dimensions of the valve on Δp_{out} (or p_{out}) is reflected through the influence of f_{w0} on Δp_{out} , and d_{ep} on Δp_{out} ; (9.54) and (9.55). With an increase in f_{w0} the change in $\Delta p_{\text{out}} = f(f_{w0})$ will pass more steeply along straight line a'nb' (Fig. 9.20). With an increase in d_{ep} the change in Δp_{out} will pass along curve c'nd'.

Values $\Delta p_{\text{out}} = \Delta p_{\text{out}} - \Delta p_{\text{out}}$: with an increase in d_{w0} (or d_{ep}) were increased, i.e., the value of the greatest deviation of outlet pressure from the nominal value p_{out} was increased: the accuracy of the operation of the reduction valve worsened. Consequently, in a reduction valve of reverse stroke a decrease in dimensions of the valve increases the accuracy of its operation.

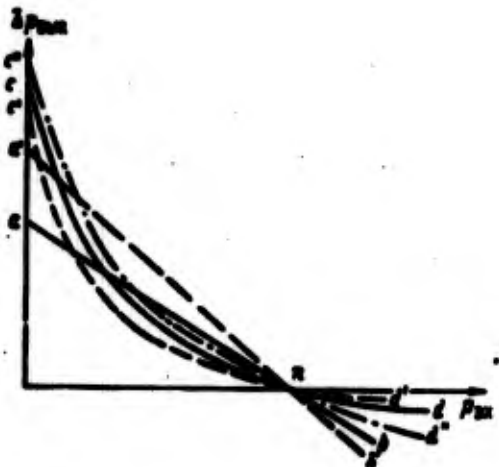


Fig. 9.20. Influence of dimensions of the valve of a reduction valve and rigidity of springs and membranes on Δp_{\max} .

For reduction valves operating according to the diagram of Fig. 9.13, the influence of the change in dimensions of the valve is reflected by the factor $1/l_{ns}$ in equation (9.57) and by the influence of d_{op} in the second member of equation (9.57). The change in l_{ns} in the first member of equation (9.57) does not affect Δp_{\max} , since with a change in l_{ns} for the improvement of the characteristic it is necessary to change l accordingly. The main influence of dimensions of the valve on Δp_{\max} is produced by the factor $1/l_{ns}$: the greater l_{ns} , the less Δp_{\max} . Consequently, the accuracy of the operation of reduction valves operating according to the diagram of Fig. 9.13 increases with an increase in dimensions of the valve.

Influence of the Rigidity of Springs and the Membrane

The influence of rigidity on Δp_{\max} is reflected by the second member of equation (9.52) or (9.57). With an increase in k the change in Δp_{\max} will pass along curve c"nd". Here, as one can see from Fig. 9.20, the magnitude of the greatest positive deflection $+\Delta p_{\max}$ will decrease.

9.5. Design of Reducing Valve

The main requirement of a reducing valve is that pressure of gas as it leaves the valve will remain within assigned constant limits and will not depend on inlet pressure. Therefore, the design

of such a valve consists in selecting those dimensions of structural elements which will best provide mutual compensation of the influence of second and third members of the equation of the characteristic of the valve. In certain pneumatic hydraulic systems these valves have a further requirement of airtightness of the throttling section shutoff.

When designing a reducing valve it is necessary to determine or to select the following values:

- a) dimensions of throttling section and valve of the reducer;
- b) necessary force of springs and their rigidity;
- c) dimensions of diaphragm or bellows, plunger, piston and their rigidity or given surface.

If a valve is balanced, it is necessary to determine the degree of instability as the difference of areas $(f_s - f_{ss})$ or $(f_{ss} - f_u)$.

Design of the valve is carried out in the following order:

1. We determine dimensions of the throttling section and valve.
2. We determine the compression force of springs of the reducing valve and dimensions of the diaphragm, bellows or plunger.
3. Knowing the force of springs and dimensions of diaphragms, we determine dimensions of springs and rigidity of springs and diaphragms.
4. From the equation of the characteristic we check whether the reducing valve satisfies assigned work conditions.

Dimensions of Throttling Section and Valve

The design conditions for determination of dimensions of the throttling section will be those conditions for which the dimensions of the throttling section, the opened valve, should be the greatest.

Such conditions are met upon termination of work of the reducing valve. At this instant the pressure of gas entering the reducing valve p_{min} will be least during the whole period of work of the valve, but its specific volume will be the greatest. Speed of flow of gas through the throttling section in this period will be least, since the pressure drop will be least. Here, pressure of gas on the entrance section according to expression (9.49) will be

$$p_{\text{min}} = p_{\text{out}} + \Delta p_{\text{per}}$$

Value Δp_{per} , the value of which is unknown, must be assigned.

At high pressures on the outlet (for example, during pressurized feed)

$$\Delta p_{\text{per}} = (0.25 - 0.5) p_{\text{out}}$$

At low p_{out} (for example, during pressurization of tanks)

$$\Delta p_{\text{per}} = (2 - 10) p_{\text{out}}$$

Area of the throttling section is determined by equation (9.25) (when $k_s = k$):

$$f_{\text{spec}} = \pi d_{\text{ep}} h$$

Substituting h from (9.33), taking equality (9.32) into account we obtain the calculation formula:

$$f_{\text{spec}} = \frac{Q}{\rho A_0 \sqrt{\frac{p_{\text{out}} \cdot p_{\text{min}}}{p_{\text{out}} + p_{\text{min}}}}} \quad (9.58)$$

where A_0 is determined depending on the value of ratio $p_{\text{out}}/p_{\text{min}}$ by formula (9.29) or (9.36) or from graphs of Fig. 9.15.

Discharge coefficient must be assigned:

$$\mu = 0.65 - 0.8.$$

If gas passes through the reducing valve for displacement of components from tanks and we know the free volume of tanks V_{ext} , pressure and temperature in the tanks P_0 and T_0 , then obviously,

$$G = V_{\text{ext}} \frac{P_0}{RT_0} \quad (9.59)$$

and then

$$f_{\text{spec}} = \frac{V_{\text{ext}} P_0}{RT_0 A_0 \sqrt{\frac{P_0}{P_{\text{ext}}}}} \quad (9.60)$$

Knowing value f_{spec} , we determine d_{min} and h . In accordance with the influence of valve area on ΔP_{max} , examined above, for reducing valves working according to Fig. 9.10, d_{min} is selected as small as possible (3-8 mm); for reducing valves represented by Fig. 9.12 value d_{min} is selected larger (15-40 mm). Width of the valve seat $h = 0.3-0.5$ mm.

Determination of Force of Springs of Reducing Valve, Dimensions and Rigidity of Springs and Sensing Devices

The compression force of a valve spring (if the valve has one) is either assigned within limits of 2-15 kgf or is calculated from the condition of maintaining airtightness of the valve. Moreover, the valve must be pressed to the seat with a force for which the specific pressure of the valve on the surface of the seat will be greater or equal to specific pressure of airtightness q_{mpn} , guaranteeing the required compactness of valve shutting. Value q_{mpn} is determined by the material of the valve and packing, and also the difference in pressures before and after the valve at which airtightness must be ensured.

Figure 9.21 gives the necessary specific pressures of airtightness for various materials of the valve and packing.

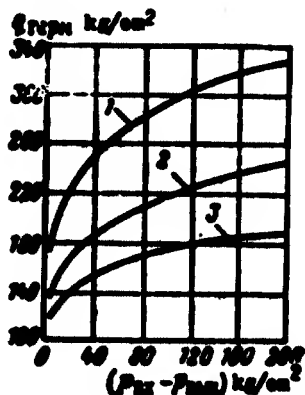


Fig. 9.21. Least specific pressures of airtightness for certain materials:
1 - fiber, hard; 2 - fiber;
3 - ebonite.

Depending on the selected (for assigned materials) necessary value q_{min} in kg/cm^2 (or N/cm^2), it is possible to calculate the force of a spring Q_1 .

Pressure of airtightness

$$Q_{min} = q_{min} F_{min} \quad (9.61)$$

where $F_{min} = \pi d_{sp}^2$ — surface area of contact of valve seat with valve in cm^2 .

Force of spring Q_1 is found from equation

$$Q_{min} = Q_1 + f_{us}(P_{min} - P_{ext}). \quad (9.62)$$

whence, taking relationships (9.49) and (9.61) into account

$$Q_1 = q_{min} F_{min} - f_{us} P_{ext}. \quad (9.63)$$

Value F_m of the surface area of the main diaphragm or bellows is assigned. F_m is proportional to the precision of the reducing valve. However, besides precision of the valve, during selection of F_m the permissible dimensions and mass of the valve are still governing factors. During determination of dimensions of the piston f_m or auxiliary diaphragm f_m for reducing valves with balancing, for improvement of the characteristic we select d_m (or d_u) greater

or less than a_m by a factor of 0.2-1.5%.

Compression force Q_2 of the main spring of the reducing valve is determined from the equation of equilibrium of forces (9.22) or (9.45) at the time of opening of the valve, i.e., when rise of the valve $h = 0$.

Since the characteristic of the valve always passes lower than a limiting value, sometimes after its design it becomes necessary to correct the compression force of the main spring, increasing it by 5-10 kgf. Therefore, during design of a spring the value of the calculation force on the spring is selected somewhat greater than the force obtained from formulas (9.22) or (9.45).

Dimensions of springs and their rigidity are determined by proceeding from structural considerations and using the usual formulas used in designs of machine parts.

Rigidity of metallic diaphragms is calculated or determined from experimental graphs built for every given type and material of a diaphragm.

Rigidity of "soft" rubber or plastic diaphragms is considered by introduction, instead of F_m of reduced area

$$F_{m \text{ eq}} F_m a_m \quad (9.64)$$

Value a_m for diaphragms with protective disks or without them (see Fig. 9.10b, d) is determined by the formula

$$a_m = 0.33 \left[1 + \frac{D_1}{D} + \left(\frac{D_1}{D} \right)^2 \right]. \quad (9.65)$$

For bellows it is possible to take $a_m = 1$.

After determination of all design parameters of a reducing valve from the equation of the characteristic we check whether the valve satisfies the assigned work conditions. For this, assigning

a series of values p_{out} (usually with an interval of 20-50 [atm(abs.)]), p_{out} is calculated. If values p_{out} do not emerge from the assigned limits, the design is considered completed. If however the characteristic of the valve emerges from the assigned limits, then, following the influence of parameters on the characteristic described above design parameters of the valve are corrected and the calculation is repeated.

Real Accuracy of Work of a Reducing Valve

Accuracy of work of a reducing valve is determined by value $\pm \Delta p_{\text{out}}$. During work of the valve the real amount of deviation of outlet pressure Δp_{out} will be greater than the theoretical value Δp_{out} obtained from calculations. The cause of deviation consists in the impossibility of absolutely precise manufacture of components of the valve and precise adjustment.

Depending on class of accuracy of manufacture of the valve, real deviation can be estimated by value

$$\Delta p_{\text{out}} = [\Delta p_{\text{out}} + (0.5 + 1.5)]. \quad (9.66)$$

It is also necessary to consider that the value of outlet pressure p_{out} is influenced also by temperature of the valve, since a change of temperature changes mechanical properties of resilient elements of the valve and their dimensions.

Example of calculation of a reducing valve

Calculate a reducing valve for reduction of pressure of air passing from the bottle with an initial pressure of 300 [atm(abs.)] (29.4 MN/m^2) to $p_{\text{out}} = 34$ [atm(abs.)] (3.33 MN/m^2).

Flow rate of air through the valve is $G = 400 \text{ g/s}$. With a decrease of inlet pressure to $p_{\text{inlet}} = 45$ [atm(abs.)] (4.41 MN/m^2) calculation deviation of outlet pressure must not exceed ± 0.5 [atm(abs.)] (0.049 MN/m^2). At the beginning of reduction, temperature of a gas in the bottle is equal to 18°C .

Solution. We determine the throttling section of the valve by formula (9.58):

$$f_{\text{spec}} = \frac{\sigma}{\mu A_0 \sqrt{\frac{P_{\text{max}} - P_{\text{min}}}{R T_{\text{min}}}}}$$

We set $\mu = 0.8$. For

$$\frac{P_{\text{max}}}{P_{\text{min}}} = \frac{34}{45} = 0.75$$

on the graph in Fig. 9.15 or by formula (9.29) we find $A_0 = 19$. Considering $n = 1.25$, we find T_{min} by formula (9.1):

$$T_{\text{min}} = T_{\text{p,ext}} = T_{\text{p,ext}} \left(\frac{P_{\text{max}}}{P_{\text{min}}} \right)^{\frac{n-1}{n}} = 291 \left(\frac{45}{300} \right)^{\frac{1.25-1}{1.25}} = 199^\circ \text{K.}$$

Hence

$$f_{\text{spec}} = \frac{0.4}{0.8 \cdot 1.9 \frac{45 \cdot 10^4}{\sqrt{291 \cdot 199}}} = 0.502 \cdot 10^{-4} \text{m}^2 = 0.502 \text{ cm}^2$$

We take the diagram of the valve of Fig. 9.12a with valve diameter $d_{\text{valve}} = 18 \text{ mm}$. We consider $d_{\text{sp}} = d_{\text{valve}}$.

We then determine the force of the spring. For improvement of the characteristic of the valve we take plunger diameter d 0.3% greater than d_{valve} i.e., $d = 18.05 \text{ mm}$. We determine the necessary force of the spring in the absence of flow, i.e., when $h = 0$:

$$Q = P_{\text{max}} f_{\text{ext}} + P_{\text{ext max}} (U_0 - f_{\text{ext}}) = \\ = 34 \frac{3.14 \cdot 1.8^2}{4} + 300 \frac{3.14}{4} (1.805^2 - 1.8^2) = 90.7 \text{ kgf} (890 \text{ N}).$$

The spring is calculated for a force $Q = 90.7 \text{ kgf}^2$ (890 N). Material of spring is silicon steel 60C2. For it $\tau = 75 \text{ kgf/mm}^2$ (736 MN/m^2); shear modulus $G = 800 \text{ kgf/mm}^2$ (7850 MN/m^2).

We assign spring index $c = D/d = 5$. For $c = 5$ coefficient $k_0 = 1.3$. Diameter of a turn of the spring

$$d = 1.6 \sqrt{\frac{k_0}{\tau}} = 1.6 \sqrt{\frac{1.3 \cdot 5 \cdot 90.7}{75}} = 4.48 \text{ mm.}$$

We select $d = 4.5$; $D = c \cdot d = 22.5$ mm.

We assign spring rigidity $k = 5$ and determine the necessary number of turns

$$t = \frac{Gd^4}{8D^3} = \frac{8000 \cdot 4.5^4}{8 \cdot 5 \cdot 22.5^3} = 7.2$$

We select the working number of turns $i = 7$.

Let us definitize the value of spring rigidity

$$k = \frac{Gd^4}{8D^3i} = \frac{8000 \cdot 4.5^4}{8 \cdot 22.5^3 \cdot 7} = 5.14 \text{ kgf/mm} (50.4 \text{ N/mm}).$$

From equation (9.46) we calculate the characteristic of the reducing valve. The calculation is given in Table 9.2.

Table 9.2.

$\frac{P_{in}}{P_{out}}$	$P_{in} (kgf/cm^2)$	$\frac{P_{in}}{P_{out}}$	A_p	$A = \pi d^2$	$\frac{x}{x-1} = \left(\frac{P_{in}}{P_{out}}\right)^{\frac{1}{2}}$	$T_{in} = \frac{1}{2} \times T_{max}$	$\frac{P_{in}}{A}$	$M_{cp} = \frac{P_{in}}{\sqrt{A \cdot T_{in}}}$	$\frac{M_{cp}}{M_{in}}$	$\frac{1}{f_{in}} (s)$
1	2	3	4	5	6	7	8	9		
200	4.34	0.1135	2.14	5.37	291	0.652	85.708	33.65		
210	3.075	0.131	2.14	5.37	264	0.745	86.238	33.9		
220	3.11	0.1545	2.14	5.37	273	0.861	86.729	34.05		
180	2.545	0.189	2.14	5.37	262	1.032	87.123	34.2		
140	1.98	0.243	2.14	5.37	250	1.30	87.42	34.32		
100	1.415	0.34	2.14	5.37	234	1.786	87.525	34.4		
60	0.848	0.567	2.13	5.34	212	2.78	87.072	34.2		
45	0.565	0.756	1.98	4.72	199	4.57	85.564	33.8		

Graphically, dependence $p_{out} = f(p_{in})$ is represented in Fig. 9.22, whence we see that outlet pressure does not exceed the assigned limits.

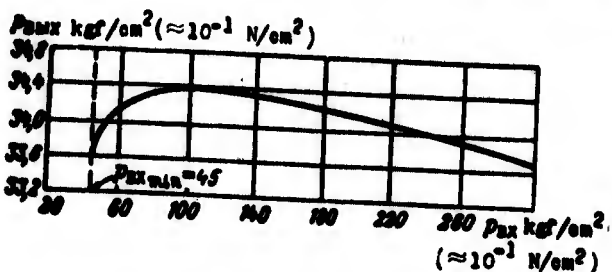


Fig. 9.22. Example of characteristic of a reducing valve.

9.6. Displacement Supply Systems with PAD and ZhAD

Besides compressed gas, for displacing components from tanks it is possible to use also hot combustion products obtained during a burn in a gas generator of solid or liquid fuel. Such gas generators we called solid fuel pressure accumulators (PAD) or liquid fuel pressure accumulators (ZhAD).

Therefore we distinguish pressure feed systems with PAD or with ZhAD.

Supply System with PAD

Besides application of PAD as a drive for turbopump assemblies and, in the first place, as a starter for spin-up of turbopump assemblies, sometimes PAD are used as even the basic unit of a pressure feed system. An elementary diagram of such a system is shown in Fig. 9.23, where components are displaced from tanks by combustion products of the powder generated during its combustion in the PAD.



Fig. 9.23. Diagram of displacement with PAD:
1 - starting PAD; 2 - PAD;
3 - reflectors; 4 - tanks;
5 - diaphragms; 6 - engine chamber.

The advantage of a system of supply with PAD as compared to a gas-pressurized system of supply consists in structural compactness and several excellent weight characteristics.

However, a great deficiency of such systems is the difficulty in obtaining stable and reliable characteristics of their work. Characteristics of a system of supply with PAD are greatly influenced by changes of external conditions, since there are changes in laws of burning of the powder as well as conditions of heat radiation from powder combustion products to the environment, to structural elements and to displaced components. Furthermore, during supply with PAD, in the tank of the oxidizer after-burning of combustion products occurs since usually the powders contain a surplus of combustible elements. Moreover, the flow of the afterburning process considerably depends on different accidental factors (for example, burst of components, their temperature, etc.). All these factors very much lower the reliability of work of the system, as a consequence of which pressure feed systems with PAD are not widely used. Examples of installations having displacement systems with PAD are the propulsion system of SAM "Typhoon" [25], the ampule propulsion system of the rocket missiles "Sparrow" and "Bull Pup" (see Fig. 9.31); and also the propulsion system of the first stage of "Diamant" (Fig. 9.24).

The engine of "Diamant" works on a fuel of nitric acid + turpentine. Thrust of the engine \approx 28 t (275 kN); time of work is 88 s. Unit PAD 11 for displacing the fuel is placed in the oxidizer tank. From PAD through pipelines 13 combustion products of the powder displace fuel from tanks of the oxidizer and fuel, where nitrogen is also used for rotation of the airborne ac turbogenerator at 400 Hz.

Properties of powders

For creation of PAD it is most difficult to ensure constancy of the flow rate of powder gases at assigned pressure.

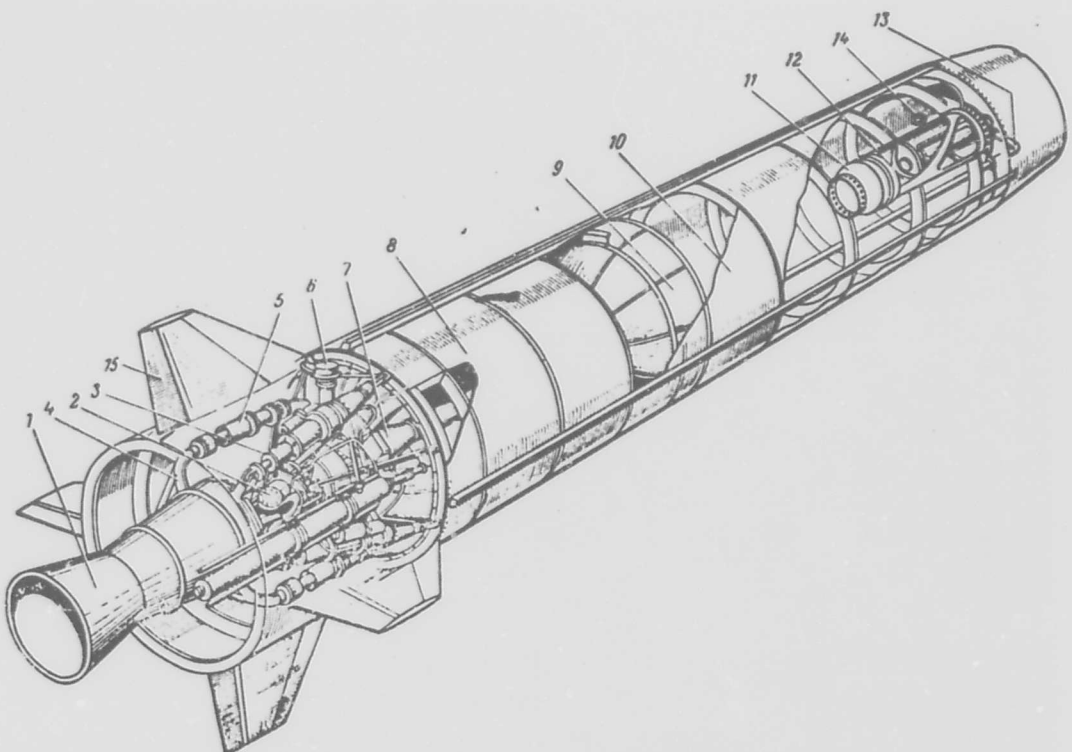


Fig. 9.24. Propulsion system of first stage of "Dismant" rocket:
 1 - liquid-fuel rocket engine; 2 - gimbal thrust pad of liquid-fuel rocket engine; 3 - hydraulic drive for control of rocket pitch and roving; 4 - fuel pipeline; 5 - telescopic connector; 6 - pipe connection for servicing; 7 - oxidizer pipeline; 8 - fuel tank; 9 - bottom of oxidizer tank; 10 - oxidizer tank; 11 - PAD for fuel feed; 12 - charge of solid fuel PAD; 13 - pipeline to oxidizer tank; 14 - hole for entrance of gases into oxidizer tank; 15 - steering for roll control.

As it is known, powder does not burn in a mass but in parallel layers from the surface. In order to obtain uniform burning of a powder cartridge in time, and consequently also constant liberation of powder gases necessary for uniform displacing of fuel from tanks, it is necessary to have a constant combustion surface. For this so-called restricted burning grains are used, part of the surface of which is covered by a composition which does not allow burning. Therefore, burning of a restricted grain can occur only on the open surface.

If it is necessary to have uniform burning in time of a powder grain, ends of it (one or both) are left open (unrestricted). For such a grain the surface of burning remains constant and equal to the area of the end (Fig. 9.25a). Consequently, the quantity of powder burning per unit of time G_s remains constant.

Figure 9.25b also shows a restricted grain with a nonuniform surface of burning which increases on account of an increase in diameter of the burning surface.

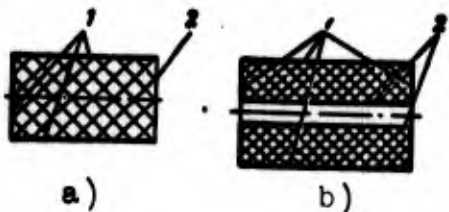


Fig. 9.25. Restricted burning grains: a) with constant surface of burning; b) with variable burning surface; 1 - armoring; 2 - burning surface.

The burning rate of a powder in the first place is determined by the pressure at which combustion occurs.

For the majority of powders the dependence of burning rate u on pressure can be determined in the form

$$u = u_1 p^\nu \text{ cm/s}, \quad (9.67)$$

where p — pressure in kgf/cm^2 ; u_1 — burning rate of powder in cm/s at a pressure of 1 kgf/cm^2 , depending on the composition of powder; ν — exponent depending on composition of the powder ($\nu < 1$).

The burning rate of powder also depends on its initial temperature [22], [147].

$$u_1 = u_{1,0} \frac{B}{B - (T - T_0)}, \quad (9.68)$$

where $u_{1,0}$ — burning rate at assigned initial temperature T_0 ; T — temperature of powder; B — physicochemical constant characterizing a given make of powder.

Values of burning rate $u_{1,0}$, exponent ν , constant $1/B$ and certain other parameters of burning of powders are given in Table 9.3.

Table 9.3. Indices of burning of certain powders [22], [27], [147].

Make of powder	Combustion temperature T_{pk} at 40-70 $[atm]$ (abs.) (4-7 mm/s^2)	Force of powder f_0 kg/cm^2	Burning rate u_0 m/s	Exponent ν	$1/B$	Density ρ_s g/cm^3	Lower limit of pressure, P_{min}	
							m^2/s	N/m^2
Dibasic, type H, HM-2, T-6	2200-2300	88000	0.700	0.6	0.0038	1.6	10	3.92
Dibasic, type M-8, T-5	3100-3200		0.885	0.69		1.6	15	1.47
IP	3160	100000	0.832	0.71	0.005	1.60		
IPN	3160	100000	0.879	0.69	0.0038	1.61	20	1.96
Mixture with $KClO_4$, type A2T	1800-2100	51000- 59000	1.24	0.7	0.002	1.77	30 (70)	4.9 6.87
Mixture with NH_4ClO_4 , type AP	1500-2500	60000- 90000	2.2	0.4		1.75	14	1.375
Mixture with NH_4NO_3 , type AN	1500-1700 1755	58000- 66000	0.4	0.5		1.55	7	0.687

When selecting fuel for PAD it is desirable that it have, first, a low combustion temperature, since this decreases heat radiation from combustion products. This facilitates conditions of work of structural elements heated by combustion products (tanks, pipelines, valves, etc.), and eliminates the need of providing special cooling of combustion products. Furthermore, desirable properties of the fuel are inertness of combustion products with respect to displaced components, low sensitivity of fuel to changes of initial temperatures, and the absence of solid particles in combustion products.

In PAD both dibasic, and mixture fuels are used. According to foreign data the fuels continue to be studied. By changing the ratio of the binder and oxidizer or inclusion of organic substances like dicyandiamide and ammonium oxalate the combustion temperature of powders of experimental brands can be decreased to $930^\circ C$. Figure 9.26 gives graphs of the change of combustion temperature depending on the content of binder and trigger additions.

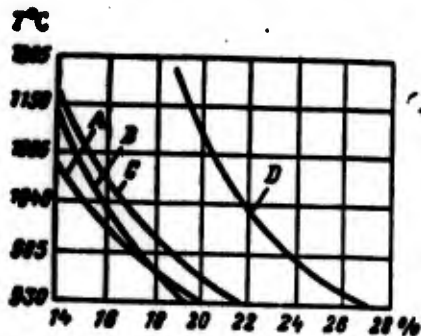


Fig. 9.26. Influence of including, in composition of fuel, different cooling additions (A, B, C) in a quantity of 10% on the theoretical combustion temperature of the fuel; D - fuel without cooling additions.

Types of PAD

According to their principle of action, powder pressure accumulators are divided into supercritical and subcritical. By use, PAD can be divided into basic and starting.

On Fig. 9.27a is a diagram of supercritical PAD. In durable body 1 is placed a powder cartridge 2 (or set of grains) of slowly burning powder. When starting the engine these grains ignite with the help of igniter 3, consisting of smoky rocket powder or a thermite mixture. Ignition of the igniter is produced with the help of an electric current. As a result of burning of powder gases at high temperature and pressures are formed which pass through throttle nozzle 4 and tube 5 and enter fuel and oxidizer tanks.

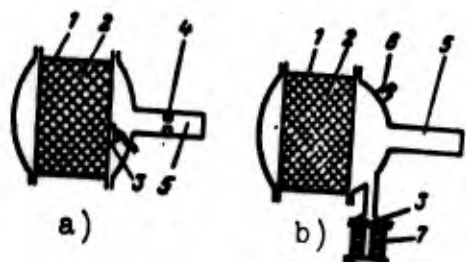


Fig. 9.27. Diagrams of PAD:
a) supercritical; b) subcritical;
1 - body; 2 - powder; 3 - igniter;
4 - throttle nozzle; 5 - pipe for
exit of powder gases; 6 - safety
valve; 7 - starting PAD.

The basic principle of work of such PAD consists of the fact that the ratio of feed pressure p_0 to pressure in the PAD chamber p_1 is less or equal to critical, i.e.,

$$\frac{p_0}{p_1} \leq \beta = \left(\frac{2}{n+1} \right)^{\frac{n}{n-1}}.$$

With such a pressure drop in the throttling nozzle, critical speed of flow of the powder gases is attained.

In view of the need for a great pressure drop p_a/p_s , pressure in supercritical PAD reaches 200-250 [atm(abs.)] ($\sim 20-25 \text{ MN/m}^2$) that leads to considerable loading of PAD. Furthermore, with such pressures there is an intense heat radiation from powder gases to walls of the PAD, leading to difficulties in organization of cooling of the unit. Therefore, at present supercritical PAD find use only as a starting unit.

In contrast to supercritical, in subcritical PAD (Fig. 9.27b) there is no throttling nozzle. The difference in pressures in PAD and in tanks ($p_a - p_s$) is small and is determined by losses in the pipeline system. Therefore, even the pressure in the chamber of subcritical PAD p_a is low, which makes it easier to use. For practical purposes one may assume that pressure in the chamber of subcritical PAD is equal to feed pressure p_s .

For preventing an increase of pressure above assigned, in subcritical PAD it is necessary to place a safety valve 6 which serves to jettison of surplus combustion products.

During work of a propulsion system with displacement feed one strives to reduce the time it takes to get into operating conditions, i.e., the time it takes pressure in tanks to reach nominal feed pressure p_s . It depends on the free volume of tanks and dimensions of gas pipelines. Depending on conditions of work of a propulsion system this time should not exceed 1-2.5 s (depending on construction). Therefore in systems with PAD, besides the main PAD there is usually an additional one, a starting PAD, working at high pressure. The starting PAD serves for rapid filling of the free volume of tanks and gas pipelines.

The charge of the starting PAD ignites from a special charge with the help of an electric spark.

Depending on time of work of PAD and combustion temperature of powder the basic PAD working to displace components, can be cooled or not cooled. A PAD is cooled usually by one of the components. Starting PAD work a very short time and therefore are not cooled.

During work of PAD on powders with high combustion temperatures, the decrease in temperature of combustion products by heat radiation to the environment, elements of construction and liquid components may be insufficient. Therefore in certain cases products of combustion of PAD are cooled by way of heat removal from them by evaporation of sublimation of specially introduced coolants.

On Fig. 9.28 is a diagram of cooling of products of combustion from PAD, by sublimation of the coolant. High temperature combustion products from the PAD enter multichannel filter 3, carried out from ammonium oxalate, as a result of sublimation of which the temperature of combustion products drops to the required level.

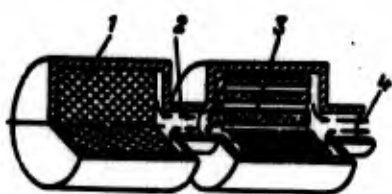


Fig. 9.28. Diagram PAD with device for cooling combustion products: 1 - powder charge; 2 - hot combustion products; 3 - multichannel filter with coolant; 4 - cooled combustion products.

Calculation of PAD

During work of PAD in the "pipelines - tanks" system the following phenomena occur:

1. Intense cooling of hot powder gases in pipelines and in tanks themselves on account of heat radiation to the environment, construction and components.
2. Evaporation of liquid components and partial solution of powder gases in them.

3. Since in powder combustion products $\alpha < 1$, then in the oxidizer tank during interaction of them with vapors of the oxidizer CO and H₂, burn, leading to an increase in temperature of gases in the oxidizer tank as compared to their temperature in the propellant tank.

All these phenomena influence the ability of powder gases to displace, and consequently also the supply of components. However it is impossible exactly to consider their influence. Therefore, during calculation of PAD we originate from the assumption that during all the time of work of PAD the gas volume of the system is filled only by powder gases. Processes of cooling, dissolution and burning of powder gases shown above are considered by introduction of experimental coefficients.

Calculations of dimensions of PAD grain originate from the following requirements.

1. The flow rate of powder gases entering tanks should be equal to the necessary volumetric flow rate of fuel (fuel and oxidizer);
2. The time of burning of grain should be equal to the time of work of the engine.

From calculations of engines we know the per-second volumetric flow rate of tanks:

$$V_{\text{sec}} = \frac{G_f}{w} + \frac{G_o}{w}. \quad (9.69)$$

On the other hand, the volume of powder combustion products formed in 1 second is equal to

$$V_{\text{sec}} = \frac{G_s}{w}, \quad (9.70)$$

where G_s — quantity of powder burning per unit time; w — density of combustion products at feed pressure p_0 .

It is obvious that

$$G_s = F_s \rho V_0. \quad (9.71)$$

where F_s — burn surface of grain; ρ — density of powder.

During pressure feed of components with the help of PAD

$$V_{ess} = V_{s,ess} = \frac{G_s}{\gamma_w}. \quad (9.72)$$

According to the equation of state of gases

$$\gamma_w = \frac{P}{RT}. \quad (9.73)$$

where R — gas constant of powder combustion products; T — temperature of powder combustion products developed if the powder burns at constant pressure; P_0 — feed pressure.

Product RT is conventionally called reduced force of powder f_0 . For the powders enumerated in Table 9.3, value $f_0 = 58,000-100,000$ kgf·m/kg ($\approx 5.8 \cdot 10^5 - 10 \cdot 10^5$ N·m/kg).

Placing expressions (9.71) and (9.73) in equation (9.72), we obtain

$$V_{ess} = \frac{F_s \rho V_0 RT}{P_0} = \frac{F_s \rho V_0 f_0}{P_0}, \quad (9.74)$$

whence we find the necessary burn surface of the powder

$$F_s = \frac{P_0 V_{ess}}{\rho V_0 RT}. \quad (9.75)$$

This formula is not final, since it includes temperature of combustion of the powder, the value of which depending on the make of powder is within limits of $1200-2500^\circ K$. In the tanks combustion products have a lower temperature, $\sim 800-1000^\circ K$. Moreover, as was already noted, the temperature of combustion products can drop due to the heat radiation from them, as well as from forced cooling.

Since the temperature of powder combustion products entering tanks is lower than the combustion temperature of the powder, for production of the necessary flow rate per second of fuel and assigned feed pressure it is necessary to burn in 1 second more powder than was determined during calculation by formula (9.75), i.e., the quantity of powder burning in 1 second should be increased in proportion to the decreases in absolute temperature of the gases.

Furthermore, the PAD chamber should produce a certain additional quantity of gas necessary for stable work of the pressure valve and for restoration of operating pressure in tanks p_0 in case it is lowered accidentally. All these factors are considered by introduction of coefficient $\psi = 1.2-3.5$.

The exact value of coefficient $\psi > 1$ is determined from experimental data when finishing the system. Strictly speaking, the lowering of temperature on account of heat radiation and the addition of special coolants can be approximately estimated. However there will always be unaccounted factors affecting the change of temperature of combustion products, and all the same it is necessary to introduce a coefficient considering the influence of these factors.

For the oxidizer tank value ψ due to afterburning will be less than for the fuel tank; for small propulsion systems the magnitude of ψ must be selected higher since in this case the relative surface of heat radiation of tanks and gas conduits is large.

The final formula for determination of the necessary surface of burning of grain taking cooling of powder gases into account will take the form

$$F_0 = \frac{p_0 V_{ext}}{\sigma T_0} \psi = \frac{p_0 V_{ext}}{\sigma T_0 f_0} \psi. \quad (9.76)$$

In order to always ensure the assigned pressures of powder gases in the tank, the burning rate of powder u in formula (9.76) is selected at the least possible operational temperature at the beginning of powder burn.

If this temperature is greater than calculation, then speed u will be greater, as a consequence of which the flow rate and pressure of gases will be greater than calculation. Surplus pressure in the chamber of a PAD will actuate the valve for relieving pressure.

Grain length L is calculated proceeding from necessary the time of work of a liquid-fuel rocket engine, τ :

$$L = u\tau \text{ cm.} \quad (9.77)$$

During calculation of the length of grain the burning rate of powder u must be selected by proceeding from the highest possible temperature of the start of burning, and consequently, from the fastest burning rate of the powder. If value u is selected according to an average or minimum temperature, length of grain L will be insufficient to ensure the necessary time of work of the engine at a high ambient temperature, and the supply of components as necessary will cease earlier than is permissible.

Starting PAD

A starting PAD is necessary in the first place for rapid initial filling of tank volumes with powder gases. Its gas productivity should ensure rapid onset of operating pressure in tanks in the whole range of operational temperatures of the liquid-fuel rocket engine.

The mass of the starting charge is determined by calculation in terms of the greatest free volumes of tanks and pipelines at the least operational temperature of liquid-fuel rocket engines. During work of the starting PAD the quantity of powder gases given off during its work should be enough to raise the pressure in volume V_{gas} to assigned feed pressure p_0 , i.e.,

$$G_{\text{gas}} = \frac{p_0 V_{\text{gas}}}{RT}$$

It is obvious that the mass of the grain before combustion $G_{\text{g.s.}}$ is equal to the mass of powder gases formed $G_{\text{g.s.}} = G_{\text{g.r.}}$

During work of the starting PAD, just as during work of the main charge powder gases entering the tank are cooled by heat radiation through walls of the system and into the displaced liquid. This lowering of temperature of gases is considered by introduction of factor $\psi > 1$. The starting PAD works in the initial moment of work of the liquid-fuel rocket engine; the tank system is heated, leading to an even greater lowering of temperature of powder gases. Therefore, for a starting PAD ψ is selected larger than for the main charge, and is equal to 5-6.

Taking the mass of powder into account

$$G_{\text{g.s.}} = \frac{P_0 V_{\text{init}}}{RT} \psi. \quad (9.78)$$

To ensure that operational conditions are reached as soon as necessary, starting PAD have quick-burning powder. For increasing the burning rate of powder the chamber of the starting PAD works at pressures considerably higher than feed pressure. Thickness of the grain is determined from the condition

$$S = u t_p,$$

where u — burning rate of powder at average pressure in the chamber of the PAD and minimum temperature during exploitation; t_p — assigned time for reaching operating conditions.

Displacement Supply with ZhAD

Liquid pressure accumulator (ZhAD) is the name of the gas generator producing combustion products for displacing fuel from tanks of liquid-fuel rocket engines by burning liquid fuels. In principle, as ZhAD it is possible to use single component and two-component gas generators. Usually two-component liquids working on spontaneously inflammable components are used. By weight

characteristics systems of supply with ZhAD are somewhat better than a gas cylinder, however they are more complicated than supply with PAD and a gas-pressurized system.

On Fig. 9.29 and 9.30 are elementary diagrams of supply systems with ZhAD.



Fig. 9.29. Diagram displacement supply with ZhAD: 1 - gas pressure accumulators; 2 - pressure reducers; 3 - tanks for ZhAD components; 4 - ZhAD; 5 - tanks; 6 - diaphragm; 7 - engine chamber.

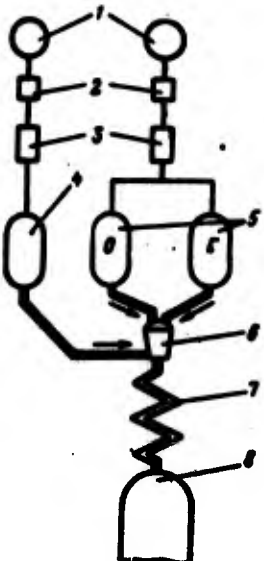


Fig. 9.30. Supply system with ZhAD with cooling of combustion products: 1 - air pressure accumulators; 2 - cut-off valves; 3 - reducing valves; 4 - tank with coolant; 5 - tanks with components for ZhAD [Translator's Note: 0 - oxygen; Г - fuel]; 6 - ZhAD; 7 - mixer; 8 - tank.

For a supply system with ZhAD, carried out according to the diagram of Fig. 9.29, by the pressure of gas the fuel components are forced from tanks 3 into ZhAD 4 of the fuel and oxidizer tanks. For lowering the temperature of combustion products the ZhAD works with a displaced excess oxidant ratio α . Besides, so that in oxidizer and fuel tanks there will not be burning of gases, ZhAD for displacing the oxidizer work with a surplus of oxidizer ($\alpha = 3-6$), and ZhAD for displacing fuel work with a surplus of fuel ($\alpha = 0.3-0.4$).

Calculation of liquid pressure accumulators in conduct in the following order.

1. Knowing the components on which ZhAD will work and the feed pressure, we assign temperature of the gas produced by the ZhAD.

2. We determine the excess oxidant ratio for which in ZhAD we obtain the rated temperature of gas. As was indicated, for ZhAD producing gas for displacing the oxidizer, we take $\alpha \gg 1$, and for ZhAD which displace fuel we take $\alpha \ll 1$.

Usually for a given fuel there are graphs of the change of combustion temperature and value RT depending on α . If such graphs are lacking, then, by tentatively assigning value α we calculate T and RT by the method shown in section 7.5.

3. Knowing RT and pressure we determine for each ZhAD the density of obtained combustion products by equation (9.73):

$$\rho_{cr} = \frac{P_1}{RT}$$

4. Obviously, just as during calculation of PAD, in each of the tanks equality (9.72) is fulfilled:

$$V_{ex} = \frac{\alpha}{\rho_{cr}}$$

where V_{ex} — per-second liberated volume of tank; G — flow rate per second of components in given reactor of ZhAD.

On the basis of formulas (9.73) and (9.72) we determine the necessary total flow rate of components in the ZhAD:

$$G = V_{\text{ext}} \gamma_{\text{cr}} = V_{\text{ext}} \frac{P_0}{RT}. \quad (9.79)$$

5. Thus, as during supply with PAD, gases entering tanks are cooled. Consequently, the flow rate per second of components must be increased in proportion to the decrease in temperature of gases formed. This increase of flow rate is considered by coefficient $\psi > 1$.

Final calculation formulas for the ZhAD reactor of the oxidizer tank

$$G = V_{\text{ext}, \text{ox}} \frac{P_0}{(RT)_{\text{ox}, 1}} \psi;$$

for the fuel tank ZhAD reactor

$$G = V_{\text{ext}, \text{fu}} \frac{P_0}{(RT)_{\text{fu}, 1}} \psi. \quad (9.80)$$

For a supply system working with a propulsion system like the "Veronica" rocket (see Fig. 9.30), components from tanks 5 are displaced by compressed gas in ZhAD 6, where combustion occurs. By addition of coolant from tank 4 combustion products are cooled to a temperature of 800°C . The gases (a mixture of combustion products and coolant vapors) enter fuel tanks for displacing the components.

For preventing the possibility of afterburning in fuel tanks the fuel of ZhAD and the coolant are selected so that gases formed will be neutral with respect to displaced components. The ratio of quantities of fuel and coolant is selected from the condition of obtaining the necessary temperature of gases. The combined flow rate of components and coolant is determined by equation (9.79), where R - gas constant, and T - temperature of mixture of combustion products and coolant vapors.

9.7. Propulsion Systems with Preliminary Fueling and Hybrid Engines [149], [150], [151]

The main advantage of liquid-fuel rocket engines as compared to solid fuel motors (RDTT) are their higher power characteristics (i.e., specific thrust). Furthermore, the advantage of propulsion systems with a liquid-fuel rocket engine is the possibility of providing multiple starting and thrust control over wide limits.

However, notable deficiencies of ZhRD as compared to RDTT are the relatively long launch preparation time and also the limited capability of prolonged storage of ZhRD in a state of launch readiness. This limits the use of ZhRD. A search for systems combining the basic advantages of liquid-fuel rocket engines with the merits RDTT has led to the development of liquid-fuel rocket engine with preliminary fueling, and also the creation of so-called hybrid rocket engines (GRD) in which part of the fuel is in a liquid state and part in a solid state.

Propulsion Systems with Preliminary Fueling

The possibility of prolonged storage and reduction of launch preparation time to a value corresponding to the preparation time of RDTT is found in liquid-fuel rocket engines with preliminary fueling. Such liquid-fuel rocket engines allow fueling long before use (from several months to several years) in order to obtain an installation possessing constant launch readiness. In general, liquid-fuel rocket engines with preliminary fueling can have either pump or pressure feed systems. For best compactness the chamber of the engine can be made as a unit with tanks or separately.

Liquid-fuel rocket engines with preliminary fueling have components which allow prolonged storage. In the ideal case such fuel should possess high chemical stability and have the lowest possible freezing point and highest possible boiling point. It is desirable that components of fuel be spontaneously inflammable.

Table 9.4 gives certain components which are useful for preliminary fueling.

Table 9.4.

Propellant components	Freezing point, °C	Boiling point at 1 [atm (abs.)] °C	Density at 20°C, g/cm³
<u>Oxidizers</u>			
Inhibited nitric acid	-54	66	1.57
Nitrogen tetroxide	-11	21	1.45
Mixture of nitric acid with nitrogen tetroxide		Depending on % content of N ₂ O ₄ in mixture	
Chlorine tri-fluoride	-76	12	1.83
Bromine pentafluoride	-60	40	2.48
<u>Fuels</u>			
Hydrazine	2	114	1.01
NDMG	-57	63	0.79
Diethylenetriamine	-65	207	0.96
Monomethyl hydrazine	-52	88	0.88
Pentaborane	-47	60	0.63

An example of an elementary diagram of a liquid-fuel rocket engine with preliminary fueling is represented in Fig. 9.31, the diagram and an outer view of the "Guardian" engine utilized for the "air-to-surface" missiles "Sparrow" and "Bullpup" [151]. Thrust of the engines are 3.9 and 5.4 t (38.2 and 53 kN). The supply system has a displacer with a PAD. Both tanks are filled at the end of manufacture, when the filler necks are completely welded or reliably hermetically sealed. The PAD and its igniter can be set in either immediately after filling the tank or (out of safety considerations) before launch. The possibility of fuel getting into the PAD cavity is prevented by diaphragms, and the cavity of the combustion chamber — by packing of injectors. Thus, a filled propulsion system constitutes, as it were, an ampule with fuel,

as a consequence of which such installations are sometimes called ampules. Launch is carried out by an electric spark which ignites the ignition charge from which PAD grain is ignited.

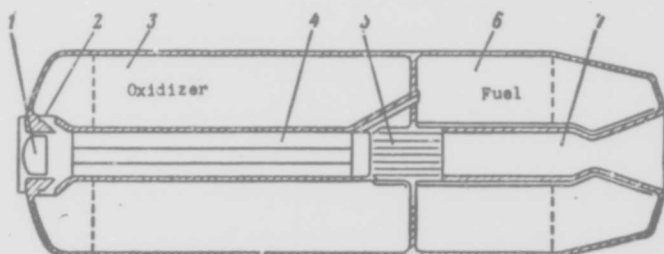
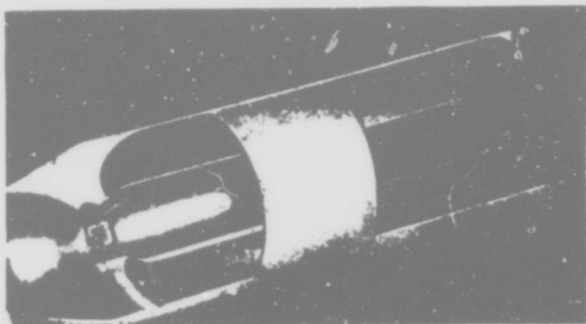


Fig. 9.31. Diagram of liquid-fuel rocket engine with preliminary fueling (ampule liquid-fuel rocket engine): 1 - igniter; 2 - diaphragm; 3 - oxidizer; 4 - PAD; 5 - chamber head; 6 - fuel; 7 - combustion chamber.

Besides the examined case of use of liquid-fuel rocket engines with preliminary fueling for missiles, it is possible to use them also for guided antiaircraft rockets, expendable aircraft boosters and the engines of spaceships [149].

Hybrid Rocket Engines

Theoretically the following fuel combinations are possible in GRD:

- liquid fuel + solid oxidizer;
- liquid oxidizer + solid fuel;
- solid fuel with a deficiency of fuel + part of the combustible in liquid form;

- solid fuel with a deficiency of oxidizer + part of the oxidizer in liquid form.

In existing fuels, oxidizers and solid fuels the best is the last of these combinations. Table 9.5 gives certain fuel components for GRD.

Table 9.5.

Fuel	Oxidizer	P_{72}		
		$\frac{\text{kgf}}{\text{kg}}$	$\frac{\text{N}}{\text{kg}}$	$\frac{\text{kgf}}{\text{l}}$
Polymer with additions of aluminum	Hydrogen peroxide	269	2840	435
	Nitric acid	273	2680	414
Hydrazine	Nitrenium perchlorate (NO_2ClO_4)	295	2895	428
	Chlorine trifluoride	293	2975	445
Lithium hydride	Fluorine	263	2580	476
	Chlorine trifluoride	318	3120	369
Lithium	Nitrogen tetroxide	375	3680	530
	Hydrogen peroxide	375	3680	566
Beryllium hydride	Fluorine	395	3895	604
	Oxygen	371	3645	486
Polymer	Mixture of liquid fluorine and liquid oxygen	343	3375	412
Aluminum hydride	Fluorine	353	3465	531

Figure 9.32 for example gives one of the most usual structural diagrams of GRD.



Fig. 9.32. Diagram of engine with hybrid fuel: 1 - PAD; 2 - oxidizer; 3 - injection device; 4 - solid-propellant grain; 5 - combustion chamber oxidizer supply; 6 - injection of oxidizer into nozzle for control of thrust vector.

Hybrid rocket engines, preserving a number of the qualities inherent in RDTT (in the first place, high volumetric specific thrust), thanks to burning of liquid components along with solid fuel, have a greater specific thrust than RDTT. For certain combinations of solid and liquid fuel attainable specific thrusts reach $365 \text{ kgf}\cdot\text{s/kg}$ ($\approx 3650 \text{ N}\cdot\text{s/kg}$). Besides high specific thrust, the use of a liquid component in GRD enable thrust control by way of a change of flow rate of the liquid component. Thus, for example, by changing the flow rate of liquid oxidizer it is possible to change the value of thrust (and specific thrust) down from the greatest value during optimum flow rate of oxidizer to the thrust obtained during burning of solid fuel alone. Figure 9.33 shows calculation and experimental graphs of the change of specific thrust depending on the quantity of liquid oxidizer used (N_2O_4 and ClO_3F). Application of liquid component also gives the possibility of reliable cooling of the engine chamber. Moreover, in GRD it is easier to store the rocket in a filled state with full launch reactives for a prolonged time. By decreasing the quantity of oxidizer in the solid fuel, it is possible to improve strength properties of the charge. A deficiency of GRD is the difficulty of organization of full combustion. From the graphs of Fig. 9.33 it is clear that experimental values of specific thrust differ from calculation by 8-10%.

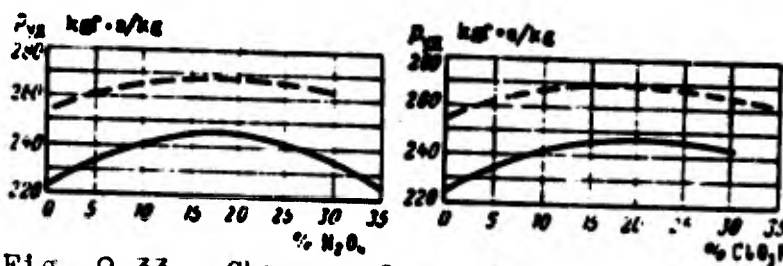


Fig. 9.33. Change of specific thrust of liquid-fuel rocket engines depending on flow rate of liquid oxidizer (N_2O_4 and ClO_3F): ---- calculation; —— experiment.

Footnotes

¹Sometimes the terms "dynamic" and "static" characteristics are used. However, these names do not correspond to terminology accepted in the theory of control, and therefore in the determination of the type of characteristic it is more convenient to use the terms accepted above.

²During calculation of dimensions of springs we use the usual formulas applied in calculations of machine parts.

APPENDIX

I. Auxiliary Graphs for Calculation of Cooling

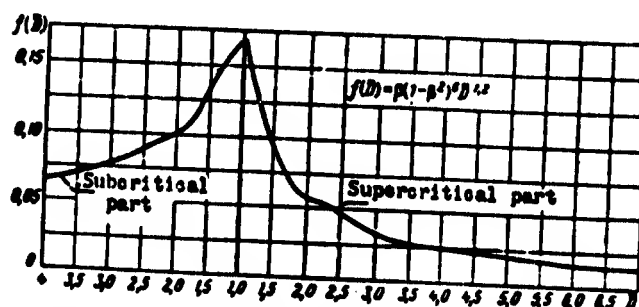


Fig. I.1. $f(D) = \beta(1-\beta^2)^{1/2} D^{1/2}$ depending on D .

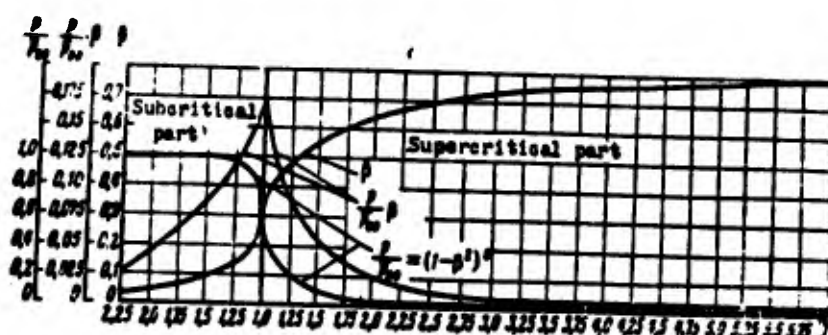


Fig. I.2. $\beta; (1-\beta^2)^{1/2}; \beta(1-\beta^2)^{1/4}; \beta(1-\beta^2)^{1/8}$ depending on D .

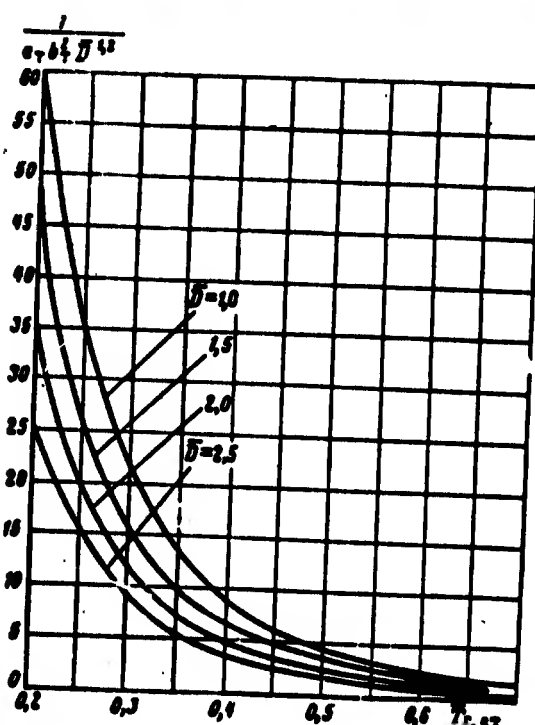


Fig. I.3. $\frac{1}{c_p D^{1/2}} = f(T_{ref,0}, D)$,
subcritical part.

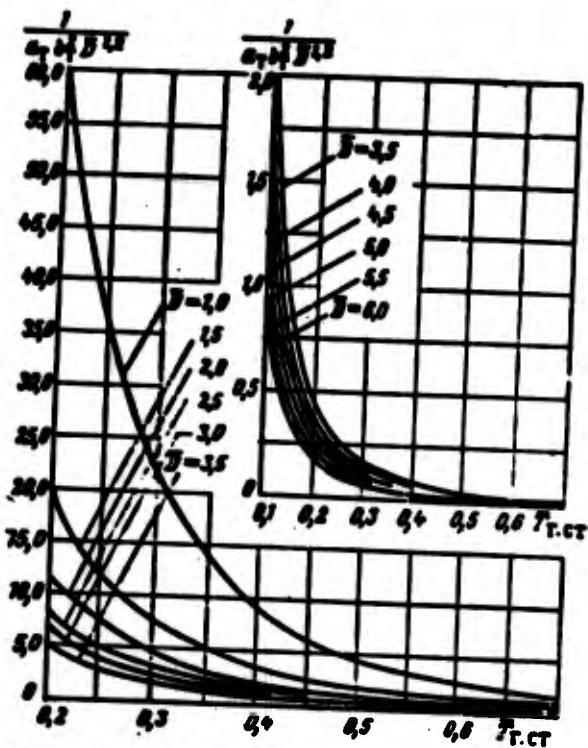


Fig. I.4. $\frac{1}{\sqrt{\nu_1 \nu_2}} = f(T_{r,cr}, \bar{D})$, supercritical part.

II. Auxiliary Graphs for Conversion of Thermal Flows

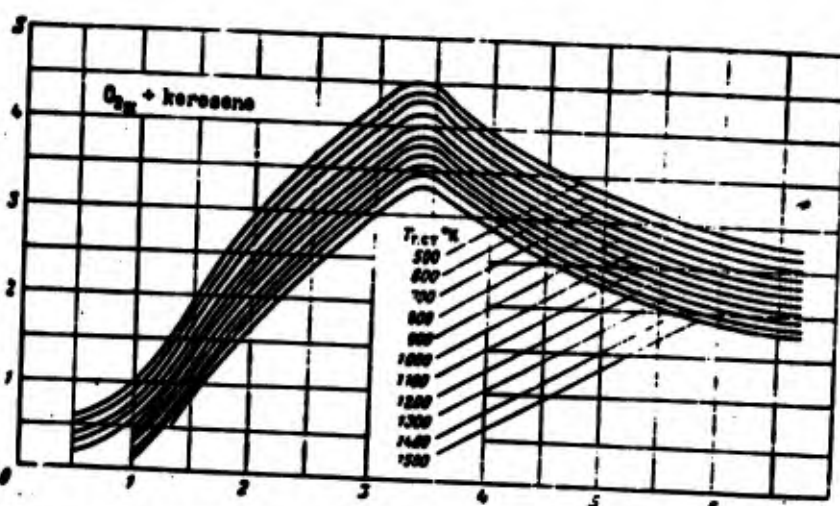


Fig. II.1.

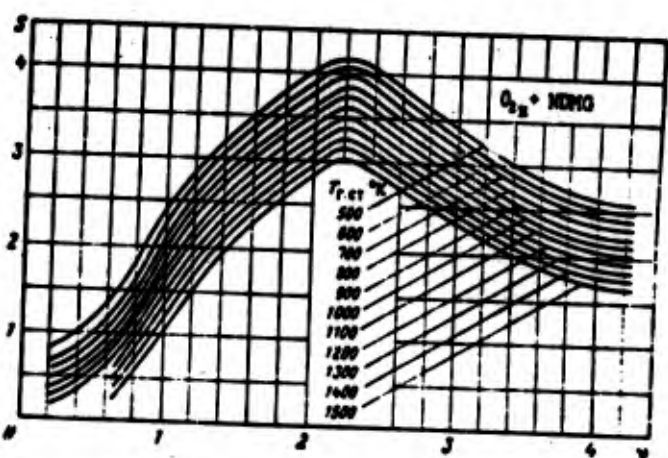


Fig. II.2.

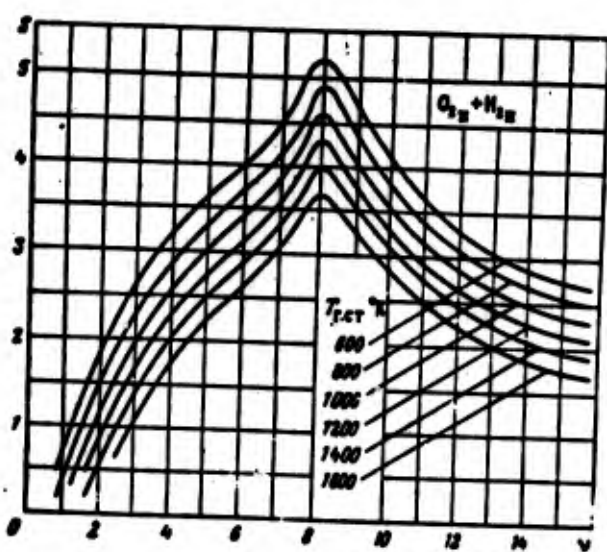


Fig. II.3.

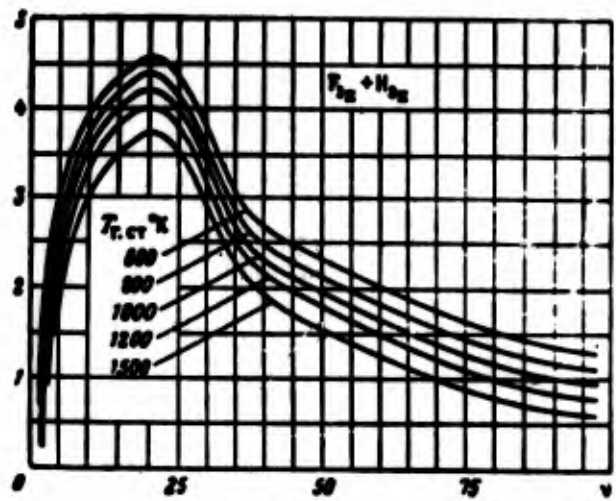


Fig. II.4.

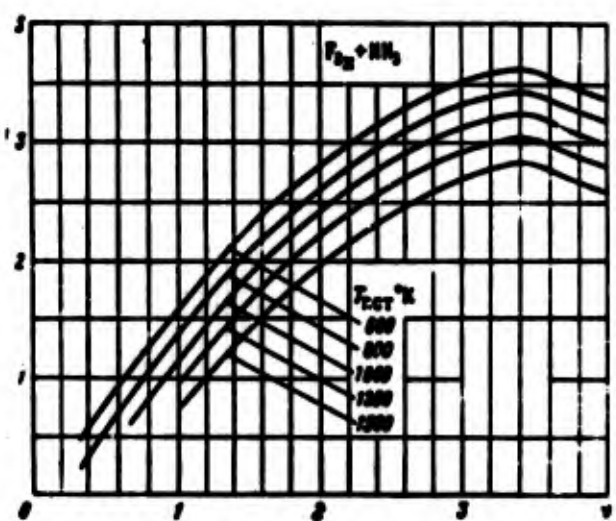


Fig. II.5.

BIBLIOGRAPHY

1. Abramovich G. N., *Prikladnaya gazovaya dinamika* (Applied gas dynamics), ITTL, 1953.
2. Alemasov V. Ye., *Teoriya raketnykh dvigateley* (Theory of rocket engines), Oborongiz, 1962.
3. Aleshkov M. N., Zhukov I. I., *Fizicheskiye osnovy raketnogo oruzhiya* (Physical bases of rocket armament). Voyenizdat, 1965.
4. Barrer M., et al. *Raketnyye dvigateli* (Rocket engines), Oborongiz, 1962.
5. Volgarskiy A. V., Shchukin V. K., *Rabochiye protsessy v zhidkostno-reaktivnykh dvigatelyakh* (Working processes in liquid-fuel engines), Oborongiz, 1953.
6. Volgarskiy A. V., et al. *Termodinamika i teploperedacha* (Thermodynamics and heat transfer), izd-vo "Vysshaya shkola", 1964.
7. Vargaftik N. B., *Spravochnik po teplofizicheskim svoystvam gazov i zhidkostey* (Reference book on thermophysical properties of gases and liquids). Fizmatgiz, 1963.
8. Vasil'yev A. P., et al. *Osnovy teorii i rascheta ZhRD* (Fundamentals of the theory and design of liquid-fuel rocket engines), izd-vo "Vysshaya shkola", 1967.
9. Voprosy goreniya raketnykh topliv (Questions on combustion of rocket fuels), Collection of translations edited by V. A. Popov, IL, 1959.
10. Vukalovich M. P., Novikov I. I., *Tekhnicheskaya termodinamika* (Technical thermodynamics), Gosenergoizdat, 1962.
11. Glushko V. P., *Zhidkoye toplivo dlya reaktnykh dvigateley* (Liquid fuel for rocket engines), izd-vo VVIA im. Zhukovskogo, 1936.

12. Yevstigneyev M. I., et al. Izgotovleniye osnovnykh detaley i uzlov aviadvigateley (Manufacture of basic parts and units of aircraft engines), izd-vo "Mashinostroyeniye", 1964.
13. Issledovaniye raketnykh dvigateley na zhidkem toplive (Investigation of liquid fuel rocket engines), Collection of translations edited by V. I. Il'inskiy, izd-vo "Mir", 1964.
14. Kvasnikov A. V., Teoriya zhidkostnykh raketnykh dvigateley (Theory of liquid-propellant rocket engines), Sudpromgiz, 1959.
15. Korolev S. P. Raketnyy polet v stratosfere (Rocket flight in the stratosphere), Voenizdat, 1936.
16. Krasnov N. F., Aerodinamika tel vrashcheniya (Aerodynamics of solids of revolution), izd-vo "Mashinostroyeniye", 1964.
17. Kosmonavtika, Sov. Entsiklopediya (Cosmonautics, Soviet Encyclopaedia), 1968.
18. Langemak G. E., Glushko V. P. Rakety, ikh ustroystvo i primeneniye (Rockets, their manufacture and use), ONTI, 1935.
19. Mel'kumov T. M., et al. Teoriya zhidkostno-reaktivnykh dvigateley (Theory of liquid-fuel rocket engines), VVIA im. Zhukovskogo, 1956.
20. Mikhaylov-Mikheyev P. B. Spravochnik po metallicheskim materialam turbinostroyeniya (Reference book on metals for turbine construction), Mashgiz, 1961.
21. Moshkin Ye. K. Dinamicheskiye protsessy v ZhRD (Dynamic processes in liquid-fuel rocket engines), izd-vo "Mashinostroyeniye", 1964.
22. Orlov B. V., Mazing G. Yu. Termodynamicheskiye i ballisticheskiye osnovy proyektirovaniya raketnykh dvigateley na tverdom toplive (Thermodynamic and ballistic design fundamentals of solid-fuel rocket motors), izd-vo "Mashinostroyeniye", 1964.
23. Paushkin Ya. M. Khimiya reaktivnykh topliv (Chemistry of rocket propellants), AN SSSR, 1962.
24. Reaktivnyye dvigateli (Jet engines), Collection of translations edited by N. G. Dubrovskiy, Voenizdat, 1962.
25. Sinyarev G. B., Dobrovolskiy M. V. Zhidkostnyye raketnyye dvigateli (Liquid-propellant rocket engines), Oborongiz, 1957.
26. Feodos'yev V. I., Sinyarev G. B. Vvedeniye v raketnuyu tekhniku (Introduction to rocket technology), Oborongiz, 1960.
27. Shevel'yuk M. I. Teoreticheskiye osnovy proyektirovaniya ZhRD (Theoretical design fundamentals of liquid-fuel rocket engine), Oborongiz, 1960.

28. Shirokov M. F. *Fizicheskiye osnovy gazodinamiki* (Physical bases of gas dynamics), *Fizmatgiz*, 1958.
29. Tsander F. A. *Problema poleta pri pomoshchi reaktivnykh apparatov* (Problem of flight with the help of rocket apparatuses), *Oborongiz*, 1961.
30. Tsiolkovskiy K. E. *Izbrannyye trudy* (Selected transactions), AN SSSR, 1962.
31. Bragg. *Rocket Engines*, London, 1962.
32. Sutton G. *Rocket Propulsion Elements*, New York-London, 1963.
33. Stanley Lehrer. Considerations in the Design of Chemical Rocket Powerplants for Space Applications, IAS Paper, 1960, No. 24.

Additional Bibliography

To Chapter I

34. Zhidkiye i tverdyye raketnyye topliva (Liquid and solid rocket propellants). Collection of translations edited by Yu. Kh. Shavlov, IL, 1959.

35. Chemical and Engineering News, 1963, Do. 39.
36. Space Aeronautics, 1963, No. 5.

To Chapter II

37. Alberg, et al. Postroyeniye optimal'nogo sopla na osnove ukorochennykh ideal'nykh sopl (Construction of an optimum nozzle on the basis of shortened ideal nozzles), Translated from English, "Raketnaya tekhnika", 1961, No. 11.

38. Bay Shi-i, Vvedeniye v teoriyu techeniya szhimayemoy zhidkosti (Introduction to the theory of flow of compressible fluids), IL, 1962.

39. Borisenko A. I. *Gazovaya dinamika dvigateley* (Gas dynamics of engines), Oborongiz, 1962.

40. Guderley G., Hantsch Ye. Nailuchshiye formy sverkhzvukovykh osesimmetrichnykh sopl (Best forms of supersonic axisymmetrical nozzles), (collection of translations), "Mekhanika", No. 4, IL, 1956.

41. Deych M. Ye. *Tekhnicheskaya gazodinamika* (Technical gas dynamics), Gosenergoizdat, 1961.

42. Zauer R. Vvedeniye v gazovuyu dinamiku (Introduction to gas dynamics), Gostekhizdat, 1947.

43. Katskova O. N., et al. Opyt rascheta osesimmetrichnykh i ploskikh sopl metodom kharakteristik (Experiment in design of axisymmetrical and flat nozzles by the method of characteristics), Tr. VTs AN SSSR, 1961.

44. Katskova O. N., Shmyglevskiy Yu. D. Tablitsy parametrov osesimmetrichnogo sverkhzvukovogo techeniya svobodno rasshiryayushchegosya gaza s ploskoy perekhodnoy poverkhnost'yu (Tables of parameters of axisymmetrical supersonic flows of freely expanding gas with a flat transition surface), izd-vo AN SSSR, 1962.

45. Kolt S., Bedel D. Kharakteristiki konicheskogo raketnogo sopla pri techenii s otryvom ot stenki (Characteristics of conical rocket nozzles during flow with breakaway from the wall), VRT, 1966, No. 3.

46. Luk'yanov N. A. K raschetu smeshannogo do- i sverkhzvukovogo techeniya gaza v ploskom sople davleniya (Design of mixed trans- and supersonic flows of gas in a flat pressure nozzle), Izv. AN SSSR, Mekhanika zhidkosti i gaza, 1966, No. 2.

47. Panichkin I. A. Nekotoryye zadachi gazovoy dinamiki (Several problems in gas dynamics), NTIO, 1953.

48. Pirumov U. G., Rubtsov V. A. Raschet osesimmetrichnykh sverkhzvukovykh kol'tsevykh sopl (Design of axisymmetrical supersonic annular nozzles), Izv. AN SSSR, MIM, 1961, No. 6.

49. Rao G. Posledniye dostizheniya v profilirovaniyu raketnykh sopl (Latest achievements in profiling rocket nozzles), Translated from English "Raketnaya tekhnika", 1961, No. 11.

50. Sternin L. Ye. K raschetu osesimmetrichnogo reaktivnogo sopla naimen'shego vesa (Design of axisymmetrical nozzle of least weight), Izv. AN SSSR, MIM, 1959, No. 1.

51. Ferri A. Aerodinamika sverkhzvukovykh techeniy (Aerodynamics of supersonic flows), ITTL, 1963.

52. Shmyglevskiy Yu. D. Nekotoryye variatsionnyye zadachi gazovoy dinamiki (Certain variational problems in gas dynamics), Tr. VTs AN SSSR, 1963.

53. Berman K., Neuffer B., "Astronautics", 1960, No. 9.

54. Green L., "Jet Propulsion", 1953, No. 1.

55. Kramer P., "Raketenforschung und Raumfahrtforschung", 1961, Nr. 4.

56. Rao G., ARS Journal, 1958, No. 6, 1960, No. 6.

To Chapter III

57. Vorodin V. A., Dityakin Yu. F. O forme plenki tsentrobezhnoy forsunki (About the form of a film of a swirl), Izv. AN SSSR, MIM, 1962, No. 2.
58. Yerastov K. N., Nikolayev Ye. G. Vliyaniye podogreva podavayemoy zhidkosti na kharakteristiki tsentrobezhnoy forsunki (Influence of preheating of liquid on characteristics of a swirl) TsIAM, 1955.
59. Klyachko L. A. K. teorii tsentrobezhnoy forsunki (Concerning the theory of swirlers), "Teploenergetika", 1962, No. 3.
60. Lyshevskiy A. S. Protsessy raspylivaniya topliva (Processes of fuel atomization), Mashgiz, 1963.
61. Makhin V. A., et al. Teoriya istecheniya kipyashchey zhidkosti cherez tsentrobezhnyu forsunku (Theory of outflow of a boiling liquid through a swirl). Izv. VUZ "Aviatsionnaya tekhnika", 1962, No. 3.
62. Makhin V. A., et al. Eksperimental'noye issledovaniye istecheniya kipyashey zhidkosti cherez tsentrobezhnyu forsunku (Experimental investigation of outflow of a boiling liquid through a swirl), Izv. VUZ, "Aviatsionnaya tekhnika", 1962, No. 1.
63. Prakhov A. P. Issledovaniye i raschet tsentrobezhnoy forsunki (Investigation and design of swirlers), Collection "Avtomacheskoye regulirovaniye aviadvigateley", Oborongiz, 1959.
64. Talakvadze V. V. Teoriya i raschet tsentrobezhnoy forsunki (Theory and design of swirlers), "Teploenergetika", 1961, No. 2.
65. Tikhonov V. B. K raschetu tsentrobezhnoy forsunki (Concerning the design of swirlers), Izv. VUZ, "Aviatsionnaya tekhnika", 1958, No. 3.
66. Shaulov Yu. Kh., Lerner M. O. Goreniye v ZhRD (Combustion in liquid-fuel rocket engines), Oborongiz, 1961.

67. Aviation Week, 1962, No. 30.
68. Astrodynamics, 1962, No. 2.
69. Flugwelt, 1961, Nr. 10.
70. Flugkörper, 1961, Nr. 8.

To Chapter IV

71. Avduyevskiy V. S., et al. Osnovy teploperedachi v aviatcionnoy i raketnoy tekhnike (Fundamentals of heat transfer in aviation and rocket technology), Oborongiz, 1960.

72. Gukhman A. A. Fizicheskiye osnovy teploperedachi (Physical bases of heat transfer), Gosenergoizdat, 1936.

73. Gukhman A. A., Ilyukhin N. V. Osnovy ucheniya o teplobmene pri techenii gaza s bol'shoy skorost'yu (Fundamentals of heat exchange during flow of a gas at high speed), Mashgiz, 1951.

74. Zhidkiy vodorod (Liquid hydrogen), Collection of translations edited by M. P. Mal'kov, izd-vo "Mir", 1964.

75. Zarubin V. S. Temperaturnyye polya v konstruktsii letatel'nykh apparatov (Temperature fields in aircraft structures), izd-vo "Mashinostroyeniye", 1966.

76. Zarubin V. S. Ob optimal'noy geometrii orebreniya na poverkhnosti teplo obmena (About optimum geometry of ribbing on a heat exchange surface), Izv. VUZ, "Mashinostroyeniye", 1963, No. 3.

77. Iyelev V. M. Nekotoryye voprosy gidrodinamicheskoy teorii teploobmena pri techeniya neszhimayemoy zhidkosti (Certain questions of the hydrodynamic theory of heat exchange during flow of incompressible fluids), DAN SSSR, 1952, t. 86, vyp. 6.

78. Iyelev V. M. Nekotoryye voprosy gidrodinamicheskoy teorii teploobmena pri techenii gaza (Certain questions of the hydrodynamic theory of heat exchange during flow of a gas), DAN SSSR, 1952, t. 87, vyp. 1.

79. Kalikhman L. Ye. Turbulentnyy pogranichnyy sloy na poverkhnosti, oblekayemoy gazom (Turbulent boundary layer on a surface streamlined by gas), Oborongiz, 1956.

80. Kol'yer Dzh. Obzor rabot po teploobmenu k dvukhfaznym sistemam (A survey of works on heat exchange to two-phase systems), IL, 1962.

81. Kutateladze S. S. Osnovy teorii teploobmena (Fundamentals of the theory of heat exchange), Mashgiz, 1962.

82. Kutateladze S. S., Leont'yev A. I. Turbulentnyy pogranichnyy sloy szhimayemogo gaza (Turbulent boundary layer of a compressible gas), Sib. otd. AN SSSR, 1963.

83. Loytsyanskiy L. G. Laminarnyy pogranichnyy sloy (Laminar boundary layer), Fizmatgiz, 1962.

84. Mikheyev M. A. Osnovy teploperedachi (Fundamentals of heat transfer), Gosenergoizdat, 1956.

85. Petukhov B. S., Royzen L. N. Teploobmen v trubakh kol'tsevogo secheniya (Heat exchange in pipes with an annular cross section), IFZh, 1963, No. 3.

86. Psarutakis. Kazhushchayasya stepen' chernoty poverkhnosti s mnogochislennymi V-obraznymi kanavkami (Apparent degree of blackness of a surface with numerous V-shaped grooves), Translated from English,

Raketnaya tekhnika i kosmonavtika", 1963, No. 8.

87. Sellers. *Vliyaniye dvukh mernogo teploobmena na temperaturu stenok kamery raketnogo dvigatelya trubchatogo tipa* (Influence of two-dimensional heat exchange on wall temperature of a tubular type thrust chamber), Translated from English, "Raketnaya tekhnika", 1961, No. 3.

88. Uvarov V. V. *O rebristykh poverkhnostyakh* (About ribbed surfaces), Izv. VUZ, "Mashinostroyeniye", 1958, No. 1.

89. Fedorov I. G. *Teploobmen i soprotivleniye shchelevykh kanalov s obaloobraznymi konischeskimi vyshtampovkami* (Heat exchange and drag of slotted channels with oval conical stampings), Izv. VUZ, "Aviatsionnaya tekhnika", 1962, No. 4.

90. Kharden. *Konstruirovaniye raketnykh dvigateley, ispol'zuyushchikh vodorod v kachestve goryuchego* (Construction of rocket engines using hydrogen as fuel). VRT, 1962, No. 8.

91. Kheyek A. *Vliyaniye temperatury gazoobraznogo vodoroda na effektivnost' okhlazhdeniya* (Influence of the temperature of gaseous hydrogen on effectiveness of cooling), Translated from English, "Raketnaya tekhnika i kosmonavtika", 1965, No. 3.

92. Khendriko, et al. *Sootnosheniya dlya koefitsiyenta teplootdachi k vodorodu pri kipenii i pri sverkhkriticheskem davlenii* (Relationship for the coefficient of heat radiation to hydrogen during boiling and at supercritical pressure). Translated from English, "Raketnaya tekhnika", 1962, No. 2.

93. Chirkin V. S. *Teplofizicheskiye svoystva veshchestv* (Thermophysical properties of substances), Fizmatgiz, 1959.

94. Shlikhting G. *Teoriya pogranichnogo sloya* (Boundary layer theory), IL, 1956.

95. Shcherbakov V. K. *Teploperedacha cherez stenku, otrebrennuya ribbing*, Izv. VUZ, "Energetika", 1962, No. 8.

96. E. I. "ADS", 1959, No. 29.

97. E. I. "Astronautika i raketodinamika", 1963, No. 5.

98. Aviation Week, 1962, No. 16.

To Chapter V

99. Artamonov V. I. *Termodinamicheskaya neustoychivost' neodnorodnogo gazovogo potoka* (Thermodynamic instability of a nonuniform gas flow), Izv. AN SSSR, MIM, 1961, No. 1, 1962, No. 3.

100. Belikov V. M., Nikitin A. N. Sborka aviatsionnykh dvigateley (Assembly of aircraft engines), izd-vo "Mashinostroyeniye", 1964.
101. Besserer K. U. Inzhenernyy spravochnik po upravlyayemym snaryadam (Engineering reference book on guided missiles), Voenizdat, 1962.
102. Bol'shakov G. F., et al. Fiziko-khimicheskiye osnovy primeneniya motornykh reaktivnykh i raketnykh topliv (Physicochemical fundamentals of the use of jet engine and rocket fuels), izd-vo "Khimiya", 1965.
103. Gurov A. F. Raschety na prochnost' i kolebaniya v raketnykh dvigatelyakh (Strength and oscillation calculations in rocket engines), izd-vo "Mashinostroyeniye", 1966.
104. Dubenets S. A. Raschet obolochek kamer sgoraniya ZhRD (Design of shells of liquid-fuel rocket engine combustion chambers), MAI, 1960.
105. Krokko L., Chang Sin-I. Teoriya neustoychivosti goreniya v ZhRD (Theory of combustion instability in liquid-fuel rocket engines), IL, 1958.
106. Krokko, et al. Poperechnyye vysokochastotnyye kolebaniya v ZhRD (Transverse high-frequency oscillations in liquid-fuel rocket engines), Translated from English, "Raketnaya tekhnika", 1962, No. 3, "Raketnaya tekhnika i kosmonavtika", 1964, No. 9.
107. Kulik F. Ye. Ustoychivost' vysokochastotnykh kolebaniy v kamere sgoraniya raketnogo dvigatelya (Stability of high-frequency oscillations in combustion chambers of rocket engines), Translated from English "Raketnaya tekhnika i kosmonavtika", 1963, No. 5.
108. Makkormak. Dvizhushchiy mekhanizm vysokochastotnoy neustoychivosti v kamere ZhRD (Mechanism of high-frequency instability in chambers of liquid-fuel rocket engines), VRT, 1965, No. 4.
109. Raushenbakh B. V. Vibratsionnoye goreniye (Vibration burning), Fizmatgiz, 1961.
110. Sinyarev G. B. Termodinamicheskiy analiz i teplovoy raschet skorostnoy kamery sgoraniya ZhRD (Thermodynamic analysis and thermal calculation of high-speed combustion chambers of liquid-fuel rocket engines), Collection of articles "Nekotoryye voprosy mekhaniki", Oborongiz, 1962.
111. Feodos'yev V. I. Prochnost' teplonapryazhennykh uzlov ZhRD (Strength of subassemblies of liquid-fuel rocket engines under heat loads), Oborongiz, 1963.
112. Khefner. Otrabotka ustoychivosti goreniya v ZhRD na toplivakh dlitel'nogo khraneniya (Adjustment of stability of burning in liquid-fuel rocket engines with storable propellants), VRT, 1966, No. 5.

113. E. I. ADS, 1959, No. 7; E. I. "Astronavtika i raketodinamika", 1963, No. 36; 1966, No. 16.

114. Aviation Week, 1963, No. 21.

To Chapter VI

115. Bashta T. M. Mashinostroitel'naya gidravlika (Machine-building hydraulics), Mashgiz, 1963.

116. Goffmen. Bol'shiye raketnyye dvigateli dlya kosmicheskikh raket i snaryadov (Large rocket engines for space rockets and missiles), VRT, 1962, No. 2.

117. Devis. Proyektirovaniye i dovodka XRL-99 (Design and finishing of XRL-99), VRT, 1963, No. 10.

118. Zegzhda A. P. Gidravlicheskiye poteri v kanalakh i truboprovodakh (Hydraulic losses in channels and pipelines), Gosstroyizdat, 1957.

119. Idel'chik I. Ye. Spravochnik po gidravlicheskim sопротивлениям (Reference book on flow friction), Gosenergoizdat, 1960.

120. Kazandzhan P. N., Tikhomirov Yu. P. Effektivnost' sistem pitaniya ZhRD (Effectiveness of feed systems of liquid-fuel rocket engines), "Vestnik vozduzhnogo flota", 1960, No. 6.

121. Nekrasov B. B. Gidravlika (Hydraulics), Voyenizdat, 1960.

122. Novyye napravleniya v kriogennoy tekhnike (New directions in cryogenic technology), Collection of translations edited by M. P. Malkov, izd-vo "Mir", 1966.

123. Porter i Stanford. Vytesnitel'nyye ustroystva dlya toplivnykh sistem kosmicheskikh korabley (Displacement device for the fuel systems of spaceships), VRT, 1966, No. 4.

124. Tikhonov N. D. Sistemy podachi ZhRD (Liquid-fuel rocket engine supply systems), Institut GVF, Riga, 1960.

125. Shevyakov A. A. Avtomatika aviatsionnykh i raketnykh silovykh ustavok (Automatics of aviation and rocket propulsion systems), izd-vo "Mashinostroyeniye", 1965.

126. E. I. "Astronavtika i raketodinamika", 1965, No. 10.

127. Flight 1961, No. 268; 1961, No. 2736; 1962, No. 2759; 1963, No. 2829.

128. The Blue Streak Propulsion System, London, 1960.

129. Rocket Propulsion Technology, 1960, vol. 1.

130. SAE Journal, 1963, No. 8.

131. Aviation Week, 1964, No. 13.

To Chapters VII and VIII

132. Abiants V. Kh. Teoriya gazovykh turbin reaktivnykh dvigateley (Theory of gas turbines of jet engines), izd-vo "Mashinostroyeniye", 1965.

133. Dobrovolskiy M. V. i Krylov Yu. V. Opredeleniye naibol'shego vozmozhnogo davleniya v kamere ZhRD, rabotayushchego po zamknutoy skheme "gaz + zhidkost'" (Determination of the highest possible pressure in the chamber of liquid-fuel rocket engines working on the "gas + liquid" closed circuit), Izv. VUZ, "Mashinos-troyeniye", 1967, No. 4.

134. Zhiritskiy G. S., et al. Gazovyye turbiny aviationsionnykh dvigateley (Gas turbines of aircraft engines), Oborongiz, 1963.

135. Yershov N. S., Ovsyannikov B. V. Osobennosti rascheta tsentrobezhnogo nasosa so shnekovym prednasosom (Peculiarities in design of centrifugal pumps with screw pre-pumps), MAI, 1961.

136. Kazandzhan P. M. Teoriya gazovykh turbin (Theory of gas turbines), izd-vo VVIA im. Zhukovskogo, 1947.

137. Loytsyanskiy L. G. Mekhanika zhidkosti i gaza (Mechanics of liquids and gases), Gizmatgiz, 1959.

138. Lomakin A. A. Tsentronezhnyye i propellernyye nasosy (Centrifugal and propeller pumps), Mashgiz, 1950.

139. Ovsyannikov B. V. Teoriya i raschet nasosov ZhRD (Theory and design of pumps of liquid-fuel rocket engines), Oborongiz, 1960.

140. Prokof'yev V. N. Tsentronezhnyye nasosy (Centrifugal pumps), izd-vo MVTU, 1948.

141. Pfleyderer K. Lopatochnyye mashiny dlya zhidkostey i gazov (Blade machines for liquids and gases), Mashgiz, 1960.

142. Rudnev S. S. Eksperimental'noye issledovaniye raboty dvukhstupenchatogo propellernogo nasosa (Experimental investigation of the work of two-stage propeller pump), Nauchnyye zapiski Khar'k. mekh.-mash. in-ta, t. IV, 1940.

143. Uvarov V. V. Gazovyye turbiny (Gas turbines), ONTI, 1935.

144. Aviation Week, 1963, No. 13.

145. Luftfahrttechnik Raumfahrttechnik, 1965, Nr. 2.

146. Space Aeronautics, 1964/65, No. 4.

To Chapter IX

147. Kurov Yu. D., Dolzhanskiy Yu. V. Osnovy proyektirovaniya porokhovykh raketnykh snaryadov (Design fundamentals of solid-propellant missiles), Oborongiz, 1961.

148. Melik-Pashayev N. I. Zhidkostnyy reaktivnyy dvigatel' (Liquid-fuel rocket engine), Voenizdat, 1959.

149. Nit, Peydzh. ZhRD s predvaritel'noy zapravkoj toplivom (Liquid-fuel rocket engines with preliminary fueling), VRT, 1962, No. 11.

150. Ordal. Smeshannyye dvigatel'nyye ustavok, VRT (Mixed propulsion systems), 1960, No. 6.

151. Flight, 1963, No. 2840.

152. Raketentechnik und Raumfahrtforschung, 1963, Nr. 3, 4; 1961, Nr. 4.

153. Space Aeronautics, 1961, No. 4.